KTH Architecture and
the Built Environment

Excavation in moraine and dense non-cohesive soil
- Numerical analysis of soil behaviour

Mattias Lindgren

Licentiate thesis
Department of Civil and Architectural Engineering
Division of Soil and Rock Mechanics
Royal Institute of Technology
Stockholm, 2012

TRITA-JOB LIC 2018
ISSN 1650-951X

Preface

The work in this thesis was carried out from March 2008 to May 2012 at the Division of Soil and Rock Mechanics, Department of Civil and Architectural Engineering at the Royal Institute of Technology (KTH). The supervisor of the work was Professor Staffan Hintze.

I would like to express my gratitude to the Swedish Transport Administration (TrV), the Development Fund of the Swedish Construction Industry (SBUF), Royal Institute of Technology (KTH) and NCC Construction Sverige AB for the financial support given to this research project.

The warmest thanks to my supervisor Staffan Hintze whose encouragement, engagement and guidance have helped me realize this work. Invaluable help and support have also been given by my co-supervisor Zein-Eddine Merouani, thank you very much!

The following group of people have contributed with knowledge and experience during the work with this research project, which is gratefully acknowledged: Håkan Eriksson (Solid Geo), Håkan Stille (KTH), Lovisa Moritz (TrV), Magnus Karlsson (TrV) and Ulf Isacsson (KTH).

Furthermore I would like to show my greatest appreciation to my colleagues at the Division of Soil and Rock Mechanics.

Finally, I would like to thank my wife Åsa who made it possible for me to conduct these research studies.

Stockholm, May 2012

Mattias Lindgren

Abstract

Excavation and moving of soil are common civil work tasks connected to the construction of buildings, roads and railways. In construction projects large amounts of soil have to be handled with different machines, tools and working methods. Soils are more or less difficult to excavate depending on their properties. The ability to excavate the soil (the excavatability) in combination with the type of work performed affects the choice of machines and tools being used. It also affects the time it takes to perform the work. The handling of soil volumes is a large part of the project cost. The cost depends on the machines and tools being used, the amount of soil being excavated and the ability to excavate the soil.

The main objectives of this study are:

- to identify parameters affecting the excavatability of soil through a literature review.
- to study and describe the excavation process in soil.
- to evaluate parameters affecting the horizontal resistive force on a wide blade with the finite element method.
- to compare and discuss the magnitude of the horizontal resistive force obtained in the finite element study with calculations using an analytical model.
- to propose a platform for further research in this area.

The excavation process and the analysis of a tool working through the soil have been studied for three types of machine-tool sets. Earlier studies from different authors have provided important parameters that affect the resistance of soil as well as form a basis for the analysis of excavation and moving soil. A two-dimensional finite element analysis of a wide blade moving horizontally in a soil mass has been performed. The purpose of the numerical analysis was to analyse and discuss the effects of different soil and soil-tool parameters on the resultant resistive force acting on the blade.

Based on the literature review, it was found that the particle size, the content of cobbles and boulders, the shear strength and the denseness of the soil affects the excavatability of the soil. When defining a model for predicting resistive forces on an excavation tool, it is necessary to study the total excavation process, including how the tool interferes with the ground, how the machine and tool moves and the methodology used for excavating and moving the soil.

Based on the numerical analysis, it was found that, for undrained cohesive soil, the resistive force increases linearly with undrained shear strength and adhesion. For non-cohesive soil the resistive force increases non-linearly with the soil friction angle and the soil-tool friction angle, and linearly with dilatancy. Extended interfaces as well as different mesh sizes significantly impacted the magnitude of the resistive force.

In order to determine the excavatability of soil and to present a new system for classification of excavatability, related knowledge is needed about the excavation process and the effect of the cobble and boulder content on the excavatability. Theoretical results obtained in this study must be verified by field tests.

Sammanfattning

Schaktning och förflyttning av jord är vanligt förkommande markarbeten vid uppförandet av byggnader, vägar och järnvägar. I byggprojekt hanteras stora mängder jord med hjälp av olika typer av maskiner, verktyg och arbetsmetoder. Jorden är mer eller mindre lätt att schakta i beroende på dess egenskaper. Jordens schaktbarhet i kombination med den typ av arbete som skall utföras påverkar valet av de maskiner och verktyg som skall användas. Schaktbarheten påverkar även den tid det tar att utföra arbetet. Hantering av jordmassor utgör en stor del av projektkostnaden. Kostnaden beror av vilka maskiner och verktyg som används, mängden jord som schaktas samt jordens schaktbarhet.

De huvudsakliga syftena med denna studie är:

- att genom en litteraturstudie identifiera parametrar som påverkar schaktbarheten.
- att studera och beskriva processen för att schakta i jord.
- att med hjälp av finita element metoden utvärdera parametrar som påverkar den horisontella resistiva kraften på ett brett blad.
- att jämföra storleken på den horisontella resistiva kraften erhållen i den numeriska studien med kraften beräknad med hjälp av en analytisk modell.
- att ta fram en plattform för vidare forskning inom detta område.

Processen att schakta och förflytta jord för tre olika kombinationer maskin – verktyg har studerats. Tidigare studier från olika författare har dels givit viktiga parametrar som påverkar motståndet från jorden dels utgör en bas för att analysera schaktning och förflyttning av jord. En tvådimensionell analys av ett brett blad som förflyttas horisontellt genom en jordmassa har utförts med hjälp av finita element metoden. Syftet med den numeriska studien var att analysera effekterna av olika jord- och verktygsparametrar som påverkar den resulterande resistiva kraften på bladet.

Baserat på litteraturstudien kan slutsatsen dras att partikelstorlek, innehåll av sten och block, jordens skjuvhållfasthet och jordens täthet påverkar jordens schaktbarhet. När man definierar en modell för att bestämma de resistiva krafterna på ett schaktverktyg vid schaktning är det nödvändigt att studera den totala schaktprocessen. Det vill säga hur verktyget interagerar med jorden, hur och i vilken riktning som maskinen och verktyget förflyttas samt vilken metod som används för att schakta och förflytta jorden.

Baserat på den numeriska studien kan slutsatsen dras att, för odränerad kohesionsjord, ökar den resistiva kraften linjärt med odränerad skjuvhållfasthet och adhesion. För icke-kohesiv jord ökar den resistiva kraften icke-linjärt med friktionsvinkeln och friktionen mellan jord och verktyg. Den ökar även linjärt med dilatansen. Att använda förlängda interface – element så väl som att använda olika storlekar på de finita elementen hade en signifikant inverkan på storleken på den resistiva kraften.

För att kunna bedöma jordens schaktbarhet och för att kunna ta fram ett nytt system för klassificering av schaktbarhet behövs ytterligare kunskap om processen att schakta i jord samt sten- och blockhaltens inverkan på schaktbarheten. De teoretiska resultaten måste även verifieras med försök i fält.

Notations

Major symbols used in the text are listed below. Other symbols are defined as they appear in text.

α	Blade angle
β	Soil failure angle
γ	Unit weight
δ	Soil-tool interaction/friction
ε	Strain in soil
ν	Poisson's ratio
ρ	Density
σ	Stress in soil
τ	Shear stress on the failure plane
Φ	Diameter, Angle of friction
φ	Angle of friction
ψ	Angle of dilatancy
BA	Blade Angle
c	Cohesion
c_a	Adhesion
c_u	Undrained shear strength
E	Elastic modulus/stiffness
F_x	Horizontal force
K_0	Coefficient of lateral earth pressure
R, $R_{interaction}$	Strength reduction factor
w	Weight, width
u_x	Displacement
u	Pore pressure
H	Horizontal load
V	Vertical load
P	Passive earth pressure
q	Surcharge

Contents

1 Introduction

1.1 Background

Excavation in soil is a common civil work connected to the construction of buildings, roads and railways. In construction projects, large amounts of soil have to be handled being excavated or moved. Soils are more or less difficult to excavate depending on their properties. The ability to excavate the soil (the excavatability) in combination with the type of work performed affects the choice of machines and tools being used. It also affects the time it takes to perform the work. The handling of soil volumes is a large part of the project cost. The cost depends on machines and tools being used, the amount of soil being excavated and the ability to excavate the soil. The type of soil being excavated, therefore, influences the total cost of the project.

In construction sites different machines and tools are used for different working operations. There are several combinations of machines, tools and methods of excavating soil. Bulldozers and scrapers use wide blades to excavate and level the soil, wheel loaders use wide buckets to move soil and excavators use narrow buckets when excavating soil. In each of these working operations the excavating tool experiences resistance from the soil, although the magnitude differs. This resistance, for example the resulting force on the tool, will vary due to working operation, the geometric outline of the tool, tool properties and soil properties. If the resistance from the soil when excavating with any tool can be predicted, the cost of excavation work can be more accurately determined.

Moraine soil is the most common type of soil in Sweden and is often dense and non-cohesive. It was formed and deposited during the latest ice age about 10 000 years ago. Moraine soil is unsorted and has particles ranging in size from clay to boulders. Depending on the process of formation, the particles can be angular or rounded in shape and loosely or densely packed. This gives a soil with varying properties, strength and deformation behaviour. The ability to excavate moraine soil will vary to a great extent depending on the nature of the soil.

The purpose of this study is to describe parameters that influence the difficulty of excavating (excavatability) moraine and dense non-cohesive soils. A parametric study to see what parameters affect the horizontal force on a wide blade was performed with the finite element method.

1.2 Earlier studies

The literature review in this study presents earlier studies relevant to the problem of excavating in soil. There are few reported results in the literature regarding excavatability classification of soil. Some studies performed in Sweden and Finland has aimed to present a classification system for excavation of soil. Some of these systems have started from a soil classification system and with results from experiments performed when excavating soil, an excavatability classification system has been created.

Different aspects of soil-tool performance have been treated in the agricultural and earth moving areas. Efficiency incitements have encouraged research in soil-tool interaction, soil movement and implement design. In the topic of agriculture research is focused on agricultural implements for cultivation. The tools used in these studies are often narrow compared to a bulldozer blade where the height of the blade is less than the length of the

blade. It is however possible to find some similarities between blades used in agricultural soil and blades used in soil at construction sites. In the matter of earth moving, both wide blades and buckets are concerned. Companies that construct blades, buckets and other equipment for earth moving conduct research in this area. Logically, this knowledge is often secret and unpublished. The knowledge of constructing tools has also been gained through practical experience and is therefore unpublished. In addition the automation of earth moving machines is a growing field of research and is motivated by improvements in productivity, efficiency and safety. The development of fast computers, techniques for controlling machines and the ability to sense the environment have enabled the progress.

1.3 Objectives

The main objectives of this study are:

- to identify parameters affecting the excavatability of soil through a literature review.
- to study the excavation process in soil.
- to evaluate parameters affecting the horizontal resistive force on a wide blade with the finite element method.
- to compare and discuss the magnitude of the horizontal resistive force obtained in the finite element study with calculations in analytical models.
- to propose a platform for further research in this area.

1.4 Scope and structure

This thesis consists of five chapters which are briefly described:

Chapter 1 gives an introduction to the area of research as well as the objectives and content of this thesis.

Chapter 2 consists of a literature review regarding aspects of soil excavation and earlier work on excavatability classification.

Chapter 3 presents a numerical study of a wide blade excavating in soil using the finite element program Plaxis.

Chapter 4 consists of a discussion where results from the performed literature review and the finite element analysis are treated.

Chapter 5 presents general conclusions of the study and recommendations for future work.

1.5 Extent and limitations

This thesis studies the ability to excavate soil. The excavation process and the analysis of a tool working through the soil is briefly studied for three types of machine-tool sets performing excavation and soil moving work in construction areas. The thesis consists of a two-dimensional finite element analysis of a wide blade moving horizontally in a soil mass. The purpose of the FE analysis is to analyse and discuss the effects of different soil and soil-tool parameters affecting the resultant resistive force acting on the blade.

2 Literature study

2.1 Introduction

This chapter presents literature related to the prediction of resistance of excavating in soil. It starts with a review of literature concerning classification of excavatability. The next sections review studies concerning excavation and earth moving with blades and buckets respectively, naturally distinguishing between working operations. In the literature most of the resistive force prediction theories used when studying buckets are developed for blades. In the section of soil properties different measures of soil is presented, relevant when studying moraine and dense non-cohesive soils. In the last section the shear strength of soil and parameters affecting the shear strength are presented.

2.2 Classification of excavatability

A number of classification systems for excavatability have been proposed in the literature. Most of these studies are from Sweden and Finland and presents attempts to group the soil after its difficulty of excavating. In theses studies the classification of excavability is based on soil classification, machine performance, excavation studies, soil properties and human experience. Also two classification systems from United Kingdom respectively Australia is presented. In several of the systems presented the classification ranges from 1 to 5 meaning that class 1 offers lowest resistance to excavation and class 5 offers the highest resistance.

2.2.1 Fransen (1951)

In guidance for performing excavation work with an excavator from the State board of water power an excavatability classification system is presented, see Table 2.1. The classes range from “very easy” to excavate to “very hard” to excavate. For each class the bulk density and relative swelling is presented. It is stated that the excavatability depends on particle size distribution, cementation, water content and porosity, since these parameters influences the strength of the soil. Excavatability is related to both loosen the material from the ground and filling the bucket. It is stated that the degree of filling the bucket is dependent on the ability of soil to flow into the bucket and filling it. The filling degree is higher for fine grained and homogenous material and lesser for soil with high boulder content.

Table 2.1. Excavatability classification of soil, modified from Fransen (1951).

Excavatability class	Bulk density (kg/m3)	Swelling coefficient	Soil (example)
Very easy	1000-1500	1,1-1,3	Loose clay, dry sand
Easy	1500-2000	1,2-1,4	River sand, gravel
Normal	1600-2000	1,3-1,5	Sandy clay, sand or gravel with cobbles, loose moraine
Hard	1800-2200	1,4-1,7	Gravel with cobbles, medium dense moraine, well blasted rock
Very hard	2000-2600	1,5-2,0	Hard dense moraine, Silt with cobbles, poorly blasted rock

2.2.2 Arhippainen & Korpela (1966)

Arhippainen & Korpela (1966) states that when creating a system for excavatability classification, it is necessary to create a system independent of machines and working methods. In this way the system is only dependent on geology and soil properties and can be used even though machines and working methods develops. In the study excavatability is seen as a difficulty of excavating only depending on characteristic physical soil properties of a soil type or layer. Parameters like what season of the year it is, weather conditions, groundwater level, the skills of the operator or the bearing capacity of the excavating machines are not considered. These parameters are considered when determining the performance of an excavating machine in terms of cubic meter of soil loaded per hour (m^3/h).

In the study an excavatability classification system have been constructed from soil classification, machine performance and earlier reported excavation studies, see Table 2.2. The classification system has been calibrated by field experiments, both in moraine soil with an excavator and in gravel with a wheel loader. In order to predict the excavatability the system was correlated to different soil survey methods.

Table 2.2. Excavatability classification, according to Arhippainen and Korpela (1966).

Excavatability class	Bulk density (kg/m^3) (unsaturated)	Seismic velocity (m/s) Above GW	Below GW	Ram sounding (bats/10 cm)	Rotation sounding (m/h)	Soil (example)
K:1	< 1,7	< 400	< 1300	0-5	> 1,5	Sorted, fine grained (sand, saturated clay)
K:2	1,7-1,9	400-800	1300-1600	5-10	1,0-1,5	Sorted with cobbles (gravel with cobbles)
K:3	1,8-2,0	800-1200	1600-1900	10-20	0,5-1,0	Dense soil or with cobbles (dry clay, sandy moraine)
K:4	2,0-2,2	1200-1700	1900-2300	20-40	0,2-0,5	Very dense and unsorted (dense moraine)
K:5	> 2,2	> 1700	> 2300	> 40	< 0,2	Hard moraine with many boulders

In the study it is concluded that when determining the excavatability of soil it is important to examine the geology of the soil layer and that the most important parameters are unsaturated bulk density and content of cobbles and boulders. In Table 2.2 the characteristics of the soil types for the different excavatability classes are presented. Moraine soil can be found in classes K:3 through K:5. Other parameters mentioned are particle size distribution, shear strength and water content.

According to Arhippainen & Korpela the excavatability decreases both with decreasing grading of particles and with increasing content of cobbles. This is because the shear strength increases or because an increasing content of cobbles will not fit in the excavating bucket. Though, in sorted soils the content of cobbles does not necessary affect the excavatability of the soil extensively but it causes difficulties when sounding in the soil. Beneath the groundwater table the soil will loosen easier but will also increase in weight and it will become more difficult to fill the bucket. In the report there is a distinction pointed out between the ability of excavating in a particular soil and the excavation capacity of a machine in a particular soil.

2.2.3 Korhonen & Gardemeister (1972)

In the report from Korhonen and Gardemeister a system for classification of excavatability was presented, see Table 2.3 and Table 2.4. It was created from a soil classification system. Soil with similar physical properties is grouped together and, according to the report, the resistance to excavation is about the same in each group. Some field experiments have been performed to determine excavation performance of an excavator through measured deformation in the excavator arm giving the resistance force of the soil. The classification system has been approximated with results from a geotechnical survey performed at the field experiments.

The fine grained soils (soil type H) are divided according to particle size and undrained shear strength. The undrained shear strength of dry clay should be at least 50 kPa to be classified H3. For the coarse grained soils (soil type K) the classification depends on particle size distribution, denseness and content of cobbles and boulders. In sand and gravel only the particle size distribution and the content of cobbles is used in classification. The moraine soil (soil type M) is divided according to the resistance to excavating measured during field experiments. It is concluded that the resistance when excavation in moraine soil depends on bulk density and content of cobbles and boulders. Particles with sizes up to 60 mm do not have a significant impact on the excavation resistance. Densely cemented moraine is classified M3 independently of the content of cobble and boulders.

Table 2.3. Excavatability classification, modified from Korhonen and Gardemeister (1972).

Soil group	Excavatability class	Soil type	Wood content (%)	Cobble content (%)	Boulder content (%)	Bulk density (Mp/m^3)
E	E1	Gyttja, dy (organic)				
	E2	Peat	< 30			
	E3	Peat	> 30			
H	H1	Clay				
	H2	Silt				
	H3	Dry-crust clay				
K	K1	Sand				
	K2	Gravel		< 30		
	K3	Esker		30-50		
		Cobble soil		> 50		
M	M1	Loose moraine without cobbles		< 30	< 10	< 1,9
	M2	Medium dense moraines without cobbles		< 30	< 10	1,9-2,1
	M3	Dense moraines				> 2,1
		Moraines with cobbles		> 30	< 10	
		Moraines with boulders			10-50	
		Boulderly soil			> 50	

Table 2.4. Weight sounding, ram sounding and seismic velocity correlated to excavatability classes, modified from Korhonen and Gardemeister (1972).

Soil group	Excavatability class	Soil type	Weight sounding	Ram sounding (bats/m)	Seismic velocity Above GW (m/s)	Seismic velocity Below GW (m/s)
E	E1	Gyttja, dy (organic)	< 50 kg			
	E2	Peat	< 50 kg			
	E3	Peat	< 50 kg			
H	H1	Clay	< 100 kg			1100-1500
	H2	Silt	< 150 hv/m			1100-1500
	H3	Dry-crust clay	> 10 hv/m		< 300	
K	K1	Sand	> 50 hv/m	> 50	200-500	1200-1600
	K2	Gravel	> 50 hv/m	> 50	400-800	1500-1800
	K3	Esker, Cobble soil			500-1100	1600-1900
M	M1	Loose moraine without cobbles		< 300	700-1000	1600-1900
	M2	Medium dense moraines without cobbles		300-700	800-1400	1800-2000
	M3	Dense moraines		> 700	1200-1600	2000-2300
		Moraines with cobbles		(> 400)	1200-1600	2000-2300
		Moraines with boulders			1200-1600	2000-2300
		Boulderly soil				

In the field experiments the resistance from the soil was measured during excavation with an excavator. Also the movement of the bucket through the soil was recorded and it was shown to be continuous in clay, sand and gravel. In esker and moraine soil the path of movement was discontinuous with curves and loops as the operator reverses the bucket to loosen a cobble or boulder. The resistance to excavation is fairly continuous in clay, sand and gravel but in moraine soil discontinuous. In moraine the resistance increases and decreases irregularly as the bucket has to take care of cobbles and boulders.

In the study it is shown how the productivity, in terms of cubic meter excavated soil per hour, is related to the resistance to excavation. Also the decrease of filling the bucket is related to the resistances to excavation for different soils. See Figure 2.1.

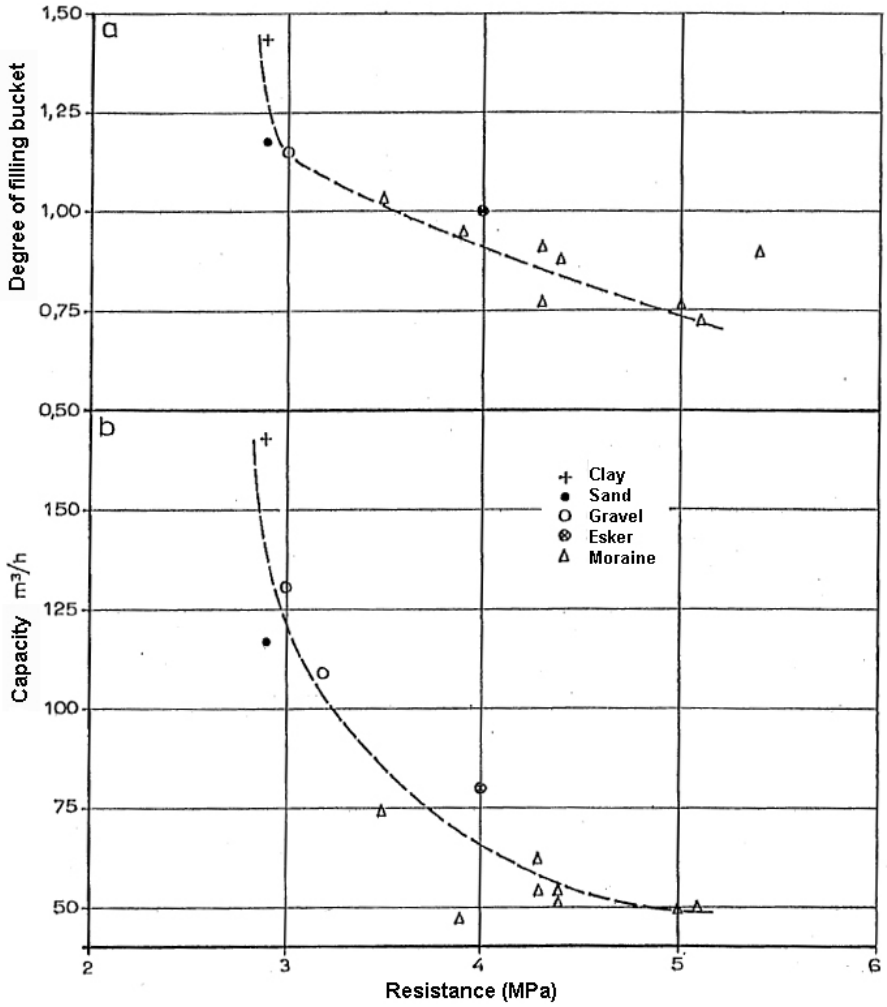

Figure 2.1. Relations between resistance to excavating and degree of filling bucket respectively capacity, from field tests, modified from Korhonen and Gardemeister (1972).

2.2.4 Swedish Road Administration (1972)

The report contains preliminary results from an internal development project at the Swedish Road Administration called "Definition of workability for different soils". In the end of 1960th and 1970th the Swedish Road Administration carried out different projects regarding earth moving and excavation work. This is the first report putting together results from Development project 2.7. This report concerns workability as a process of several stages involving soil loosening (excavation), loading, transportation, unloading and compaction. The workability of the soil refers to a general definition of the properties of the soil affecting the choice of method and machines to use in the earth moving process. The workability is based on the same soil and rock parameters that determines the resistance to soil loosening, the tendency of soil liquefaction, the bearing capacity during excavation and the bank bearing capacity and soil compaction properties.

In the study other factors concerning the choice of machines to use is presented: The quality of the road leading to the excavation area affects transportation possibilities. If the depth of the ground water table is above or close to the excavation depth the soil probably is wet affecting the bearing capacity of the soil and the rolling ability of tires. The size of the

working space affects the ability of using some types of machines. What time of the year and weather it is gives different conditions for excavation work. During winter low temperature gives increased bearing capacity but also increased resistance to soil loosening. Rain gives an increased water content of soil resulting in lower bearing capacity.

In the study a system for classification of soils related to workability is presented. With the classification system it is possible to classify soil and rock properties that affect the excavation work and to choose machines appropriate for the type of work. The system is constructed to be a combination of one classification scheme for classification of workability from soil properties and another for choosing machines. The systems for classification of values in both of these systems are based on experience. The first classification scheme involves rating the above mentioned parameters affecting the workability (resistance to soil loosening, tendency of soil liquefaction, bearing capacity during excavation, bank bearing capacity and soil compaction properties) according to soil properties. The rating scale has the range: 1 (good), 2 (normal), 3 (bad) and 4 (very bad). From soil surveys in field and laboratory, soil properties are retrieved for soils with finer particles, coarser particles and moraines.

The soil loosening (excavation) part of this study involves classification of the excavatability. The classification scheme is fairly detailed and concerns several common geotechnical survey methods used today, see Table 2.5. Vane and cone tests can be used to classify fine sediments and cobble and boulder content can be used for coarse grained sediments. The values of the grading system are based on human experience and results from three road projects were soil investigation and excavation studies have been carried out. Though, no references are presented and it is not stated if the work in these studies is directly connected to the classification system constructed.

Table 2.5. Excavatability classification system presented by the Swedish Road Administration (1972). Values for different geotechnical methods and soil properties divided into excavatability classes. Modified from Swedish Road Administration (1972).

Resistance to loosening soil:		Small	Normal	Large	Very large
Excavatability class:		1	2	3	4
Seismic velocity above GW	m/s	300	800	1300	1800
Seismic velocity below GW	m/s	1200	1600	2000	2400
Weight sounding	hv/0,2m	5	10	25	-
Ram sounding	bats/0,2m	10	20	40	60
Density in situ	t/m^3	1,8	2,0	2,2	2,4
Vane test	Mp/m^2	3	5	-	-
Cone test	Mp/m^2	3	5	-	-
Cobble content (Ø 6-20 cm)	%	10	15	30	40
Boulder content (Ø 20-60 cm)	%	1	6	10	20
Boulder content (Ø > 60 cm)	%	2	4	6	10
Geological determination of boulder content	-	1	2	3	4

In the report “Field tests regarding workability of different soils at road 805 Allån – Alanäs”, Swedish Road Administration (1977) results from field tests in a road project were presented. In the project the workability classification system proposed in Swedish Road Administration (1972) was used. The construction of the road comprised excavation and moving of 230 000

m^3 of soil. At the location of the project the soil consisted of a 1-3 meter stratum of moraine with few blocks and beneath that shale. In the beginning of the project a soil workability classification was performed. During the construction work the workability classification regarding resistance of soil loosening and bearing capacity during excavation was followed up. The results of the predicted and "measured" workability classification values seem to show on good agreement. Though, the classification system showed to be too extensive and complicated. According to the study the affect of water content in the soil do not considerably change the resistance of soil loosening. Not in comparison to other parameters.

2.2.5 Magnusson (1973)

In the report a classification of soil into excavatability classes is proposed, see Table 2.6. The classification is based on field experiments of horizontal excavation with a bulldozer in clay, sand and moraine soil. The results from the experiments are compared to theoretical calculations. In the classification scheme different soils are classified into one of five classes depending on the magnitude of the force on the blade at an excavation depth of 10 cm and when 3 m^3 of soil is accumulated in front of the blade. This means that the excavated length is different for different soils. In order to determine the excavatability of a soil mass common geotechnical surveying methods like weight sounding, ram sounding and seismic have been correlated to the experimental results and the classification scheme.

Table 2.6. Proposed classification of soil regarding excavatability, modified from Magnusson (1973).

Class	Resultant Force (kN)	Soil type
5	160-250	Clay moraine, very dense Moraine, silty-sandy dense
4	100-160	Clay moraine, dense Moraine, silty, medium dense
3	65-100	Sand, dense Clay, stiff Moraine, sandy-gravely, loose
2	40-65	Sand, medium dense Clay, medium stiff
1	0-40	Sand, loose Clay, soft

Excavation tests were performed with a bulldozer and the force on the blade was measured during 12 to 13 tests in each type of soil. It was noted that the excavation force, performing at a constant depth, increased during the excavation as the volume of the accumulated soil increased. When the blade could not hold more soil spillage occurred and the force reached a constant value. It was concluded that one part of the total force regards cutting soil loose and another part to push the accumulated soil in front of the blade. It was stated that the former force was related to the peak shear strength and the latter to the residual shear strength. As the blade moves pieces of soil will break up from the ground. This piece of soil is created as the

shear strength of the soil is reached and a failure zone is formed in the soil. The point of attack of the force on the blade moved upwards as the volume of the soil increased in front of the blade. When spillage occurred the point of attack dropped. This took place in a cyclic order. It was difficult for the operator to keep the blade in level during excavation as the soil accumulated, which could have affected the results.

Tests were carried out in uniform sand with a soil friction angle of about 40 degrees and a bulk density of about 1,75 t/ m^3, see Figure 2.4. The soil was homogenously accumulated in front of the blade and the total force reached a constant value for a critical length of excavation. At this point the volume of the soil spilling over and along the sides of the blade was approximately equal to the volume of the loosened soil. The density decreased 10% during excavation. As for the sand 12 excavation tests were performed in clay soil, see Figure 2.3. The clay was firm and over consolidated with an in situ shear strength of about 90 kPa, soil friction angle of 34 degrees and bulk density of about 1,95 t/ m^3. The firm clay soil was broken into pieces during excavation. The pieces rolled around in front of the blade. The density decreased 20 – 30% during excavation. Tests were performed in silty sandy gravely moraine with a normal content of boulders and a bulk density of 2,3 t/ m^3 in top soil and 1,9 t/ m^3 at 2 m depth, see Figure 2.2. In moraine the force required for loosen the soil was greater than the one to push the loosened soil in front of the blade. The content of cobbles and boulders decreased the ability of excavating in the moraine soil and peaks of the force were noted. The volume of the moraine soil accumulated in front of the blade was less, about 2/3 of the volumes for clay and sand. The density decreased 25% during excavation. For all soils it was concluded that the velocity had no affect on the force on the blade. Excavations were performed in velocities between 0,3 m/s and 0,9 m/s.

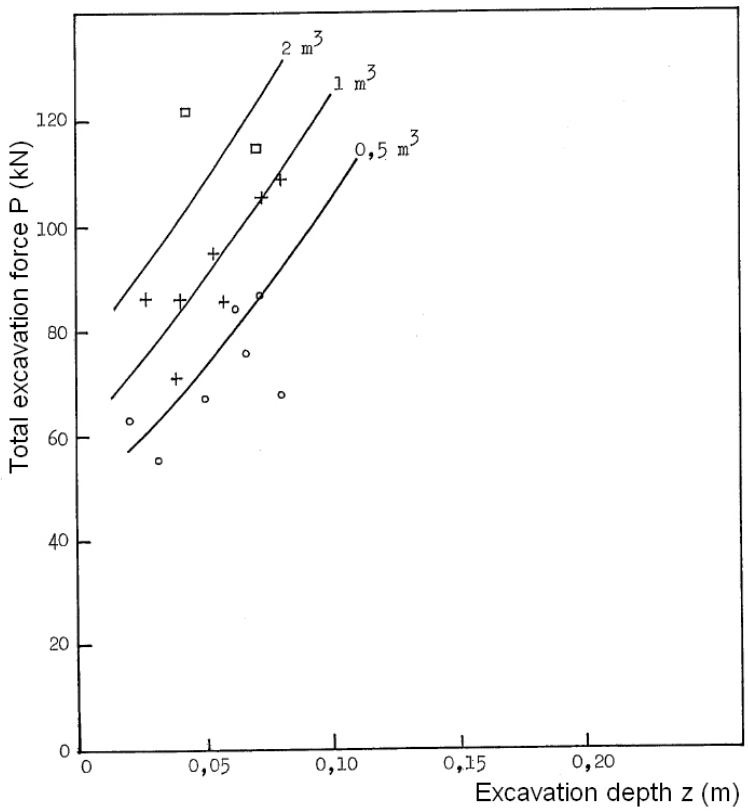

Figure 2.2. Results from excavation in moraine, modified from Magnusson (1973).

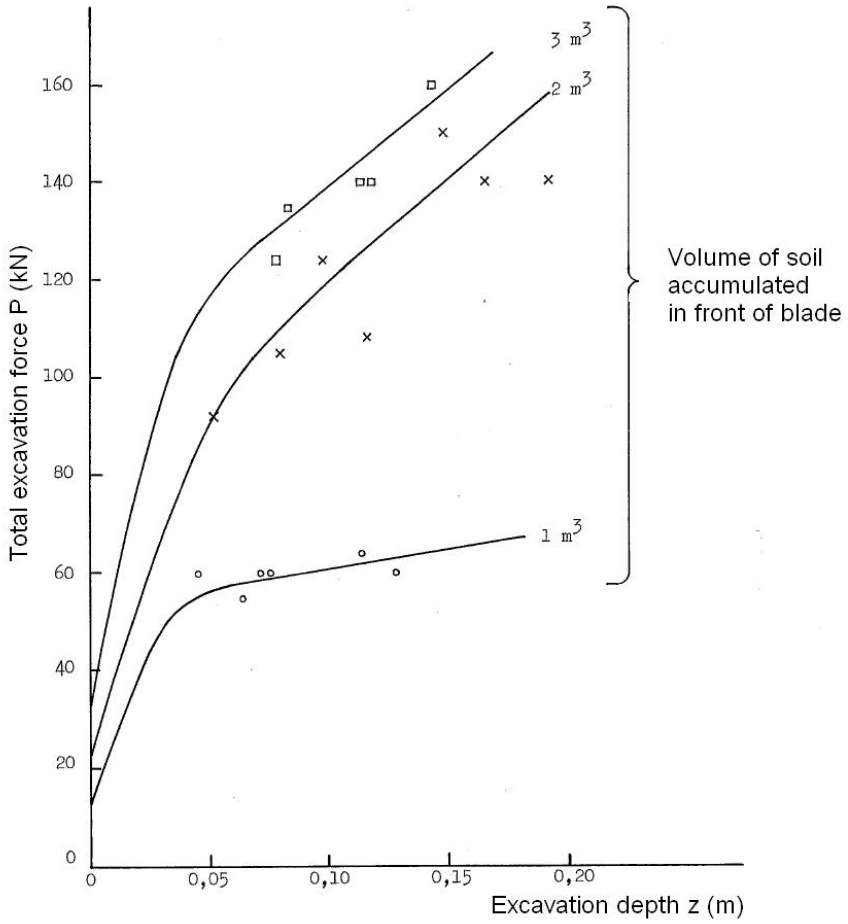

Figure 2.3. Results from excavation in clay, modified from Magnusson (1973).

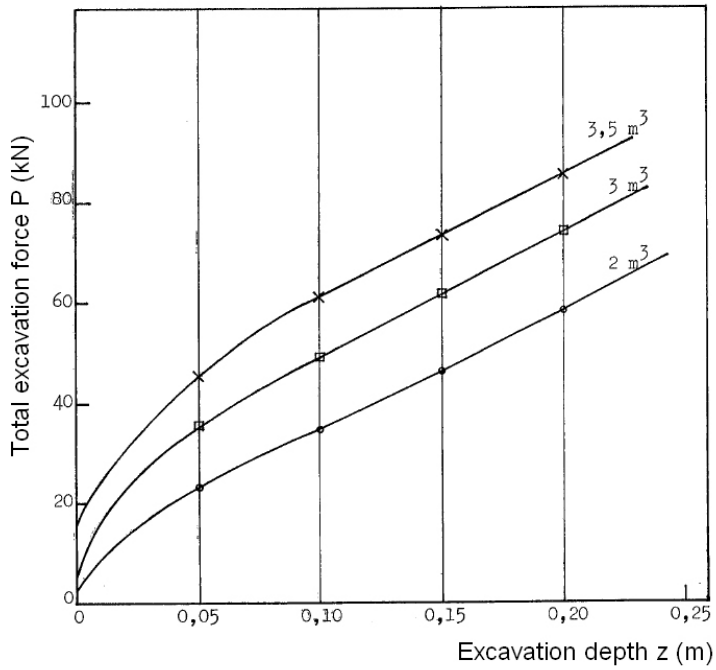

Figure 2.4. Results from excavation in sand, modified from Magnusson (1973).

In the theoretical calculations of the resistive forces in clay and sand a concept according to Hettiaratchi et al (1966) of different soil volumes in front of a bulldozer blade was used, see Figure 2.5. The total horizontal force was supposed to be composed of three different forces: the force required to break loose the soil from the ground, the force caused by the volume of soil that is superimposed the loosened soil and the force required to push the accumulated soil that is already loosened in front of the blade. The soil loosening force was calculated according to the equation of Reece (1964) that builds on passive earth pressure theory of Coulomb. For the moraine soil the resistive force or pressure acting on the edge of the blade was calculated according to the method of Prandtl. This method is used to calculate bearing capacity of foundations. In the method the stresses occurring in a zone with soil in plastic state (Prandtl zone) is considered, see Figure 2.6. Also the passive pressure from a Rankine zone was assumed to cause resistance to soil loosening. In the method the accumulated soil in front of the blade was considered to cause a superimposed pressure on the ground.

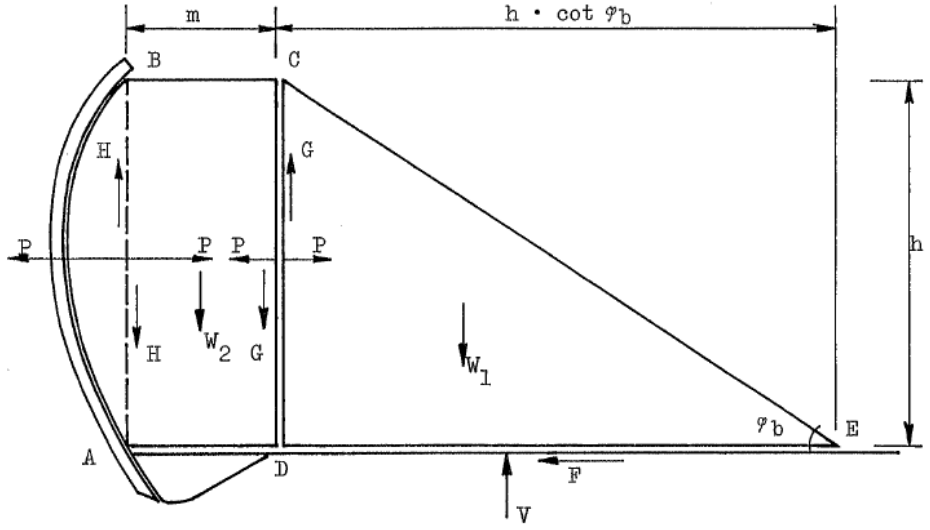

Figure 2.5. Different volumes of soil in front of a bulldozer blade, according to Hettiaratchi et al (1966).

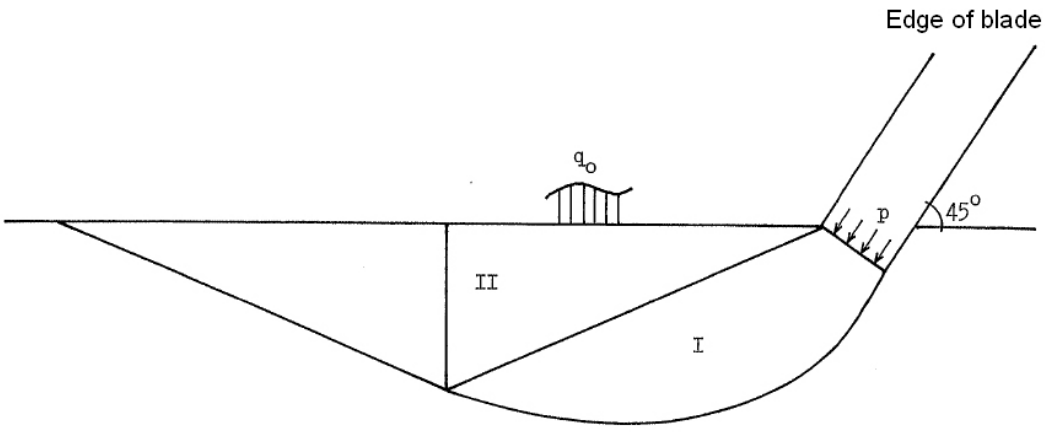

Figure 2.6. Rupture of soil according to the method of Prandtl with the Prandtl zone (I) and the passive zone (II), modified from Magnusson (1973).

The calculated force was about 14% greater than measured force in sand, see Figure 2.7. In clay the calculated and measured forces were about the same. The force caused by the volume of soil that is superimposed the loosened soil was considerably greater than the other two forces according to Reece (1964) method. In moraine soil the calculated force exceeded the measured force with about 5%.

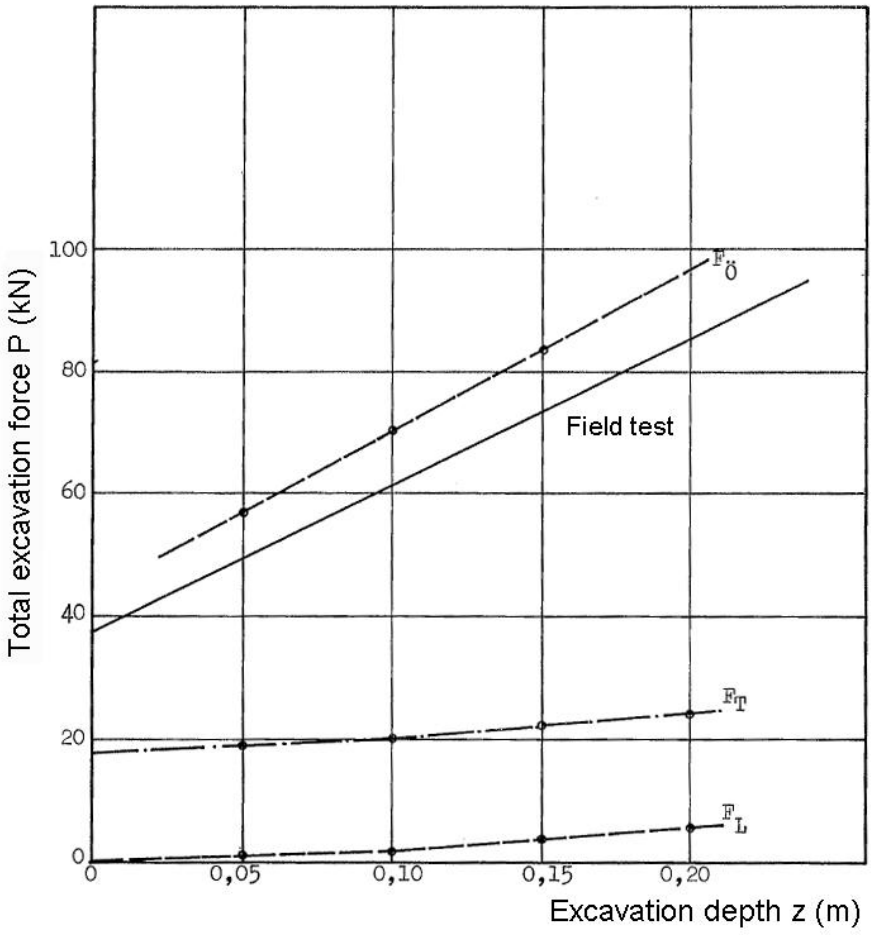

Figure 2.7. Calculated and measured forces on the blade for 3,5 m^3 of sand excavated, modified from Magnusson (1973).

In the report experiments to find out the soil-metal friction and adhesion was performed. For sand the soil-metal friction angle, δ was 27°, for clay δ was 36,5° and moraine δ was 36°. Also the movement of the soil in front of the blade was studied through small marbles placed in the soil. The soil seemed to move upwards along the blade and then forward, see Figure 2.8.

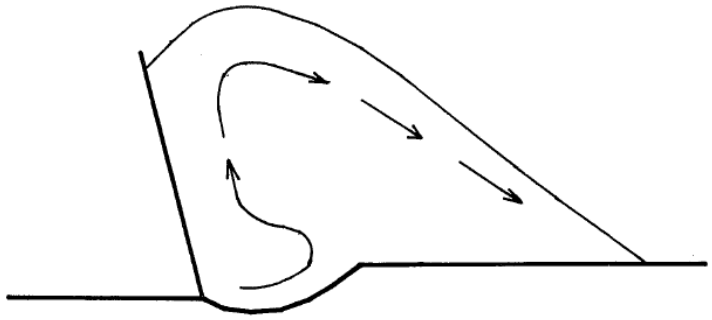

Figure 2.8. Movement of marbles in front of the blade, modified from Magnusson (1973).

2.2.6 Swedish Road Administration (1976)

Final results from internal development project of the Swedish Road Administration called "Definition of workability for different soils". In the end of 1960th and 1970th the Swedish Road Administration carried out different projects regarding earth moving and excavation work. This is the second and last report with results from Development project 2.7. This report aims at defining what soil parameters affect the capacity of earth moving. The workability is classified through classifying the excavatability of soil and the bearing capacity of soil. Here, the excavatability involves the parameters of the soil affecting the capacity during excavation and loading. Factors determining the excavatability are resistance to soil loosening and the extent of filling the bucket with soil. Bearing capacity refers the ability of the soil to carry machines.

In the report several factors affecting the capacity of machine performance are presented: properties of the material (soil), geometry of the excavation place, properties of the machine, properties of the machine driver (skills), and the organization of the work. Other factors affecting the capacity or effectiveness of earth moving are: the excavatability of soil, height of excavation work (bench height), rotation angle, time for waiting, and volume of transported soil. In the study results from excavation work is presented, see Figure 2.9. It is an example of how soil parameters, such as relative density and boulder size affect the capacity of an excavation machine with a 1,2 m^3 bucket. The relative affect is graded from 1 (low affect) to 3 (high affect).

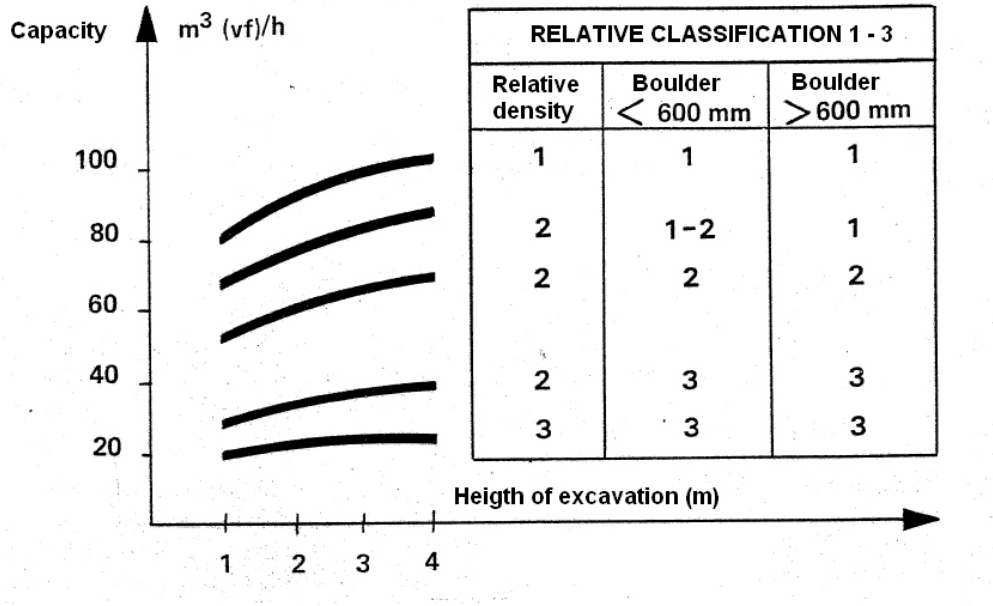

RELATIVE CLASSIFICATION 1 - 3		
Relative density	Boulder < 600 mm	Boulder > 600 mm
1	1	1
2	1-2	1
2	2	2
2	3	3
3	3	3

Figure 2.9. Capacity of excavator excavating in moraine with a 1,2 m^3 bucket, modified from Swedish Road Administration (1976).

According to the report the resistance of loosening the soil from the ground, see Figure 2.10, depends on soil parameters such as: relative density, particle size distribution, cohesion, cementation and if the soil is frozen (tjäle). The ability of filling the bucket with soil depends on soil parameters such as: relative density, particle size distribution, boulder size, friction angle, cohesion and water content. Other parameters are soil dilatancy, the volume change of excavated material, and soil adhesion to the bucket.

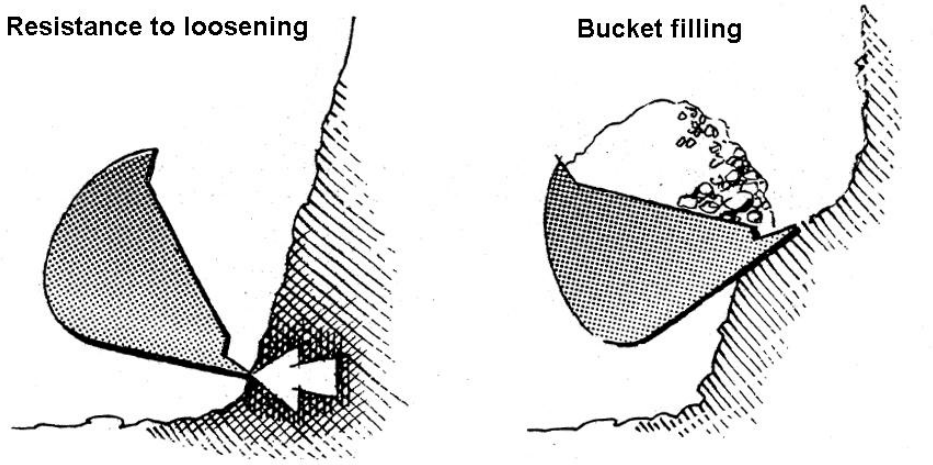

Figure 2.10. Schematic figures of the concepts of resistance of soil loosening respectively ability of filling the bucket, modified from Swedish Road Administration (1976).

Table 2.7. Soil classification due to excavatability, modified from Swedish Road Administration (1976). In the figure boulders have a diameter Ø > 0,2 m according to an older soil classification system.

Class	Material
1	Agricultural soil Loose sand Clay Dy (organic soil) Gyttja (organic soil)
2	Silt Sand Gravel Gravely sand Sandy gravel Clay (depending on w.c. and dry crust thickness)
3	Moraine with few boulders - Gravely moraine - Sandy moraine - Sandy - silty moraine Clay (depending on w.c. and dry crust thickness)
4	Moraine with normal to very few boulders - Normal moraine - Clayey moraine Moraines with normal to boulderly or with large boulders - Gravely moraine - Sandy moraine - Sandy - silty moraine Moraine clay Sandy gravel Clay (depending on w.c. and dry crust thickness)
5	Boulderly moraines or moraines with large boulders - Normal moraine - Clayey moraine

In the report the workability of the soil is classified through classification of excavatability and classification of bearing capacity. The classification systems are based on results from excavation studies during field tests. The classification of excavatability of the soil is based on cobble and boulder content and results from geotechnical sounding (rams sounding and weight sounding) and seismic velocity. The excavatability of the soil is rated in a scale from 1 to 5. “1” refers to low resistance of loosening the soil and good ability of filling the bucket. “5” refers to high resistance of loosening the soil and poor ability of filling the bucket. The classification scheme is based on the soil classification presented, see Table 2.7. The system for excavatability classification is divided into two parts: one for fine grained soils, see Table 2.8, and one for coarse grained soils, see Table 2.9. In the Swedish soil classification system valid during 1970th the particle size of cobbles was defined having a diameter between Ø 20-200 mm and boulders with Ø > 200 mm.

Table 2.8. Excavatability classification; coarse grained soils, modified from Swedish Road Administration (1976).

Class	Ram sounding (bats/20 cm)	Seismic velocity (m/s) Above GW	Below GW	Boulder content Ø > 200 mm (weight %)	Boulder content Ø > 600 mm (weight %)	Soil (example)
1	< 5	400	1400	0	0	Loose sand
2	10	500	1500	7	5	Silt, sand, gravel
3	50	700	1700	15	7	Gravel with cobbles, sand moraine
4	150	1000	2000	30	15	Esker with boulders, gravel moraine
5	0	1300	2400	40	20	Dense moraine boulderly, Loose rock

Table 2.9. Excavatability classification; fine grained soils, modified from Swedish Road Administration (1976). Stiff clay: 50 kPa < τ_{fu} < 100 kPa.

Class	Weight sounding (hv/20cm)	Ram sounding (bats/20cm)	Seismic velocity (m/s) Above GW	Below GW	Boulder content Ø > 200 mm (weight %)	Boulder content Ø 20-200 mm (weight %)	Soil (example)
1	< 5	< 5	-	-	0	0	Medium stiff clay (τ_{fu} < 50 kPa)
2	10	10	600	1400	5	15	Stiff clay, silt
3	>25	50	900	1600	7	30	Very stiff clay (τ_{fu} > 100 kPa), Sandy silty moraine
4		150	1200	1800	10	40	Clay moraine, Silt moraine
5		0	1500	2200	15	55	Dense clayey moraine, Dense rocklike sediment

2.2.7 Magnusson & Orre (1985)

The report is a review and combination of results from earlier studies regarding excavation, excavation performance in soil and earlier classification systems. The aim of the report is to present an excavatability classification system that is practical to use. The classification of excavatability is divided into five classes. The excavatbility system is mainly based on the studies from the Swedish Road Administration, the Finnish studies of Arihippainen et al (1966) and Korhonen et al (1972) and the study of Magnusson (1973). The incitement for creating a new system was partly because of the introduction of a new soil classification system. Therefore in this study the definition of a cobble is between 200–600 mm diameter and of a boulder above 600 mm diameter. The result of the study, which is the excavatability classification chart, is a consolidation of knowledge from the earlier studies. The results from

the earlier excavatability studies (Figure 2.12) are combined into a single chart (Figure 2.11). The field diagonally drawn across the chart represents the resistance to excavating from easy to very difficult excavated soil. In the study it is concluded that the resistance to excavating in soil depends on relative density, particle size density, cohesion, cementation and frozen soil. The ability of filling a bucket is dependent on relative density, soil particle distribution, boulder size, internal friction angle, cohesion, water content, adhesion, frozen soil and the geometrical outline of the excavated area. The excavatability of a soil is primary determined from the bulk density and the content of cobbles and boulders in the soil. Secondary, the values from the sounding resistance and seismic can be used. As guidance also the soil type examples can be used.

In the classification chart (Figure 2.11) the bulk density (1,6 – 2,25 t/m^3) and the “relative” loosening resistance (0 – 360 kN) are prompted along the vertical axis. The “relative” resistance is seen as guiding values and gives a hint of the magnitude of the resistance to loosening the soil. Along the horizontal axis values from ram sounding (HfA), point pressure sounding (Trs), weight sounding (Vim) and seismic velocity can be used. In the most right column example of soil types are displayed. In the lower right corner the classification of cobble or boulder content can be performed and then used with a soil type in the classification chart.

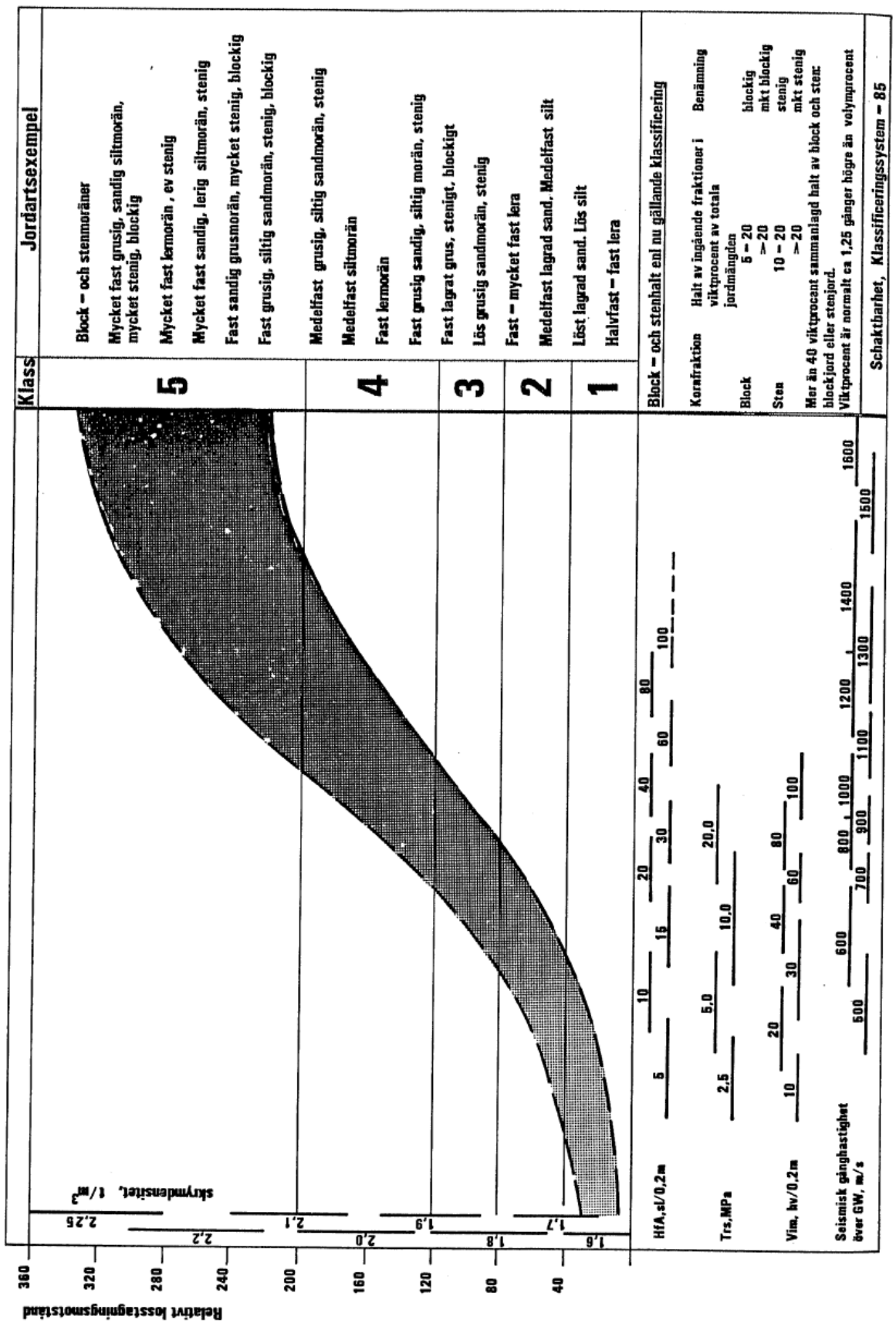

Figure 2.11. Excavatability classification chart (in Swedish), according to Magnusson and Orre (1985).

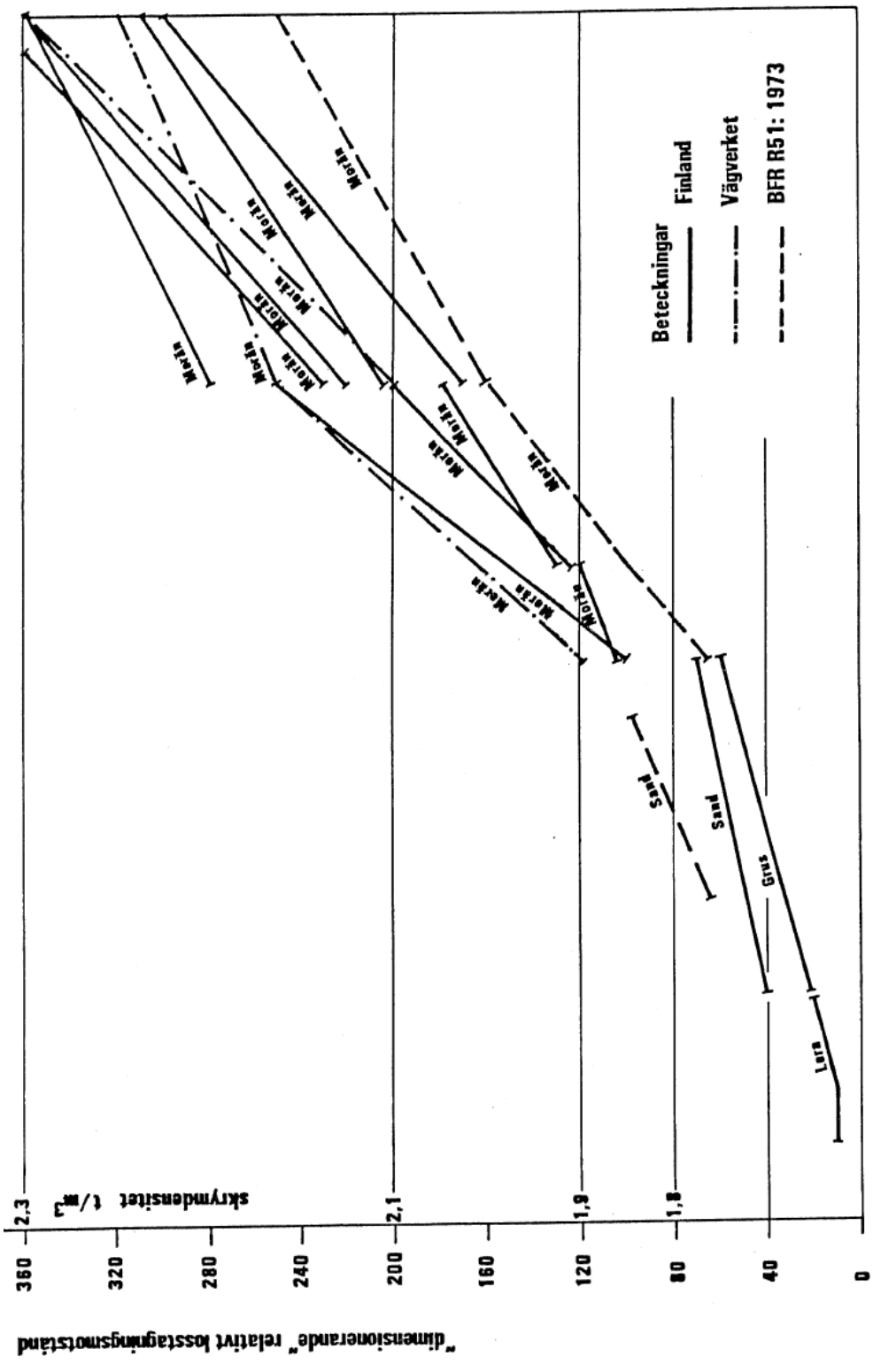

Fig. 2.2 Exempel på relativt losstagningsmotstånd i olika jordar

Figure 2.12. Results from earlier excavatability studies (in Swedish), according to Magnusson and Orre (1976).

2.2.8 Wilkinson (1997)

WWW-pages for road design education describing the process of earthwork and a diggability (excavatability) classification system used in United Kingdom.

In the study it is stated that when performing earthworks it is important to have knowledge about the material you are working with otherwise technical problems or cost overruns can occur. Through site investigation this can be known. According to Wilkinson (1997) there are many ways of classifying the soil in terms of its ease of excavation, including seismic techniques. According to the study, the most common excavatability classification system used in the United Kingdom, at present, is the Ease of Digging scale or diggability. This classifies the soil or rock material in one of four categories:

E Easy digging - Loose free running soils eg sands, fine gravels.
M Medium - Denser cohesive soils eg clayey gravel, low PI clays
M-H Medium to Hard - eg broken rock, wet heavy clay, gravel with boulders
H Hard - material requiring blasting and hard high PI clays

Soil and rock material will increase in volume when excavated. It is therefore necessary to use a bulking factor to determine the increased volume of the material during excavation. The bulking factor is defined as:

Bulking factor = volume after excavation/volume before excavation

Table 2.10. Classification of excavatability and typical values of the bulk density and the bulking factor for different materials, modified from Wilkinson (1997).

Material	**Bulk Density t/m^3**	**Bulking Factor**	**Diggability (excavatability)**
Clay (Low PI)	1.65	1.30	M
Clay (High PI)	2.10	1.40	M-H
Clay and Gravel	1.80	1.35	M-H
Sand	2.00	1.05	E
Sand & Gravel	1.95	1.15	E
Gravel	2.10	1.05	E
Chalk	1.85	1.50	E
Shales	2.35	1.50	M-H
Limestone	2.60	1.63	M-H
Sandstone (Porous)	2.50	1.60	M
Sandstone (cemented)	2.65	1.61	M-H
Basalt	2.95	1.64	H
Granite	2.41	1.72	H

2.2.9 Resource Management Technical Report 298 (2005)

The Department of Agriculture at State of Western Australia have collected and described qualities, characteristics and capabilities of land resources to be used when making decisions about management, development and conservation of land resources, see Table 2.11. One land quality considered is the ease of excavation of soil in building construction or earthworks. This is normally performed at 30-150 cm depth in soil, whereas cultivation is performed at 0-30 cm depth. The chart gives an indication of the range of ease of excavation as described by different parameters.

Table 2.11. Ease of excavation rating, modified from Department of Agriculture at State of Western Australia (2005).

Characteristic	Ease of excavation rating[1]			
	High (H)	Moderate (M)	Low (L)	Very low (VL)
Depth to rock (cm)	Very deep (> 150 cm)	Deep (80-150 cm)	Moderately shallow to Moderate (30-80 cm)	Very shallow to Shallow (<30 cm)
Slope (%) All soils except very deep sands	Flat to Moderate (<15%)	Moderate (15-30%)	Mixed (MX)	Steep (> 30%)
Very deep sands (>150 cm deep)	Flat to Gentle (<10%)		Moderate (10-15%)	Moderate to Steep (>15%) and Mixed (MX)
Stone within profile (% volume) (include cemented gravels)	Few to Common (<20%)	Many (20-50%)	Abundant (>50%)	-
Rock outcrop (% surface area)	None (<2%)	Slight (2-10%)	Rocky to Very rocky (10-50%)	Rockland (>50%)
Waterlogging risk	Nil to moderate	High	Very high	Very high
Surface condition and soil texture	All coarse sand to clay loams, Non-hardsetting clays	Hardsetting clay or heavy clay	-	-
Soil texture and arrangement within top 100 cm	All coarse sand to clay loams, Moderate to well structured clays, Shrink-swell clays	Poorly structured clay or heavy clay layer present within top 100 cm	-	-

[1] Rating determined by the most limiting characteristic.

2.3 The excavation process

During the construction phase in infrastructure and building projects the soil is excavated and transported to or from the construction area for different purposes. Especially roads and railways are often very long and cover big areas which means that in a project several thousands m^3 of soil have to be handled. Depending on the ability of excavating the soil different machines or combinations of machines are used together with different types of tools in excavation and earthmoving work. There are several combinations of machines, tools and

methods of excavating in soil material, but a more thorough review of this is not the aim of this study.

Usually the work task involves one machine, for example a bulldozer, or a set of machines such as an excavator and a dumper. Common machines for excavation and earth moving are excavators, wheel loaders, bulldozers and scrapers. Transporting soil is often carried out by dumpers or trucks.

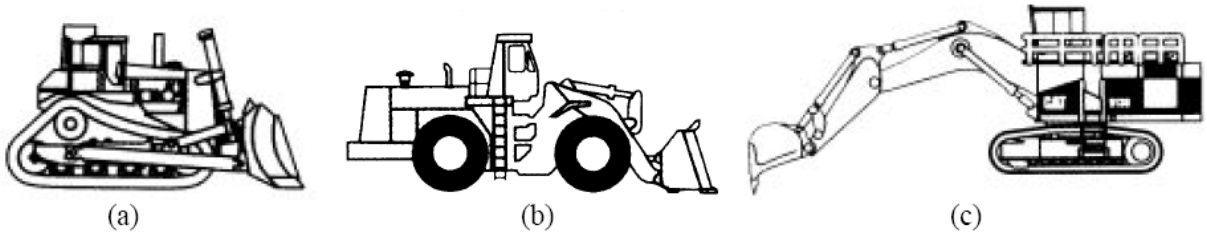

Figure 2.13. Three examples of machines for excavation and earthmoving: (a) bulldozer (b) wheel-loader (c) backhoe excavator, modified from Singh (1997).

For this study, three types of machine-and-tool sets for excavation and earthmoving work are distinguished: 1. A bulldozer or scraper with a wide blade, 2. A wheel or track loader with a wide bucket, 3. An excavator with a narrow bucket. For all of these sets the soil is excavated but with different tools and working methods. The bulldozer both looses the soil and pushes the loosened soil in front of the blade as it moves at a constant phase forward. With a wheel loader the wide bucket will penetrate and withdraw the loosened soil, in most cases, from a pile of soil. The wheel loader will load soil and unload the soil to a dumper in a repetitive way. An excavator will penetrate and loosen the soil with the bucket loading it on a dumper or just moving it. It will also be done in a repetitive manner.

For productivity not only loosening of soil with a bucket is important, also the degree of filling it is significant. The actual volume of a filled bucket can be higher than the struck volume or the rated volume because of soil heap. Depending on material the heap will differ.

Depending on what type of tool is used and how it is used different forces will act on the tool and the soil failure will look in a certain way. How the soil will deform and fail depends on the shape and size of the blade or bucket, angle of attack, soil-blade properties, soil properties, etcetera. The amount of force or energy that is needed to excavate the soil depends on the deformation and failure of the soil. When analyzing the soil failure or the forces acting on a blade or bucket a certain phase of the excavation process is studied. For each machine-and-tool set different phases in the excavation process can be defined and distinguished respectively. These have been described in some literature and the approaches of some authors are presented below.

The soil cutting with narrow blades has been studied by many researchers in the agricultural area. These blades and ploughs are mainly used for tillage; that is, cutting and loosening of soil in order to create a furrow for seeds. The soil cutting process of a narrow blade is similar to the one of a wide blade, see the chapter 2.4. In the construction industry narrow blade tools are not widely used since it does not allow for moving large volumes of soil. The process of soil cutting with narrow blades is not discussed more in this chapter.

2.3.1 Bulldozer with a wide blade

The work cycle of a bulldozer with a wide blade consist of a short penetration phase followed by a continuous cutting-and-moving phase. The cutting-and-moving phase occurs for a certain length, moving the material from its original place, and is mostly performed at constant depth and speed. Since the penetration phase for a bulldozer blade is short in relation to the cutting-and-moving phase the penetration of the material has not been considered by all of the authors below.

In a mechanical analysis Hettiaratchi et al. (1966) defined the volumes in front of a bulldozer blade with three parts, see Figure 2.14. They are the volume of cut soil, the soil accumulated in front of the blade causing an overburden on the cut soil and the part of the accumulated soil displaced forward (triangular wedge). The equation of Reece (1964) was used to calculate the soil cutting force and the weight of the soil volumes in front of the blade affected the horizontal force.

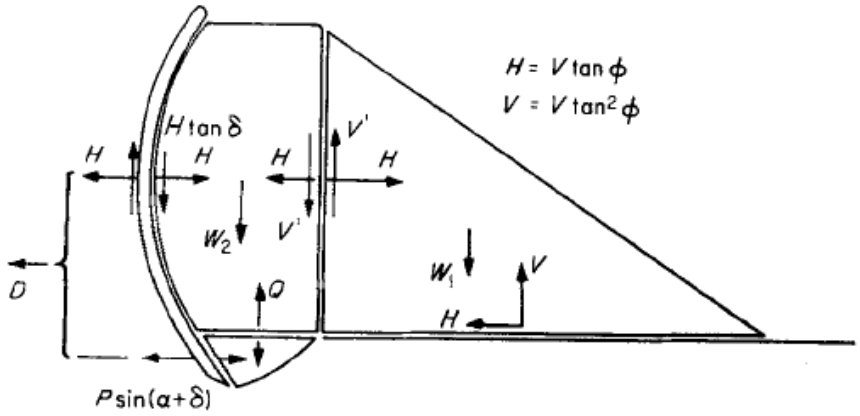

Figure 2.14. Simplified failure pattern in front of bulldozer blade according to Hettiaratchi et al. (1966).

Through observing and analyzing experiments Qinsen & Shuren (1994) stated that the excavation process of wide blades can be divided into two parts: the earthmoving process on the ground and the soil cutting process under the ground. Qinsen & Shuren observed that the cut soil, volume abdgf, slide up along the blade surface and then fall down in front of the blade. The accumulated soil, volume fgde, was displaced forward during blade movement, see Figure 2.15.

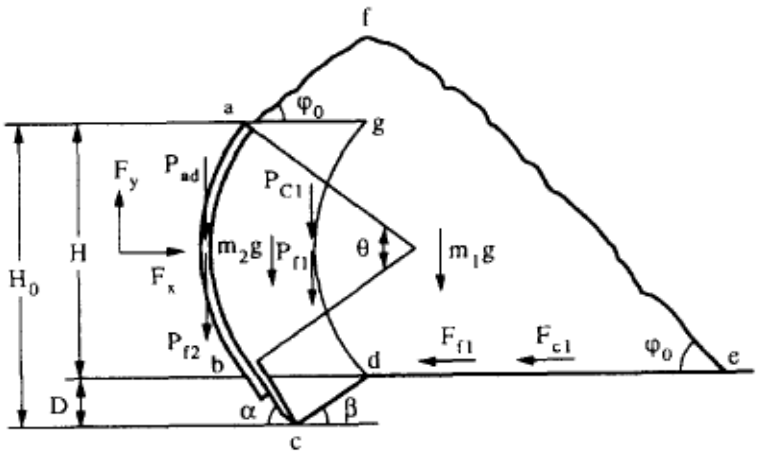

Figure 2.15. The forces acting on the soil in front of the blade, according to Qinsen & Shuren (1994). The earthmoving process concerns the soil within the area of abdef. The soil cutting process concerns the soil within the area of bcd.

In a three dimensional soil cutting model proposed by Xia (2008) the block of soil continuously cut and the soil pile accumulating in front of the blade was described, see Figure 2.16. Even tilted blade operations and complex terrain conditions are considered in the model. Forces acting on the blade were defined even considering dynamic forces due to acceleration of the soil.

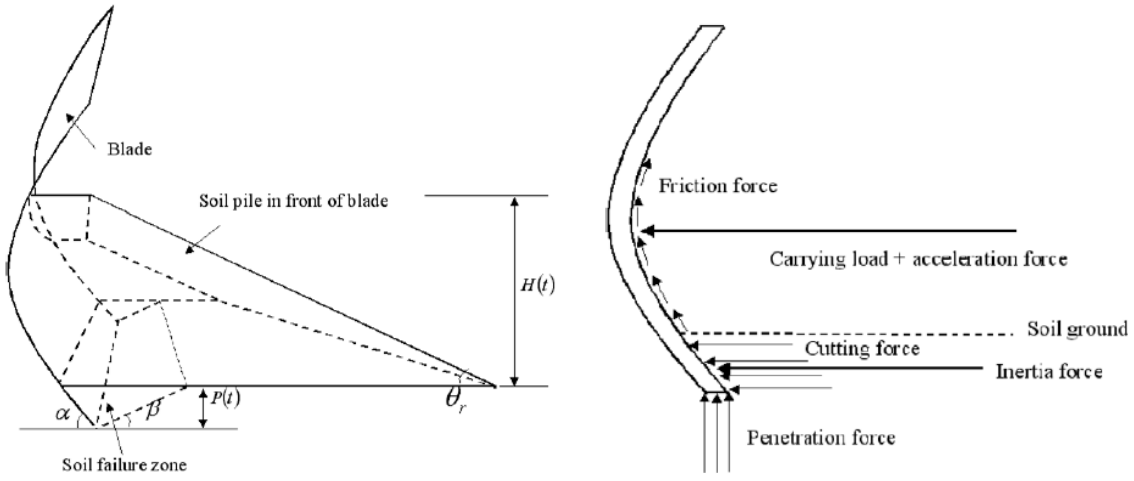

(a) (b)

Figure 2.16. (a) Schematic description of soil pile and soil cutting block in front of a wide blade, (b) forces acting on the blade, according to Xia (2008).

2.3.2 Loader with a wide bucket

The wheel loader work cycle consists of loading and filling the bucket with soil, reversing and travelling to the receiver, unloading, reversing and returning to loading position, Volvo GPPE performance manual (2009). See Figure 2.17. In the excavatability point of view the bucket filling process is of interest and described by some authors below.

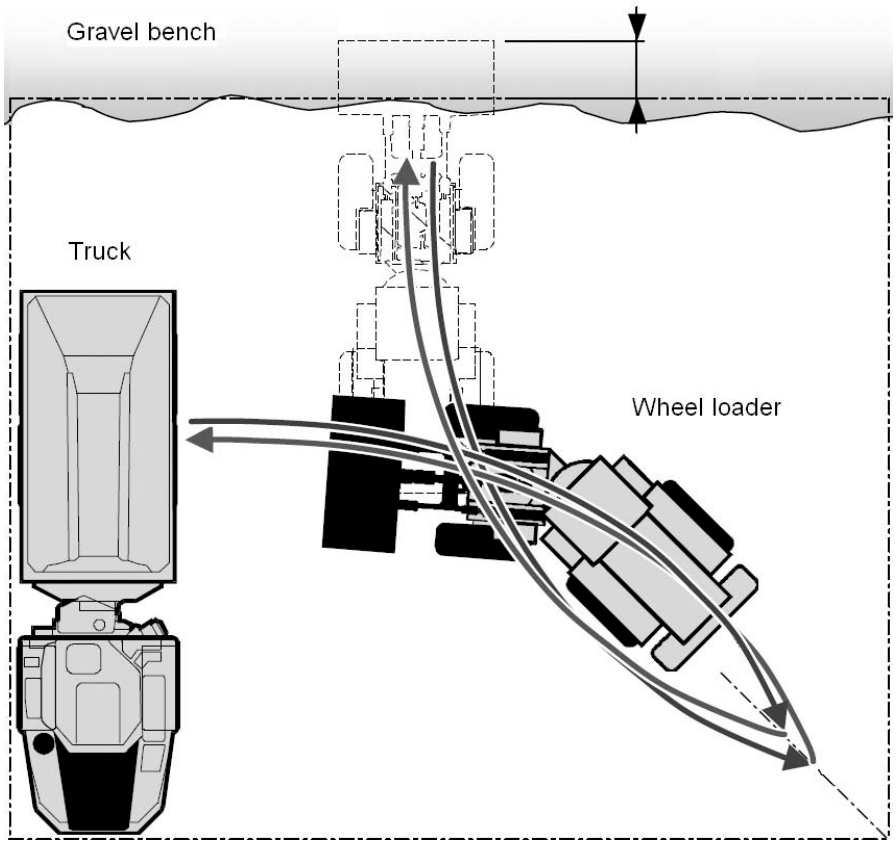

Figure 2.17. Plan view of the work cycle of a wheel loader loading a dumper, modified from Filla (2005).

The bucket filling process of a wheel loader has been described by Filla et al. (2005). A common bucket filling process, also used by Ericsson & Slättengren (2000), includes forcing the bucket into the soil pile, tilting and lifting the bucket to loosen (cutting) the soil and withdraw the filled bucket from the pile. In the filling process proposed by Filla et al. (2005) the bucket is also forced horizontally into the soil pile. In the next phase the bucket will cut the soil following a path parallel to the soil pile slope, since this is assumed to be an efficient way of filling the bucket, see Figure 2.18. The bucket is moved on a velocity vector with bearing of the soil pile slope angle, ε. The filling ends as the wheel loader reverse and the bucket is lifted.

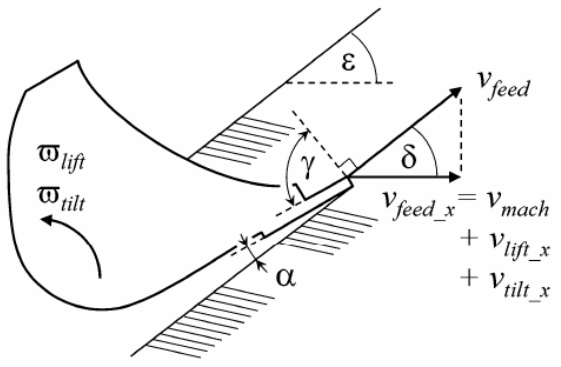

Figure 2.18. Bucket filling approach according to Filla et al. (2005).

Filla (2005) have reviewed a study of automatic control of rock or soil loading with a wheel loader by Wu (2003). According to Filla (2005), Wu (2003) proposes that the loading cycle consist of the attacking, crowding and scooping phases, see Figure 2.19. Due to different material properties both the crowding and the scooping procedure can be varied through different strategies. With “hard-scooped” material small oscillations are implemented in the bucket tilt angle. With “easy-scooped” material the bucket is tilted back faster than with “normal-scooped” material.

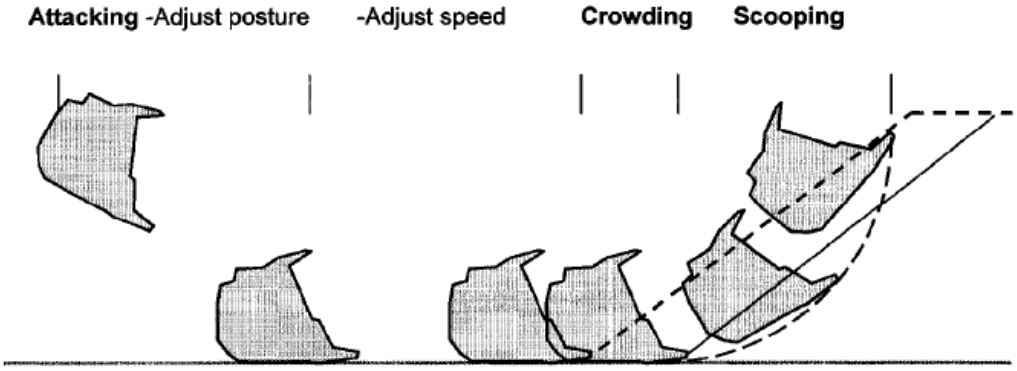

Figure 2.19. Operations of excavation task, according to Wu (2003), modified from Filla (2005).

Also Hemami (2008) have studied the loading and excavation process concluding that the main objective is to fill the bucket, with minimum energy required. Hemami proposes that automatic loading can be performed through the definition of a trajectory and the motion control to lead the tool through the defined trajectory. Controlling the motion of the bucket is important in cases when, for example, obstacles are encountered in the media excavated, see Figure 2.20.

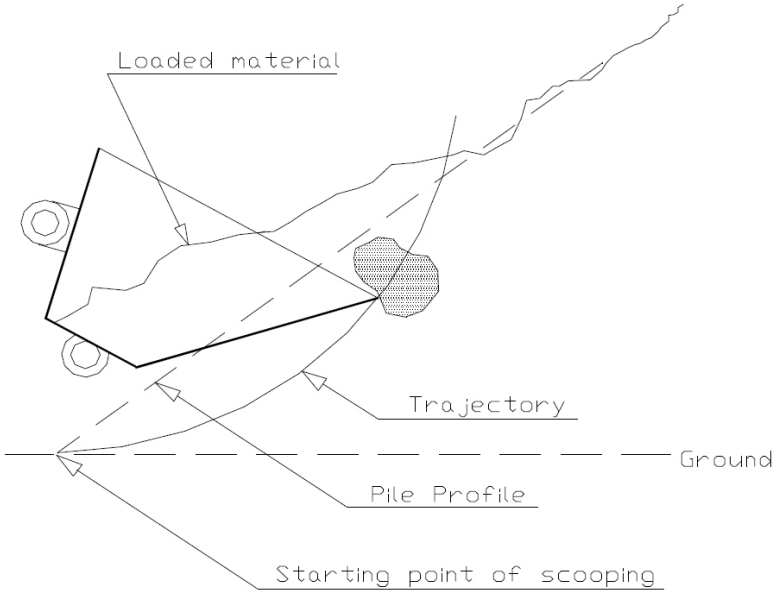

Figure 2.20. Loading of bucket according to Hemami (2008).

2.3.3 Excavator with a narrow bucket

The excavator work cycle consists of penetrating the soil, filling and lifting the bucket, slewing to the desired location, dumping the material and returning to the digging position, Volvo GPPE performance manual (2009). The machine stays in one position as long as there is material to excavate. In the excavatability point of view the penetration and cutting of soil and filling the bucket is of interest and has been approached by some authors below.

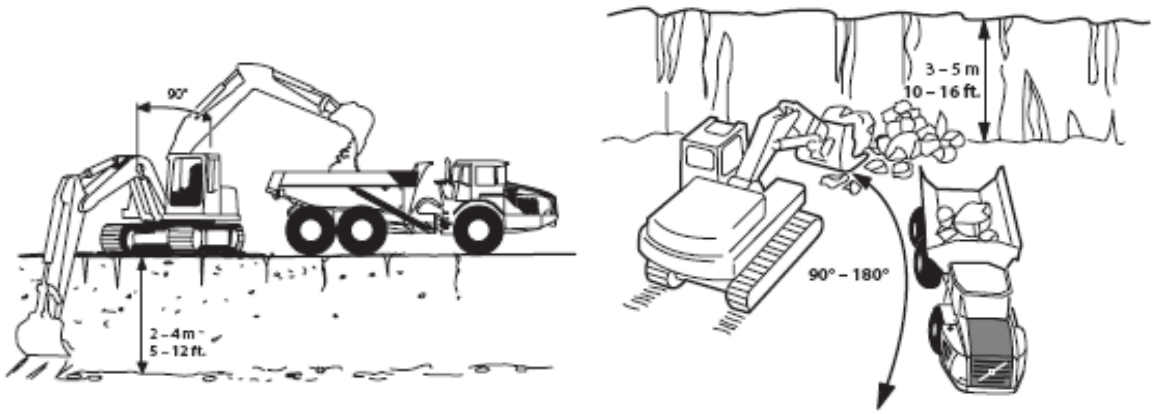

Figure 2.21. Excavating and loading with excavator, from Volvo GPPE performance manual (2009).

Broms (1966) stated that excavation with an excavator concerned the actions of penetration and movement of the soil. Blouin et al. (2001) defined three different earthmoving actions with an excavator bucket: penetration, cutting and loading (scooping of material).

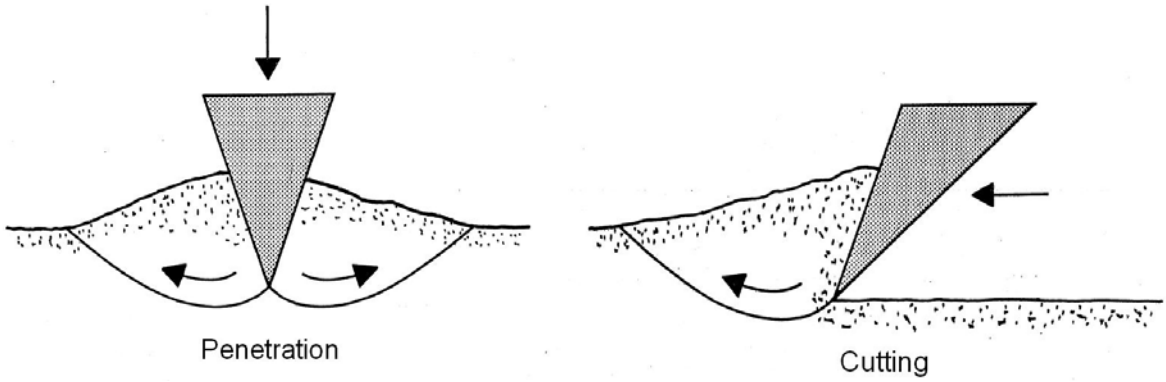

Figure 2.22. Penetration respectively cutting (movement) of the soil mass, modified from Broms (1966).

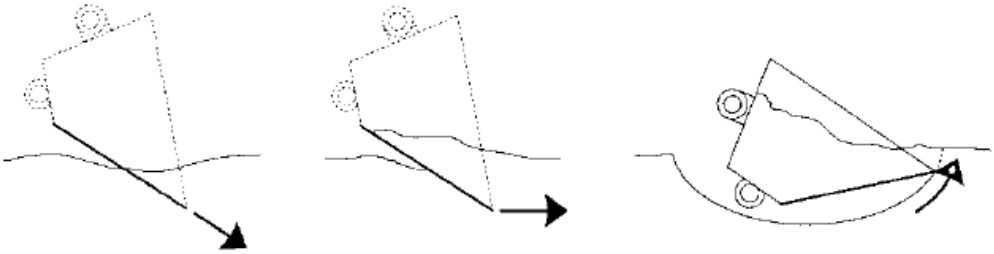

a) penetration b) cutting c) loading (excavation)

Figure 2.23. Earthmoving actions modified from Blouin et al. (2001).

Singh (1997) discusses that excavation work is most influenced by soil properties and that soil behaviour is a very complex phenomena. He divides the soil-tool interaction during excavation into two problem areas. The first concern what happens when a bucket sweep along a trajectory in the soil: forces involved, soil movement and bucket filling. He states that no model exist that can explain this problem fully, since soil is such a complex material. The second problem concerns the effect of the soil on the tool, that is, the resistive forces acting on the tool as it moves through the soil. Singh (1997) reports on different ways of approaching the latter problem in the literature. Some researches have tried to estimate the cutting resistance based on empirical results. Others have developed models to predict resistive forces on agricultural tools, based on first principle mechanics including parameters such as internal soil friction, soil-tool friction and tool properties.

Cannon (1999) have studied systems for automated truck loading with a hydraulic excavator. It is assumed that the excavator is placed on the top of a bench, removing material from the bench. The automated excavation operation was modelled as four basic stages, see Figure 2.24. First, the boom is lowered until contact is made with the ground. Second, in the pre-dig stage the bucket penetrates the ground and the bucket rotates to a dig position. In the dig stage, the material is pushed into the bucket. In the last stage the bucket is rotated to capture the material and lift it from the ground. These stages are based on observations of expert human operators. The forces in the ground applied by the bucket during digging follows a soil hardness index which is provided externally.

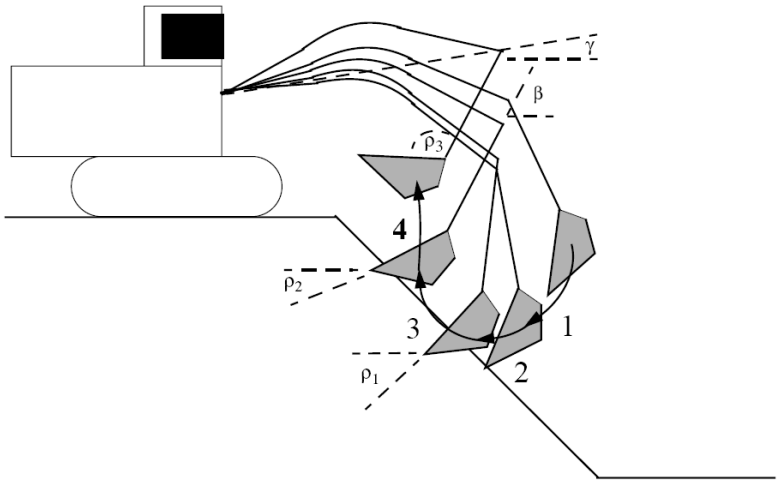

Figure 2.24. Basic excavation stages, modified from Cannon (1999).

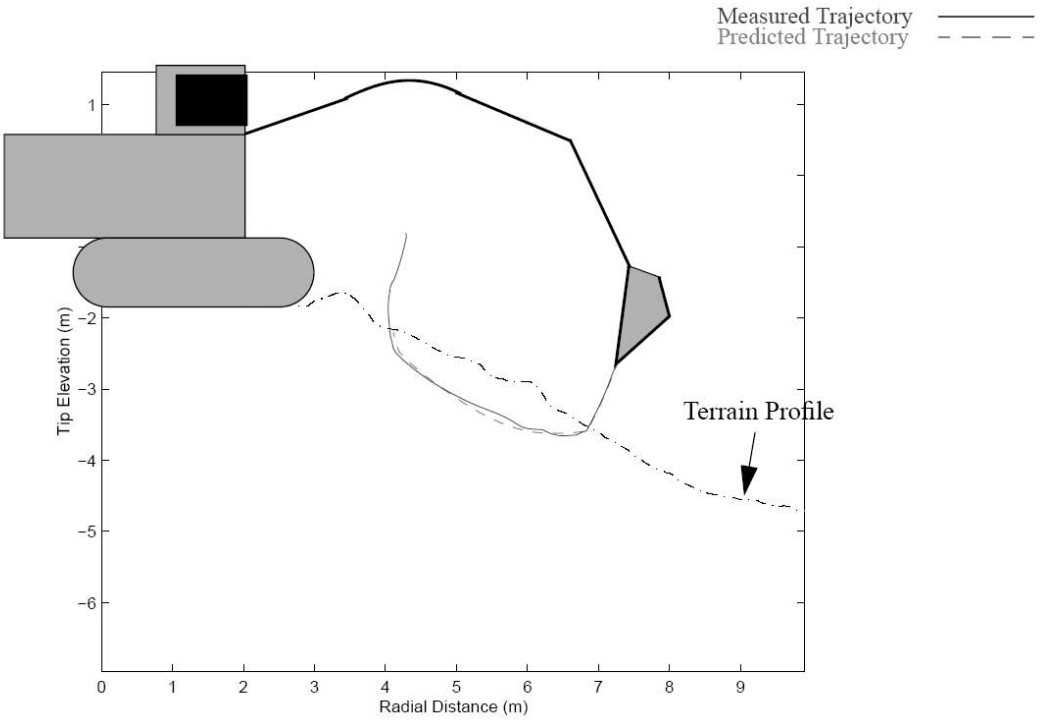

Figure 2.25. Bucket tip trajectory, modified from Cannon (1999).

In their work with an automated robotic excavator, Bradley and Seward (1998) have studied how skilled excavator operators perform excavation work. Two basic strategies were identified: penetrate and rotate or penetrate and drag. See Figure 2.26. The strategy of penetrating and rotating was used in soft ground, like sand, which easily could be penetrated by the bucket. After the bucket was forced into the soil vertically, to a certain depth, it was rotated and filled in the same time. The strategy of penetrating and dragging was used in harder ground. After the operator first had penetrated the ground he then adjusted the angle of attack of the bucket to "plane off" material as the bucket was dragged back towards the body of the excavator. The observations showed that altering the angle of attack of the bucket and the direction which the bucket was dragged was tactical variations used by the operators. These operations are influenced by the bucket geometry.

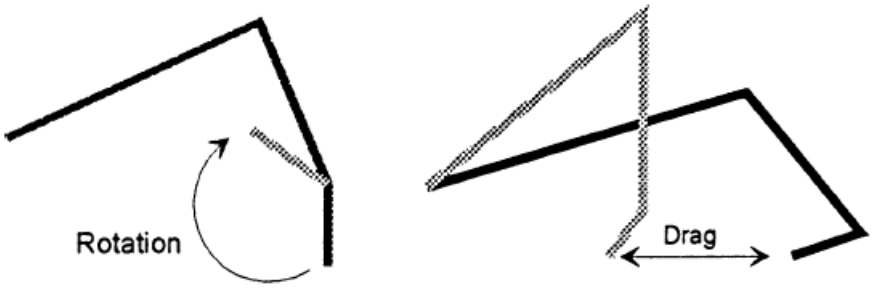

a) Use of rotation to fill bucket b) Bucket filled by dragging

Figure 2.26. Strategies of excavating in soil by skilled operators, according to Bradley and Seward (1998).

Haga et al. (2001) proposed a method for controlling level excavation with an automated excavator. The front attachment of an excavator consists of boom, arm and bucket. Each of these parts is actuated by individual cylinders, allowing for movement in circular arcs. In level excavation the boom tip height must be controlled so that the bucket tooth tips can move horizontally. Haga et al. (2001) described the hydraulic excavator work cycle for general excavation of ditches with four stages, see Figure 2.27.

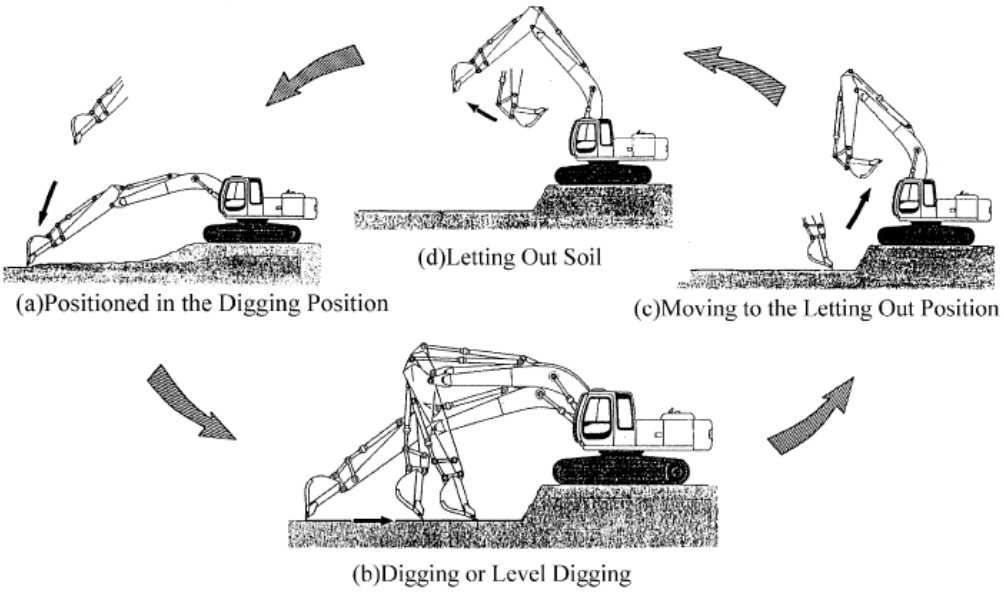

Figure 2.27. Excavator work cycle at level excavation, according to Haga et al. (2001).

2.4 Studies related to excavating and moving soil

This chapter consists of reviews of studies on narrow blades (tines), wide blades, narrow buckets and wide buckets. In these reviews different aspects of cutting, excavating and moving soil is studied. Such as: the type, shape and extent of failure of soil in front of a tool, the prediction of horizontal (draft) and vertical forces on a tool and the effect of different parameters on these forces, such as tool depth, tool width, rake angle (blade angle), tool speed, shear strength of soil and soil-tool friction and adhesion. Some of these reviews are reviews or state of the arts themselves. Most of the reviews present models for predicting forces on a blade or a bucket. Several studies of blades have been performed in the agricultural area and many studies regarding buckets have been carried out in research about automated excavation. Even though narrow blades are not widely used in the construction area the research about narrow blades can potentially be used in the analyses of excavation and moving soil. The models to predict forces on narrow blades do often use passive earth pressure theory as basis, but with specific failure zones in the soil assumed. In several of these models the failure zone have a three dimensional shape.

In the literature, it is generally assumed that narrow blades give rise to three dimensional failure problems, whereas for wide blades, the side effects can be neglected and assumed to involve two dimensional failures problems. In several studies concerning narrow buckets, a two dimensional failure problem is assumed, and models developed for blades are used for prediction of forces. According to McKeys (1985) the side-walls of an excavator bucket constrain the failure in the soil to a volume directly ahead of the bucket thus causing a two dimensional soil failure. Studies of wide buckets are often performed in a two dimensional analysis, according to the literature.

2.4.1 Narrow blades

In this chapter laboratory experiments performed by Selig & Nelson (1964) studying the soil failure caused by a narrow blade is presented. Also force prediction models by Hettiaratchi & Reece (1967), McKeys & Ali (1977), Godwin & Spoor (1977), Stafford & Tanner (1983) and Swick & Perumpral (1988) are shown. In reviews by Hettiaratchi (1965), Hettiaratchi (1988), Zein Eldin & Al-Janobi (1995) and Godwin (2006) soil failure shapes, prediction of forces on earthmoving tools and the affects from different parameters on the forces on a tool was discussed.

2.4.1.1 Selig & Nelson (1964)

Selig and Nelson (1964) made observations of soil cutting with narrow blades with a two-dimensional glass box apparatus to study the failure phenomena, see Figure 2.28. Three types of soil were used: a medium-dense, dry Ottawa sand, a silty clay, and a plastic clay. Four different situations were studied: a vertical blade in all soils, a blade inclined 45 degrees to the rear in silty clay and plastic clay, an L-shaped blade with horizontal cutting edge in all soils, and a blade inclined 20 degrees forward in sand. See Figure 2.29. The soil deformation and mode of failure were studied and photographed. Narrow blades was used; about 0,1 m wide working at a depth of about 0,165 m.

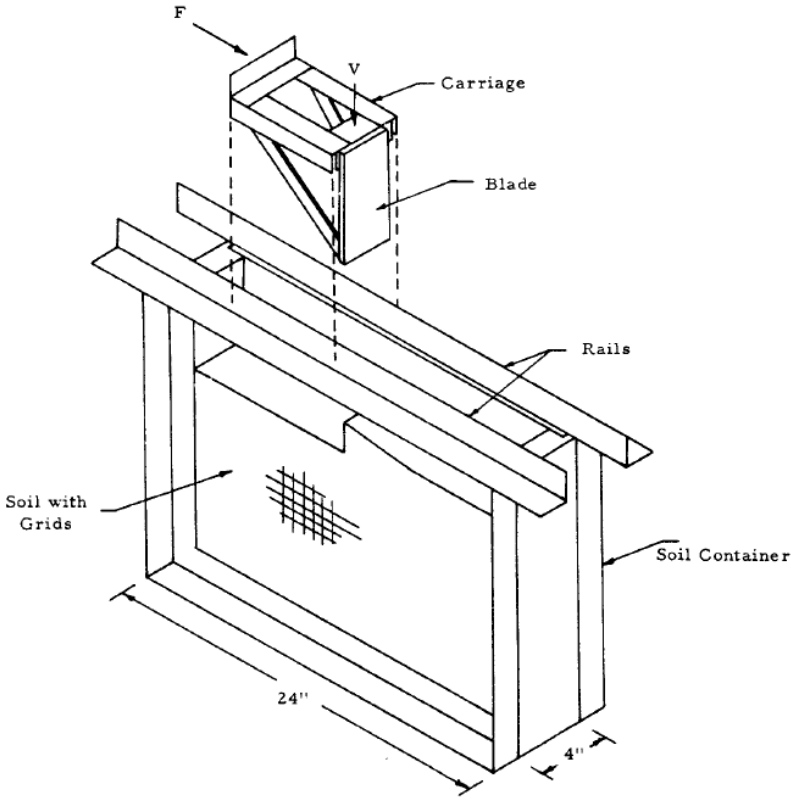

Figure 2.28. Glass box apparatus with blade fixture, Selig and Nelson (1964).

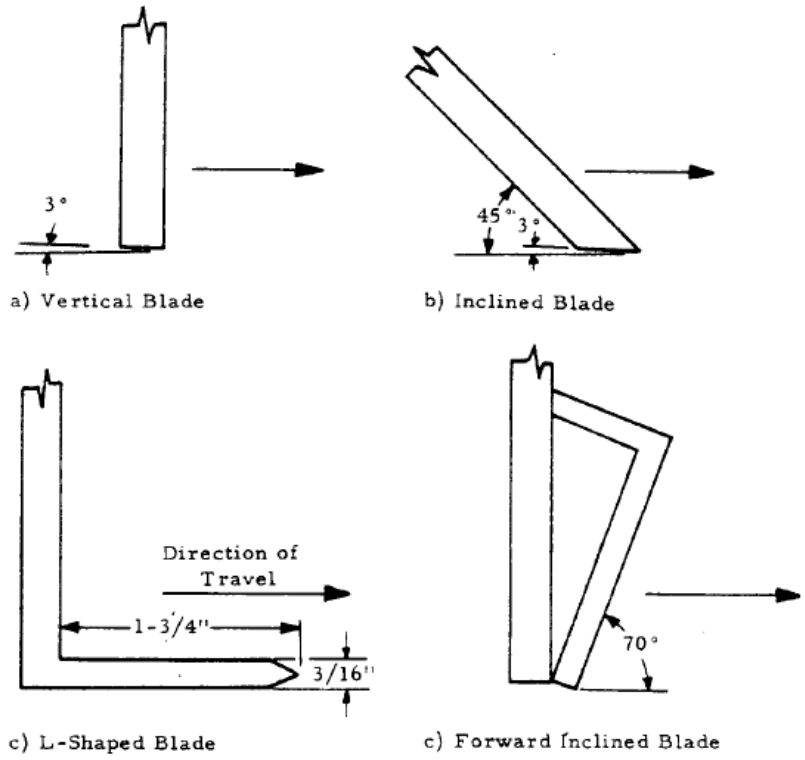

Figure 2.29. Geometry of blades used in experiments, Selig and Nelson (1964).

According to Selig & Nelson the results indicates that there are two principal mechanisms of failure occurring: passive shear failure and tensile failure or splitting. Depending on the

application of the blade, one of them predominates. The first mechanism involves that the forward motion of the blade is prevented by passive resistance of the soil. When the force of the blade is sufficiently great to overcome this passive resistance, shear failure occurs along a specific surface of the soil. As the blade continuous to move, after a certain displacement a new surface becomes critical and the next failure occurs there. The soil is removed through this discontinuous manner of series of failures and displacements. The geometry of the failure surfaces observed generally agreed to those assumed by earth pressure theories. Though, in the observations the size of the failure region decreases as the overburden build up in front of the blade, which differs from the earth pressure theory. Similarly the inclination of the failure surface decreases. In sand the angle between the failure surface and the soil surface were greater than the theoretical angle of 45 – ø/2 degrees in the beginning of the test, but were less after large blade movement. In cohesive soil the angle of intersection was always less than the theoretical angle.

The second mechanism occurs if the surface of the blade is parallel to or at small angle to the direction of motion of the blade. This could, according to Selig and Nelson, occur to blades at angles 45 degrees and steeper, when the adhesion or friction between the soil and blade is not great enough to develop passive pressure.

The tests showed that the failure pattern in sand generally occurred through passive shear failure, see Figure 2.30. The soil particles adjacent to the blade remained in place during test and the slippage occurred in the soil around. In silty clay and plastic clay, passive shear failure occurred for the vertical blade, and a tensile failure or splitting, due to uplift, for the inclined blade, see Figure 2.31. The L-shaped blade initiated a tensile crack and when the vertical part of the blade come into contact with the soil a shear failure occurred through the rupture zone.

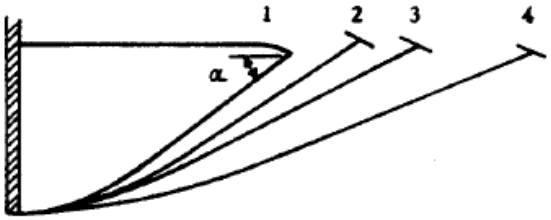

Failure No.	d, "	α, °
1	3/8	34
	5/8	36
2	2	30
	2-1/2	33
3	5	28
4	6-3/4	22
	7-1/2	21

Figure 2.30. Comparison of failure surfaces for a vertical blade in medium-dense sand, Selig and Nelson (1964).

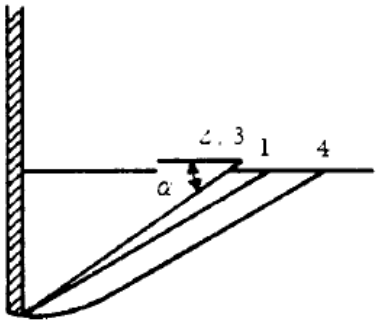

Failure No.	d, "	α, °
1	5/8	31
2	3-5/8	35
3		35
4	6-7/8	30

Figure 2.31. Comparison of failure surfaces for a vertical blade in plastic clay, Selig and Nelson (1964).

2.4.1.2 Hettiaratchi (1965)

The paper reviews research in the area of earthworking tools and cutting blades. Hettiaratchi reported on analytical work of Payne (1956) on narrow blades (tines). Payne performed a detailed analysis of the mode of failure of soil. According to Hettiaratchi (1965), Payne (1956) concluded that the failure plane followed Ohde's (1938) logarithmic spiral and that a vertical wedge of soil was formed in front of the blade. According to Hettiaratchi (1965), Payne (1956) he classifies narrow blades those having a depth/width ratio greater than unity and blades as those having a depth/width ratio less than 0,5.

Hettiaratchi (1965) also reported on experimental work carried out by O'Callaghan and Farrelly (1964) on narrow tines, see Figure 2.32. They presented an equation for the draught of narrow vertical tines. They assumed that the transition from vertical to horizontal plane of deformation of the soil occurs at a depth of 0.6 of the width of the vertical tine. The assumed failure mechanism is shown in Figure 2.49 in Chapter 2.4.1.8. According to Hettiaratchi (1965), O'Callaghan and Farrelly (1964) have proposed that the draught force, D (horizontal force) can be predicted as follows:

$$D = c(d\text{-}kw)N_c + 0{,}5\gamma(kw)^2K_\gamma + c(kw)K_c \qquad (2\text{-}1)$$

Where d is working depth, w is tool width, N_c is the Prandtl bearing capacity factor for a vertical blade and K_γ and K_c are passive earth pressure coefficients. The shape factor k can be set to 0,6, according to O'Callaghan and Farrelly.

$$N_c = \cot(\varphi)\tan^2(\pi/4 + \varphi/2)\, e^{\pi\tan(\varphi)} - 1) \qquad (2\text{-}2)$$

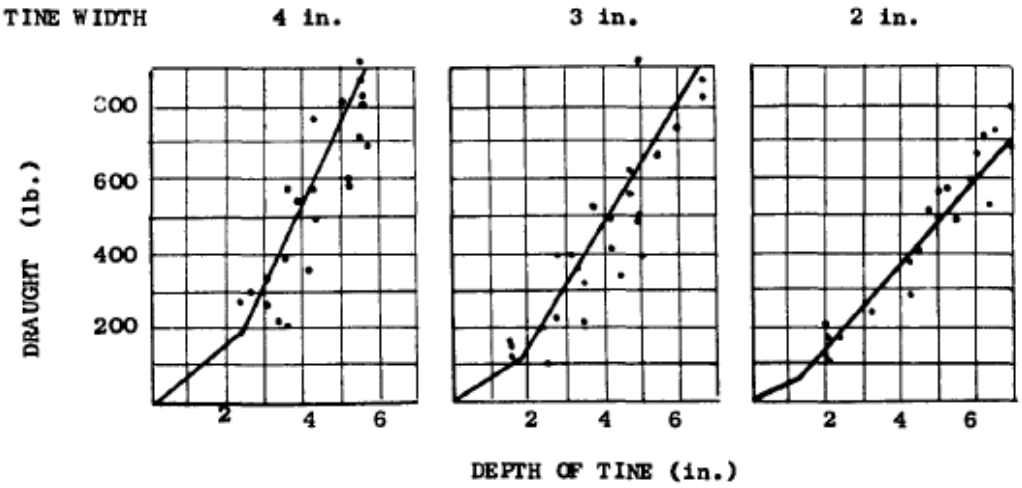

Figure 2.32. Results from O'Callaghan and Farrelly (1964) on narrow tines, according to Hettiaratchi (1965).

2.4.1.3 Hettiaratchi & Reece (1967)

Hettiaratchi and Reece (1967) performed an extensive analysis on three dimensional soil failures of narrow blades. They assumed that the soil failure surface consisted of vertical and horizontal failure surfaces, see Figure 2.34. A model in form of a set of equations to calculate the forces on the blade was presented. Experiments with a 2 inch wide rigid steel tine in a soil

bin were performed and the draught force vs the aspect ratio (depth, z / blade width, b) was plotted. The theory over predicts the forces for the smaller values of aspect ratio.

The forward failure, P_f, the sideways failure, P_s, draught, D and lift forces, L can be calculated as follows:

$$P_f = \gamma z^2 b N_\gamma + czbN_c + c_a zbN_a + qzbN_q \quad (2\text{-}3)$$

$$P_s = [\gamma\,(d + q/\gamma)^2\, wN_{s\gamma} + cwdN_{sc}\,]\,K_a \quad (2\text{-}4)$$

$$D = P_f \sin(\alpha + \delta) + P_s \sin(\alpha) + c_a z \cot(\alpha) \quad (2\text{-}5)$$

$$L = P_f \cos(\alpha + \delta) + P_s \cos(\alpha) + c_a z \quad (2\text{-}6)$$

The N – factors can be found in Hettiaratchi and Reece (1967).

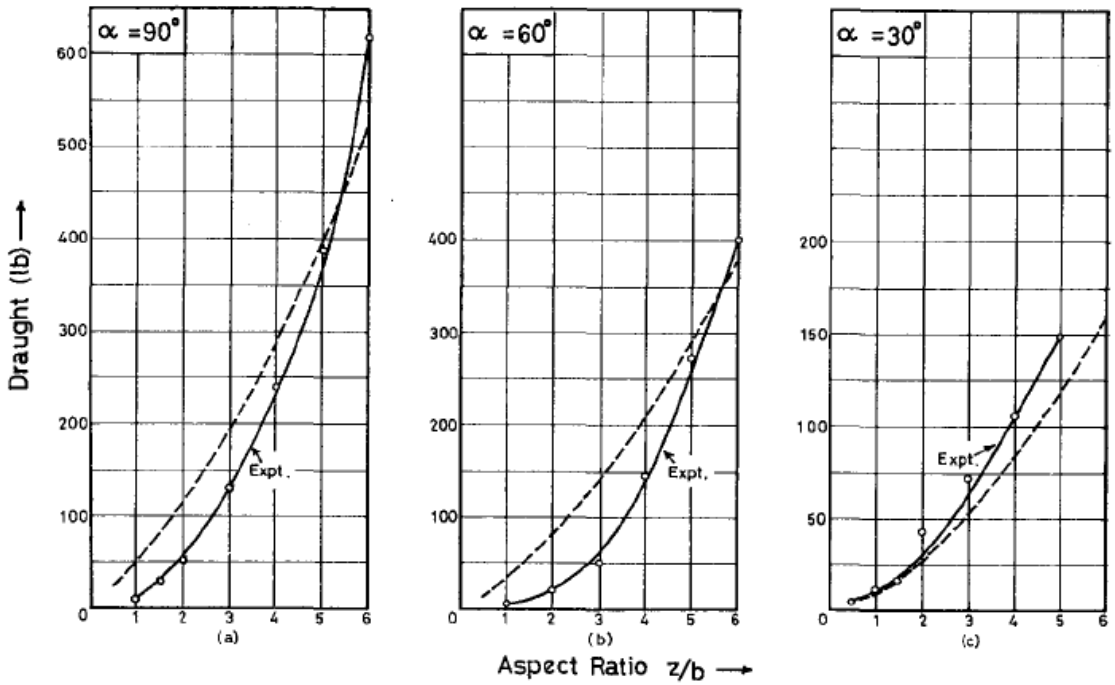

Figure 2.33. Comparison between calculated and experimental values of the draught force. Angle of internal friction of soil, Ø = 32°, soil-interface angle of friction, δ = 25.5°, cohesion, c = 0.2 lb/in^2, soil-interface adhesion, c_a = 0, γ = 0.06 lb/in^3. α = blade angle. From Hettiaratchi and Reece (1967).

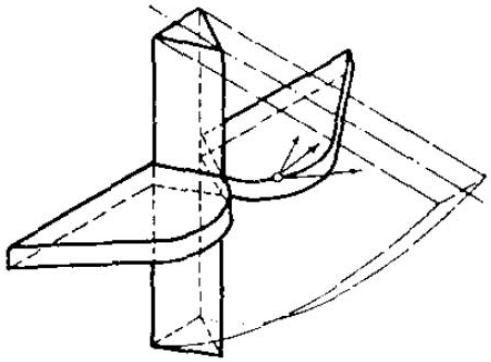

Figure 2.34. Forward and sideways soil failure according to Hettiaratchi and Reece (1967).

Experimental results performed by Payne (1956) and O'Callaghan and Farrelly (1964) were also presented. Values of the draught force from the experiments were compared with values calculated by the draught force model developed, see Table 2.12.

Table 2.12. Comparison between values from experiments and predicted values, Hettiaratchi and Reece (1967).

Source	Soil and blade variables					Draught force (lb)		
	$\phi°$	c (lb/in²)	z (in.)	b (in.)	z/b	Expt.	Calculated $\delta/\phi=0{\cdot}8$	Calculated $\delta/\phi=0{\cdot}5$
Payne [5] $\gamma=0{\cdot}06$ lb/in³	26	2·3	4·1	1	4·1	246	375	181
				2	2·1	336	733	351
				3	1·4	434	1073	510
				4	1·0	818	1397	675
	25	3·07	4·5	1	4·5	361	532	242
				2	2·2	494	1042	471
				3	1·5	630	1528	685
				4	1·1	770	1991	886
				3/8	14·0	49	25	15
	22·5	0·34	5·6	2	2·8	82	123	70
				3	1·9	103	182	102
				4	1·4	125	238	132
O'Callaghan and Farrelley [7] $\gamma=0{\cdot}055$ lb/in³ (Averaged values)	7	7·5	4·0	2	2·0	380	540	417
				3	1·3	500	782	604
				4	1·0	550	1005	778
	3	23·0	3·0	2	1·5	750	1505	795
				3	1·0	900	2185	1136
				4	0·75	1200	2816	1440

2.4.1.4 McKeys & Ali (1977)

McKeys and Ali (1977) proposed a model for cutting of soil with narrow blades. The model concerns a three-dimensional soil failure surface and builds on passive earth pressure theory. The model assumes that the failure shape can be divided into three soil segments in front of the blade: a triangular wedge in the middle and two circular crescent sections on the sides, see Figure 2.35 and Figure 2.36.

The passive force P, in front of the blade, can be calculated with the following equation:

$$P = (\gamma d^2 N_\gamma + cdN_c + qdN_q)\, w, \qquad (2\text{-}7)$$

where the N – factors can be calculated as follows:

$$N_\gamma = (r/2d)[1 + 2r \sin(\rho) / 3w] / (\cot(\alpha+\delta) + \cot(\beta+\varphi) \qquad (2\text{-}8)$$

$$N_c = (1 + \cot(\beta) \cot(\beta+\varphi))[1 + r \sin(\rho) / w] / (\cot(\alpha+\delta) + \cot(\beta+\varphi) \qquad (2\text{-}9)$$

$$N_q = (r/d)[1 + r \sin(\rho) / w] / (\cot(\alpha+ \delta) + \cot(\beta+\varphi) \qquad (2\text{-}10)$$

where β is chosen for the minimum N_γ by trial and error.
Definitions according to the figures below.

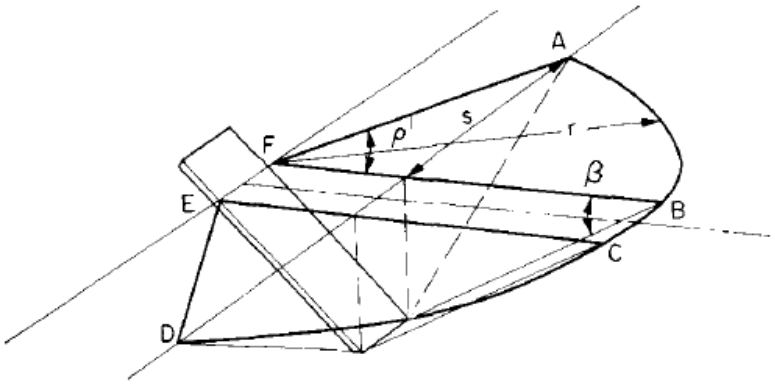

Figure 2.35. Soil failure model proposed by McKeys & Ali (1977).

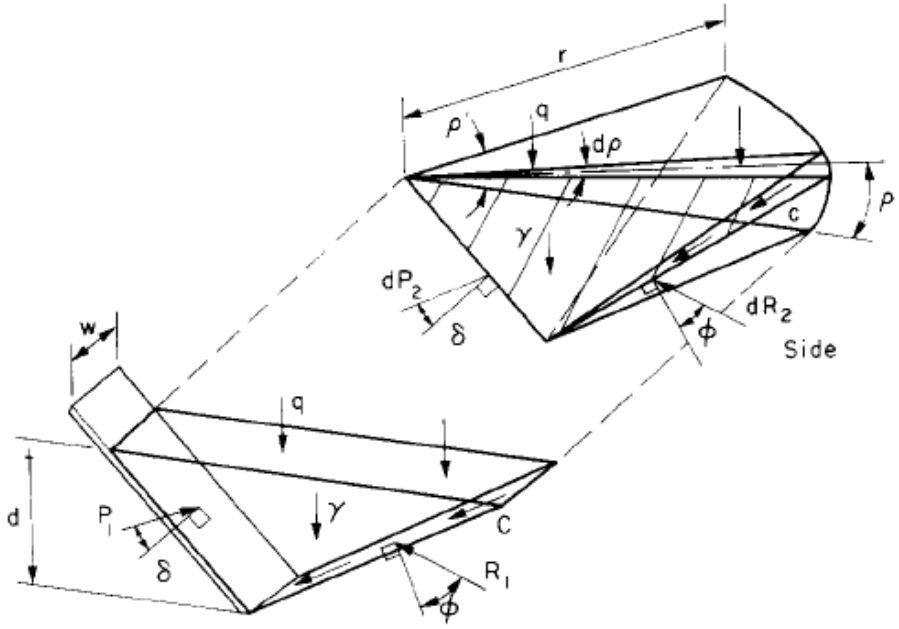

Figure 2.36. Forces acting on the centre and side soil segments, McKeys & Ali (1977).

Table 2.13. Predicted and measured forces for rectangular blades operating in sand and sandy loam. Se figures below. From McKeys & Ali (1977).

α°	w cm	w/d	β°	$N_{\gamma H}$	N_{cH}	H kg	H Measured kg
Sand: d = 5 cm, φ = 35°, δ = 23°, c = 0.00232 kg/cm², γ = 0.00153 kg/cm³							
90	5	1	38	8.65	17.76	2.68	2.75
	15	3	36	6.10	11.92	5.57	5.5
	25	5	35	5.19	9.90	7.83	8.0
60	1.25	0.25	42	14.26	28.75	1.10	0.75
	5	1	38	4.94	9.26	1.48	1.5
	15	3	36	3.49	6.12	3.07	3.0
	25	5	35	2.97	5.04	4.31	5.5
30	1.25	0.25	63	9.80	11.24	0.63	0.5
	5	1	53	3.49	3.66	0.90	1.0
	15	3	49	2.46	2.50	1.85	2.5
	25	5	45	2.08	2.10	2.60	3.5
Sandy loam: d = 3.175 cm, φ = 35°, δ = 23°, c = 0.0362 kg/cm², γ = 0.0016 kg/cm³							
90	2.54	0.80		10.26	22.0	6.84	8.0
	5.08	1.6		7.45	15.29	9.54	10.0
	10.16	3.2		5.98	11.71	14.65	14.25
	20.32	6.4		4.79	8.97	22.52	22.0

The calculated horizontal draft force was verified through experiments with a rectangular steel blade in a soil bin, see Figure 2.37 and Figure 2.38 as well as Table 2.13. Tests were performed in well graded sand and sandy loam at different blade angles and there was a good agreement between calculated and measured values. The results indicate that the draft force increases with blade angle and blade width.

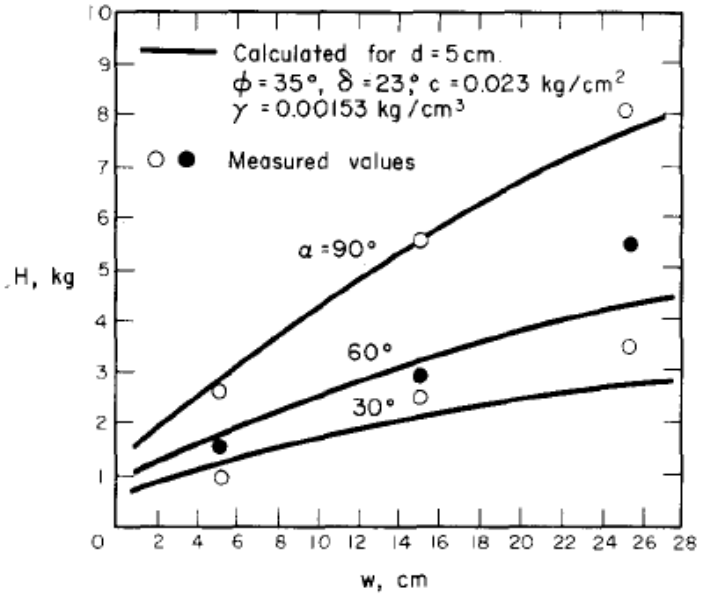

Figure 2.37. Calculated and measured horizontal forces for blades in moist sand, McKeys & Ali (1977).

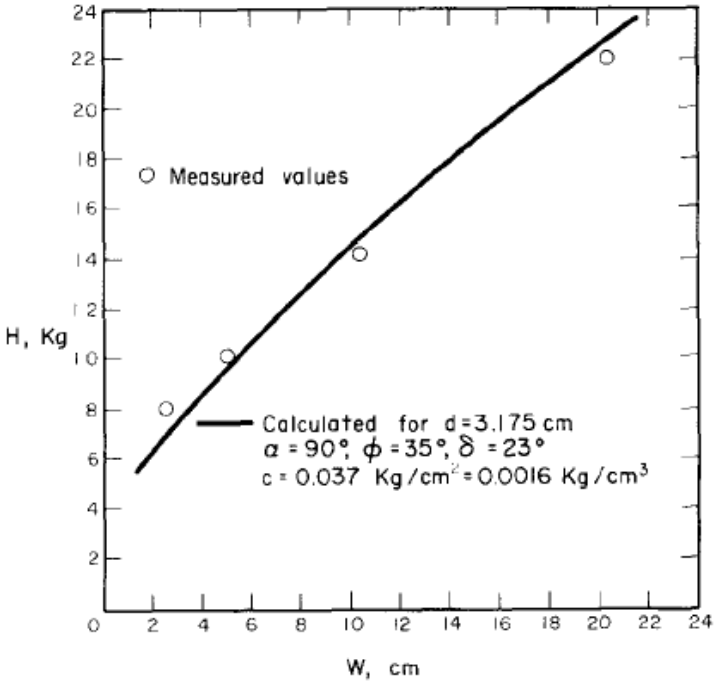

Figure 2.38. Calculated and measured horizontal forces for blades in compact sandy loam, McKeys & Ali (1977).

2.4.1.5 Godwin & Spoor (1977)

Godwin and Spoor (1977) proposed a force prediction model developed for tines for a wide range of working depth to tine width ratios. Their model assumes that the failure shape is of crescent failure shape above a critical depth and that only lateral failure occurs below this depth, see Figure 2.39. This was based on observations of the soil failure pattern in compact sandy loam in a glass-sided box. For all tine widths and rake angles a compacted soil wedge was observed in front of the tine. As the aspect ratio (depth/width ratio) increased the soil failure developed into the two failure shapes of crescent and lateral failure.

The crescent failure shape is very similar to McKeys and Ali (1977) with a wedge segment in front of the blade and two crescent shaped segments on the sides. The shape of the lateral failure, occurring beneath the critical depth, is composed by a vertical triangular wedge in front of the blade and two segments on the sides of the blade. The type of failure is similar to that beneath a footing, with logarithmic spiral boundaries. The force prediction model for the upper crescent failure zone consists of a passive pressure in front of the blade and the passive force resulting from the soil wedges aside the blade. The resultant passive force, P in front of the blade, can be calculated as proposed by Hettiaratchi et al (1966). The N – factors can be determined using a numerical analysis presented by Sokolvskij (1960).

$$P = \gamma z^2 N_\gamma + cz\, N_c + c_a z\, N_a + qz\, N_q \qquad (2\text{-}11)$$

The total horizontal force, H for the linear and curved side sections is given by:

$$H = [\gamma d_c^2 N_\gamma + c d_c N_c + q d_c N_q]\,[w + m d_c \sin(\cos^{-1}(\cot(\alpha)/m))]\sin(\alpha+\delta) + c_a w d_c\,(N_a \sin(\alpha+\delta) + \cos(\alpha)) \qquad (2\text{-}12)$$

where $m = r/d_c$.

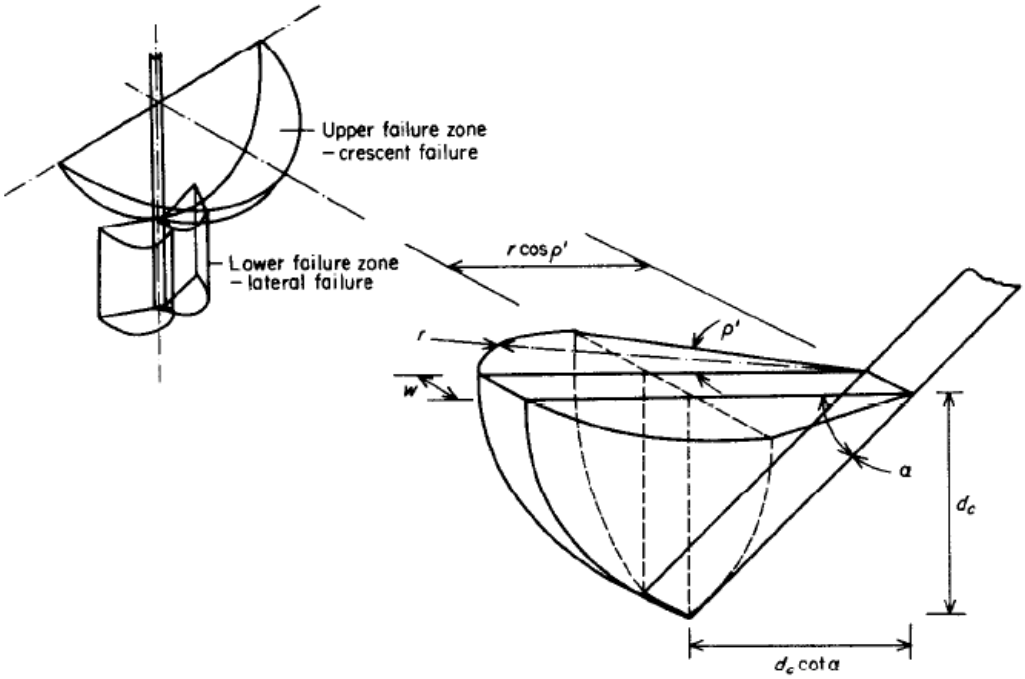

Figure 2.39. Conceptual mechanism of soil failure (left) and crescent geometry (right), according to Godwin and Spoor (1977).

Experiments were performed in a soil bin at two depths (165 mm and 115 mm), and the predicted and measured horizontal and vertical forces on the tine were plotted. The agreement between the model and the experimental values were acceptable for the horizontal force. The model values increased non-linearly with blade width while the experimental values had a linearly increase with blade width.

Experiments were performed in loose and compacted soil. The results show that the horizontal and vertical forces, obviously, are greater in the compacted soil than in the loose soil. The difference in this case was about a factor of ten. The following soil properties were used:

Compacted soil: $\varphi = 37{,}5°$, $c = 4{,}6$ kN/m^2, $\delta = 22°$, $c_a = 0$, $\gamma = 1500$ kg/m^3.
Loose soil: $\varphi = 34°$, $c = 0$, $\delta = 22°$, $c_a = 0$, $\gamma = 1100$ kg/m^3.

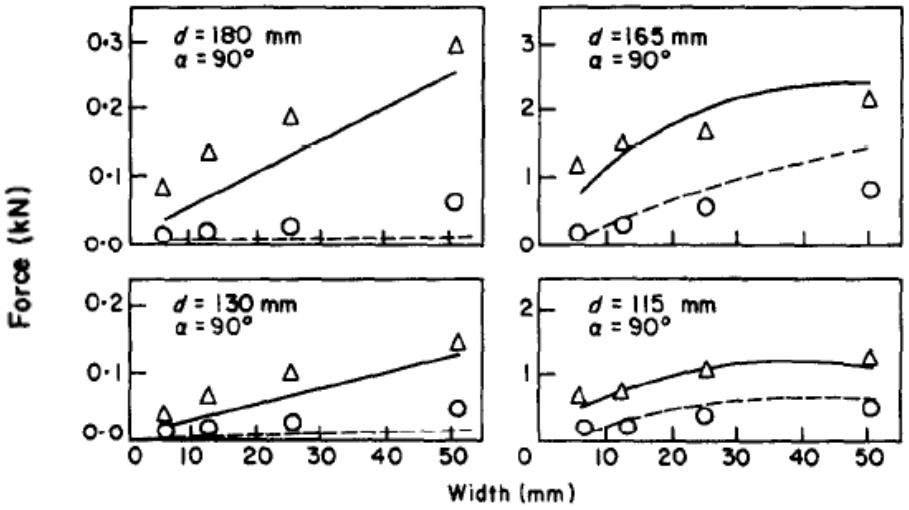

Figure 2.40. Comparison between predicted forces (horizontal – soild line, vertical dashed line) and measured forces (horizontal – triangles, vertical – circles) in uncompacted soil (left) and compacted soil (right). After Godwin and Spoor (1977).

2.4.1.6 Stafford & Tanner (1983)

Stafford & Tanner (1983) report on the effect of deformation rate on soil shear strength. In laboratory experiments the effect have been examined for three typed of soil:a sandy clay loam (soil 1) and a clay soil (soil 2). The shear of soil occurred at 0.0015 – 5 m/s sliding speed. The cohesion was found to vary logarithmically with deformation rate for a range of moisture contents. According to the experiment the soil internal friction angle was independent of deformation rate. The residual shear strength did not vary in a consistent way with deformation rate.

The relationship between shear stress and shear strain were investigated for a normal stress of 470 kPa, see Figure 2.41 below. For lower moisture contents the curves showed typical brittle soil failure pattern, for higher moisture content the failure pattern was like plastic soil. In the experiment some problems were experienced with resonance of the transducer assembly at high deformation rates. The shear strength was plotted against the normal stress and there was a linear relationship for all sets of data, see Figure 2.42. The shear behaviour of the soils was found to follow the Coulomb model. The values of peak and residual stresses are more uncertain at rates above 2.5 m/s.

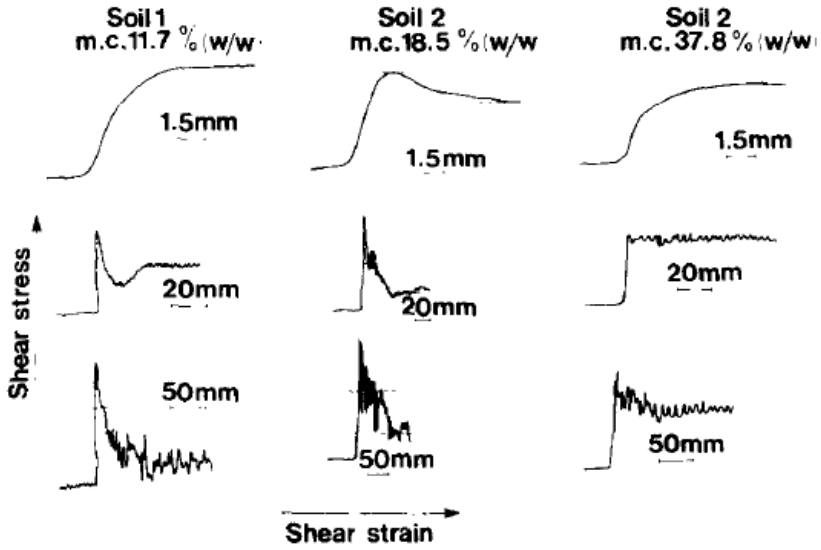

Figure 2.41. Stress – strain curves at normal stress of 470 kPa. Deformation rates: top 0,0015 m/s, middle 2 m/s and bottom 5 m/s, Stafford & Tanner (1983).

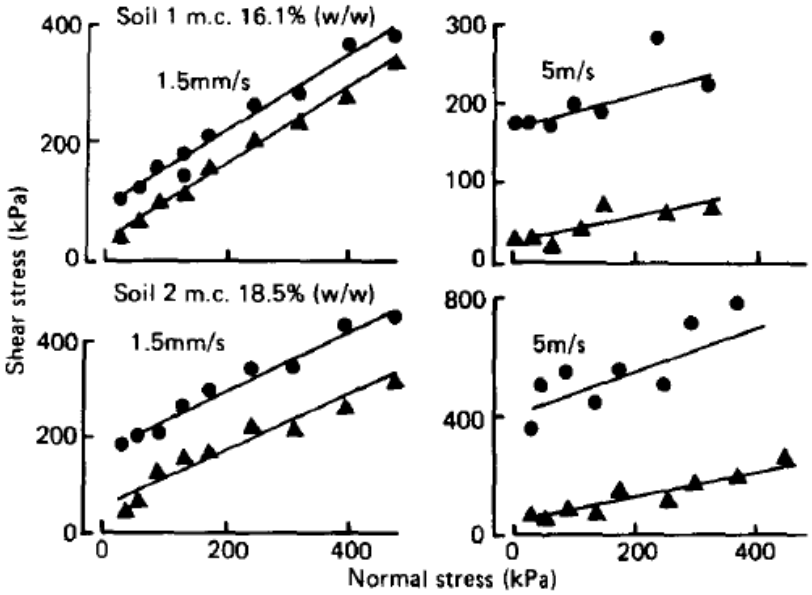

Figure 2.42. Variation of the peak (dots) and residual (triangles) shear stresses with normal stress, according to Stafford & Tanner (1983).

The relationship between cohesion and deformation rate were investigated for both peak and residual strength. The peak cohesion was plotted against the deformation rate and it showed on a logarithmic relationship, see Figure 2.43. The residual cohesion values were also plotted against deformation rate. There was no apparent relationship noted more than a tendency of a slight increase of the residual cohesion with deformation rate. The scatter in the plot may be due to difficulty interpreting the stress-strain relationship.

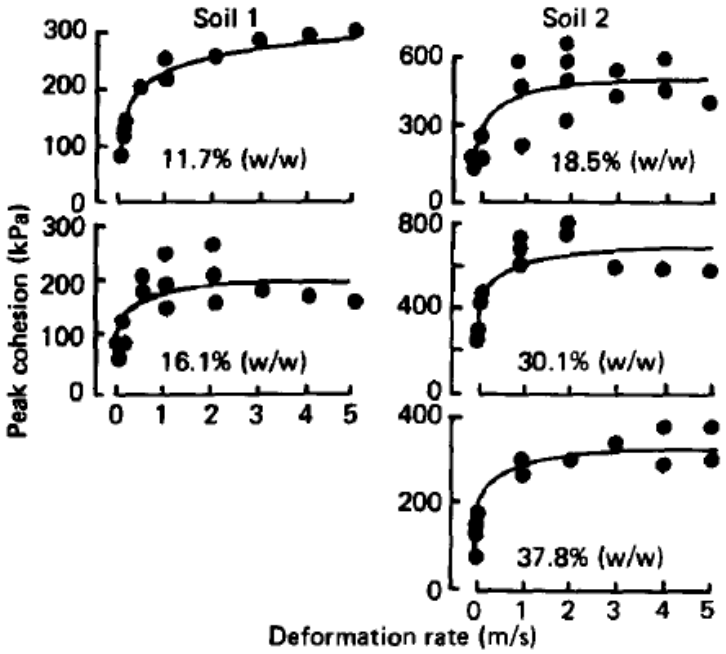

Figure 2.43. Variation of the peak cohesion with deformation rate at different moisture content, according to Stafford & Tanner (1983).

Neither the peak nor the residual angles of friction showed any relationship with deformation rate. Though, there was a significant decrease in the peak friction angle of the clay soil as moisture content was increased. The increase in the residual friction angle was barely significant.

The experiments are performed under confined conditions were the soil sample was not allowed to freely dilate during shearing. It is showed earlier that in a compression test the soil strength is greater during confined conditions than under unconfined conditions. Tests showed that the cohesion was reduced when the confining pressure was removed. The internal friction angle was not affected, see Figure 2.44. The experiments were performed on a clay soil with moisture content of 30.1 % at the deformation rate of 1 m/s.

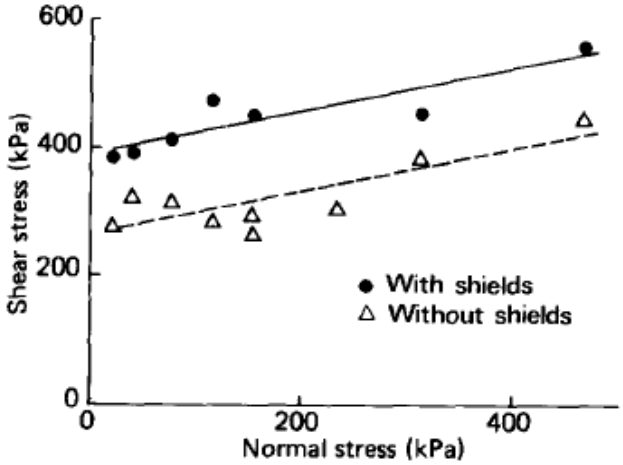

Figure 2.44. Effect of confining shields around the clay samples on the shear stress – normal stress relationship, Stafford & Tanner (1983).

Stafford & Tanner argues that the residual shear strength is, in general, of less importance than the peak shear strength in the machine/soil interaction area.

2.4.1.7 Swick & Perumpral (1988)

Swick and Perumpral (1988) presented a model for predicting forces on narrow tillage tools under dynamic conditions. The model includes effects due to shear rate, acceleration force and soil-metal friction. The model assumes soil failure trough three segments in the soil, very similar to Goodwin and Spoor (1977) soil failure model. The soil failure model consists of a triangular wedge in front of the blade and circular wedges on the sides, see Figure 2.45. The soil experiments were carried out in a soil bin with artificial soil (sand, fine clay and mineral oil) for verification of the model. The predicted and observed draft forces were compared and the predicted values tend to be lower than the observed ones. Also the prediction error, the difference between predicted and observed values, was plotted against the depth-width ratio, see Figure 2.46. It shows that large under predictions of the force appear to be due to under predictions of the size of the failure wedge. Similarly over predictions of the force are over predictions of the size of the failure wedge.

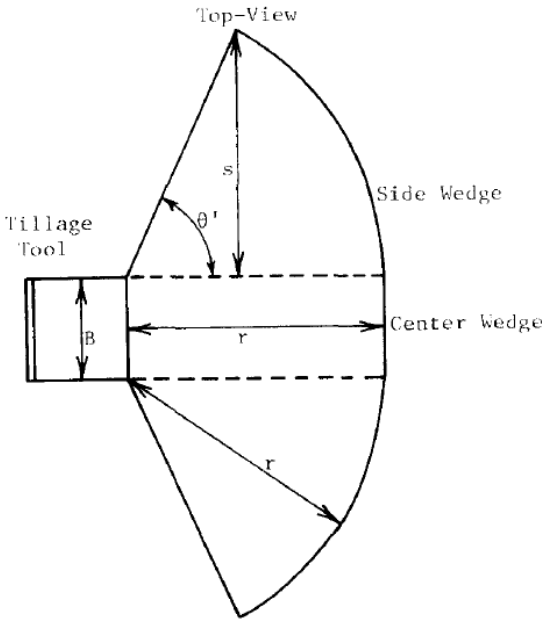

Figure 2.45. Top-view of soil failure wedges assumed in the model, Swick and Perumpral (1988).

Experiments with artificial soil in a direct shear box were carried out to determine the effect of shear rate on soil strength and soil-metal friction parameters, see Figure 2.47 and Figure 2.48. Tests were performed in three displacement rates: 0,08, 8,3 and 21,2 mm/s. The results show that the shear rate had no effect on soil strength or soil-metal friction. This does not agree to other studies of, for example, Stafford and Tanner (1983) who observed an increase in shear strength with increasing shear rate. According to the authors these disagreements could depend on differences in apparatus and soil types as well as differences in loading conditions during tests.

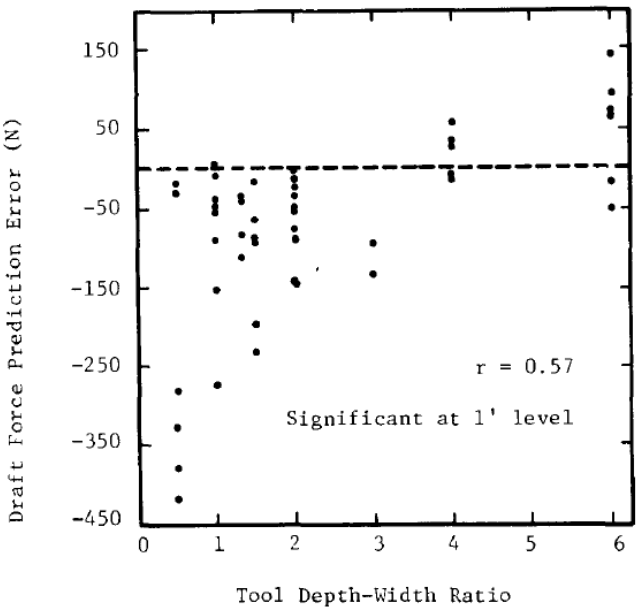

Figure 2.46. Effect of tool depth-width ratio on draft force prediction error, Swick and Perumpral (1988).

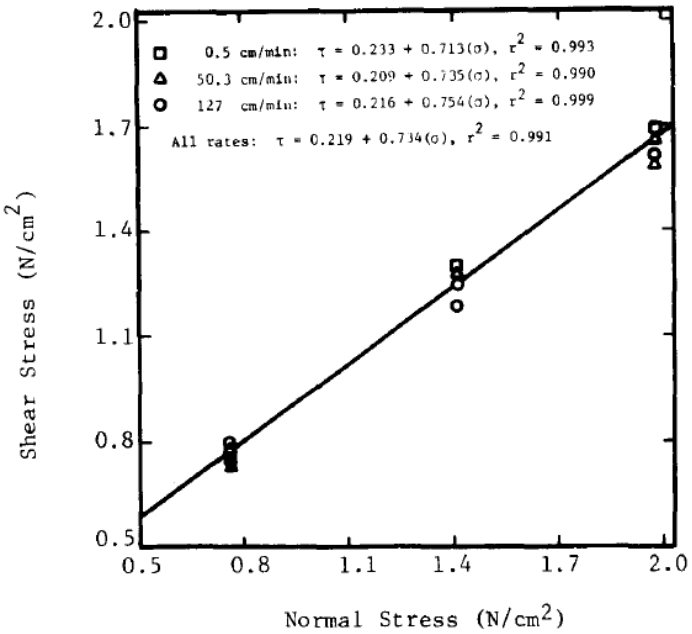

Figure 2.47. Shear and normal stress relationship from direct shear tests with artificial soil, Swick and Perumpral (1988).

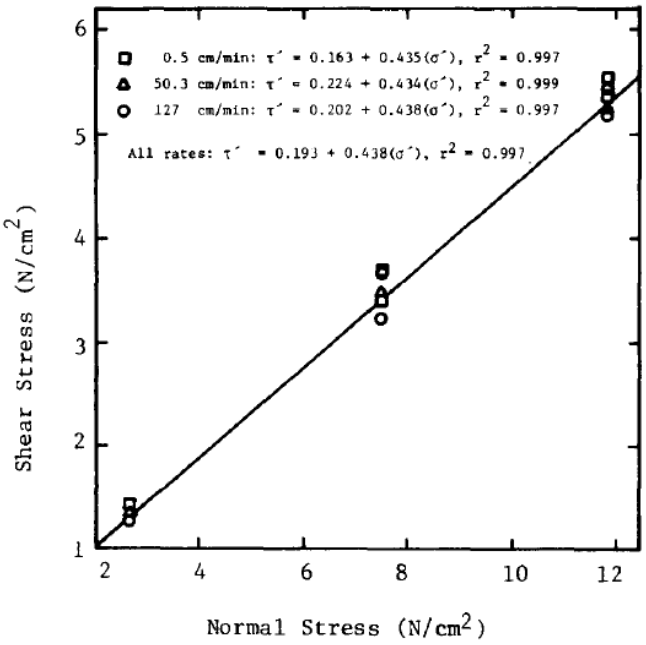

Figure 2.48. Shear and normal stress relationship from soil-metal friction test with artificial soil, Swick and Perumpral (1988).

2.4.1.8 Hettiaratchi (1988)

In this paper Hettiaratchi (1988) reviews and discusses soil mechanics and how it is related to soil-tool interaction. Soil-implement mechanics involves the analysis of soil forces on machine elements, identifying soil-disturbance zones during soil failure and the problems of wearing of tool surfaces. This is closely related to passive earth pressure theory in civil engineering. According to Hettiaratchi all earth pressure problems involves some basic factors: the external loads and their displacements, internal stresses and relating displacements, a failure criterion for the soil and a failure mechanism. There are different methods for formulating the failure mechanism: limit analysis methods and slip-line methods.

In two dimensional passive earth pressure problems the task of determining the failure mechanism is done through distinguishing a rupture zone in the soil, within were the shear and normal stresses are at the border to failure. According Hettiaratchi (1988) a well known form of rupture zone is Ohde's (1938) logarithmic spiral boundary. Other solutions have been proposed by Sokolovski (1960) using a numerical method and Reece (1964) using a variant of the logarithmic spiral surface. According to Hettiaratchi (1988) the passive earth pressure coefficients proposed by Reece (1964) have been presented by Hettiaratchi and Reece (1974).

In a two dimensional problem the Mohr-Coulomb failure criterion is a function of only two principal stresses. In a three dimensional problem of determining the failure mechanism thus will involve solving partial differential equations for complex boundary conditions. Another way of approaching a solution of a three dimensional problem would be the formulation of a failure mechanism that harmony with practical observations. When an acceptable failure boundary has been stated the forces can be evaluated through static equilibrium.

Hettiaratchi (1988) reports on several researchers trying to analyze the forces acting on rigid tines (narrow blades) and the three dimensional rupture zones formed in front of the tool

through semi-empirical models. The observed failure shapes and models developed differ from one researcher to another, see figure below. According to Hettiaratchi (1988), O'Callaghan and Farrelly (1964) reported that the failure shape of a deep tine was divided into a crescent formed failure shape closer to the surface and lateral failure at a critical depth and below. The critical depth is a function of the aspect ratio (depth/width ratio) and the blade angle of the tine.

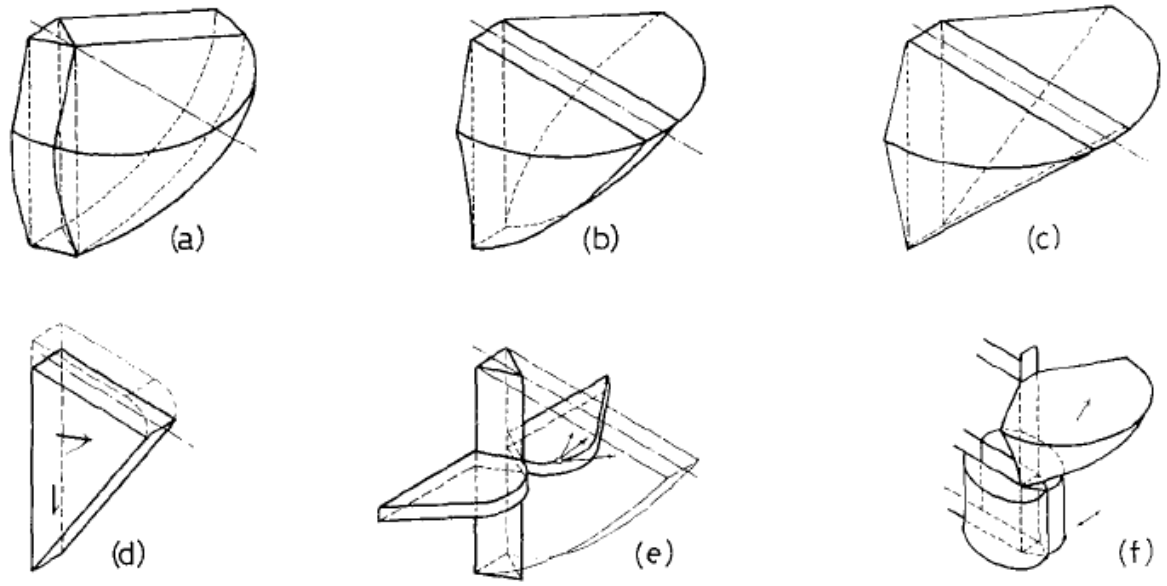

Figure 2.49. Failure surfaces used in analyses of narrow blades proposed by different authors; (a) Payne (1956), (b) Godwin and Spoor (1977), (c) McKeys and Ali (1977), (d) Perumpral et al. (1983), (e) Hettiaratchi and Reece (1967), (f) O'Callaghan and Farrelly (1964). From Hettiaratchi (1988).

Hettiaratchi (1988) discusses complex soil-failure problems which can be caused when cutting with, for example, disc tools and mouldboard ploughs. These problems cannot be solved through mathematical methods used in two-dimensional problems or by semi-empirical three-dimensional theories. They involve complex geometry of soil failure as well as acceleration and velocity of soil which has to be handled through kinematic and dynamic analysis. Hettiaratchi proposes that experiments in soil bins and model testing are good techniques to obtain understanding in this area. Model testing and dimensional analysis have to be done with caution. Dimensional analysis can be used in order to categorize quantities and units and the relation between them. Also the similarity between the theoretical model and the prototype can be evaluated. All the non-dimensional groups have to be the same in both the model and the prototype if a complete similarity should be obtained. Consider the static force P that is a function of some parameters assembled in non-dimensional groups:

$$P/\gamma z^2 = f\,(c/\gamma z,\ q/\gamma z,\ \varphi,\ \delta) \qquad (2\text{-}13)$$

Glass-box experiments are useful in examining the ruptured surface in the soil and the movement of soil by the tool prototype. According to Hettiaratchi (1988), these experiments are only suitable for two-dimensional problems and three-dimensional examples have to be handled through elaborate methods, like X-rays, or through location of marker particles embedded in soil.

2.4.1.9 Zein Eldin & Al-Janobi (1995)

In their review Zein Eldin and Al-Janobi discusses the effects of different parameters on soil-tillage tool interaction. The geometrical shape of the tool in mind is not stated in the review but it is assumed, with leading from references, that a tillage tool is a rectangular wide or narrow blade. From studies of dimensional analyses of soil tool interaction they divide the parameters into four groups: tool parameters, soil parameters, soil-tool interface parameters, and surcharge conditions. The review is focused on tool parameters affecting soil-tool interaction. Tool parameters include depth, width, blade angle, speed, aspect ratio (depth/width) and tool shape (curvature of blade). Soil parameters are cohesion, angle of internal friction, bulk density and moisture content. The soil-tool interface parameters are soil-metal friction angle, adhesion, tool sharpness and wear conditions. The surcharge condition involves the case when the tool operates below the soil surface and is expressed by a uniform pressure on the surface.

Zein Eldin and Al-Janobi concludes that the draft (horizontal force) is proportional to and increases with depth. They propose that theoretically the draft force, P can be explained as variant of the Fundamental Earthmoving Equation by Reece (1964).

$$P = \gamma d^2 N_\gamma + cd\, N_c + c_a d\, N_{ca} + qd\, N_q + \gamma v^2 d\, N_a \qquad (2\text{-}14)$$

In this equation the weight component of the force increases with square of depth and the other components; cohesion, adhesion, surcharge and acceleration, increases with depth. In practice the actual response depends on the relative magnitude of the components. If the weight term dominates the relationship is parabolic, if the other terms dominate it is linear. If the relative magnitudes of the terms are about the same, the relationship will be quadratic. Zein Eldin and Al-Janobi claims that studies show on a linear relationship between the tool width and cutting force although nonlinear relations also have been reported by Goodwin and Spoor (1977). The vertical force on a blade has shown to increase linearly with both tool depth and width. Though, theoretically the vertical force can increase non-linearly with depth.

Zein Eldin and Al-Janobi reports that from a blade angle of zero degrees, measured from the vertical plane, the force decreases to an optimum at a blade angle of about 10 to 20 degrees. At further increase of the blade angle causes an increase of the draft force. An explanation of this initial effect can be that the tool has a larger area in contact with the soil at very small blade angles. But at increasing blade angle the area in contact will decrease. The vertical force will generally increase with blade angle up to an optimum at about 10 and 20 degrees. After that it will decrease with blade angle. At a blade angle of about 50 to 70 degrees the force change sign and starts to act upwards.

Zein Eldin and Al-Janobi claims that, when the soil has accumulated in front of the blade, a curved blade behaves as a plane blade. The tool-soil friction, δ, then becomes equal to the soil friction angle, φ, and the adhesion, c_a equals zero which leads to a higher draft force for a curved blade than a plane one. Zein Eldin and Al-Janobi concludes that the draft force generally increases with speed. Studies show that the relationship is linear, exponential, second order polynomial or parabolic. Also there are studies that show on no relationship between force and speed. Tool speed affects the draft force due to three different reasons: inertia required to accelerate the incoming blocks of soil, effect of shear rate on soil shear strength, and effect of shear rate on soil metal friction. For sandy soils the effect of inertial forces has been found to be significant causing the draft force to increase with the square of speed. For cohesive soils the shear strength increase with shear rate has been found to be more

significant causing the draft force to increase exponentially with shear rate. The relationship between the vertical force and speed is linear for both cohesive and sandy soils. Though, both draft and vertical forces are components of the cutting force. Therefore it would be expected that the relationships are the same for the draft and the vertical force. Zein Eldin and Al-Janobi also reports on simulation results showing that the draft force increases with the increase of cohesion, soil friction angle, adhesion and soil – metal friction.

Zein Eldin and Al-Janobi have gathered results from earlier studies about parameters affecting soil disturbance and soil failure geometry. There is a linear relationship between rupture distance ahead of blade and depth. Similarly it is a linear relationship between the rupture distance perpendicular to the blade and depth. The effect of speed on the disturbed area of soil is not clarified, though, the degree of soil breakup increases with speed. The reporting is not consistent.

2.4.1.10 Godwin (2006)

Godwin (2006) has performed a review of the relationships between the geometry of the narrow blade (tillage tool) and soil physical properties. The soil failure pattern differs with width and depth of the blade.

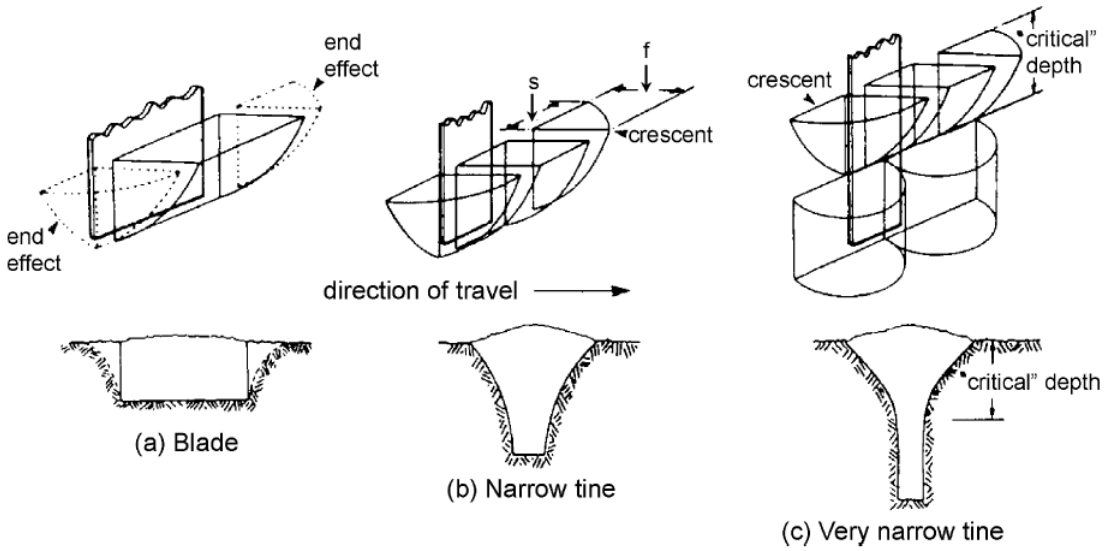

Figure 2.50. Effect of the implement depth to width ratio on soil failure, from Godwin (2006).

According to Godwin blades with blade angles greater than about 70 degrees produces upward vertical forces, which have to be counterbalanced with weights or by the tractor. Godwin concludes that both the horizontal and vertical forces increase at an increasing rate for a vertical tine. Small changes in the working depth can affect the magnitude of the horizontal force significantly, see Figure 2.51. According to Godwin the blade width affects the magnitude of the horizontal and vertical forces, see Figure 2.52. The influence of the width is greater for very narrow tines than for wide blades. The blade angle increases the magnitude of the forces on the blade, see Figure 2.53. Goodwin proposes that the point were the vertical force changes between upward and downward force is at approximately a critical blade angel, $\alpha_c = 90 - \delta$, were δ is the soil tool friction angle. The horizontal and vertical forces increase with speed. Goodwin shows on experimental data with a narrow tine in frictional soil were the forces increase almost linearly with speed.

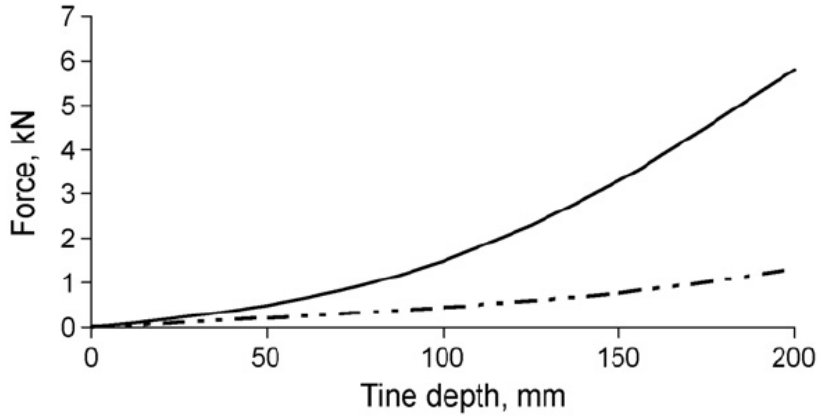

Figure 2.51. Effect of blade depth on horizontal (solid line) and vertical (broken line) forces acting on a vertical blade, Godwin (2006).

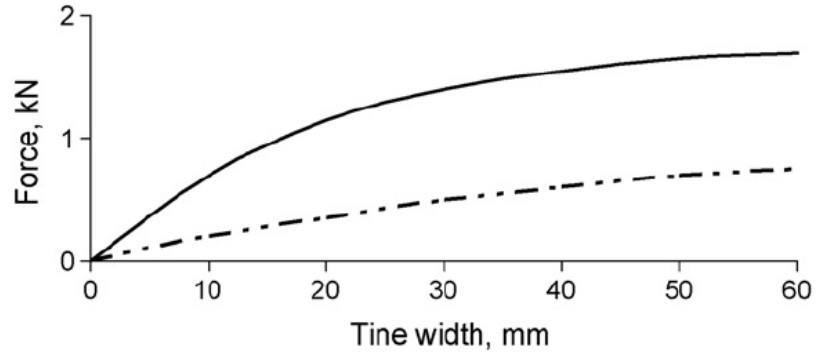

Figure 2.52. Effect of blade width on horizontal (solid line) and vertical (broken line) forces acting on a vertical blade, Godwin (2006).

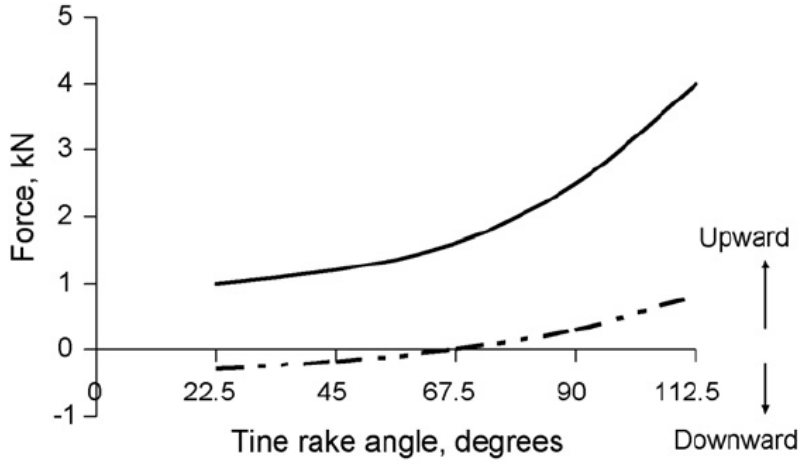

Figure 2.53. Effect of blade (rake) angle on horizontal (solid line) and vertical (broken line) forces, Godwin (2006).

2.4.2 Wide blades

In this chapter force prediction models by Reece (1964), McKeys (1989) and Qinsen & Shuren (1994) are presented. In Hettiaratchi (1965) work from Osman (1964) and Siemens et al. (1964) is presented.

2.4.2.1 Reece (1964)

In the paper Reece (1964) proposes an equation describing the force on a soil cutting blade when performing earth moving work. Reece argues that since the soil involved in an earth moving action is brought to a complete failure the methods of soil mechanics can be used. Therefore he suggests that all soil forces can be described by a single equation. Reece refer to Osman's (1964) experimental work on wide cutting blades and his theoretical solution. Osman found the relevant variables involved in a typical earth moving problem and suggested a dimensionless equation. According to Reece (1964), Osman (1964) proposed that the dimensionless groups are: cohesion, internal friction, soil-metal friction, soil-metal adhesion, surcharge and blade angle (shape of tool element).

$$P/\gamma b^2 = f\,(c/\gamma b,\ \varphi,\ \delta,\ q/\gamma b,\ c_a/\gamma b,\ \theta) \qquad (2\text{-}15)$$

Reece claimed that Osmans equation could be replaced by a more specific equation consisting of four terms. These terms represent the effects of the cohesion of the soil, its weight, surcharge loading and the adhesion developed between blade and soil. The N-factors are dimensionless numbers describing the shape of the soil failure surface. These factors depend on the internal soil friction, soil-tool friction, blade angle and the angle of soil failure with the horizontal. Charts with N – factors can be found in the paper by Reece (1964).

$$P = \gamma b^2 N_\gamma + cb\, N_c + c_a b\, N_{ca} + qb\, N_q \qquad (2\text{-}16)$$

This equation is similar to the bearing capacity equation described by Terzaghi (1943).

In order to determine the limiting equilibrium of a soil mass it is necessary to know the shape of the failure surface. According to Coulomb this shape would be such that the force required to cause soil failure would be a minimum. A Coulomb material will have failure planes lying at angle of $90 - \varphi$ to each other. The failure shape assumed in this paper is logarithmic spiral shape closest to the blade and a plane in the Rankine passive zone, see Figure 2.54.

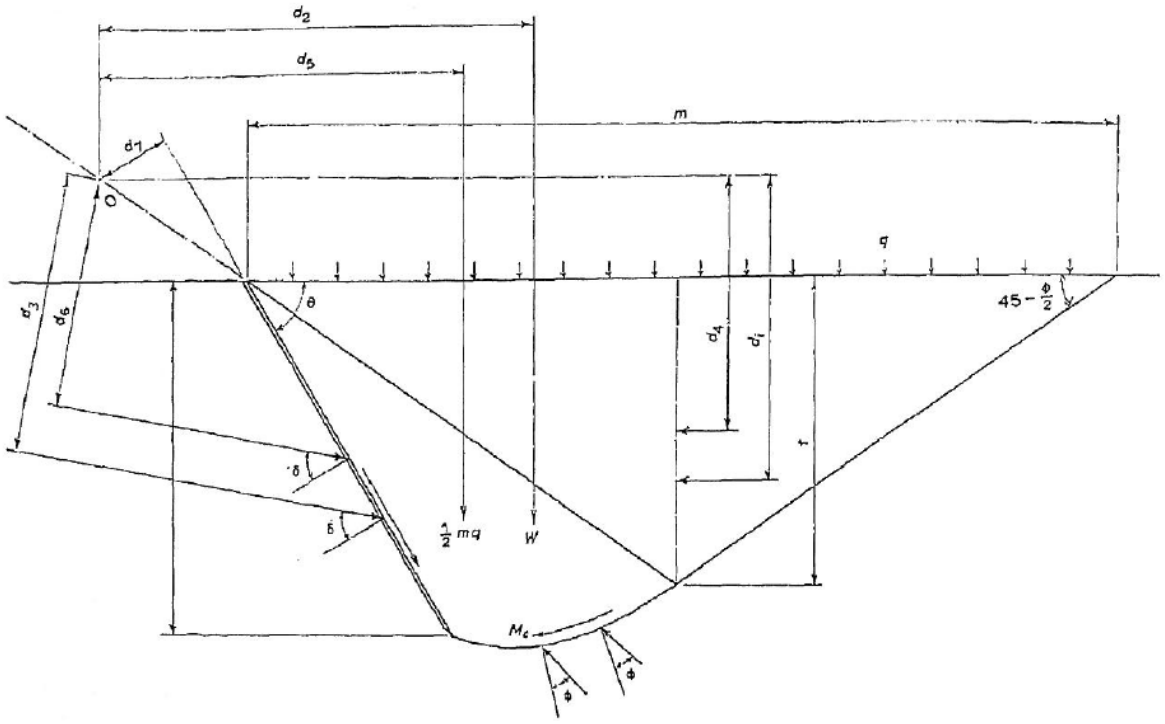

Figure 2.54. The forces acting on the soil failure zones in front of the cutting blade, Reece (1964).

2.4.2.2 Hettiaratchi (1965)

The paper reviews research in the area of earth working tools and cutting blades. Hettiaratchi (1965) concluded that narrow tools, called tines, give rise to a three dimensional failure problem in soil whereas wide tools, called blades, involves two dimensional soil failures.

Hettiaratchi (1965) presented the work of wide blade theory of Osman (1964) who tested two-dimensional soil cutting with varying blade angles and soil types. Osman attempted to verify two theories for passive earth pressure acting on the blade: Coulomb´s solution for granular material and Ohde´s (1938) logarithmic spiral method. Osman performed laboratory experiments on three types of soil: a purely non-cohesive dry sand, a cohesive stiff clay and a c – ø type of soil. He also experimented with smooth and rough surfaces on the blade as well as plane and curved blades. According to Hettiaratchi (1965), Osman (1965) concluded that Coulomb´s wedge solution only held for smooth blades of small rake angles working in non-cohesive soils, but that Ohde´s (1938) solution gave remarkable accuracy of prediction of the forces acting on the blade. Results from the experiments shows that the horizontal force increases with blade angle in both clay and sand. The increase is slightly nonlinear. See Figure 2.55.

Osman performed advanced calculations and dimensional analysis and presented the variation of the draught force with different parameters. It seems like the horizontal force increases exponentially with increasing soil friction angle, if it is assumed that the gravitational force is constant. See Figure 2.56.

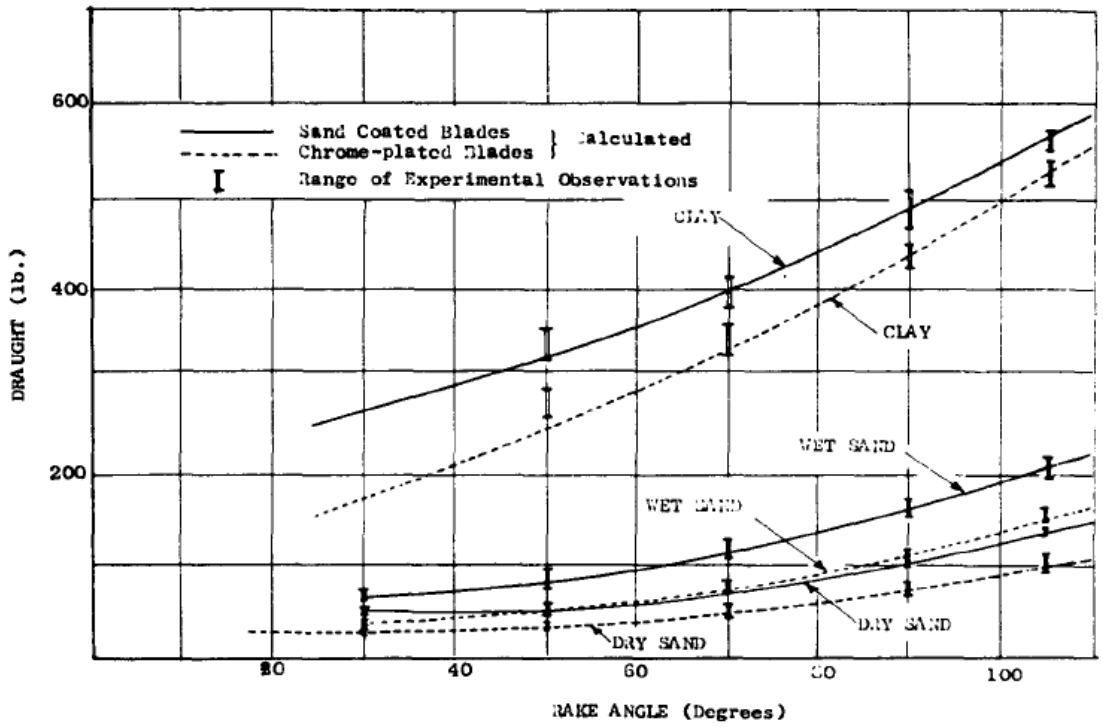

Figure 2.55. The increase of the horizontal force with increasing blade angle in both clay and sand proposed by Osman (1964), according to Hettiaratchi (1965).

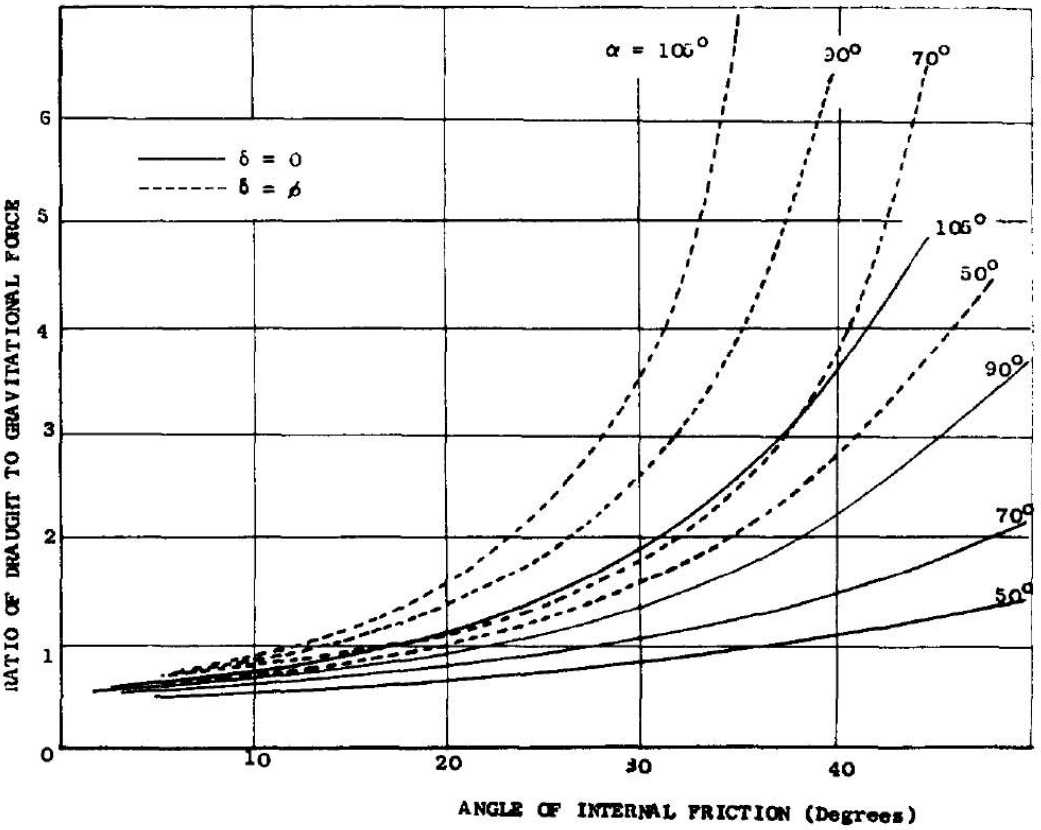

Figure 2.56. Predicted values from Osman (1964), according to Hettiaratchi (1965). Solid line: $\delta = \varphi$, dashed line: $\delta = 0$.

Hettiaratchi also reported on experimental work carried out by Siemens et al. (1964). They investigated the mode of failure of the soil and noted a fluctuation of the force on the tool during cutting. According to Hettiaratchi (1965), Siemens et al. (1964) observed that the maxima occurred at the beginning of each slip plane and that the minima corresponded to when the slip planes were fully developed. Siemens et al. (1964) showed that each slip plane originated at the tip of the tool and that the plane continues upwards to the soil surface at the angel of 45 – ø/2 degrees.

2.4.2.3 McKeys (1989)

Two dimensional analytical calculations of the total horizontal force on a blade have been carried out by McKeys (1989). His approach builds on passive earth pressure theory proposed by Coulomb and Rankine. His approach have been used and referred to in earlier studies, for example: Luengo et al (1998), Cannon (1999) and Shmulevich et al (2007). The model builds on earlier work of McKeys (1985) and is very similar to force prediction model proposed by Reece (1964).

In McKeys' (1989) method the resultant force required to move a blade in soil is calculated as the passive pressure mobilized in the soil. As for a retaining wall, it is assumed that the soil failure occurs along an internal rupture surface, a slip line, as the blade is moving towards the soil. The failure surface has shown to be curved due to, for example, friction between the soil and the blade. In the model the failure surface is approximated to be linear for easier calculations, which is assumed to have acceptable error effects on the calculated resultant forces. As passive failure occurs in the soil in front of the blade a wedge of soil is loosened. Studying this soil wedge in static equilibrium the forces acting on the wedge can be calculated.

Figure 2.57 and Figure 2.58 illustrates the forces acting on the soil wedge and a bulldozer blade respectively. As the passive force, P, the weight, W and surcharge, Q acts on the blade a resultant force, R will develop on the soil wedge. The components of the resultant, R consists of the normal stress component and the shear stress component on the soil failure surface (not shown in figures). The passive force, P is composed of the normal force component and the frictional resistance force component on the blade (not shown in figures). The adhesive resistance force acting along the blade is defined as: c_aL_1.

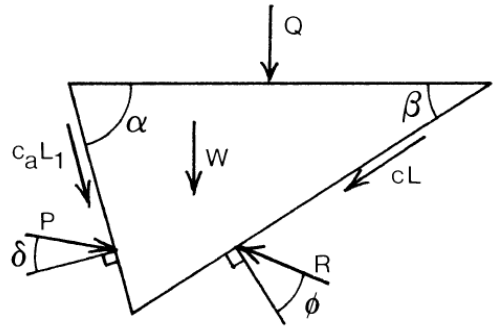

Figure 2.57. The general passive soil failure wedge model, according to McKeys (1989).

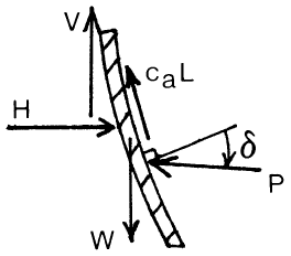

Figure 2.58. Forces acting on the blade in static equilibrium, McKeys (1989).

McKeys (1989) proposes three equations to be used to calculate the soil force, P, and the horizontal, H, and vertical, V, components of the forces to move the blade.

$$P = (\gamma h^2 K_\gamma + ch\, K_c + c_a h\, K_{ca} + qh\, K_q)w \quad (2\text{-}17)$$

$$H = P\sin(\alpha + \delta) + c_a hw\cot(\alpha) \quad (2\text{-}18)$$

$$V = P\cos(\alpha + \delta) - c_a hw + W \quad (2\text{-}19)$$

The soil force, P, consist of components related to the weight of the soil, the soil internal cohesion, the adhesion between the soil and the blade and the weight of overburden. Each component contains a coefficient, K_i that varies with wedge geometry, soil friction angle and the friction between the soil and the blade.

$$Kp = (\cot(\alpha) + \cot(\beta)\sin(\beta + \varphi)) / 2\sin(\alpha + \beta + \delta + \varphi) \quad (2\text{-}20)$$

$$Kc = \cos(\varphi) / \sin(\beta)\sin(\alpha + \beta + \delta + \varphi) \quad (2\text{-}21)$$

$$Kca = -\cos(\alpha + \beta + \varphi) / \sin(\alpha)\sin(\alpha + \beta + \delta + \varphi) \quad (2\text{-}22)$$

$$Kq = 2Kp \quad (2\text{-}23)$$

where

$$\beta = \cot^{-1}[(\sqrt{((\sin(\alpha + \delta)\sin(\delta + \varphi)) / \sin(\alpha)\sin(\varphi) - \cos(\alpha + \delta + \varphi)) / \sin(\alpha + \delta + \varphi)}] \quad (2\text{-}24)$$

2.4.2.4 Qinsen & Shuren (1994)

The paper studies the soil cutting process of a bulldozer blade and provides a mathematical model for soil-blade interaction. The two-dimensional model is constructed for predicting vertical and horizontal forces and can be used for computer simulations. Experiments with a soil bin have been conducted in order to validate the model. There were good correlations between predicted and observed vertical respectively horizontal resultant forces.

The mathematical model was created partly from prior observations. Some assumptions are based on “observing and analysing a lot of experiments”. None of these experiments or other work is presented or referred to. According to Qinsen & Shuren the soil cutting process of blades can be divided into two parts: the earthmoving process on the ground, the soil within

the area of abdef, and the soil cutting process under the ground, the soil within the area of bcd see Figure 2.59 and Figure 2.60.

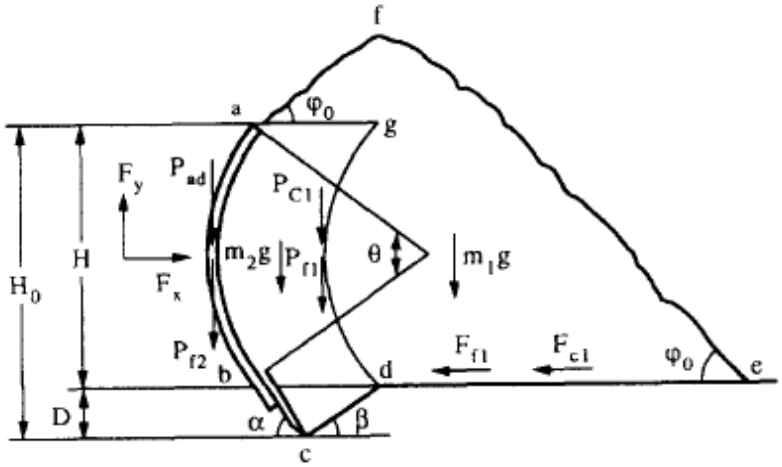

Figure 2.59. The forces involved in the soil cutting processes, according to Qinsen & Shuren (1994).

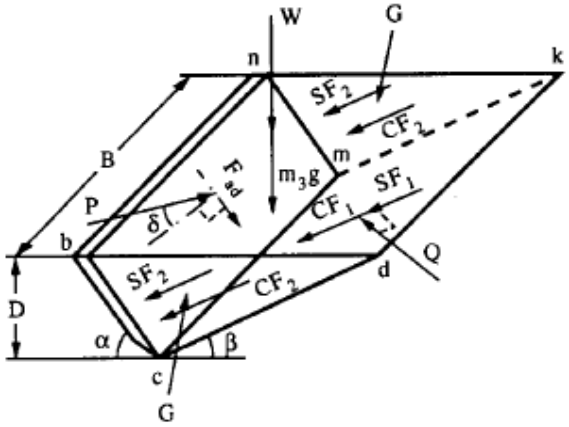

Figure 2.60. The forces acting on the wedge in front of the cutting edge of the blade, from Qinsen & Shuren (1994).

The authors divided the soil cut on the ground into a soil pile moving on the ground (fgde), and the soil sliding up between the blade and the soil pile (abdgf). This is helpful in determining forces in the soil sliding up along the blade acting on the wedge beneath. Different relationships for the various vector forces are set up in the article. The authors assumes that, according to the passive earth pressure theory, a passive failure occur when the resistance by the soil wedge is minimum. In the paper the rupture surface is assumed, from observations, to be a plane (c-d in figure). Below are the resultant forces on the blade presented, draft force, F_x and vertical force, F_y.

$$F_x = P \sin(\alpha + \delta) + F_{f1} + F_{c1} \quad (2\text{-}25)$$

$$F_y = P \cos(\alpha + \delta) - (P_{f2} + P_{ad}) \quad (2\text{-}26)$$

The resultant forces are the maximum forces in the soil cutting process. According to the authors cohesive forces (CF1 and CF2) acting on the wedge change after the blade is fully loaded. This causes the resultant forces on the blade to vary with change of displacement of

the blade. Since it is difficult to mathematically model this fluctuation of forces the authors assume that the blade cutting depth change with the cohesive forces. It is assumed that the blade is cutting soil on the inclined plane at a variable depth of the cutting blade, changing from a maximum to a minimum of depth. Although the supposition does not agree with the actual process, the result of the supposition is similar to that of the actual process. Thus the depth, D of the cutting blade in the expressions for the cohesive forces varies with change of time:

$$D(t) = V\,(t - NT_0)\tan(\beta) \qquad (2\text{-}27)$$

where V is the velocity of the blade, t is the time, T_0 is the period of D(t) and N is the number of times of T_0 repetition. $T_0 = D\cot(\beta) / V$ and $N = \text{int}(t / T_0)$.

Laboratory experiments where performed to examine the validity of the model. Soil cutting tests were conducted in a soil bin with Loess, a kind of sandy clay from China, with moisture content of about 16% and density of 1,753 g/cm^3. Tests were performed at velocities ranged from 0 to 5 km/h and the reaction force on the blade was sensed by dynamometers. The cutting blade had a width/depth ratio of about 20. Results show on good agreement between predicted and measured values for draft and vertical forces.

The paper presents results of the effects of soil density and tool depth on the draft force. It is claimed that both the mean draft force and the fluctuation amplitude of the draft force vary as the soil density varies, see Figure 2.61 and Figure 2.62. Though, according to the results presented, it is not clear whether it is the soil density or the tool depth that affects the fluctuating amplitudes of the draft force.

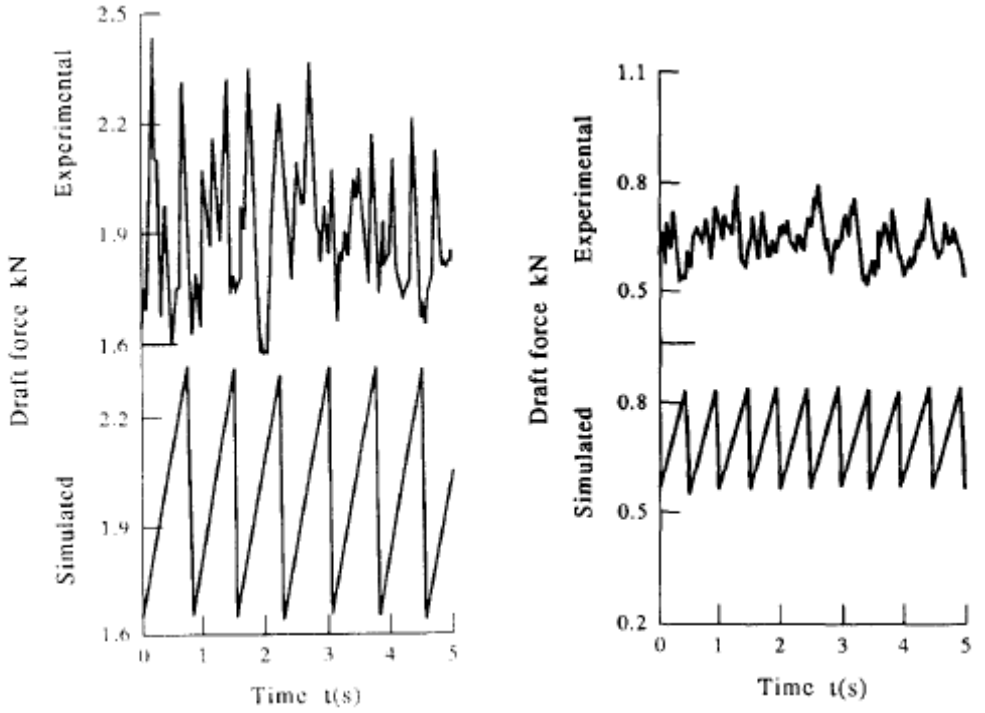

(D = 30 mm, γ = 1.85 g/cm^3, V = 0.223 m/s) (D = 23 mm, γ = 1.62 g/cm^3, V = 0.252 m/s)

Figure 2.61. Comparison of the fluctuations of observed and predicted draft force, from Qinsen & Shuren (1994).

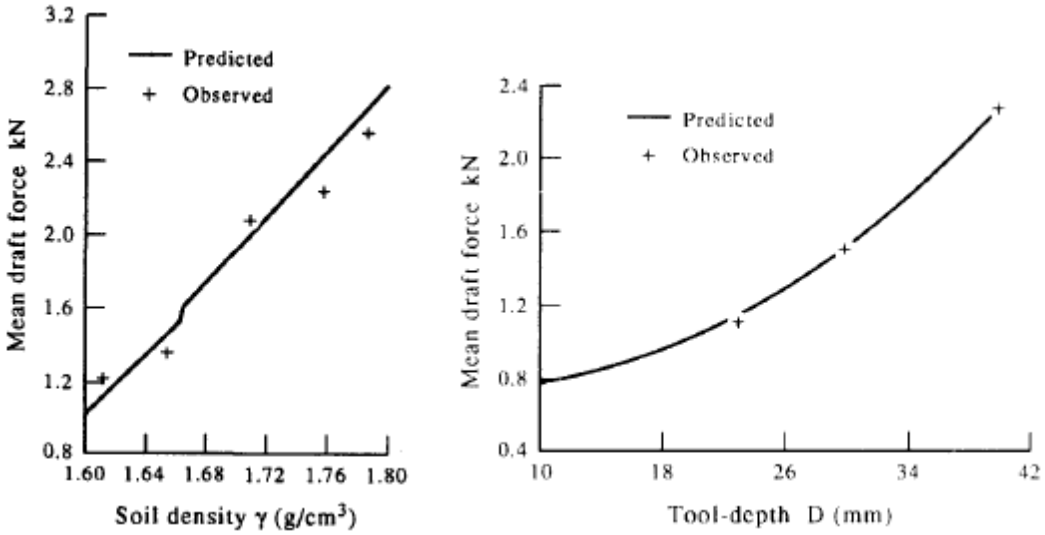

Figure 2.62. Comparison of the mean observed and predicted draft force as related to soil density (left) respectively tool depth (right), from Qinsen & Shuren (1994).

The results also show that the frequency of fluctuation of the draft force is considerably affected by the velocity of the blade, see Figure 2.63.

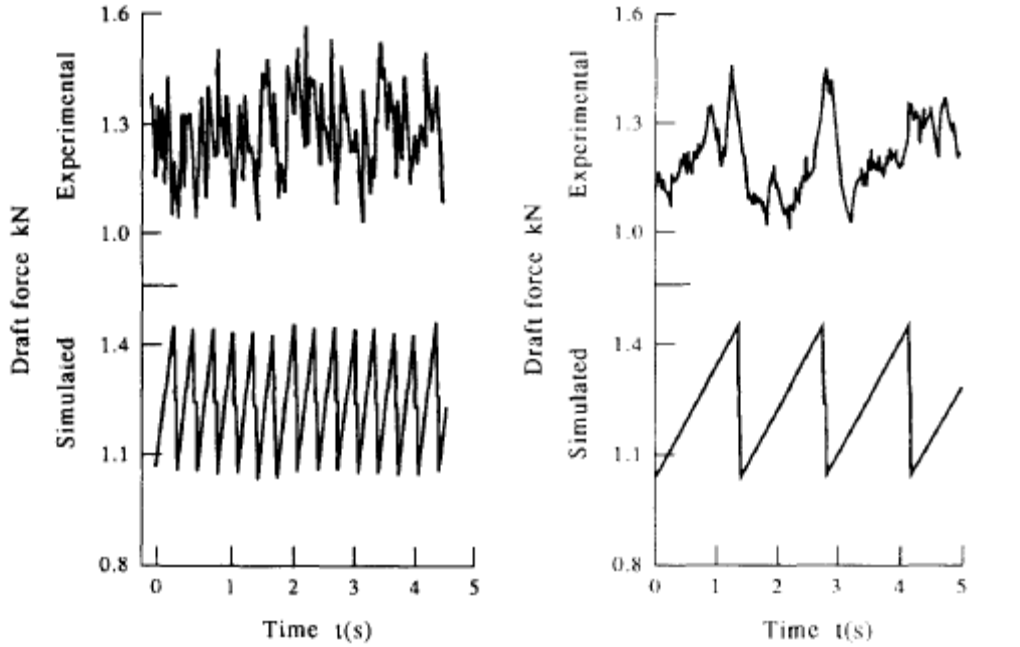

Figure 2.63. Comparison of the fluctuations of observed and predicted draft force. Velocity low (left) and high (right), from Qinsen & Shuren (1994).

The model cannot predict the force on the blade when the velocity of the blade is high because it is formulated neglecting soil inertial forces. When velocity is low (< 20cm/s), the mean draft force do not essentially vary with the change of velocity. When velocity is high (> 30 cm/s), the experimental results increase but predicted results remain unchanged, as the velocity increases, see Figure 2.64.

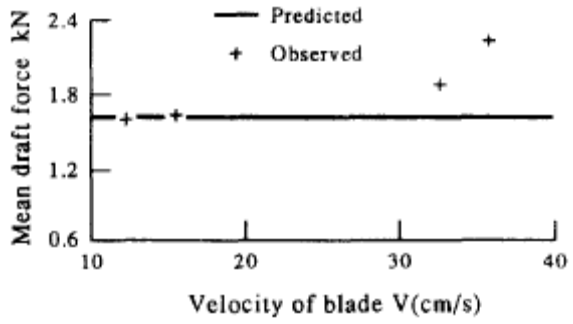

(D = 15 mm, γ = 1.86 g/cm^3)

Figure 2.64. Comparison of the mean observed and predicted draft force as related to velocity, from Qinsen & Shuren (1994).

2.4.3 Results from experiments in the literature with blades

In this chapter results from experiments in some studies have been gathered and presented. These studies concerns experiments with narrow and wide blades and show the effects from different parameters on the horizontal force on the blade. In this study we are interested in the horizontal force needed to break the soil loose from the ground. This occurs after a short displacement and no soil have accumulated in front of the blade. The effect from parameters like blade depth, blade width, blade angle, speed and different soil properties are presented. The experiments are performed in clay, sand or sandy clay. A two dimensional analysis is considered in this study. Most experiments have been performed with wide blades (w/d ratio > 10), though, in a few cases the w/d ratio has been between 1 and 5. Some experiments have been carried out with blades in a glass sided box, having a w/d ratio of about 1. In a glass box, where the box sides are along the sides of the blade, the soil is assumed to move forward and a two dimensional analysis can be considered.

Yong and Hannah (1977) presented force-displacement curves for experiments in a glass sided box with clay soil, see Figure 2.65. The values are compared to values predicted by a two dimensional finite element model.

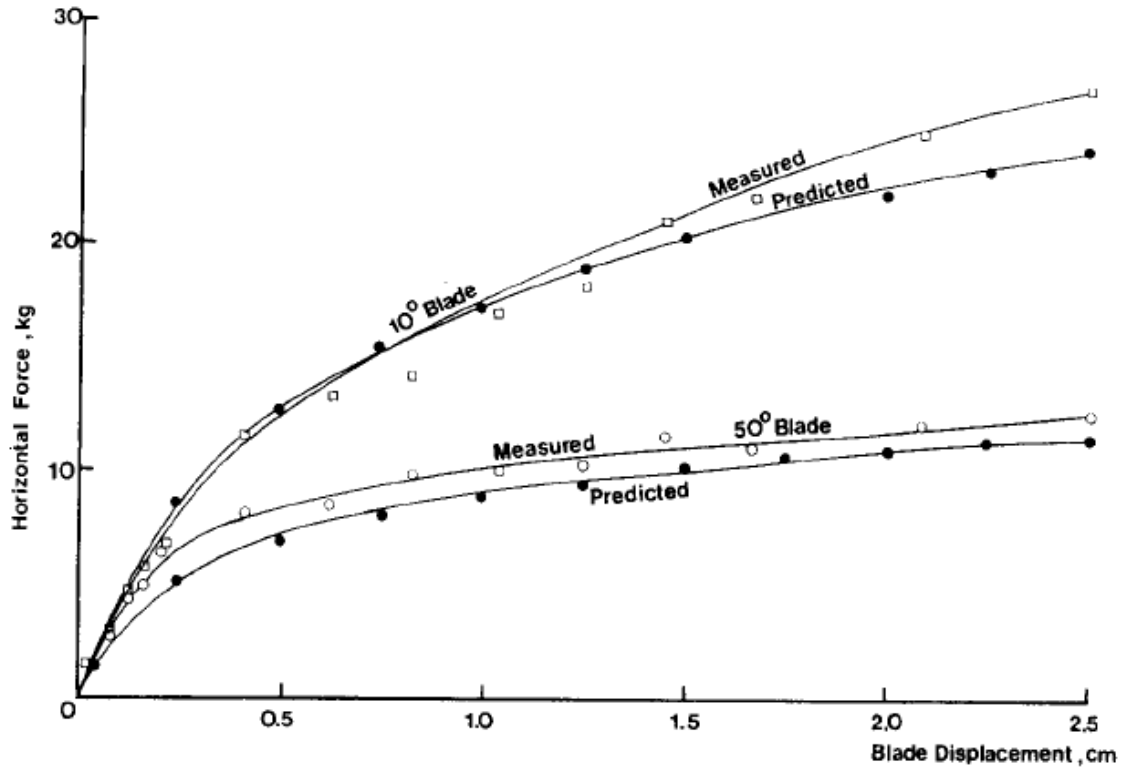

Figure 2.65. Force – displacement curves in clay soil, from Yong and Hanna (1977). Blade angles inclined 10 respectively 50 degrees to the vertical.

2.4.3.1 Effect of blade depth

Results from laboratory experiments with a wide blade in sandy clay (loess) by Qinsen and Shuren (1994), show on a slightly non-linear to linear increase of the horizontal force with depth, see Figure 2.66. The experiments were performed at a blade angle of 45° and in sandy clay with a bulk density of 1753 kg/m^3. Yong and Chen (1970) have achieved the same results in their experiments in sand.

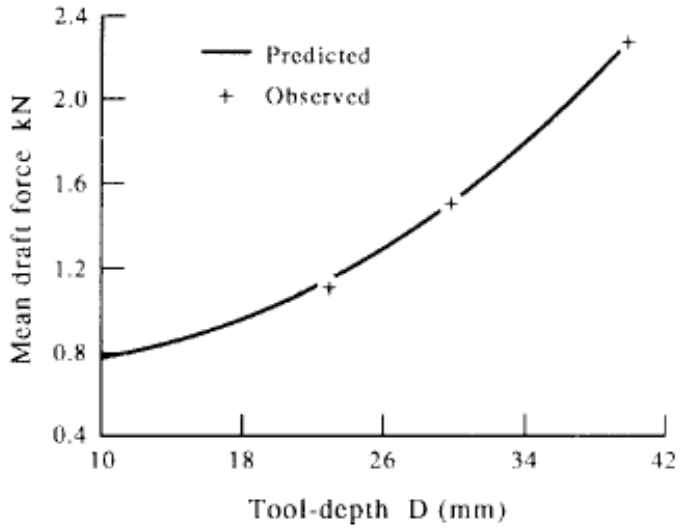

Figure 2.66. Increase of horizontal force with depth in sandy clay, Qinsen and Shuren (1994).

2.4.3.2 Effect of blade width

Results from laboratory experiments in sand performed by McKeys and Ali (1977) shows that the horizontal force increases with the width of the blade, see Figure 2.67. These experiments were conducted at a w/d ratio ranging from 1 to 5. The results seem to show on a linear relationship. Experiments were performed in moist sand with a soil friction angle of φ=35°, soil-interface friction angle of δ=23°, cohesion, c=0.023 kg/cm^2, soil-interface adhesion, c_a=0 and bulk density of γ=0,00153 kg/cm^3.

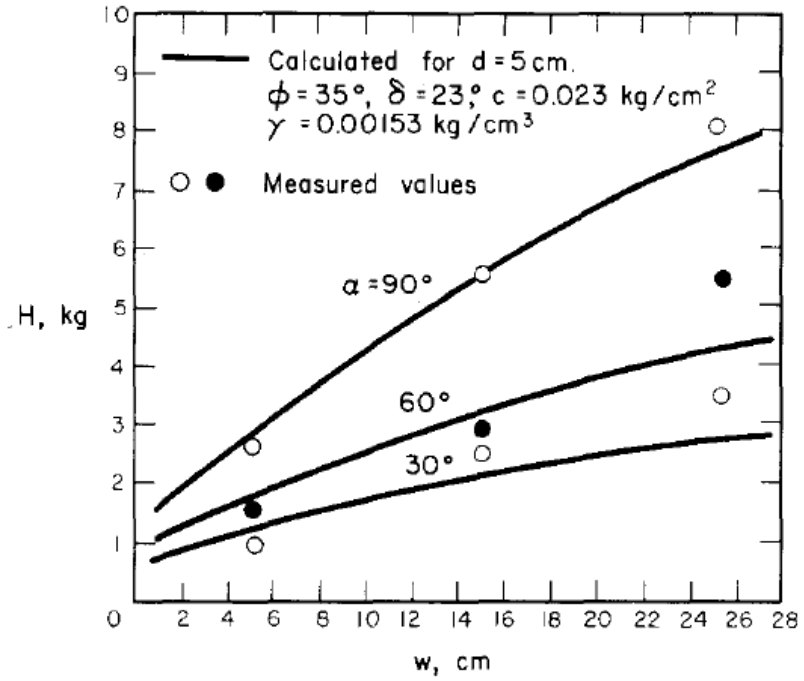

Figure 2.67. Values from experiments performed in sand, by McKeys and Ali (1977).

2.4.3.3 Effect of blade angle

Experimental results by Osman (1964) presented by Hettiaratchi (1965) shows that the horizontal force increases with rake (blade) angle in both clay and sand, see Figure 2.68. The increase is slightly nonlinear, which also is shown in the results from McKeys and Ali (1977) in sand, see Figure 2.37 in Chapter 2.4.1.4.

In Figure 2.69 and Figure 2.70 results from experiments in clay soil in a soil bin is presented, Yong and Hannah (1977). The experiments are performed in a soil glass box allowing for a two dimensional analysis. The horizontal force increases with displacement as well as blade angle. It is shown that the vertical force is negative when the blade has an inclination between 70 and 80 degrees with the horizontal (10 to 20 degrees with the vertical). This means that the soil will force the blade upwards for large blade angles.

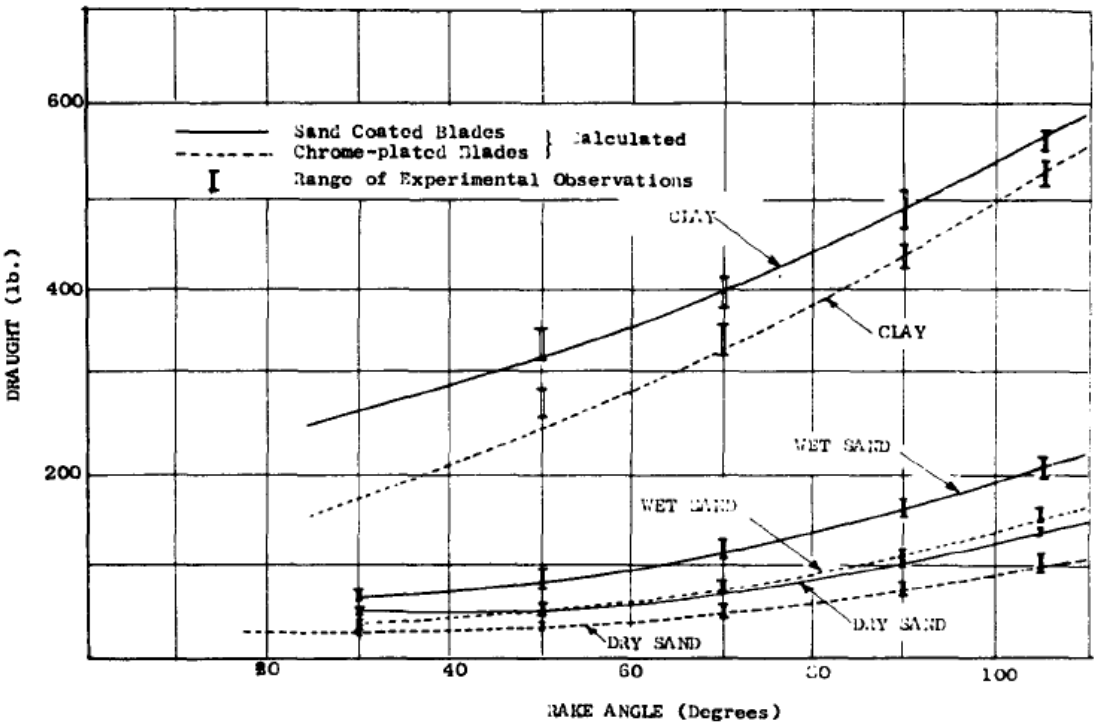

Figure 2.68. The increase of the horizontal force with increasing rake (blade) angle in both clay and sand, proposed by Osman (1964), according to Hettiaratchi (1965).

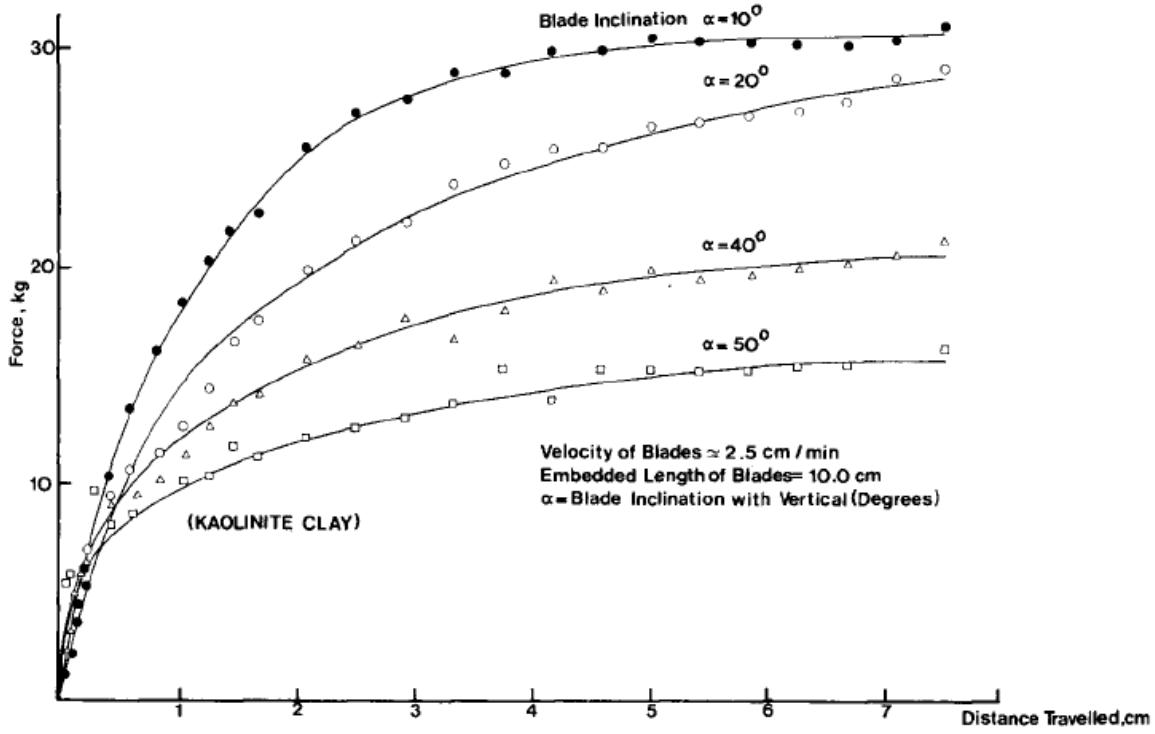

Figure 2.69. Variation of the horizontal force at different blade angles, Yong and Hannah (1977).

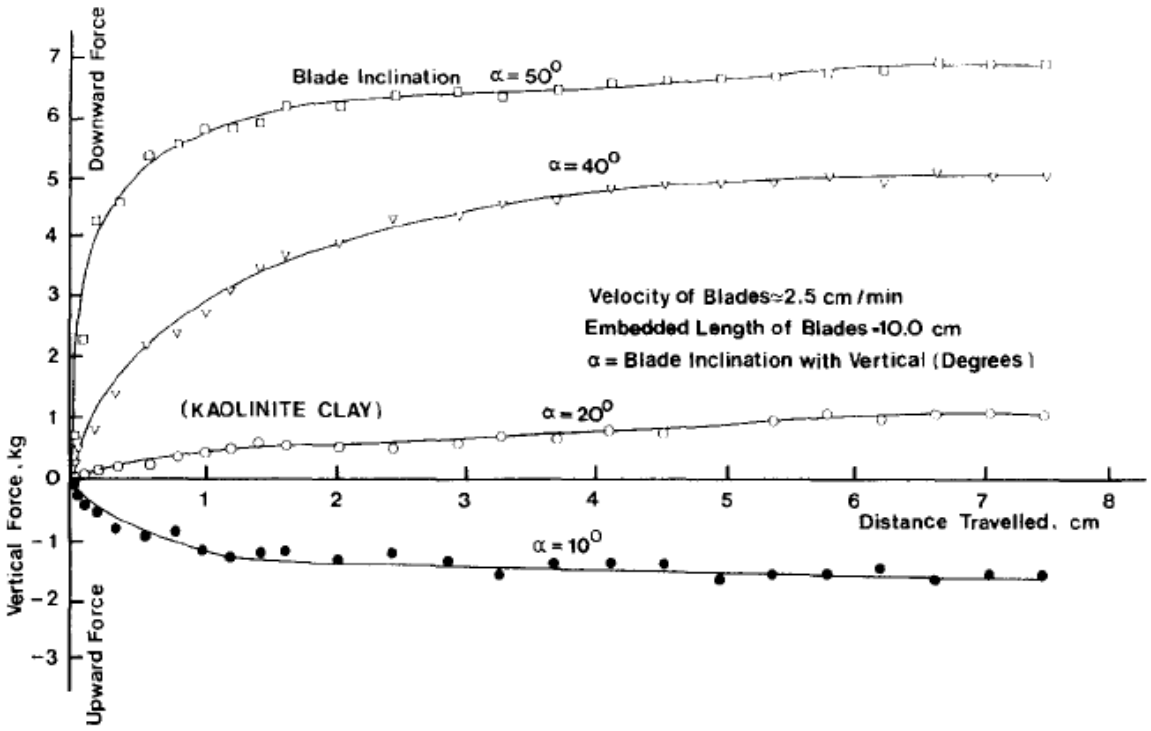

Figure 2.70. Variation of the vertical force at different blade angles, Yong and Hannah (1977).

2.4.3.4 Effect of soil properties

According to experimental results from Osman (1964), presented by Hettiaratchi (1965), the ratio between the horizontal and gravitational force is affected by the soil friction angle and soil-tool friction angle. It seems like the horizontal fore increases non-linearly with increasing soil friction angle, if it is assumed that the gravitational force is constant.

Results from Qinsen and Shuren (1994) shows that the horizontal force increases linearly with increasing soil density in sandy clay (Loess), see Figure 2.71.

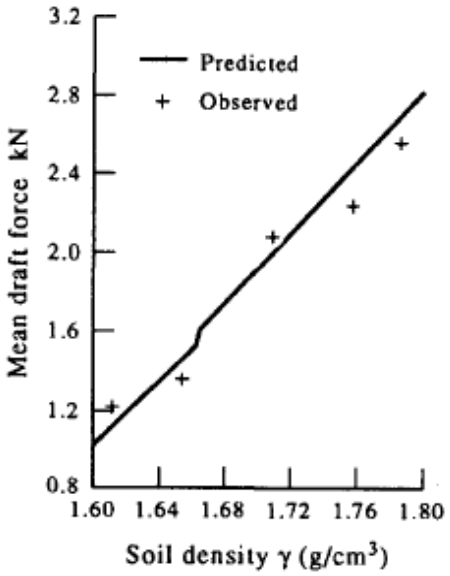

Figure 2.71. Results from experiments in sandy clay by Qinsen and Shuren (1994).

Godwin and Spoor (1977) have conducted experiments with a narrow blade (w/d < 1) in loose (uncompacted) and compacted sand, see Figure 2.72. The result shows the difference in magnitude of the horizontal force between the uncompacted and compacted sand with a factor of about 10. It is not clear if the force increases linear or nonlinear with width in compacted sand. Even though a narrow blade is used it is reasonable to believe that the same effect would show for a wide blade.

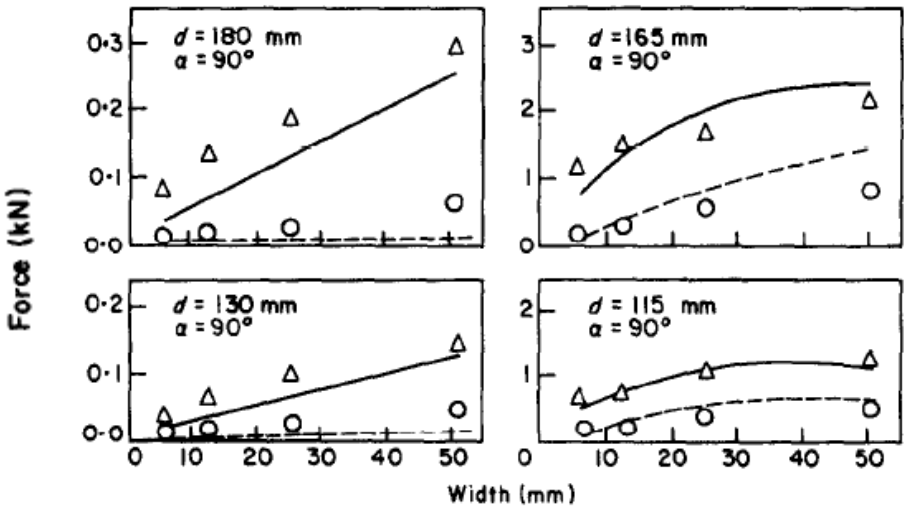

Figure 2.72. Experimental and predicted values in uncompacted (left) and compacted (right) sand, Godwin and Spoor (1977). Circles shows the vertical measured force, triangles shows the horizontal measured force and lines shows predicted values.

Jafari (2008) presents results from numerical modelling of a narrow blade displaced in soil, see Figure 2.73. The effect of soil properties on the horizontal and vertical forces was investigated through a parametric study. It is shown that an increase of the cohesion and friction angle of the soil will cause an increase of the horizontal and vertical forces on the blade. A variation of Poisson's ratio between 0,1 and 0,33 have not yielded significant

changes of the forces. Even though a narrow blade was studied the same trend but with another magnitude of the horizontal force would appear for a wide blade. Therefore the results are interesting.

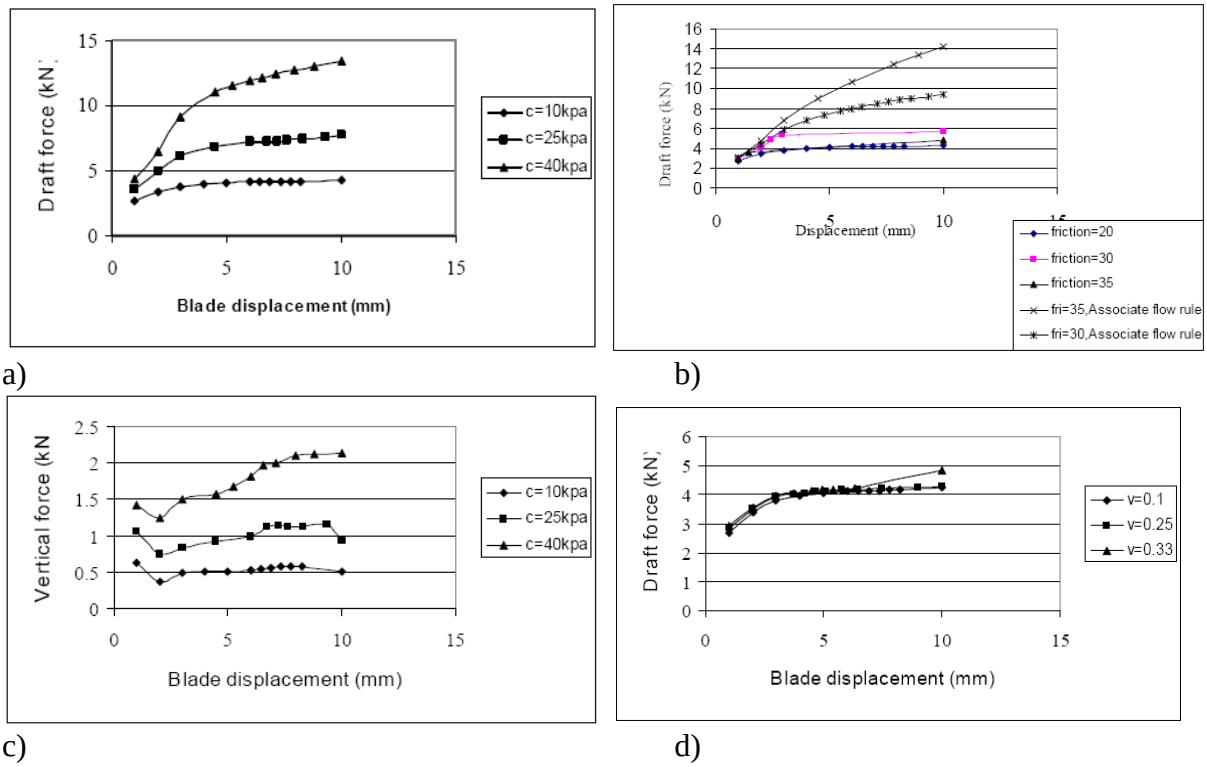

Figure 2.73. Variation of the horizontal force with blade displacement for different values of a) cohesion, b) soil friction angle and d) poisons ratio. In c) the variation of the vertical force for different values of cohesion is displayed. From Jafari (2008).

2.4.3.5 Effect of speed

According to experimental results in clay soil from Dechao and Yusu (1992) and Qinsen and Shuren (1994) the horizontal force increases with velocity of the blade, see Figure 2.74 and Figure 2.75. The vertical force decreases with velocity. The experiments by Dechao and Yusu (1992) were performed at a w/d ratio of 3,75.

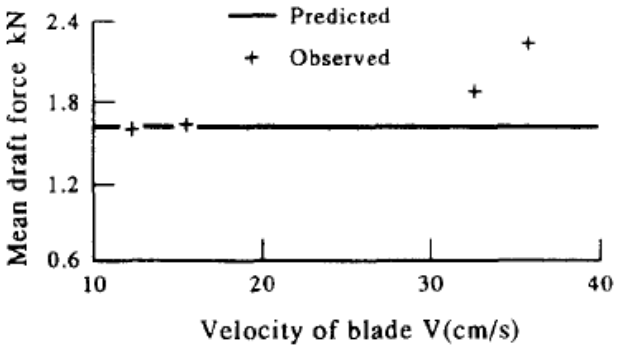

Figure 2.74. Results from experiments in sandy clay, from Qinsen and Shuren (1994). Cutting depth, D = 15 mm, unit weight, γ = 1,86 g/cm^3.

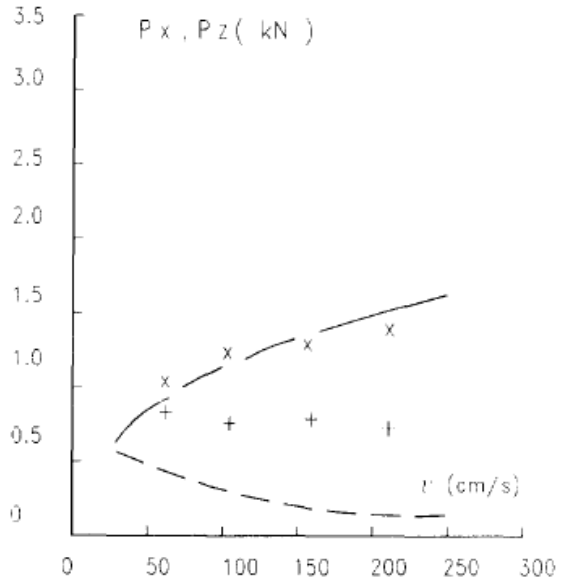

Figure 2.75. Experimental (x – horizontal force, + – vertical force) and predicted results in clay from Dechao and Yusu (1992).

2.4.4 Buckets

In the past three decades a significant amount of research has been carried out in the area of automation of excavating machinery, Hemami et al. (2009). Automatic excavation is interesting for industries like construction, mining and road work because the possibility of increasing cost-effectiveness and safety for workers as well as working in hazardous places, Hemami (1995). Autonomous loading or excavation concerns the functions of loading, navigating, obstacle detection, obstacle avoidance and unloading. Research conducted in the area are related to and can be categorized on the following aspects: type of excavating machine, application, control methodology, sensors and machine instrumentation, actuation and feedback, force or power analysis and motion analysis, Hemami (1995). In this study the resistance of the soil during excavation is of interest. Below some studies concerning methods and models for estimating the resistive forces on buckets during excavation are presented.

In this chapter force prediction models by Hemami (1994), Luengo et al (1998) and Ericsson & Slättengren (2000) are presented. Singh (1995), Singh (1997) and Blouin et al (2001) discuss different aspects of excavation as well as force prediction. Nezami et al. (2007) have performed some discrete element simulations of a wide bucket excavating in a soil pile and compared the results to ones achieved through laboratory experiments. In the Volvo GPPE performance manual (2009) excavatability and bucket filling is discussed.

2.4.4.1 Hemami (1994)

Hemami (1994) have performed an analysis of the various forces involved during the scooping and loading operation of a Load-Haul-Dump loader. In the paper these five forces were defined related to the motion and dimension of the bucket. The force due to weight of the loaded material, f_1, has been discussed in detail. Hemami declares that in order to perform

automatic excavation effectively it is necessary to make the tip of the bucket to follow an appropriate curve as it counteracts with the resistive forces and torques. Therefore information is needed about the path of the cutting edge and about the forces and torques acting on the bucket. The motion of the bucket during loading is defined by a basic nominal trajectory causing a rotation of the bucket, see Figure 2.76. When the bucket moves in the trajectory forward and upward translations are needed because of the heterogeneity of the material loaded and to avoid obstacles, like large pieces of rock, encountered.

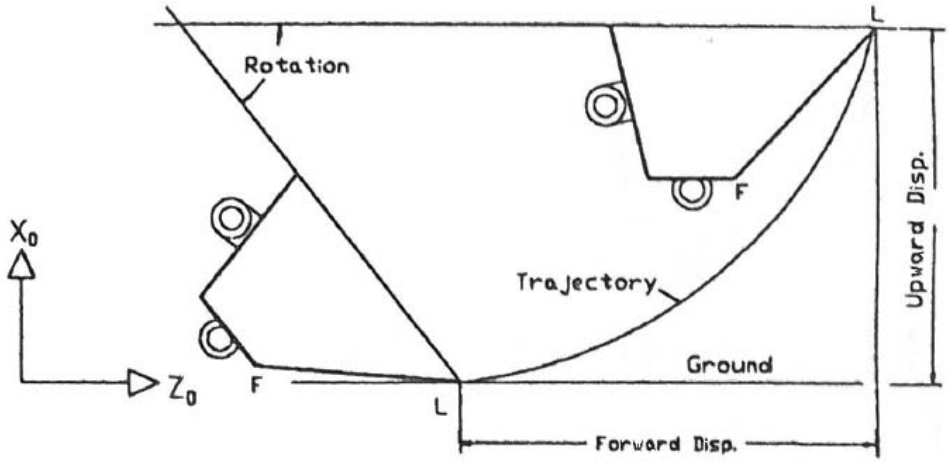

Figure 2.76. Bucket trajectory during loading, modified from Hemami (1994).

Forces and torques, acting on the bucket, changes continuously during the scooping and loading action. Hemami defines four forces acting on the bucket, see Figure 2.77 (left): the weight of the loaded material, f_1 the resistance to compaction of the unloaded material, f_2 the friction on the walls of the bucket, f_3 and the penetration and cutting resistance, f_4. In order to move the loaded material also the inertia force has to be considered, f_5, see Figure 2.77 (right). Below the various forces are discussed in detail.

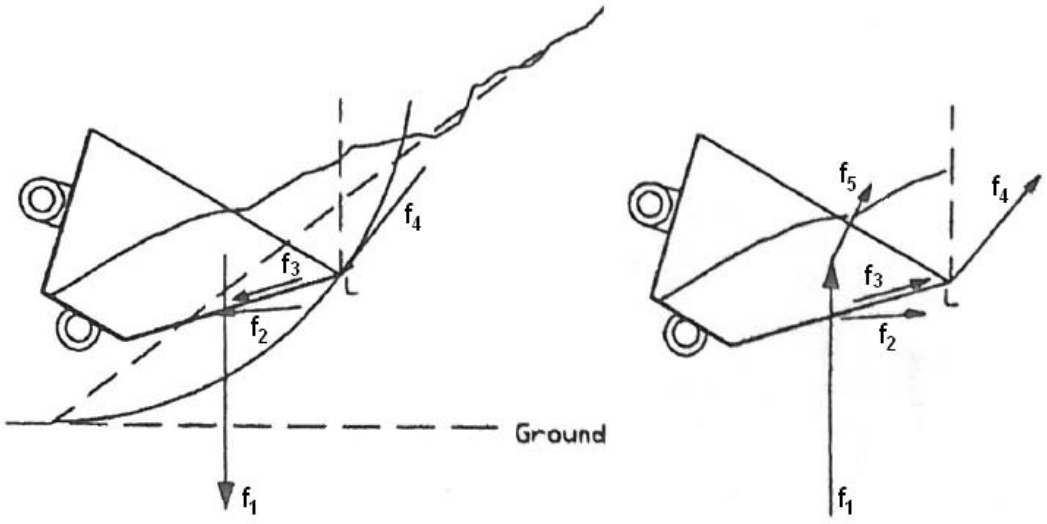

Figure 2.77. Forces involved in loading action, modified from Hemami (1994). Resistive force components from material (left) and forces to be overcome by the bucket (right).

The force to compensate for the weight of the loaded material, f_1 acts in the centre of mass and varies in magnitude and acting point with the motion of the bucket. The force is related to the volume of the loaded material, at each instant of motion. Calculating per unit width of the bucket, the area of the loaded material can be divided into two parts: A_1 (LFF'L') and A_2 (MLL'), see Figure 2.78. A_1 and A_2 are then defined as:

$$A_1 = {}_0\int^{\beta} 0{,}5\ \rho^2\ d\beta \qquad (2\text{-}28)$$

Where β is the orientation of the bucket in relation to the horizontal line and ρ is an approximation of the length L'L as the orientation of the bucket (β) changes during motion.

$$A_2 = 0{,}5\ \rho\ (l\ \tan(\nu) - h) \qquad (2\text{-}29)$$

Where ν is the slope of the pile, h is the upward displacement and l is the forward displacement of the bucket tip. The upward and forward displacements have been determined by Hemami and Daneshmend (1992). The calculation of point of action of f_1 been done in Hemami (1994).

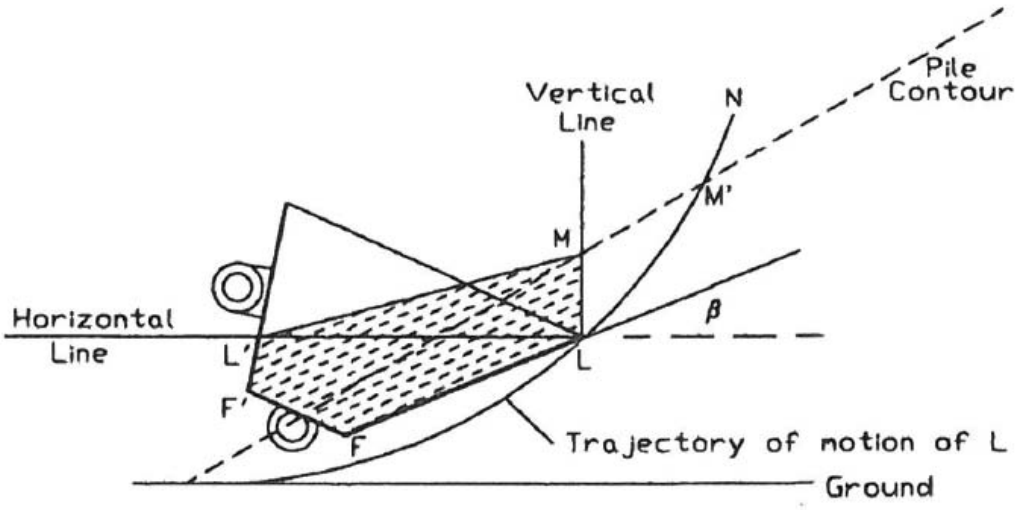

Figure 2.78. Modelling of the bucket and the loaded material in a general instant, according to Hemami (1994).

The resultant force due to compaction resistance of unloaded material, f_2 depends on the motion of the bucket. It develops if the bucket motion is such that the bucket has a direct pressure on the material. It pushes the material to make room for the bucket.

The resultant force due to friction on the walls of the bucket, f_3 acts in the opposite direction as the motion of the bucket. The magnitude of the force depends on the size of the area of the bucket in contact with the material and the coefficient of friction between the bucket and the material. According to Hemami a basic approximation of this force could be that it increases linearly from zero at the starting point to a maximum when the sides and the front are in contact with the material. Then it decreases linearly to zero at the end point, the highest point of the trajectory.

The digging resistance of the material, f_4 depends on the cutting edges and the material properties. This force acts on front and side cutting edges of the bucket. The specific digging resistance is referred to the resistance (depending on physical and mechanical properties of the material) for a unit length of bucket edge. According to Hemami (1994) the understanding of the basic principles of digging and scooping is not yet developed. Blouin et al. (2001) have defined this force as the penetration – cutting force. Hemami declares that when pushing a bucket into soil both f_3 and f_4 develops whereas when the bucket is withdrawn from the soil only f_3 exists.

The force to move the material inside and above the bucket, f_5 is concerned with the acceleration of the material as the bucket follows a trajectory. This force depends on the weight and acceleration of the material (the inertia) at each instant. The calculation of the force has not been performed by Hemami (1994).

According to Hemami (1994) these five forces presented varies during the scooping and loading process. At each instant of time the magnitude of these forces have to be provided in order to control the motion of the bucket.

2.4.4.2 Singh (1995)

In order to plan its actions a robotic excavator requires a method that allows it to predict the resistive forces that it experiences as it scoops the soil. In the paper a method for a robot to predict the resistive forces and to improve the predictions based on experience is presented. Singh proposes a two dimensional model presented by McKeys (1985) for cutting of soil with a wide blade to calculate the resistive forces. The model builds on passive earth pressure theory and the wedge theory of Coulomb. Even though the geometrical difference between a wide blade and an excavator bucket Singh prefer to use this model for a first analysis. Singh concludes, according to McKeys (1985), that the side-walls of an excavator bucket helps pushing the soil into the bucket and to constrain the failure to a volume directly ahead of the bucket. This indicates, according to Singh, that it is sufficient to use a two dimensional analysis, as for an infinitely wide blade. Though, Singh notes that there are other differences between modelling a flat blades and a bucket: The curved surface of buckets and blades captures the soil in front of the tool and after a certain amount of scooped material additional travel of the tool will result in compression, in addition to shearing, of the soil. Blades mostly perform at a constant depth opposed to excavation buckets which often operates in uneven terrain. Excavator tools will be required to rotate at various rates while soil cutting tools translate at a fixed orientation. Singh also concludes the disadvantages of using the soil cutting model chosen: The model ignores dynamic effects, it approximates the curved failure surface with a plane, it presumes a uniform surcharge of the failure wedge, it assumes the soil to not be confined and thus ignoring dilation of soil and it models the force just before failure which not always is the case.

2.4.4.3 Singh (1997)

This paper is a state of the art in automation of earthmoving and reviews work in different disciplines, such as: sensing technologies, remote operation, trajectory control, mechanism models and soil-tool interaction modelling. Singh divides excavation models into three categorize: Kinematic models, which use geometric relationships, for example relating the joint angles of an excavator or loader to the pose (location and orientation) of the bucket's tip. Dynamic models, which use relationships of quantities such as inertia, friction, cohesion and

acceleration, to relate joint torques to the motion of an excavator's limp. The third type of model characterizes the interaction between the tool and the soil. Singh concludes that soil behaviour is a very complex phenomena and soil can behave rather anisotropic. He identifies two issues in the work of characterizing the interaction between a tool and the soil. First: what happens when a bucket sweeps along a trajectory in the soil? Second: what is the affect of the terrain upon the tool? To the first question no model exists, to the second question it is possible to use a resistive force prediction model. Both questions can be solved using finite element methods, though, these methods are to slow for on-line evaluation of forces and other parameters.

According to Singh (1997) a large body of work exists on estimation of resistive forces acting on tools. He refers to research by Alekseeva et al. (1985) and Zelenin et al. (1985) trying to estimating the cutting resistance based on empirical results with different earthmoving machines. According to Singh (1997) also extensive literature is found on models for estimating forces experienced in tools needed for tillage of agricultural soil, referring to research by, for example, Reece (1964), Siemens et al. (1965), Luth and Wismer (1965) and Hettiaratchi and Reece (1967). Singh concludes that these models are based on theory of bearing capacity of foundations and developed for blades moving through soil with different tool geometries and orientations. Some literature has been found on the mechanics of a bucket moving through the terrain. Singh (1997) refers to research by Hemami (1994), Bisse et al (1995) and Malaguti (1994). Malaguti has proposed that the resultant resistive force is composed of the soil-penetration force, the soil-cutting force and the filling force. Singh concludes that the best estimation of resistive forces requires experimentally determined values. In situ tests provide the best results but also experiments with small scaled models of a tool give good predictions.

2.4.4.4 Luengo et al. (1998)

The paper presents a model for predicting resistive forces in an excavating bucket during excavation. The predicted forces are used in modelling the closed loop behaviour of a bucket in automated excavation. In the paper this model actually is made up of two models: a soil-force model and a force-tool model. The soil-force model is a reformulation of the soil cutting model by Reece (1964), in which the resistive force depends on soil and tool parameters. Reece (1964) model is improved in order to count for sloping ground and compaction of soil in the bucket during excavation. The force-tool model connects the force in the bucket with the pressure in the hydraulic cylinders when excavating in the soil. In the paper a method for estimating soil parameters φ, c, β and δ from measured force data is also presented. These parameters vary because topography and soil properties vary. It is essential to know these parameters in order to optimize the automated excavation process. Only the reformulated soil cutting model proposed by Luengo et al. (1998) will be reviewed.

Reece (1964) equation, that builds on bearing capacity theory of Terzaghi (1943), is presented below and the N – factors depend on soil frictional strength, tool geometry and soil-tool strength properties.

$$P = (\gamma b^2 N_\gamma + cd\, N_c + c_a d\, N_{ca} + qd\, N_q)\, w \qquad (2\text{-}30)$$

McKeys (1985) presented a variant of Reece (1964) equation, assuming a plane failure surface forming a wedge of soil in front of the blade. The resistive force was derived from static equilibrium of the wedge, see figure below.

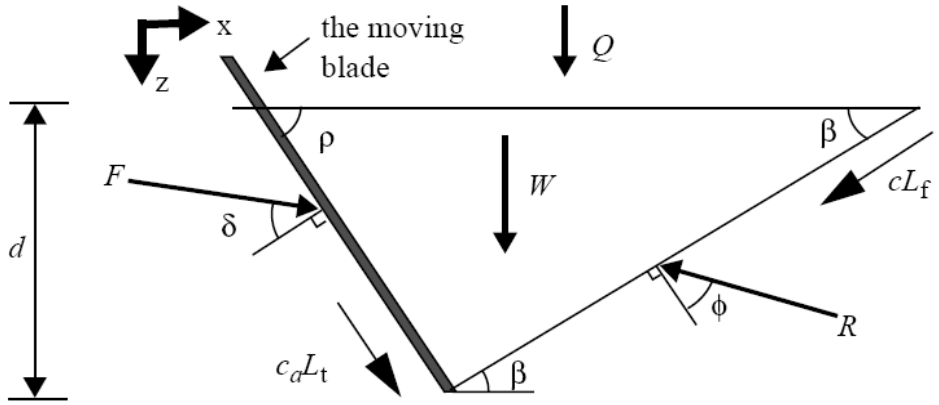

Figure 2.79. Static equilibrium analysis using an approximation of the failure surface, according to Luengo et al. (1998).

The components of the resistive force can be expressed:

$$F_x = F \sin(\rho+\delta) + c_a L_t \cos(\rho) - R \sin(\beta+\varphi) - cL_f \cos(\beta) = 0 \quad (2\text{-}31)$$

$$F_z = -F \cos(\rho+\delta) + c_a L_r \sin(\rho) - R \cos(\beta+\varphi) + cL_f \sin(\beta) + W + Q = 0 \quad (2\text{-}32)$$

Giving the total resistive force:

$$F = (W + Q + cd\,[1 + \cot(\beta)\cot(\beta+\varphi)] + c_a d\,[1 - \cot(\rho)\cot(\beta+\varphi)]) / \cos(\rho+\varphi) + \sin(\rho+\varphi)\cot(\beta+\varphi) \quad (2\text{-}33)$$

This equation can be formulated as Reece (1964) equation. The values of the N – factors will be different, because of the plane failure surface.

$$N_\gamma = (\cot(\rho) + \cot(\beta)) / 2\,[\cos(\rho+\delta) + \sin(\rho+\delta)\cot(\beta+\varphi)] \quad (2\text{-}34)$$

$$N_c = (1 + \cot(\beta)\cot(\beta+\varphi)) / (\cos(\rho+\delta) + \sin(\rho+\delta)\cot(\beta+\varphi)) \quad (2\text{-}35)$$

$$N_q = ((\cot(\rho) + \cot(\beta)) / (\cos(\rho+\delta) + \sin(\rho+\delta)\cot(\beta+\varphi)) \quad (2\text{-}36)$$

It is assumed that the sidewalls of the bucket do not allow shearing in direction transverse to the bucket motion. Therefore a two dimensional model can be used. Also it is assumed that the inertial forces of the soil are negligible since accelerations during digging are typically low. It is also assumed that the

In the paper a reformulation of McKeys (1985) variant of Reece (1964) model is performed to account for additional phenomena. In the model proposed by Luengo et al. (1998) the total force acting on the bucket has been decomposed into three main forces. The shear or cutting force, F_s, is the force to shear the soil away from itself. The gravity force, F_g, accounts for the total gravitational force acting on the bucket. The remoulding force, F_r, is the force required to remould and compress the soil in the bucket. Additional force is required as the bucket begins to fill up with soil, to form the soil in the bucket and then to compress it. The model by Luengo et al. (1998) accounts for a sloping ground, see Figure 2.80. This is made through the

terrain profile angle, α, affecting the N_w – factor. The terrain profile angle, α, is included in the blade angle, ρ. The volume of the material swept by the bucket, V_s, is defined by the shaded area in Figure 2.80.

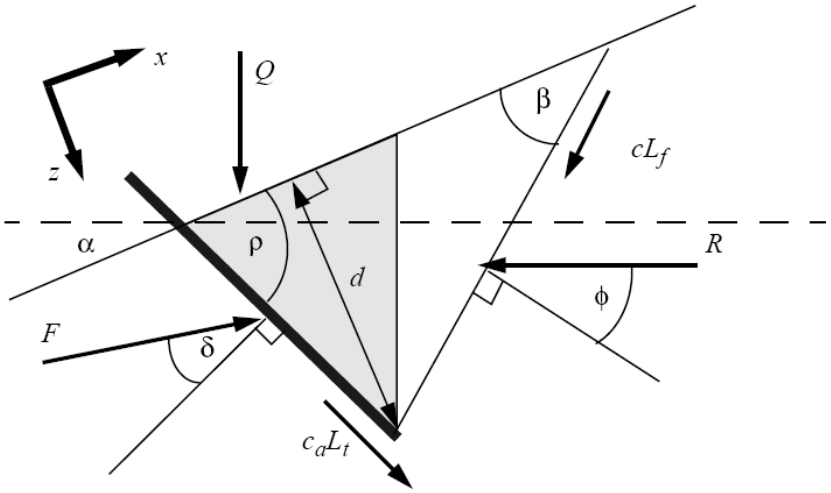

Figure 2.80. The reformulated model proposed by Luengo et al. (1998).

The reformulated equation proposed by Luengo et al. (1998) is written as:

$$F_s = d^2 w\gamma g N_w + cwdN_c + V_s\gamma g(N_q - 1), \quad (2\text{-}37)$$

where the N – factors can be calculated as follows:

$$N_w = ((\cot(\beta) - \tan(\alpha))(\cos(\alpha) + \sin(\alpha)\cot(\beta+\varphi)) / 2\,[\cos(\rho+\delta) + \sin(\rho+\delta)\cot(\beta+\varphi)] \quad (2\text{-}38)$$

$$N_c = (1 + \cot(\beta)\cot(\beta+\varphi)) / (\cos(\rho+\delta) + \sin(\rho+\delta)\cot(\beta+\varphi)) \quad (2\text{-}39)$$

$$N_q = (\cos(\alpha) + \sin(\alpha)\cot(\beta+\varphi)) / (\cos(\rho+\delta) + \sin(\rho+\delta)\cot(\beta+\varphi)) \quad (2\text{-}40)$$

The gravity force, F_g, and the remoulding force, F_r, can be expressed as:

$$F_g = V_s\gamma g \quad (2\text{-}41)$$

$$F_r = V_s\gamma g d \quad (2\text{-}42)$$

2.4.4.5 Ericsson & Slättengren (2000)

Ericsson and Slättengren (2000) propose a method of simulating forces acting on a wheel loader bucket when excavating gravel or other granulated material. The method has been implemented in a model for simulation of forces in lift and tilt cylinders of a wheel loader, using the computer software ADAMS. Excavation experiments in gravel have been performed and measured values show good correlation with predicted values. The authors identify different phases in the excavation process: the penetration of the gravel pile (2,5-4 s.), the cutting of soil (4-10 s.), the retraction of the bucket from the gravel pile (9,5-10 s.), the

driving phase when moving the soil (10-14 s.) and the unloading of the bucket (14-18 s.). See figures below.

The force model consists of three specific models that characterize the three first phases of the excavation process: the penetration pressure model, the soil cutting model and the inertia force. The penetration pressure model used by Ericsson and Slättengren (2000) is based on a model proposed by Bekker (1956) for continuous loading of a soil material.

$$P = ((k_c / b) + k_\varphi) z^n \qquad (2\text{-}43)$$

In this model z is the penetration depth, b is the blade width and K_φ, K_c and n are soil stiffness parameters, which can be derived in McKeys (1985).

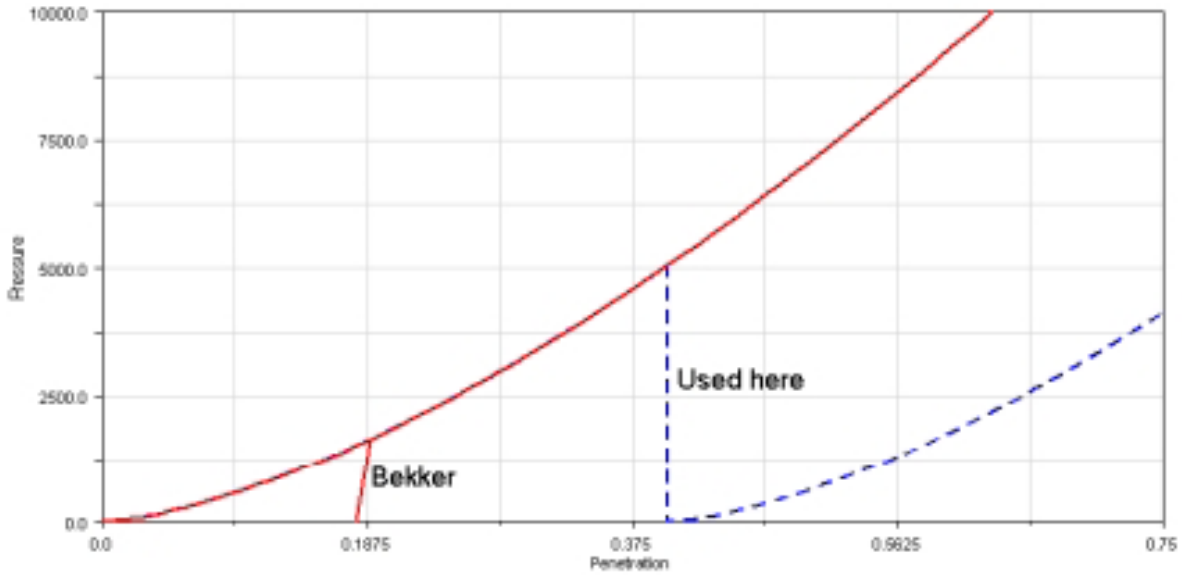

Figure 2.81. The increase of pressure (vertical axis) with penetration depth (horizontal axis) according to the model by Bekker (1956) and the proposed excavation penetration pressure model, from Ericsson and Slättengren (2000).

The soil cutting force and the volume of broken soil is determined through force equilibrium, see Figure 2.82. The authors assume a plane failure surface between b and c, noting that the failure plane more likely is a logarithmic spiral in reality.

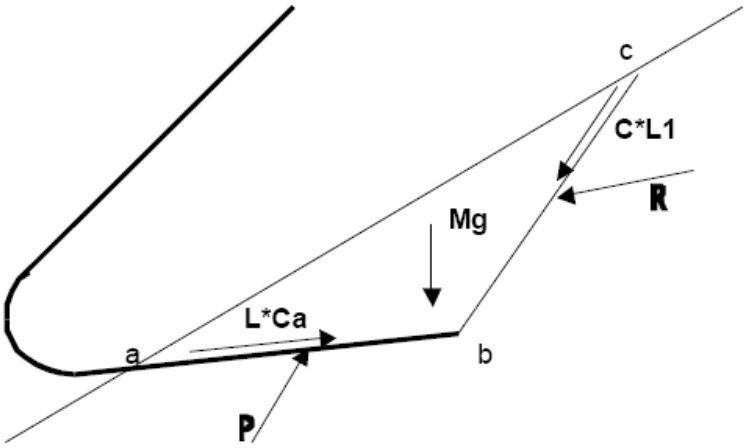

Figure 2.82. Forces acting on the soil wedge, from Ericsson and Slättengren (2000).

The system of equilibrium is solved numerically in each step where a break of the soil occurs and minimizes the breaking force P. The soil cutting force components are calculated for each time the bucket moves inwards and upwards.

$$F_z = P\cos(\delta-\alpha) + c_aL\sin(\alpha) - Mg - cL_1\sin(\beta+\theta) + R\cos(\varphi+\beta+\theta) = 0 \qquad (2\text{-}44)$$

$$F_x = P\sin(\delta-\alpha) + c_aL\cos(\alpha) - cL_1\cos(\beta+\theta) - R\sin(\varphi+\beta+\theta) = 0 \qquad (2\text{-}45)$$

Where θ is the angle of the pile relative to the horizontal plane, β is the cutting angle of the soil, angle a-c-b, α is the angle between the bucket and the horizontal plane, δ is the angle between the normal to the lower plane of the tool and the force P, and d is the penetration normal to the surface of the pile, the distance from line a-c to point b. Also $L = d / \sin(\theta - \alpha)$ and $L_1 = d / \sin(\beta)$.

The bucket will be loaded once a piece of soil is cut loose. When the bucket is retracted the pile will not support any overloading of the bucket. According to Ericsson & Slättengren (2000) the excessive material will then fall out and the volume of the material will be determined by the bucket angle and the allowed topping volume determined by the internal friction angle of the material.

The inertia forces acting on the bucket is calculated through the mass of the loaded material and the position of the center of gravity of the soil volume, F = m*a. The bucket angle determines the center of gravity position of the loaded material.

Measurements of cylinder forces during excavation in a gravel pile show on good correlation to predicted (simulated) values, see Figure 2.83 and Figure 2.84. Average gravel size was 35 mm. No other values of the soil parameters have been presented.

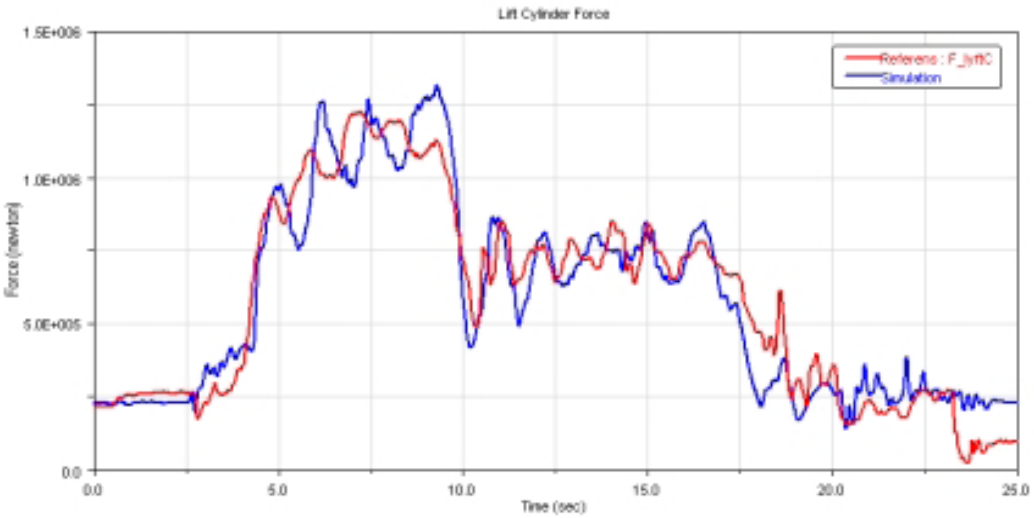

Figure 2.83. Correlation between measured (light red curve) and predicted (dark blue curve) lift cylinder forces, from Ericsson and Slättengren (2000). The vertical axis shows the force (N) and the horizontal axis shows time (s).

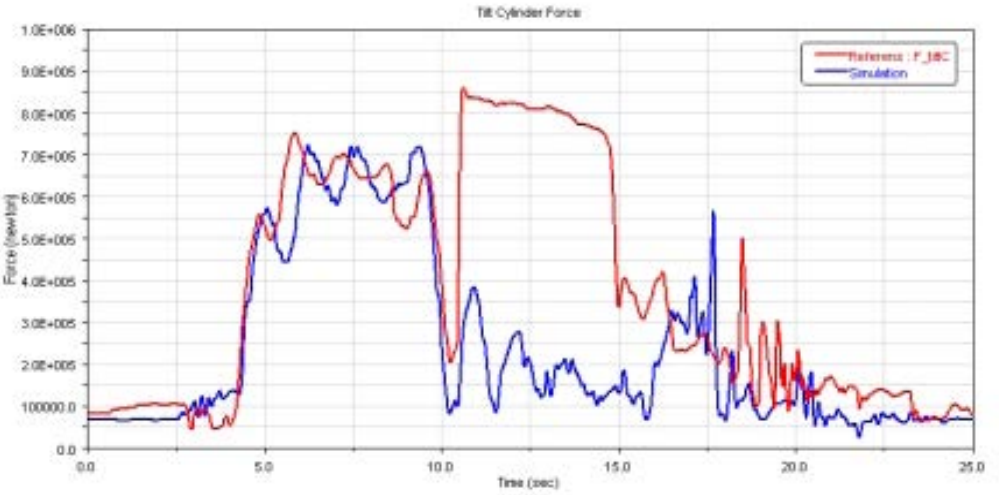

Figure 2.84. Correlation between measured (light red curve) and predicted (dark blue curve) tilt cylinder forces, from Ericsson and Slättengren (2000). The vertical axis shows the force (N) and the horizontal axis shows time (s).

2.4.4.6 Blouin et al. (2001)

The paper reviews previous work on forces on blades or buckets of excavation machines. Different models for penetration, cutting and excavating soil are reviewed and compared as well as common practices for characterization of soil and associated tool actions. The objective is to integrate formulations of penetration and cutting forces to those for excavation. This is to mathematically express the resistive force that a medium exhibits to a tool during excavation in terms of parameters of the medium, the tool and the tool motion.

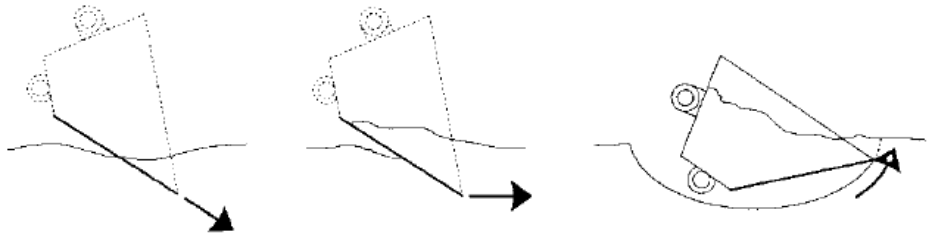

a) Penetration b) Cutting c) Loading (Excavation)

Figure 2.85. Earthmoving actions according to Blouin et al. (2001).

The authors define different earthmoving actions: penetration, cutting and excavation, see figure above. Penetration is the insertion of a single solid body into a medium of infinite depth. The tool is of longitudinal shape and the depth of operation is controlled. Cutting is a lateral motion of a blade-like body into a semi-infinite medium. The blade is working at a constant depth and the speed and the blade angle are constant. Blades are seen as narrow, wide or infinite wide and are considered infinitely wide when the width is about six times greater than the depth. Excavation is defined as the action of loading a bucket or a shovel comprising a combination of penetration, cutting the material, followed by scooping the material to remove it. Blouin et al. claims that a bucket can be defined as an infinitely wide blade since the bucket has sidewalls and almost no material moves perpendicular to the motion of the tool.

In earthmoving modelling the soil is generally assumed to be homogenous, continuous and isotropic, which almost never is the behaviour in reality. The soil characteristics can vary significantly due to, for example, geological differences causing the mechanical properties of a soil mass to change and the soil will be heterogeneous. Earthmoving actions causes large discontinuous strains in the soil mass which results in restructuring and alteration of the volume of voids, thus, the soil mass is not continuous. An isotropic behaviour means that the reaction of a medium to external stresses is not dependent on the direction of application. Though, this is not the case when bulk handling of undisturbed soil. Soil properties such as density, friction, cohesion and adhesion are important parameters when describing soil-tool interaction. Blouin et al. claims that these parameters are assumed to be constant during an earthmoving action. Though, when water is added to soil, the adhesion increases logarithmically with increasing soil-tool sliding speed. Blouin et al. claims that using elasticity and plasticity theory requires continuity of the medium. For a penetration task performed in a frictional soil (particulate medium) the plasticity theory does therefore not explain the phenomenon because the continuity assumption is invalid.

Cutting or excavation involves a failure of the soil. Shear failure is concerned when modelling the interaction of a cutting tool and a medium exhibiting a plastic behaviour. When cutting with a wide blade different mechanisms causes the force. The first mechanism is related to the acceleration of the material as the tool moves, the second mechanism considers the changing of the medium strength. Blouin et al. claims that it has been noted that resistive forces observed during cutting are of the same nature as those encountered during penetration. They also conclude that the exact relationship between penetration and cutting has not been determined yet.

In the paper of Blouin et al. (2001) various models for two- and three dimensional soil-cutting with blades are presented. Models from Osman (1964), Gill and Vanden Berg (1968), Swick

and Perumpral (1988) and McKeys (1985) are reviewed. In the models the effect from different parameters, such as weight, surcharge, cohesion, adhesion, soil friction, soil-tool friction and inertia, on the resultant force is considered.

In the paper also models for excavation with buckets are presented. In these models forces or parameters encountered during penetration and cutting are also considered. In addition forces related to the sides and the bottom of the bucket must be brought into account. Blouin et al. claims that excavation can be associated with the action of cutting with an infinitely wide blade and they conclude that there is little connection between the side effects of a blade and those of a bucket. Therefore two dimensional models are used in the formulation of the excavation models. In the paper of Blouin et al. (2001) models from Alekseeva et al. (1985), Zelenin et al. (1985), Hemami (1994) and Balovnev (1983) are presented. Different authors consider different force components in their models. In Figure 2.86 (a) Hemami (1994) defines the following resistive forces acting on a bucket during an excavation task: the weight of the material in the bucket (f_1), the compacting resistance of unloaded material (f_2), friction forces between the tool and the soil (f_3) and the penetration and cutting resistance (f_4). Though, in an excavation task also the inertia force for the loaded material (f_5) and the force to move the empty bucket (f_6) have to be considered as can be seen in Figure 2.86 (b). Hemami et al (2007) states that the penetration and cutting force, f_4 is the dominant force of the forces $f_1 - f_4$.

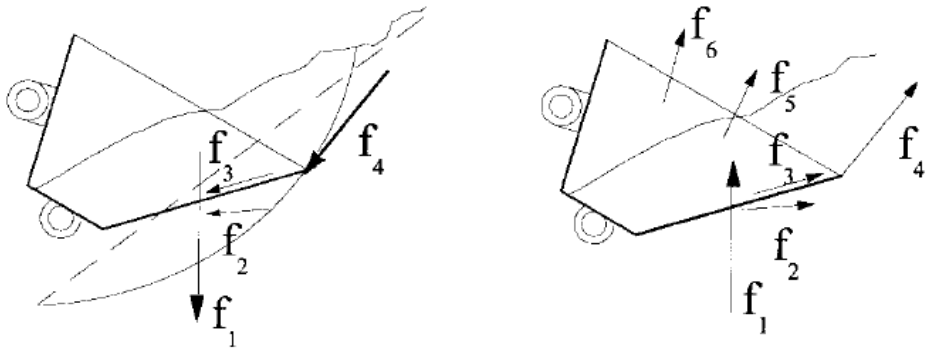

a) b)

Figure 2.86. Force components during a loading task, according to Blouin et al. (2001). (a) Resistive forces from the soil. (b) Forces needed to move the bucket.

The review of the soil cutting and excavation models in this paper is included in another paper of Lipsett and Moghaddam (2011). Lipsett and Moghaddam conclude that soil-tool interaction models assume soil to be homogenous and isotropic and that tools have simple geometries and steady motion through the soil. These are reasonable assumptions as long as the strain rate of the soil is not too high. If the strain rates are considerable, dynamic modelling of the soil-tool interaction is needed.

2.4.4.7 Nezami et al. (2007)

The paper presents a series of discrete element simulations that replicates laboratory experiments performed to measure the forces acting on a bucket of a front end loader. The experiments involved excavation in a soil bin with a bucket of 1/12 of scale of a real bucket of the 988G Caterpillar front end loader. Excavations were executed in a pile of gravel with

angular particles and sub-angular particles of different bulk density and internal friction angle (pile slope angle). The experiments were performed with different initial pile heights, initial bucket elevations and pile slope angles, see Figure 2.87.

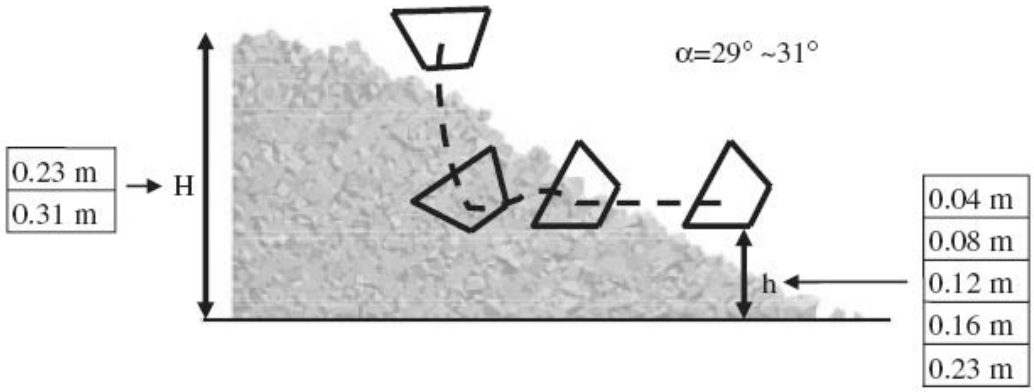

Figure 2.87. Bucket-soil experiment layout were α is the pile slope angle, from Nezami et al. (2007).

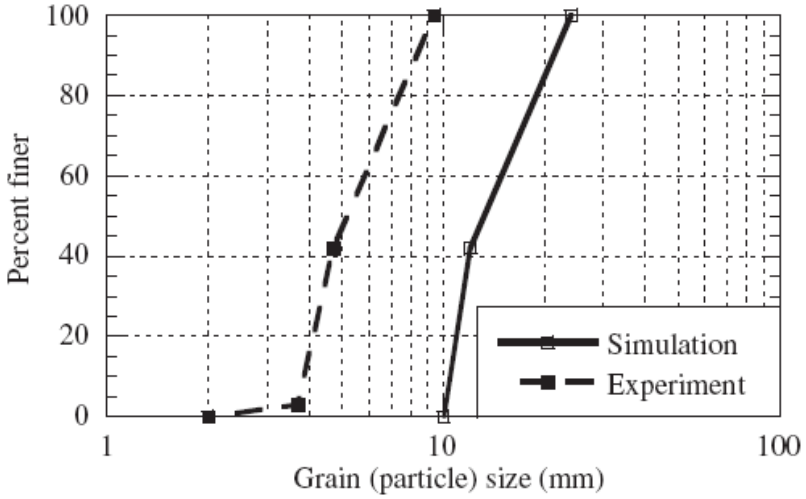

Figure 2.88. Grain size distribution of particles used in the simulation respectively the experiment, from Nezami et al. (2007).

Discrete element simulations were performed with polyhedral particles of six different shapes. The number of particles was the same for each shape. Nezami et al. claimed that particles with polyhedral shape better represents the geometry of the gravel particles than spherical particles or clusters do. The particle size in the simulations was about three times larger than in the experiments in order to keep computational effort low, see Figure 2.88. The inter-particle friction angle in the simulations was adjusted to the initial pile slope angle in the experiments. Nezami et al. concluded that the results from the experiments and the simulations were comparable and consistent, see Figure 2.89 and Figure 2.90. The horizontal forces increased initially as the bucket penetrated the gravel pile and then reduced to zero when the bucket left the pile. Vertical forces increased as the gravel particles entered the bucket. Nezami et al. claimed that the (initial) difference between the simulated vertical force and the experimental vertical force was due to larger particle size in the simulation.

Simulations with particles of smaller size showed that the simulated vertical force approached the experimental vertical force.

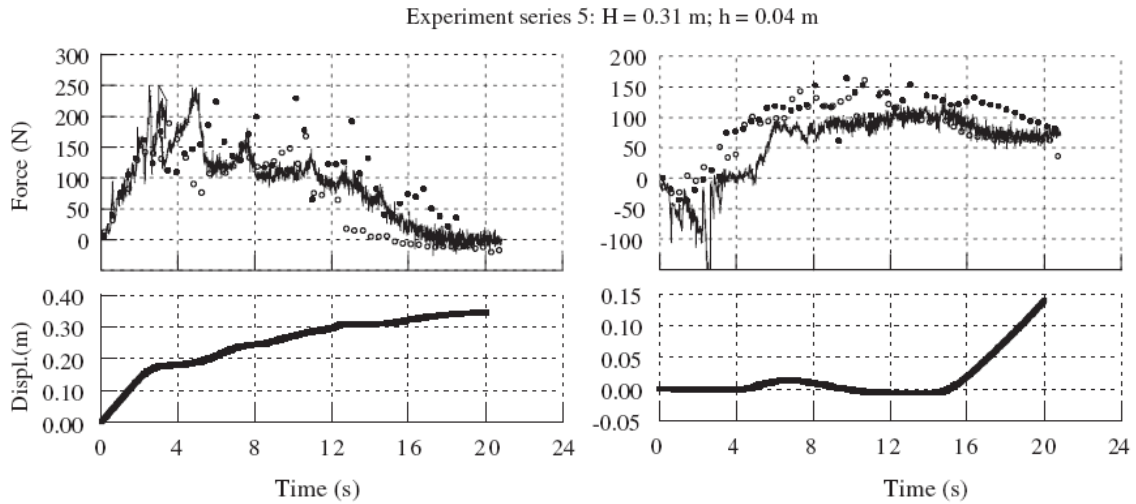

Figure 2.89. Simulated and measured bucket forces and bucket displacement trajectories. Initial elevation of bucket, h = 0,04 m. Horizontal force (left) and vertical force (right). Experiment with angular particles (circles) and sub rounded particles (dots) and simulations (solid line), from Nezami et al. (2007).

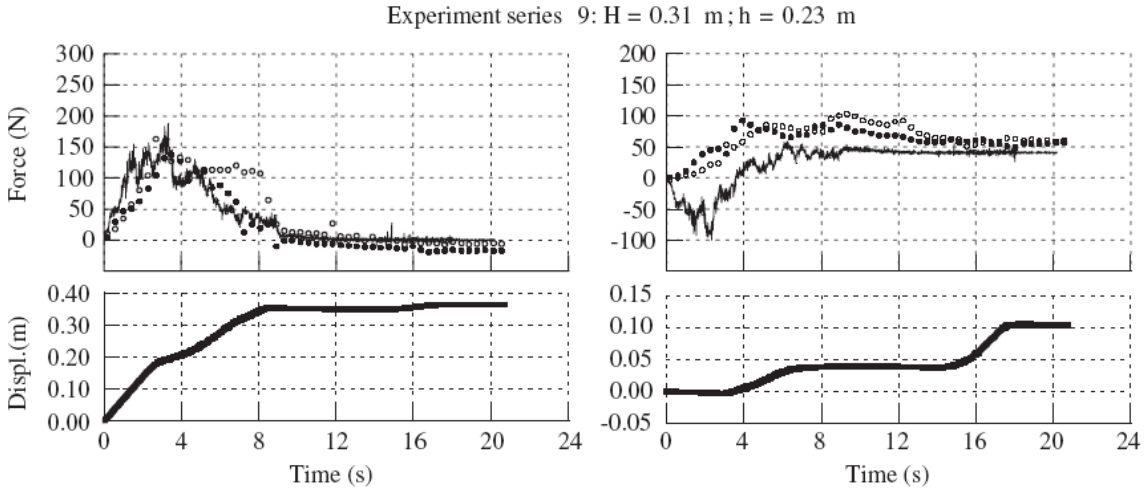

Figure 2.90. Simulated and measured bucket forces and bucket displacement trajectories. Initial elevation of bucket, h = 0,23 m. Horizontal force (left) and vertical force (right). Experiment with angular particles (circles) and sub rounded particles (dots) and simulations (solid line), from Nezami et al. (2007).

2.4.4.8 Volvo GPPE performance manual (2009)

The manual is an aid in predicting the cycle time, production and cost for moving materials with excavators, wheel loaders or dumpers (articulated haulers). In the book excavatability of different materials (excavation classes), bucket filling and choice of appropriate bucket is discussed.

In Volvo GPPE performance manual (2009) different materials are classified according to the excavatability of the material. Soil and rock material is grouped into excavation classes from 1 through 5, see Table 2.14. Class 1 involve little resistance to loosening the soil and a high degree of filling the bucket which indicates high performance of loading equipment. Class 5 concerns high resistance to loosening the soil and a small degree of filling the bucket which indicates low performance of loading equipment. For excavation of class 5 material blasting or ripping is required.

Table 2.14. Classification of material according to its excavatability (diggability), modified from Volvo GPPE performance manual (2009).

Class	Characteristic	Example of material
1	Easy digging	Unpacket earth, sand-gravel, ditch cleaning, wood chips, saw dust.
2	Medium digging	Packet earth, tough dry clay, soil with less than 25% rock content.
3	Medium to hard digging	Well blasted rock or hard packed soils with up to 50% rock content.
4	Hard digging	Averagely blasted rock or tough soils with up to 75% rock content.
5	Very hard digging	100% rock content and poorly blasted. Examples are: granite, basalt, greywacke, sandstone, caliche, dolerite, certain limestones. Hard frost.

Some soils have a higher degree of filling the bucket than others. Dense or tight soil, without voids, like clay has higher fill factor then gravel which contains large voids. Actual bucket volume depends on the rated volume of the bucket and the fill factor, see Figure 2.91 and Figure 2.92. The rated volume is the volume of a bucket heaped with soil. The angle of heap (the slope) is different for narrow excavator buckets and wide wheel loader buckets. The actual bucket volume is defined as the rated bucket volume times the fill factor. Different bucket fill factors are presented below.

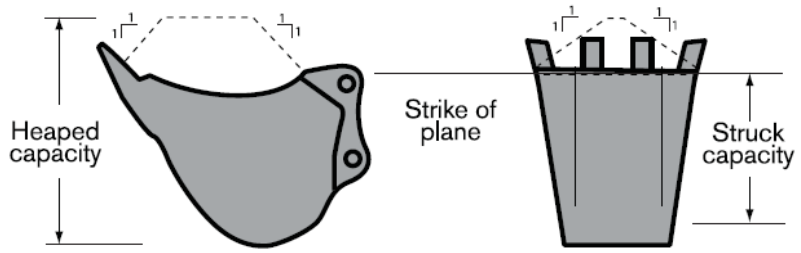

Figure 2.91. Material heap on excavator bucket, Volvo GPPE performance manual (2009).

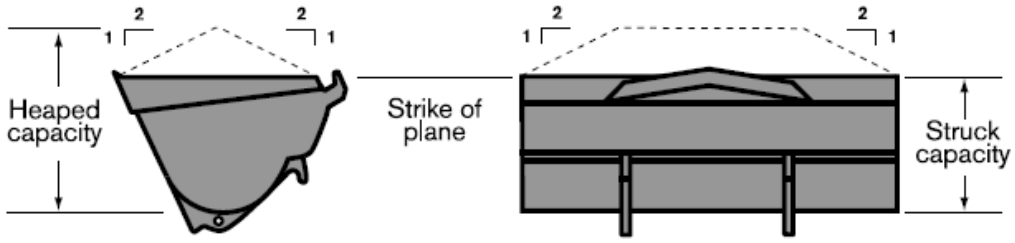

Figure 2.92. Material heap on wheel loader bucket, Volvo GPPE performance manual (2009).

In Volvo GPPE performance manual (2009) it is stated that the selection of an appropriate bucket to the excavator is of greatest importance. Even a bucket of lower capacity can actually increase productivity due to faster cycle times. The most important considerations when evaluating buckets are the bucket width and bucket tip radius. A bucket that is too wide can have difficulties in penetrating harder material but the loading time can improve when handling lower class material, such as loose sand. Narrow buckets have a smaller area of contact with the material and can therefore penetrate high class material, for example blasted rock. In wide buckets, due to the large opening, the flow of material will be faster, both in and out of the bucket, than for narrow buckets. If the bucket tip radius is too large a loss of the breakout force will occur, resulting in lower efficiency. Another important factor when choosing bucket is the ability of the excavator to load the bucket for every cycle. If the bucket is too large for the material class it can result in a small bucket fill factor, long cycle time and accelerated component wear.

For wheel loaders the crucial factor of the capacity of the loader is the ability to fill the bucket during each work cycle. Right size and shape of the bucket is important and, as for an excavator, a large bucket can result in lower productivity if the material is difficult to fill. It is recommended to have a variety of buckets to change between since different factors affect the ability of excavating in soil. These factors concern, for example, soil properties, condition of wheel loader, operator skills and the transport distance. The buckets have different proportions and can be equipped with bolt-on edges or teeth depending on combination of factors prevailing.

Table 2.15. Fill factors excavators, Volvo GPPE performance manual (2009).

Material	Bucket filling (%)
Earth / Sandy Clay	100 - 110
Hard and Compacted Clay	95 - 110
Sand / Gravel	95 - 110
Rock - well blasted	75 - 95
Rock - averagely blasted	60 - 75
Rock - poorly blasted	40 - 60

Table 2.16. Fill factors for wheel loaders, Volvo GPPE performance manual (2009).

Material	Bucket filling (%)	Density (ton/m^3)
Earth / Clay	~ 110	1,50 - 1,60
Sand / Gravel	~ 105	1,60 - 1,70
Aggregate	~ 100	1,65 - 1,80
Rock	< 100	~ 1,70

2.5 Prediction of resistive forces

In several studies of excavating and moving soil the theory of passive earth pressure on structures has been used for prediction of forces on blades and buckets. The passive pressure developed during excavation acts on the blade as a resultant resistive force from the soil. In this chapter some aspects of the passive earth pressure theory is treated. Since the research carried out in this area concerns passive earth pressures on structures the conditions of passive pressure will be assumed in this chapter.

A passive earth pressure arises when a structure moves towards the soil. The earth pressure resists the lateral movement of the structure but can also provide a stabilizing force. For several types of structures, like anchor blocks, retaining walls, pile caps and bridge abutments, the passive earth pressure helps resisting the movement of the structure.

As Duncan and Mokwa (2001) describes it: the passive resistance on a moving structure depends on four factors. (1) The amount and direction of the movement of the structure; depends on if the vertical component of the passive resistance is large enough to cause a vertical movement of the structure. In the case of an anchor block with relatively low weight, the upward passive component could be sufficient to move the structure. (2) The soil strength and stiffness; were a greater strength gives a larger possible passive pressure. The stiffness affects the passive pressure at a given amount of movement. (3) The interface friction and adhesion; where the magnitude of interface friction depends on three factors: the roughness of the interface and the soil (properties of the soil), a small amount of shear displacement across the interface to mobilize interface friction and vertical equilibrium of the structure. Additional shear stresses occur on the soil-structure interface when cohesive soil adheres to a structure. The maximum value of adhesion is equal to the cohesion of the soil. (4) The shape of the structure; since conditions at the ends of a structure are quite different from those in the middle of the structure. Short and long structures as well as two and three dimensional analyses will give different passive pressures.

If the passive pressure on the soil is too high and the ultimate strength of the soil is reached a rupture surface will develop in the soil mass. The shape of this failure surface depends on the roughness of the structure. If the surface of the wall causing soil displacement is rough, shear forces develops between the wall and the soil, causing a curved failure shape in the soil.

2.5.1 Calculating passive earth pressure

Several models and methods have been proposed in trying to calculate and simulate the passive earth pressure. Different methods have different approaches and, for example, considers the soil as a continuum or particulate medium, assumes a two or three dimensional analysis and assumes analytical or numerical analysis. Numerical methods, such as finite element and finite difference methods have recently been used for passive earth pressure calculations in different studies, see for example Shamsabadi and Nordal (2006), Shiau et al (2008) and Shiau and Smith (2006). The results from these studies show a good agreement with results from experiments, limit equilibrium methods and limit analysis methods.

There are two classical earth pressure theories: Rankine (1857), who considers the passive pressure in terms of stresses and Coulomb (1776), who treats the problem through equilibrium of forces. Other well known methods have been proposed by Ohde (1938) (Logarithmic spiral method), Caquot and Kerisel (1948) and Sokolovski (1960). Most of these methods assume that a volume of soil is loosened in front of the structure when the ultimate shear strength of

the soil is exceeded. Depending on model, the assumed shape of failure in the soil will differ. These models do not consider pre-failure stresses or deformations of the soil and will give the ultimate passive pressure of the soil.

Results from Duncan and Mokwa (2001) show the difference of the Kp – value calculated with Coulomb, Rankine and Log spiral methods for different δ/φ – ratios, no backfill inclination and φ = 40°, see Table 2.17. It can be seen that the values agree well for lower δ/φ – ratios.

Table 2.17. Comparison of Kp values computed with Rankine, Coulomb and Log Spiral methods, from Duncan and Mokwa (2001).

Wall friction (δ/ϕ) (1)	Rankine Theory (K_p) (2)	Coulomb Theory (K_p) (3)	Log Spiral Theory (K_p) (4)
0	4.6	4.6	4.6
0.2	NA	6.3	6.6
0.4	NA	9.4	9.0
0.6	NA	15.3	11.9
0.8	NA	30.4	15.5
1.0	NA	92.6	17.5

Note: NA = not applicable.

Zhu and Qian (2000) have proposed a new limit equilibrium method for calculating passive earth pressure that builds on a log spiral failure surface. The method divides the log spiral part and the plane part of the sliding mass into triangular slices. Results from their method seem to agree well with Sokolovski's method and with Coulomb's method when the interface friction angle is low, see Table 2.18.

Table 2.18. Comparison of Kp values computed with Coulomb and Sokolovski methods and the method from Zhu and Qian (2000). "This paper" refers to Zhu and Qian (2000).

ϕ (°)	δ_p (°)	Coulomb	Sokolovski	This paper
10	0	1.42	1.42	1.42
	5	1.57	1.56	1.55
	10	1.73	1.66	1.66
20	0	2.04	2.04	2.04
	10	2.64	2.55	2.56
	20	3.52	3.04	3.06
30	0	3.00	3.00	3.00
	15	4.98	4.62	4.61
	30	10.10	6.55	6.59
40	0	4.60	4.60	4.59
	20	11.77	9.69	9.66
	40	92.58	18.20	18.24

With limit analysis methods the upper and lower bounds on the failure force can be defined, Hong (2001). The upper bound calculation is concerned with velocity conditions and energy dissipation. The lower bound calculation is concerned with equilibrium and yield conditions, Hong (2001).

Shiau and Smith (2006) have performed numerical analyses with the finite difference method of the passive pressure on a retaining wall with a non-cohesive soil, see Figure 2.93. The results show that values from the analysis of the passive earth pressure coefficient, Kp are in good agreement with values calculated with the Log spiral method and the limit analysis method by Shiau et al. (2008).

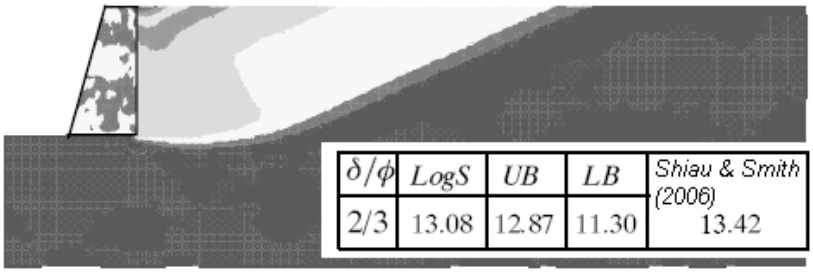

Figure 2.93. Results from numerical computations of the passive earth pressure. Kp – values calculated with different methods, modified from Shiau & Smith (2006).

Shiau et al. (2008) performed finite element limit analyses of passive earth resistance in non-cohesive soil, see Table 2.19 and Figure 2.94. The calculated upper and lower bound values were compared to values calculated with other methods. There seems to be a good agreement between the methods comparing δ/φ – ratios. Only the values of Coulomb differ for higher δ/φ – ratios.

Table 2.19. Comparison of Kp – values computed by different methods, from Shiau et al (2008). "This paper" refers to Shiau et al (2008). All methods calculated with a vertical interface and φ' = 40°.

δ/ϕ'	$K_p = 2P_p/\gamma H^2 = 2P_{p,h}/\gamma H^2 \cos\delta$						
	Coulomb Theory	Caquot and Kerisel (1948)	Log Spiral Method (Duncan et al., 2001)	Sokolovski (1960)	Upper Bound (Chen, 1975)	Upper Bound This paper	Lower Bound This paper
0	4.60	4.59	4.60	4.60	4.60	4.61 (16)	4.60 (16)
1/3	8.15	8.13	8.17	—	7.73	7.79 (20)	6.87 (15)
1/2	11.77	10.36	10.50	9.69	10.08	10.03 (35)	8.79 (17)
2/3	18.72	13.10	13.08	—	13.09	12.87 (60)	11.30 (15)
1	92.72	17.50	17.50	18.20	20.91	20.10 (64)	18.64 (24)

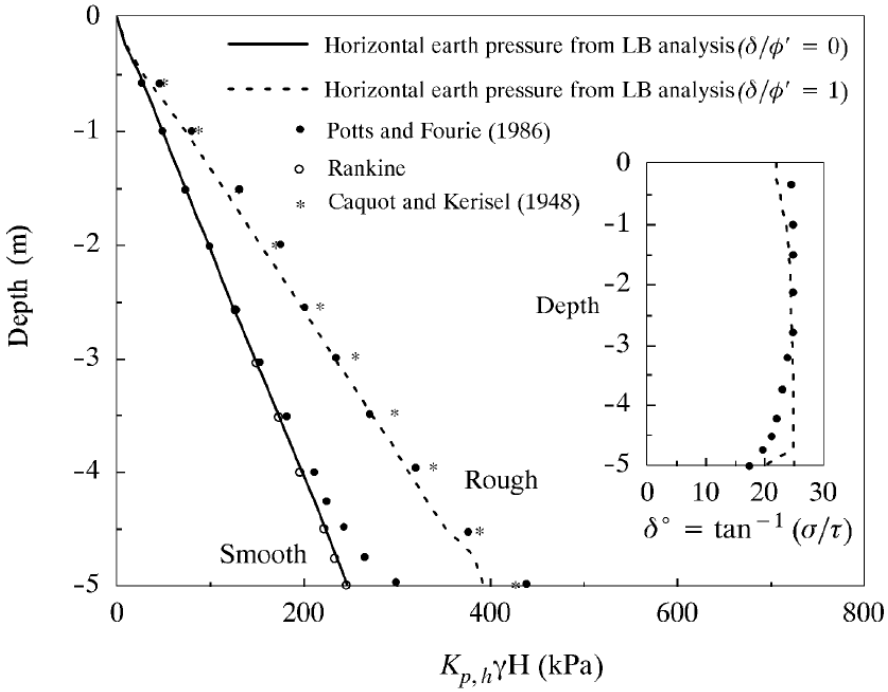

Figure 2.94. Comparison of the distribution of the passive earth pressure with depth for smooth and rough walls, Shiau et al (2008). All methods calculated with a vertical interface and φ' = 25°.

2.5.2 Passive earth pressure methods

As mentioned above the classical passive earth pressure methods assume that a volume of soil is loosened in front of the structure when the ultimate shear strength of the soil is exceeded. At this point the methods assume that the volume of soil is in static equilibrium and all of the forces and moments acting on the volume of soil will cancel each other out. Depending on method the assumed shape of failure in the soil will differ as well as if the roughness of the wall is considered or not. In the methods of Rankine (1857) and Coulomb (1776) a plane failure shape is assumed whereas in the method of Ohde (1938) the failure shape is, according to Terzaghi (1943), a combination of a logarithmic spiral and a plane. Other authors use failure shapes of circles, as Rahardjo and Fredlund (1983) or ellipses, as Caqout and Kerisel (1948), according to Rahardjo and Fredlund (1983). Zhu and Qian (2000) and Janbu (1957), according to Rahardjo and Fredlund (1983), have used a divided failure shape, in combination with an analysis with the method of slices.

A curved failure surface develops when the wall friction is considered. Coulomb (1776) considered wall friction but assumed a plane failure surface to simplify the calculations. According to Terzaghi (1943) it would for non-cohesive materials be sufficient to assume a plane failure surface if the wall friction is small. Since Coulomb's method consider wall friction but assumes a plane failure surface Terzaghi (1943) concludes that Coulomb's method only gives correct results for small values of wall friction, up to φ/3. For higher values of wall friction the difference between Coulomb's plane failure surface and a curved failure surface is too high. Duncan and Mokwa (2001) proposes that the Log spiral method gives better results than Coulombs method for conditions where $\delta > 0{,}4\varphi$. Das (2006) proposes that

the angle of wall friction, δ' can be taken equal to the soil friction angle, φ' in loose granular soil. For dense granular soil in backfills, δ' is in the range of $\varphi'/2 < \delta < 2\varphi'/3$.

The limit equilibrium methods do not consider pre-failure stresses or deformations of the soil. They are only concerned with the ultimate passive pressure at failure and can not say anything about the load – deflection behaviour of the soil. In some studies though, the behaviour has been approximated with a hyperbolic load-deflection curve and compared to experimental data. Hyperbolic relationships have been proposed by Duncan and Mokwa (2001) and Shamsabadi et al. (2007). Also the Hardening soil model in Plaxis is based on a hyperbolic relationship and have been used in some studies; for example Shamsabadi and Nordal (2006) and Rollins et al (2010). In these studies, as well as in Stewart et al. (2007), the hyperbolic model was fitted with experimental results of passive earth pressure on bridge abutments and seems to show on good agreement. It should be mentioned that there were no loose soils involved in these tests.

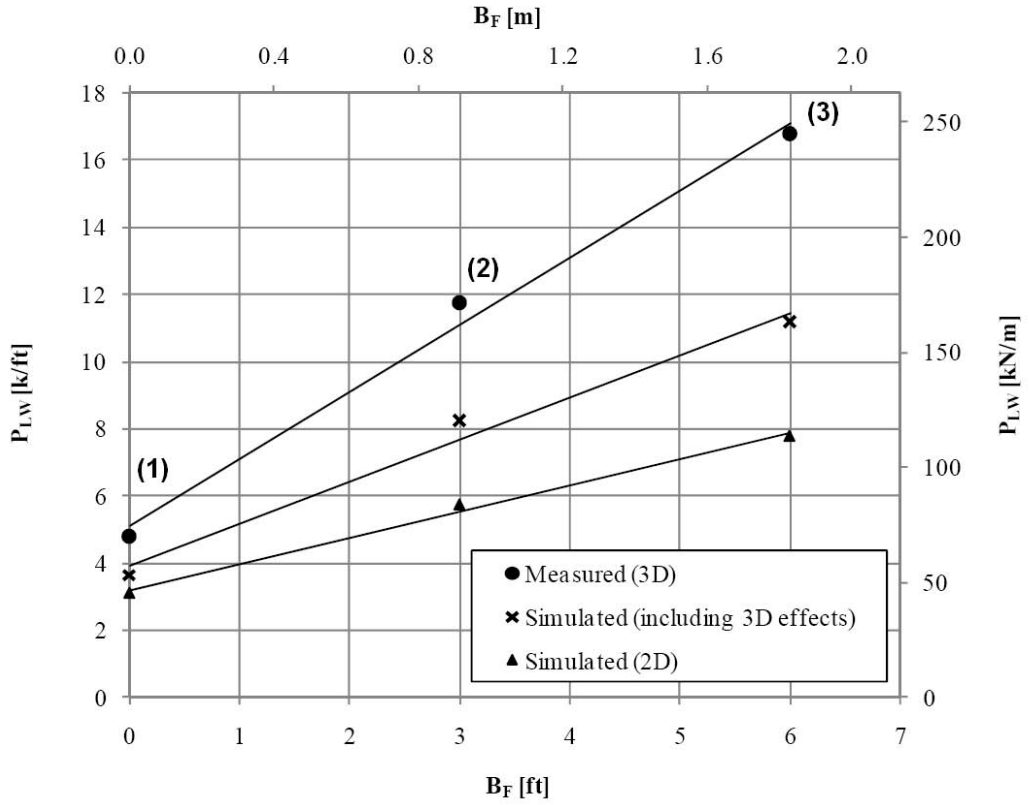

Figure 2.95. Results from field experiments and finite element simulations of the maximum passive resistance of a pile cap displaced in (1) loose silty sand, (2) 0,91 m wide gravel backfill before loose silty sand and (3) 1,83 m wide gravel backfill before loose silty sand. Modified from Rollins et al. (2010).

In the literature different authors have considered three dimensional soil failures in front of the structures during displacement, see for example Duncan and Mokwa (2001), Shamsabadi and Nordal (2006) and Rollins et al. (2010). In analyses of structures like bridge abutments and pile caps the 3D effect has shown to be significant. Since the width of the abutment is limited the two dimensional methods for passive pressure give too low values. Rollins et al. (2010) have performed field experiments and finite element analyses of a pile cap with a width/depth ratio of 5,18 m/1,12 m = 4,6. The passive resistance of the two dimensional

simulation was about half of the measured passive resistance. When the simulated passive resistance was corrected for 3D-effects according to the method of Brinch Hansen (1966), it was about two thirds of the measured passive resistance, see Figure 2.95.

2.5.2.1 Rankine's theory

In Rankine's theory the stress conditions in a soil element at failure is considered. As the soil mass is subjected to a horizontal passive pressure due to movement of a structure the horizontal effective principal stress will increase. Ultimately the stresses will reach their highest values when the soil fails. In this Rankine state the major principal stresses can be expressed as:

$$\sigma'p = \sigma'o \tan^2(45 + \varphi'/2) + 2c' \tan(45 + \varphi'/2) \quad (2\text{-}46)$$

where $\sigma'o = \gamma z$. The coefficient of Rankine's passive earth pressure, Kp is the ratio of the effective stresses. For non-cohesive soil Kp is defined as:

$$Kp = \sigma'p/\sigma'o = \tan^2(45 + \varphi'/2) \quad (2\text{-}47)$$

The total passive resistance, Pp per unit length of the wall is:

$$Pp = \tfrac{1}{2} Kp\, \gamma H^2 + 2c' (\sqrt{Kp})H. \quad (2\text{-}48)$$

For Rankine's passive state it is assumed that the slip planes of shear failure of the soil will make a $(45 - \varphi'/2)$ – degree angle with the horizontal direction. The lateral stress becomes the major principal stress. Rankine's theory is based on the relationship between the vertical and lateral pressure on a vertical plane in non-cohesive soil on a frictionless structure. Rankine's theory has been developed to consider inclined backfills and inclined walls; see for example Chu (1991). This will change the Kp – value.

2.5.2.2 Coulomb's theory

In Coulomb's theory the equilibrium of a wedge of failed soil in front of a structure is considered. To calculate the passive pressure, the weight of the soil wedge, the shear strength of the soil and the friction of the wall are considered. The shear strength of soil is defined by Coulomb shear failure equation for non-cohesive soils: $\tau = \sigma'_N \tan \varphi'$. From the equilibrium of forces on the wedge the passive pressure can be derived. It is assumed that the size of the soil wedge is determined through the soil failure angle, β giving the minimum passive force, P_{min}. Coulomb's theory assumes a plane failure surface and non-cohesive soil. It considers inclination of the backfill and the wall as well as soil-wall friction interaction.

The passive pressure, Pp for non-cohesive soil on a structure is expressed as:

$$Pp = \tfrac{1}{2} Kp\, \gamma H^2 \quad (2\text{-}49)$$

where Kp is the coefficient of passive pressure according to Coulomb and defined:

$$Kp = ((\sin(\alpha + \varphi)/\sin(\alpha))/(\sqrt{(\sin(\alpha - \delta) - \sqrt{[(\sin(\varphi + \delta)\sin(\varphi + \beta))/\sin(\alpha - \beta)]}))^2 \quad (2\text{-}50)$$

2.5.2.3 Ohde's logarithmic spiral method

The logarithmic (log) spiral method have been described by Terzaghi (1943), Duncan and Mokwa (2001) and other researchers. It seems that this method originates from Ohde (1938). According to Duncan and Mokwa (2001) the log spiral method can be used through charts, tables, graphic solutions or numerical calculations. Different variants of the log spiral method consider one or more of the following parameters: soil cohesion and friction, inclined wall and backfill and soil-wall friction.

In the log spiral method the failure mechanism is assumed to consist of a Prandtl zone near the wall and a Rankine zone close to the ground surface, see Figure 2.96. The failure surface consists of the lower logarithmic boundary of the Prandtl zone and the plane failure surface beneath the Rankine zone. The solution considers the equilibrium of moments around the centre of the logarithmic spiral from the weight of the Prandtl zone, W, the passive pressure of the Rankine zone, E_{PR}, the reaction force from the ground, F, and the passive pressure from the wall, E_P. The shape of the logarithmic spiral surface is defined by the radius:

$$r = r_0 \, e^{(\theta \tan\varphi)} \tag{2-51}$$

were r_0 is the initial radius from the centre of the spiral to the foot of the wall, θ is the angle between r and r_0 and φ is the soil friction angle. The resultant reaction force F acts along the spiral surface and passes through the spiral centre, thus causing no moment.

The passive pressure, E_P is solved for different widths of the Prandtl zone, giving different lengths of the logarithmic radius. The minimum value of the passive pressure, E_P is solved through iterations and corresponds to the value when failure occurs in the soil mass.

Duncan and Mokwa (2001) consider three parts of the passive pressure, E_P:

- Resistance due to weight and angle of internal friction of soil, $P_{p\varphi}$.
- Resistance due to surcharge on the ground, P_{pq}.
- Resistance due to cohesion of the soil, P_{pc}.

The smallest total passive pressure is expressed as the smallest sum of the three components. They found numerical difficulties for values of the interface friction angle, $\delta < 2°$.

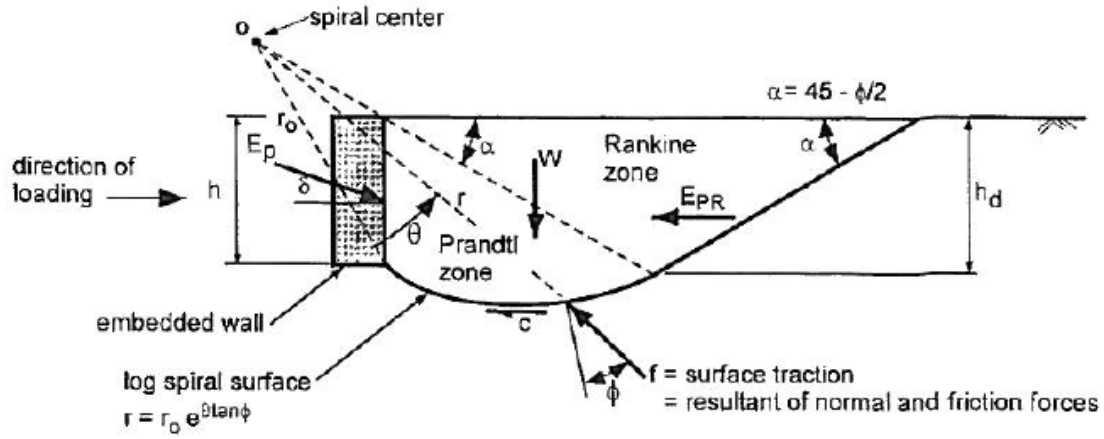

Figure 2.96. Log spiral failure mechanism, from Duncan and Mokwa (2001).

Mokwa and Duncan (1999) have developed an Excel spreadsheet called PYCAP to calculate the passive earth pressure with the log spiral method. It considers the three components of the passive pressure concerning weight, surcharge and cohesion as noted by Duncan and Mokwa (2001); $E_P = P_{p\varphi} + P_{pq} + P_{pc}$. The passive earth pressure coefficients are then calculated as follows:

$$K_{p\varphi} = 2P_{p\varphi} / \gamma H^2 \quad (2\text{-}52)$$

$$K_{pq} = P_{pq} / qH \quad (2\text{-}53)$$

$$K_{pc} = P_{pc} / 2cH \quad (2\text{-}54)$$

When the wall friction, $\delta < 2°$ the passive earth pressure coefficient of Rankine is used instead, $K_p = \tan^2(45 + \varphi/2)$.

This method is suitable for soil with $\varphi > 0°$ and c – φ soils. For soils with $\varphi = 0°$, cohesive soils, Mokwa and Duncan (1999) have developed another method for calculating the ultimate passive pressure, P_{ult}. The method is based on a wedge model with plane failure surface as developed by Reese (1997).

2.5.3 Soil-interface friction and adhesion

The roughness of the surface of the structure and the soil friction properties causes soil-interface friction, δ and adhesion, c_a. As a structure is displaced into a soil mass the soil will be compressed and moved upward. This upward motion of the soil causes an upward shear on the structure. To compensate the upward shear force a downward component of the passive pressure has to be developed. This will cause the resultant passive force Pp to be inclined at an angle of δ.

The shearing stress developed on the surfaces within a soil mass during failure is usually defined as:

$$\tau = c + \sigma_n \tan(\varphi) \quad (2\text{-}55)$$

According to Terzaghi (1943) the shearing stress on the contact surface from the moving soil mass can be defined in a similar way (per unit area):

$$p_{pt} = c_a + p_{pn} \tan(\delta) \quad (2\text{-}56)$$

were p_n is the normal component of the passive earth pressure, per unit area. The values of c_a and δ may be equal to or smaller than c and φ respectively. An upward motion of the soil mass will give a positive value of δ whereas a downward motion will give a negative value of δ.

According to Terzaghi (1943) the normal component of the total passive earth pressure can be expressed as below, accounting for inclined wall, cohesion, surcharge, weight and adhesion:

$$P_{Pn} = (H / \sin(\alpha) (cK_{Pc} + qK_{Pq} + 0{,}5\gamma HK_{P\gamma} + c_a) \quad (2\text{-}57)$$

Considering wall friction the total passive force Pp can then be expressed as:

$$P_P = P_{Pn} / \cos(\delta) \qquad (2\text{-}58)$$

Different values of the interface friction and adhesion have been presented in the literature. The values differ depending on the interface material and soil properties. In NAVFAC (1986) values for the interface friction angle, the friction factor and adhesion have been presented for different interface materials and soil types, see Table 2.22.

It is convenient to characterize the interface friction in terms of a δ/φ – ratio. Duncan and Mokwa (2001) have presented values for this ratio for different interface material and soil types, see Table 2.20. They also propose that adhesion can be characterized through the c_a/c – ratio and suggests values from about 0,5 for stiff soils to about 0,9 for soft soils. Also in Fine (2011) values for the δ/φ – ratio have been proposed, see Table 2.21.

Table 2.20. δ/φ – ratios presented by Duncan and Mokwa (2001).

Soil type (1)	Structural Material: Steel (δ_{max}/ϕ) (2)	Concrete (δ_{max}/ϕ) (3)	Wood (δ_{max}/ϕ) (4)
Sand	0.54	0.76	0.76
Silt and clay	0.54	0.50	0.55

Note: δ_{max} = interface friction angle, ϕ = angle of internal friction of soil.

Table 2.21. Recommended values on the δ/φ – ratio, according to Fine Ltd. (2011).

Material	Concrete		Steel		Wood	
Surface	Smooth	Rough	Smooth	Rough	Smooth	Rough
Loose noncohesive soil	0,85	0,9	0,7	0,8	0,75	0,8
Firm noncohesive soil	0,8	0,8	0,6	0,7	0,7	0,7
Dense noncohesive soil	0,7	0,7	0,5	0,7	0,65	0,65
Silt	0,8	0,9	0,6	0,8	0,8	0,9
Clayey soil	0,8	0,9	0,5	0,7	0,7	0,8
Clay	0,8	0,9	0,5	0,6	0,6	0,7

Table 2.22. Ultimate interface friction factors, tan (δ), interface friction angles, δ and adhesion, ca for different soil sand interfaces, modified from NAVFAC (1986). 1 psf = 0,0479 kPa.

Interface Materials	Friction factor, tan [delta]	Friction angle [delta] degrees
Mass concrete on the following foundation materials:		
Clean sound rock	0.70	35
Clean gravel, gravel-sand mixtures, coarse sand...	0.55 to 0.60	29 to 31
Clean fine to medium sand, silty medium to coarse sand, silty or clayey gravel	0.45 to 0.55	24 to 29
Clean fine sand, silty or clayey fine to medium sand	0.35 to 0.45	19 to 24
Fine sandy silt, nonplastic silt	0.30 to 0.35	17 to 19
Very stiff and hard residual or preconsolidated clay	0.40 to 0.50	22 to 26
Medium stiff and stiff clay and silty clay	0.30 to 0.35	17 to 19
(Masonry on foundation materials has same friction factors.)		
Steel sheet piles against the following soils:		
Clean gravel, gravel-sand mixtures, well-graded rock fill with spalls	0.40	22
Clean sand, silty sand-gravel mixture, single size hard rock fill	0.30	17
Silty sand, gravel or sand mixed with silt or clay	0.25	14
Fine sandy silt, nonplastic silt	0.20	11
Formed concrete or concrete sheet piling against the following soils:		
Clean gravel, gravel-sand mixture, well-graded rock fill with spalls	0.40 to 0.50	22 to 26
Clean sand, silty sand-gravel mixture, single size hard rock fill	0.30 to 0.40	17 to 22
Silty sand, gravel or sand mixed with silt or clay	0.30	17
Fine sandy silt, nonplastic silt	0.25	14
Various structural materials:		
Masonry on masonry, igneous and metamorphic rocks:		
Dressed soft rock on dressed soft rock	0.70	35
Dressed hard rock on dressed soft rock	0.65	33
Dressed hard rock on dressed hard rock	0.55	29
Masonry on wood (cross grain)	0.50	26
Steel on steel at sheet pile interlocks	0.30	17

Interface Materials (Cohesion)	Adhesion c+a, (psf)
Very soft cohesive soil (0 - 250 psf)	0 - 250
Soft cohesive soil (250 - 500 psf)	250 - 500
Medium stiff cohesive soil (500 - 1000 psf)	500 - 750
Stiff cohesive soil (1000 - 2000 psf)	750 - 950
Very stiff cohesive soil (2000 - 4000 psf)	950 - 1,300

2.6 Soil properties

The magnitude of the resistance from the soil when a blade or bucket moves into the soil depends on the properties the soil. As demonstrated by Godwin and Spoor (1977), the resistive force was about ten times higher for a dense compacted soil than for a loose uncompacted soil. This chapter presents different properties that affect the strength of the soil as well as some methods for measuring these properties.

2.6.1 Particle size distribution

The particle size distribution and relative density of a soil determine the compressibility and shear strength of the soil. This is significant for soils with coarser fractions.

From a grain size curve information can be retrieved about the total percent of a given grain size, the total percent of larger or finer of a given size and the uniformity of the range in grain size distribution, see figure below. The grading of the grain size curve can be represented by the uniformity coefficient, $c_u = d_{60}/d_{10}$, which roughly represents the slope of the grain size distribution curve. A large coefficient represents a large range in grain sizes and the soil is well graded. Moraine is commonly multi graded. For gap-graded soils, soils with an uneven grain size distribution curve, the uniformity coefficient is not representative. For these soils the coefficient of curvature, c_z is a better measure.

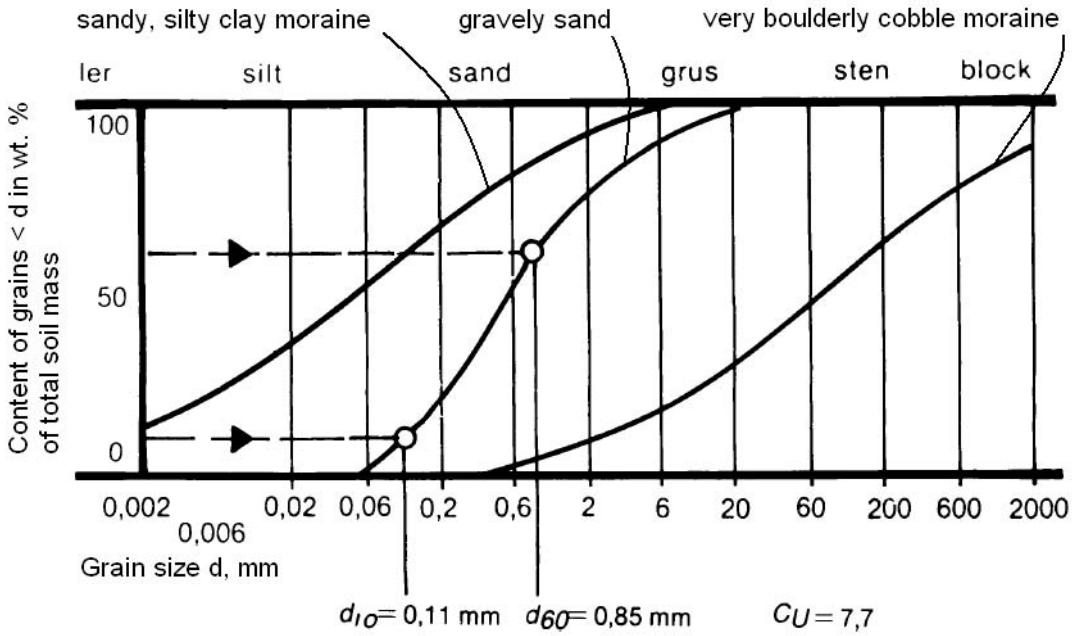

Figure 2.97. Characteristic grain-size distributions in moraine and sand. An example of how the uniformity coefficient is determined for gravely sand is also presented. Modified from Larsson (2008).

The coefficient of curvature, $c_z = 2\ (d_{30}) / d_{10}\, d_{60}$, is a measure of the shape of the grain size distribution curve. For values of c_z about 1 the soil is considered as well graded. For c_z much less than 1 and much larger than 1 the soil is regarded as poorly graded. The values of the uniformity coefficient and the coefficient of curvature can be classified into following groups, Larsson (2008):

Grading	c_u	c_z
Even graded	< 5	< 1
Medium graded	5-15	< 1
Multi-graded	> 15	$1 < c_z < 3$

2.6.1.1 Moraine/c-φ soil

Moraine soil is the most common type of soil in Sweden and covers about 75% of the country, SGI (2011). Moraine is an unsorted sediment soil that consists of particles ranging from finest clay to largest boulder in size, Lundqvist (1993). In Sweden the moraine soil is classified according to particle size and content of boulders at the surface. The composition of particles depends on which rock types and original soil types that the moraine consists of. For geotechnical purposes moraine soil is often defined as a c – φ soil.

Moraine soil was formed by material transported and deposit by the ice during the last ice age about 10 000 years ago. When the ice moved, the bedrock was eroded and material was broken loose. Also existing soil deposits were captured and moved by the ice. The materials were crushed and altered inside and in under the ice. As the ice melted the material was deposited. The bedrock was polished and the material formed contained particles of different sizes. The moraine is divided into two types depending on if the soil was formed by material deposited from the inner parts of the ice or from the bottom of the ice. The moraine formed by material transported in under the ice or in the bottom part of the ice, lodgement moraine (bottenmorän), is common in large areas of Sweden and has been deposited directly on the bedrock, Karlsson & Hansbo (1984). Since the soil had the great pressure from the ice on it the moraine soil was compressed and consolidated into a very dense material. The main part of the material comes from the local bedrock since it was relatively shortly transported by the ice. The particle size distribution of the moraine depends on the hardness and weathering of the rock from which it was formed. The moraine formed by material transported on or inside the ice, ablation moraine (ytmorän), was deposited as the ice melted away. This created a relatively loose material since it was not previously consolidated. The particles of the ablation moraine have sharper edges than the lodgement moraine. The material does in practice lack finer particles and it has been deposited in hills or in a layer covering the lodgement moraine.

In large parts of Sweden the moraine soil was formed from the old bedrock and in the soil the fractions of gravel and sand dominate, Karlsson & Hansbo (1984). The boulder and cobble content is high and the soil is clayey. In areas with sedimentary rocks with small particles the moraine is clayey, clayey moraine or clay moraine, and that lacks boulders. Clay moraines in southern parts of Sweden often contain lime. In areas with bedrock of sandstone the fraction of sand dominates and the moraine is usually silty. Boulder and cobble content is high.

The geology and the movement of the ice are parameters that have decided the properties and composition of the moraine. The strength properties of the rock have affected the particle size and particles size distribution of the moraine. Bedrock with high strength has given a moraine that contains large particles. The ice did not melt and did not move at an even pace; therefore it stopped at some positions longer time than others. This has given a moraine soil with increased crushed material in it. Moraine that have been transported a relatively long distance have been crushed more and it consists of finer particles. Moraine soil can be grouped as: boulder and cobble moraine, coarse grained moraine, mixed grained moraine, fine grained moraine and silty moraine.

2.6.2 Content of cobbles and boulders

A sample of soil containing gravel and cobbles to a certain degree do always contain cobbles and boulders. Even in sand there are some cobbles and boulders. If the uniformity coefficient, c_u is grater than 9 a relatively high content of cobbles and boulders is to be expected. This is valid for moraine as well. In moraines the content of cobbles can be high even if the content of boulders is low. The content of boulders in moraines can be grouped as follows, Larsson (2008):

Type of moraine	**Content of boulders**
Coarse grained moraine	Very boulderly
Mixed grain size moraine	Boulderly to very boulderly
Fine grained moraine	Some content of boulders to boulderly

Sediments and eskers formed of the ice of melt water contain gravel and cobbles but also some boulders. It is common that an esker with gravel and cobbles the content of boulders are 5-10 % of weight. In a esker with sand and gravel the content of boulders is often small, Larsson (2008). Generally the content of cobbles can be as high as 25 % of weight in sandy gravel and about 15 % of weight in gravely sand.

2.6.3 Porosity

In non-cohesive soil the particles are in direct contact with each other. The contact points become less in a soil with coarser particles and uniform particle sizes. Non-cohesive soil in situ can have porosity greater than 50 % due to particle shape and valve formation. If the soil is well graded with different particles sizes, the voids in between coarser particles are filled with finer particles and a very dense soil is formed. For example some moraines can have porosity as low as 10 %. Usual values of porosity for clay and silt are between 25 and 75 % and for sand and gravel between 15 and 45 %, Larsson (2008). The porosity, n is defined as; $n = V_{void}/V_{total}$.

2.6.4 Relative density

The state of compactness of granular soil can be expressed by the relative density, Dr. It is defined as:

$$Dr = (e_L - e)/(e_L - e_D) \qquad (2\text{-}59)$$

where
e_L = void ratio in loosest state
e_D = void ratio in densest state
e = void ratio in situ, defined as; $e = V_{void}/V_{solid}$

Since it is difficult to determine void ratios the unit weight can be measured instead. The state of compactness and the relative density is empirically related. For a loose sand Dr is very small and for a very dense sand Dr is very large. The relative density can be determined in situ through the Standard Penetration Test (SPT). The soil can be classified according to the state of compactness as below:

Designation	**Relative density, Dr (%)**
Very loose	0-15
Loose	15-35
Medium dense	35-70
Dense	70-85
Very dense	85-100

Another measure of the compactness of the soil is the relative firmness of the soil. It can not be directly translated from relative density but follows the same designation at large. Different geotechnical sounding methods can be used to determine the relative firmness of the soil, see Table 2.23 below. The soil can also be classified with the Cone Penetration Test (CPT).

Table 2.23. Classification of the relative firmness of soil with different geotechnical sounding methods, from Bergdahl et al. (1993).

Relative firmness	Point pressure sounding, qc (Mpa)	Ram sounding (bats/0,2m)	Weight sounding (half rounds/0,2m)
Very low	0 - 2,5	0 - 4	0 - 10
Low	2,5 - 5,0	2 - 8	10 - 30
Medium high	5,0 - 10,0	6 - 14	20 - 50
High	10,0 - 20,0	10 - 30	40 - 90
Very high	> 20,0	> 25	> 80

2.6.5 Soil friction angle

When defining the shear strength of soil, the soil friction angle, φ, is used. According to Cernica (1995) the value of the soil friction angle is influenced by:

1. The state of compaction (denseness) and the void ratio of the soil. The friction angle increases with decreasing void ratio (increasing density), but not linearly.

2. Particle size distribution. A well-graded soil usually gives higher friction angle than uniform-sized soil. (Soils with the same relative density).

3. Coarseness, shape and angularity of the grains. Angular grains causes interlocking between particles more effectively than round grains do, thereby creating a larger friction angle.

4. Mineralogical content. Grains of soft minerals may crush more easily and thereby reducing the interlocking or bridging effects. This causes lower friction angles than for harder grains. In sand only particles with mica content will affect the friction angle because of high void ratio and loose interlocking.

2.6.6 Cohesion

When defining the shear strength of soil the cohesion parameter, c, is used. Depending on if a drained or undrained situation is considered the value of the cohesion will be different. The shear strength of soil depends on the composition of the soil, how it has been formed and if it

has been consolidated before. The shear strength of cohesive soil depends on type of soil, type of loading, preconsolidation pressure and degree of consolidation. For undrained cohesive soil the undrained shear strength parameter c_u, is used. In overconsolidated clay that is considered drained, the cohesion have empirically been determined to: $c' = 0{,}1\ c_u$ or $c' = 0{,}03\ \sigma'_c$, where σ'_c is the preconsolidation pressure, Larsson et al. (2007).

2.7 Soil behaviour

The strength of the soil depends on the properties of the soil particles as well as how close the particles are placed together (the denseness). In this chapter the affect of different properties of the soil on the strength of the soil is presented. Soil strength is generally expressed with the shear strength were the soil friction angle and the cohesion are important parameters. The soil friction angle varies with properties and denseness of the soil.

2.7.1 Stresses in soil

The in-situ soil stress, at a given depth, can be divided into different components, Cernica (1995):

1. Stresses induced by the weight of the soil above
2. Fluid pressures (pore water pressure)
3. Stresses introduced by externally applied loads

Stress is defined as load per unit area and describes the intensity of the force, see Figure 2.98. In soils the total stresses are separated into stresses between particles and stresses induced by pore water pressures. Stresses between particles are referred to as effective stresses. For an element in a soil mass the stresses can be calculated as follows:

Pore water pressure, $u = \gamma_w h_w$
Effective stress, $\sigma' = \gamma_d h_1 + \gamma_b h_w$
Total stress, $\sigma = \sigma' + u$

δu may be added to account for any changes in the pore water pressure.

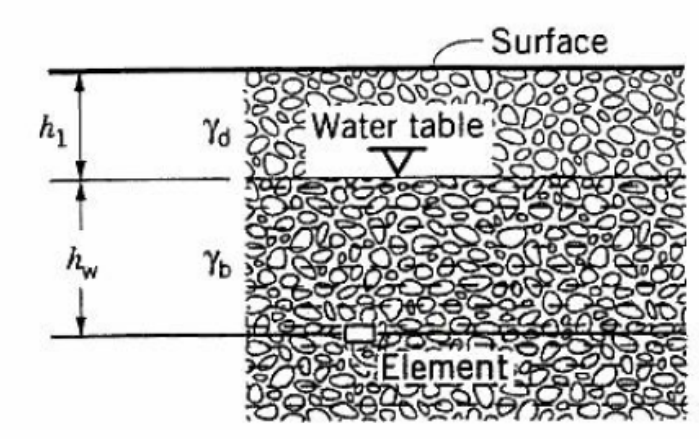

Figure 2.98. Stresses on a soil element, Cernica (1995).

2.7.2 Strength of soil

The resistance to breaking loose a piece of soil from the surrounding soil is determined by the strength of the soil and boundary conditions. To find out the strength of a type of soil you can study the deformation of a specimen of soil from an applied force. Depending on if the specimen is confined to move in some direction the deformations will be different. At a sufficiently large deformation the soil will break and the force acting on the soil specimen at this moment is the breaking force. Soils usually break through tensile, compressive or shear failure. In most situations the soil specimen is compressed and the strength of the soil is determined by the shear strength. The breakage can occur in a slip line through the material, were the highest induced stresses are greater than the shear strength.

The shear strength of soil depends on the friction between the particles and the normal stress acting on the rupture surface. The relationship between the shear stresses and the normal stresses in soil was stated by Coulomb:

$$\tau = \sigma'_N \tan \varphi' \qquad (2\text{-}60)$$

If the particles in the soil are moved closer together, for example through an external pressure, the normal force between the contact points will increase, causing an increase of the shear strength. Also, if the particles in the soil are closely packed, as in a dense soil, the shear strength will be higher than for a soil with loose structure. For these reasons the expression for the relationship between the shear stresses and the normal stresses is then extended with the cohesion parameteer:

$$\tau = \sigma'_N \tan \varphi' + c' \qquad (2\text{-}61)$$

In saturated cohesive soil the particles are surrounded by water and have almost no physical contact. In the contact points, even if there is no normal force between the particles, a tangential force can be transmitted and this is what is referred to as true cohesion.

Soil that is not classified as cohesive or non-cohesive soil can in Sweden be called Mixed soil, Axelsson (1998). Mixed soil is defined as soil with < 40% content of boulders and cobbles of total weight and 15-40% content of silt and clay of weight of soil with diameter < 60 mm. Typical mixed soils are siltey or clayey sand or gravel. In a mixed soil with a relatively small content of clay the smaller clay particles are attached on and around the larger particles. This makes the contact between the larger particles to decrease and the bonding to weaken. It has been shown that at clay content as little as 15-25% the soil will behave as a clay soil in shear strength point of view, Axelsson (1998). Also humus particles attached to soil particles can strengthen or weaken the bonding between the soil particles.

The shear strength at failure can also be expressed in terms of the effective major and minor principal stresses σ'_1 and σ'_3 at failure at a particular point in the soil mass. Shear failure can be represented by the intersection between Mohr's circle for stresses and Coulomb's linear function for shear strength. The coordinates of the tangent point are τ_f and σ'_f , where:

$$\tau_f = ½(\sigma'_1 - \sigma'_3) \sin 2\theta \qquad (2\text{-}62)$$

$$\sigma'_f = ½(\sigma'_1 + \sigma'_3) + ½(\sigma'_1 - \sigma'_3) \cos 2\theta \qquad (2\text{-}63)$$

where θ is the theoretical angle between the major principal plane and the plane of failure. From Figure 2.99 and the law of sine the following relationship can be obtained:

$$\sin\varphi' = [½(\sigma'_1 - \sigma'_3)] / [c'\cot\varphi' + ½(\sigma'_1 + \sigma'_3)] \quad (2\text{-}64)$$

After rearranging the equation the Mohr-Coulomb failure criterion can be stated:

$$(\sigma'_1 - \sigma'_3) = (\sigma'_1 + \sigma'_3)\sin\varphi' + 2c'\cos\varphi' \quad (2\text{-}65)$$

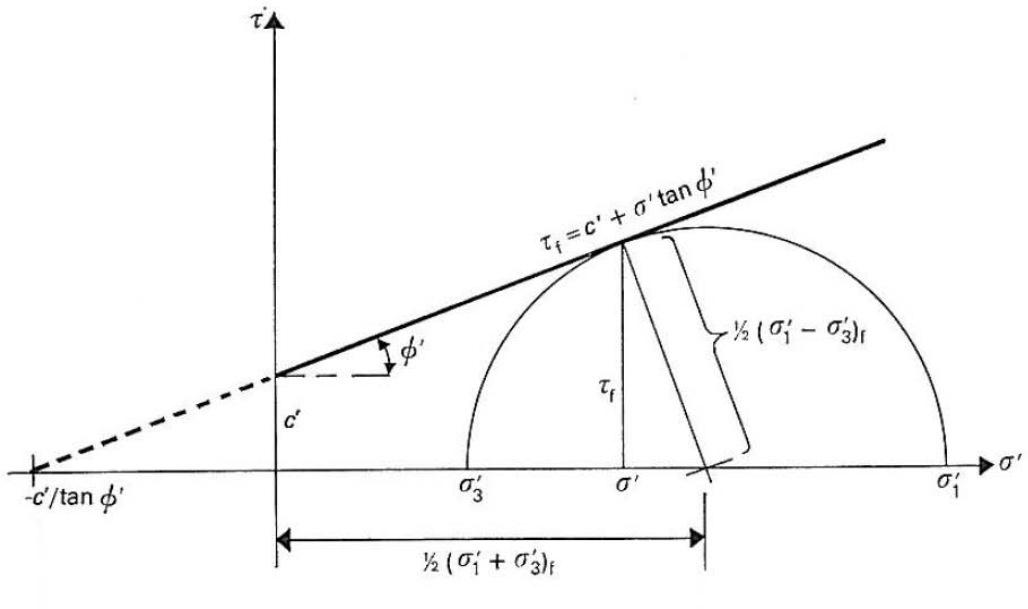

Figure 2.99. Shear strength in c-φ soil, modified from Hansbo (1975).

2.7.2.1 Drained and undrained conditions

Depending on loading of the soil and consolidation properties of the soil the shear strength is evaluated when the soil is drained or undrained. In coarser (non-cohesive) soil the shear strength of drained soil is of most interest since it is assumed not to hold water. In finer (cohesive) soil the pore pressure that is build up at deformation will affect the effective pressure between the soil particles and thus causing the undrained shear strength of soil to be important. When deformations take place over a long time and consolidation of the soil will occur the drained shear strength of the soil will be of significance.

The drained shear strength mainly depends on soil friction angle, deformation properties and prevailing stresses in the soil, Larsson (2008). If the volume of the soil is constant at plain shear the soil is at a critical state. The shear strength is then:

$$\tau = \sigma'_N \tan\varphi'_{cr} \quad (2\text{-}66)$$

The value of the critical state angle, φ'_{cr} depends on mineral of soil and particle shape. Observed values of sands are 32° for quartz sand and 37-40° for sand with feldspar content.

In saturated fine-grained soil like silt, the shear strength can be significantly reduced due to high pore pressures. When the pore pressure increases the shear strength approaches zero and

failure will occur. The soil can be saturated from capillary water. The shear strength is expressed:

$$\tau = c' + (\sigma - u_w) \tan \varphi' \quad (2\text{-}67)$$

In saturated cohesive soil, when the load is applied quickly and can not consolidate, pore pressures are building up in the soil. The effective stresses will be of about the same magnitude nevertheless what stress level the soil exhibited before loading, Larsson (2008). The shear strength for undrained cohesive soils can be expressed:

$$\tau_f = c_u \quad (2\text{-}68)$$

2.7.3 Parameters affecting the strength of non-cohesive soil

The shear strength of soil is highly dependent on the friction angle, φ, of the soil. The friction angle is often seen as a property of the material, with constant value, Larsson (1989). In that case the friction angle is only valid for a certain point, or at least a confined space, of the soil. This is because the friction angle is changing with relative density (void ratio) of soil, particle size, particle size distribution, angularity of soil particles and normal stress. Also there are other effects, such as different minerals having different friction properties and angularity, hardness and cracks of soil particles causing a change in relative density of the soil.

At shear failure in a non-cohesive soil the displacement of the particles is caused by rolling, sliding and twisting. The displacement occurs in a direction where the particle will be given the least resistance. This causes the particles to move in different directions which seldom are in the principal direction. Therefore the presence of voids in the soil mass will affect the shear strength. Below the effect of voids in the soil mass and other different parameters on the soil friction angle is presented.

2.7.3.1 Voids in the soil mass

If there is enough voids in a soil mass the particles in the shear zone will be able to move into these voids allowing for a relative movement of the soil masses. If there are not enough of voids and the particles are in close position relatively to each other the particles are not free to move and the soil is dense. Then the particles have to push the other particles or roll over them, there is some degree of interlocking between the particles. This demands more energy and thereby increases the shear strength of the soil. As the particles in the dense soil moves the volume of the soil mass will increase, see Figure 2.100. This is called dilatancy. If the soil has wide particle size distribution (high uniformity coefficient) the smaller particles in the soil mass will fill the voids in between the larger particles. This increases the denseness. Since the presence of voids depends on particle shape and particle size distribution good measures on the expected dilatancy or compression of a soil mass during loading are relative density, I_D and the uniformity coefficient, c_u.

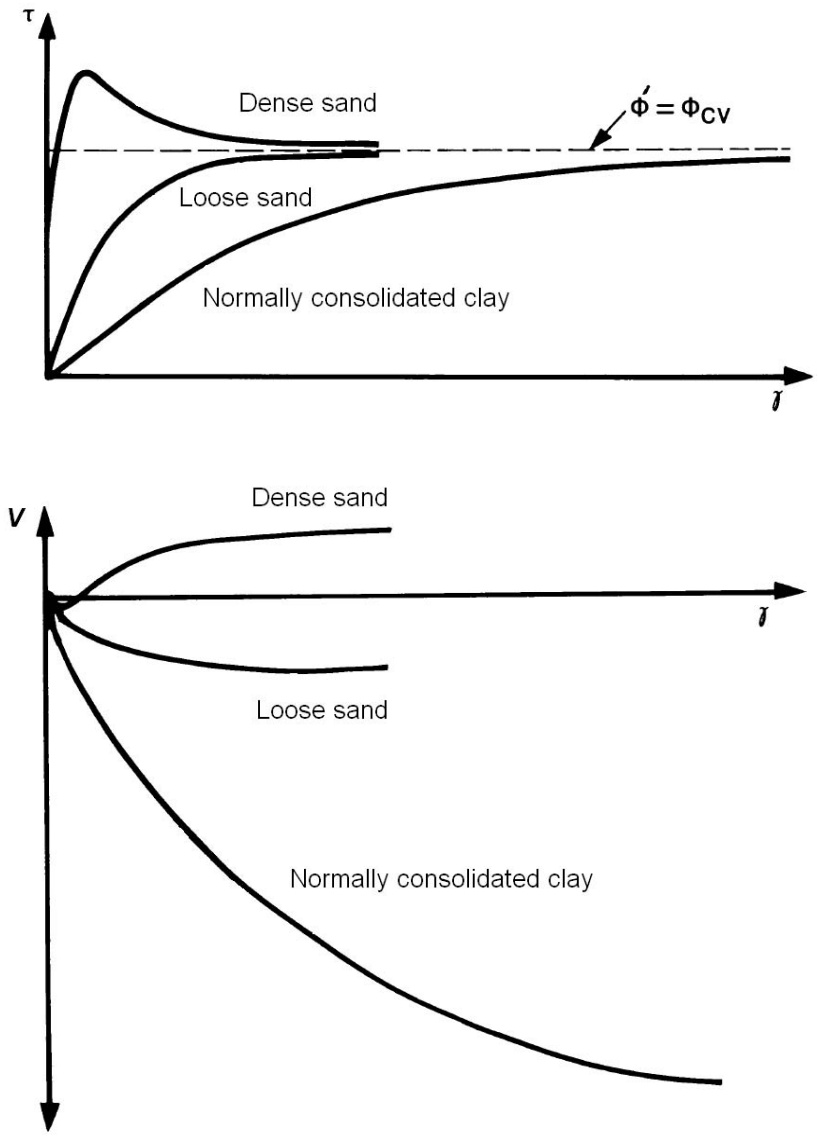

Figure 2.100. Mobilized shear strength during drained shear tests for soils at different relative density (upper figure). At large shear strains a residual shear strength value, corresponding to a critical soil failure angle, φ', will be reached independently of the initial relative density of the soil. This occurs when the volume change of the soil will stop (lower figure). Modified from Larsson (2008).

In dense soil the shear stress increases rapidly due to the small movement of the soil particles. After a relatively short shear displacement the interlocking decreases and the shear stresses needed to continue the shear displacement is reduced. As the shear displacement continues eventually the soil specimen becomes loose enough to allow particles to move without any further volume increase and the shear stress becomes constant at a residual value. The peak stress is usually used to define the failure of the soil. Very dense, well graded soils consisting of angular particles will give the greatest degree of interlocking.

In loose soil, with a large ratio of voids, the interlocking is insignificant and the particles are able to move relatively freely. As the soil mass is compressed the shear stresses increases.

With continued shear displacement the volume decreases as the particles are moved towards each other. The shear stress will increase and reach a residual value when the soil will not be compressed anymore.

Theoretically the void ratio of unconsolidated and undrained specimen of soil is constant during compression. Practically, sampling and preparations result in an increase in void ratio. For a fully saturated soil under undrained condition any increase of the all-round pressure results in an equal increase in pore water pressure. This is regardless of its effective stress value from the beginning.

2.7.3.2 Mineralogical content and shape of particles

The shearing resistance is also dependent on the minerals of the particles, the particle shape and the surface roughness. Different materials have different properties of friction. If the particle has smoother and rounded shape the resistance to sliding, twisting and rolling will decrease. Also, a smooth and rounded shape gives better contact between the particles allowing for decreased crushing. If the particles are crushed in the contact points the particles will follow the principal direction of the shear displacement causing the volume of the soil and the shearing resistance to decrease. Crushing of particles is decreasing with decreasing particle size, since the amount of contact points will increase. Since the void ratio decreases with increasing uniformity coefficient, c_U, the crushing also will decrease indirectly. In some materials the addition of water can have the effect that the hardness will decrease and the crushing of the particles will increase. The crushing also increases with increasing normal and shear stresses. For very high stresses the crushing of the material is so extensive that the volume increase due to dilatancy will not be notable even if the material is very dense. The crushing also increases with increasing angularity and decreasing hardness of particles.

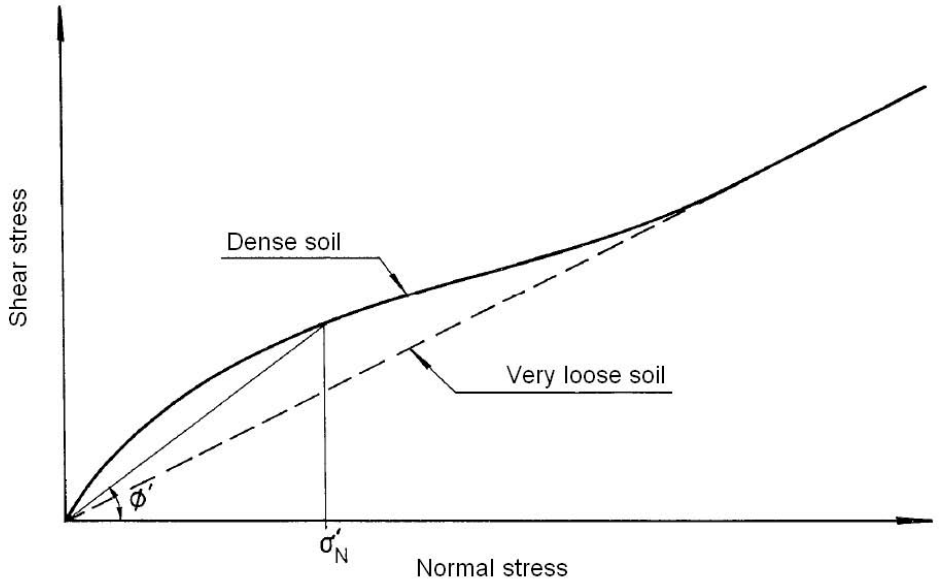

Figure 2.101. The shear stress – normal stress for dense and very loose non-cohesive soil, modified from Larsson (1989).

As the soil dilates with increasing denseness and increasing crushing at higher stress levels the relation between the shear strength and normal stress will be curved, see Figure 2.101.

For a dense non-cohesive soil high friction angles is obtained at low normal stresses. As the normal stress increases the friction angle decreases due to crushing. At very high normal stresses the friction angle approaches a constant value and no volume increase occurs in the soil. The value is about the same as for very loose soil at large deformation. This shows that the friction angle reaches a critical value for large deformation regardless of its initial relative density. The effects of the dilatancy in dense soil at low normal stresses can result in that the shear strength can be more than twice the shear strength for loose soil. After rupture has occurred in the dense soil the shear strength will decrease with increasing deformation. In most cases the friction angle is defined as the secant angle between the line formed through the origin of coordinates to a point on the curve and the horizontal. It is also possible to state the friction angle and the cohesion for a certain range of stress.

2.7.3.3 Anisotropy

The shear strength is affected by the anisotropy of the soil, that is, the soil has different properties in different directions. If the particles are longer, more rectangular than quadratic, the friction angle is different in the directions of the stresses and the displacements. The shear strength will change if the longer particles, having a random direction from the beginning, will have a direction parallel with the shear displacement during deformation. Also in what direction the soil have been consolidated causes anisotropy of the soil. The shear strength will differ depending on the direction of consolidation.

2.7.3.4 Boundary conditions

The value of the friction angle is highly affected by the boundary conditions prevailing, that is if the stresses or the deformation of the soil specimen is limited. An in situ condition is often thought to correspond to a plain strain condition were the soil deforms in two directions and is restricted in the third direction. The stresses can develop in three directions but the deformations can only take place in two directions which restricts the movement of the particles. This makes it more difficult to compare plain strain tests with triaxial tests, were deformations can take place in all directions. The friction angle, and thereby the shear resistance, is higher at plain strain tests than at triaxial tests. In some cases, when the horizontal stresses are equal in all directions, triaxial tests are preferred.

2.8 Conclusions

2.8.1 Classification of excavatability

In the literature of earlier excavatability studies several parameters affecting the ability of excavating in soil are presented. These parameters are summarized in Table 2.24 below. In most of the studies in the literature review it is proposed that particle size (distribution), water content, cementation and content of cobbles and boulders are parameters that affect the excavatability.

Also parameters used for determining the ability of excavating (excavatability) in soil are presented in the literature, see Table 2.25. The result shows that bulk density and the content of cobbles and boulders are parameters that are used to describe the excavatability in most of

the studies. But also results from geotechnical investigation methods like weight sounding, point pressure sounding, ram sounding and seismic are considered when determining the excavatability.

Table 2.24. Parameters affecting the excavatability of soil summarized from different studies.

Study		Particle size distribution	(unsaturated) bulk density	(undrained) shear strength	water content	cementation	porosity	geology	denseness	content of cobbles	content of boulders	relative density	frozen soil	cohesion	friction angle	adhesion	dilatancy
Fransen (1951)		x			x		x										
Arhippainen & Korpela (1966)			x		x			x		x	x						
Korhonen & Gardemeister (1972)	Fine	x		x													
	Coarse	x							x	x	x						
	Moraine		x			x				x	x						
Swedish Road Administration (1976)		x			x	x				x	x	x	x	x	x	x	x
Magnusson & Orre (1985)		x			x	x				x	x	x	x	x	x	x	

Table 2.25. Parameters used to determine excavatability in earlier classification systems.

Study		Bulk density (unsaturated)	Swelling factor	Content of cobbles	Content of boulders	Geological estimation of boulder content	Seismic velocity	Weight sounding	Ram sounding	Rotation sounding	Point pressure sounding	Vane test	Cone test
Fransen (1951)		x	x										
Arhippainen & Korpela (1966)		x					x		x	x			
Korhonen & Gardemeister (1972)	Fine						x	x					
	Coarse			x			x	x	x				
	Moraine	x		x	x		x		x				
Swedish Road Administration (1972)	Fine	x					x	x	x			x	x
	Coarse			x	x	x	x	x	x				
	Moraine	x		x	x	x	x	x	x				
Swedish Road Administration (1976)	Fine			x	x		x	x	x				x
	Coarse				x		x		x				
Magnusson & Orre (1985)		x		x	x		x	x	x		x		

2.8.2 The excavation process

In this study of different excavation processes for earth moving and excavation tasks, three combinations of machine-and-tool sets have been distinguished: a bulldozer or scraper with a wide blade, a wheel loader with a wide bucket and an excavator with a narrow bucket. This division is based on the work task expected and the type of material to be handled.

From studies of bulldozers with wide blades it can be concluded that there is a soil cutting process under the ground and a soil moving process on the ground. The initial penetration phase is short in relation to the cutting-and-moving phase which is continuous. The soil cut by the blade moves upwards along the blade surface and falls down in a pile in front of the blade. The soil accumulated in front of the blade is moved along with blade movement.

In studies of wheel loaders with wide buckets the bucket filling process is interesting from an excavatability point of view. It involves penetration of the soil, cutting or loosening the soil and to withdraw the bucket from the soil while filling the bucket. Both soil in natural state (for example a gravel bank) and soil in piles are handled with wheel loaders.

In studies of excavators with narrow buckets the excavation process has been approached in different ways. Most authors define at least three distinct phases: penetrating, cutting and loading the soil. Usually the loading phase includes rotation of the bucket to scoop the soil and fill the bucket. Bradley and Seward (1998) concluded that the excavation process consisted of two phases: penetration and rotating or penetration and dragging. The strategy of rotating the bucket was used in soft soil and dragging in hard soil, indicating that the soil strength affects the excavation process.

2.8.3 Studies related to excavating and moving soil

In chapter 2.4 studies of different aspects of cutting, excavating and moving soil are presented. From the literature it can be seen that several soil, tool and soil-tool parameters affect the ability of excavating and moving soil. Several researchers have performed mechanical analyses and presented force prediction models for blades and buckets displaced in soil. In most models the blade has been modelled when placed in soil, during the cutting phase. In analytical models the total force has been calculated for a given volume of soil in a state of static equilibrium in front of the blade. In several models the passive earth pressure theory has been used to calculate the soil resistance. Numerical modelling has been performed in both two and three dimensions.

In literature found on buckets several models consider the cutting phase, using a force prediction model developed for a blade. Other researchers have defined different force components acting on the bucket during the motion along a trajectory, such as Hemami (1994). Ericsson and Slättengren (2000) have modelled the excavation process of a wheel loader bucket; during the penetration, cutting and loading phases. In Volvo GPPE performance manual (2009) the ability of filling a bucket with soil is discussed. The degree of filling is dependent on the type of soil excavated were the porosity of the soil and the angle of heap are governing parameters.

2.8.4 Prediction of resistive forces

In predicting the resistance from the soil during excavation with a blade or a bucket, several methods have used the theory of passive earth pressure on structures as a basis. Passive earth

pressure develops when a structure moves towards the soil. According to Duncan and Mokwa (2001) the passive resistance depends on four factors; the amount and direction of the movement of the structure, the soil strength and stiffness, the interface friction and adhesion as well as the shape of the structure.

Several methods for calculating the passive earth pressure have been proposed; analytical and numerical. In chapter 2.5 the three classical earth pressure methods by Rankine and Coulomb as well as the logarithmic spiral method are presented. The methods of Rankine and Coulomb assume a plane soil failure surface whereas Ohde's (1938) method considers a combined one with a logarithmic spiral and a plane. The method by Rankine does not consider soil-interface interaction. The classical earth pressure methods consider a two dimensional analysis. Though, for example researchers like Duncan and Mokwa (2001), Shamsabadi and Nordal (2006) and Rollins et al. (2010) have conducted three dimensional analyses of passive earth pressure problems.

2.8.5 Soil properties

The values of the properties of the soil have an impact on the magnitude of the resistance of soil during displacement by a blade or bucket. In particular the size of soil particles, the denseness and the shear strength of the soil will influence the resistance. The soil friction angle and cohesion are parameters used to define the shear strength. The soil can be defined according to the content of the most common particle size by percent of weight, the distribution of sizes of particles in the soil and the degree of cobbles and boulders in the soil. The denseness of soil can be classified according to the porosity or relative density of the soil. Also the penetration resistance measured through different geotechnical sounding methods gives a relative magnitude of the denseness of the soil. Since the particle size and denseness vary to a great extent in moraine soil, the magnitude of these measures are in particular significant when determining soil resistance.

2.8.6 Soil behaviour

In most situations the strength of the soil can be expressed by the shear strength of soil. Generally the shear strength is expressed through the Mohr-Coulomb equation were the soil friction angle and the cohesion are important parameters. The shear strength is different if the soil is cohesive or non-cohesive under drained or undrained conditions. The resistance to soil loosening is directly related to the shear strength of the soil.

The shear strength of the soil depends on the properties of the soil particles as well as how close the particles are placed together and what direction they have. Properties like particle size, shape and hardness as well as porosity and anisotropy of the soil affects the shear strength. The soil friction angle therefore varies with the properties and the denseness of the soil.

3 Numerical analysis of excavation in soil

3.1 Introduction

A way of determining the excavatability in a certain soil is to determine the excavation resistance of the soil, the resistive force. The resulting force, experienced for example in a bulldozer blade, will be different for different machines and tools. The resulting force will vary due to working operation, the geometrical outline of the tool, tool properties and soil properties.

In several studies of narrow and wide blades has the focus been to study the shape of the failure surface in the soil and to formulate a force prediction model, see chapter 2.4. The results show that these models predict the forces developed in the blade with reasonable accuracy. The models generally assume the soil to be an elastic perfectly plastic material and that the Mohr-Coulomb failure criterion can be applied. It is also assumed that passive failure occurs in the soil along a slip surface as the blade passes through the soil.

Different types of failure surfaces have been considered such as linear, curved and logarithmic. It has been proposed that narrow blades normally give rise to three dimensional failure problems in soil. In the case of a wide blade however, it is considered that side effects on the blade can be neglected since they have small effects on the total force. Therefore a wide blade theoretically can be simplified to involve a two dimensional soil failure problem.

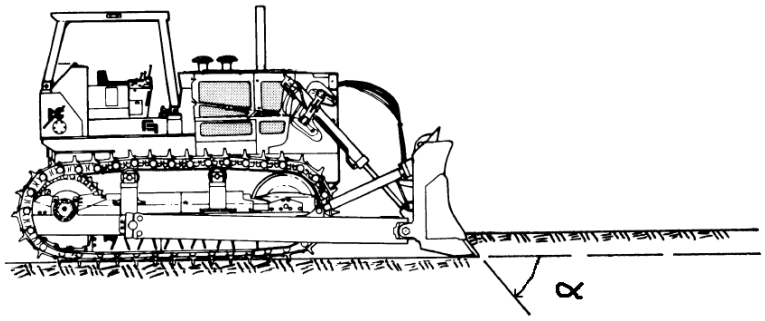

Figure 3.1 Bulldozer with blade and definition of blade angle, α. Modified from McKeys (1989).

The purpose of the numerical analysis in this study was to model the soil-tool interaction of a two dimensional blade in cohesive and non-cohesive soil with the computer program Plaxis, using the Finite Element Method, and to compare the predicted horizontal resistive force on the blade with the force predicted with a analytical model as well as results from experiments in the literature. Also an attempt to model moraine soil as a c-φ soil was carried out.

To simplify the approach in this study, the blade was modelled as a simple flat plate in two dimensions moving horizontally in the soil mass, see Figure 3.2. The cutting phase of the excavation process was studied to see the magnitude of the horizontal force required to break the soil loose. The very beginning of the cutting phase is considered were no soil has accumulated in front of the blade. This is consistent with earlier studies of blades moving in soil, see chapter 2.4. Two types of soils have been defined and used in this study: one cohesive soil with no internal friction and one “non-cohesive” soil with only 0,3 kPa of

cohesion in it. A parametric study to see the effects of different soil, tool and soil-tool parameters on the horizontal force have been carried out. Before the parametric study a convergence study have been performed to see the impact of extended interfaces, mesh coarseness and soil model on the horizontal force. In chapter 3.2 assumptions considering the finite element study is presented.

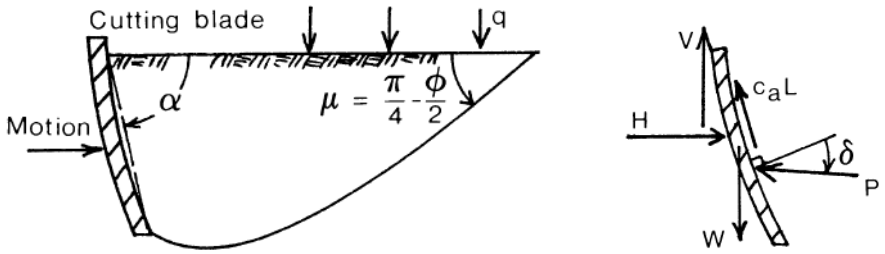

Figure 3.2. Simplified geometry of bulldozer blade and the forces acting on the blade, from McKeys (1989).

3.2 Modelling in Plaxis

The behaviour of a flat blade displaced horizontally through a soil mass has been studied. A numerical approximation of the two dimensional behaviour using the finite element method was performed with the Plaxis 2D computer software. The situation modelled concerns the blade excavating in the soil horizontally at a constant depth and the level of the soil behind the blade was lower than the level ahead of the blade. When modelling blade movement with finite element techniques the soil mechanical behaviour and the soil-tool interaction have to be considered, Mouazen et al (1998) and Davoudi et al (2008).

The finite element technique enables analysis of materials, like soils, that have a nonlinear behaviour, through numerical approximation of displacements in the material. The material body (soil mass) is divided into elements that are connected to its neighbouring elements with nodal points. Through a simple geometrical model the blade and the soil mass were defined. The objects were assigned different material and interface properties as well as a predefined displacement of the blade. The finite element model was generated from the geometrical model were lines and nodes composed a mesh of elements. The soil mass was composed with 15-node triangular elements which provides a very accurate prediction of stress-strain distributions in the soil. In the model the blade and the interfaces between the soil and the blade were generated as special types of elements.

For each nodal point displacement functions are defined and solved through numerical calculations. The size and the boundaries of the total finite element mesh was chosen after ensuring that the sides of the soil mass would not interfere with the stresses generated from the displaced blade. The boundaries of the mesh were assigned to be fixed.

In the next chapters generated figures of the blade in the soil mesh shows soil being cut along a failure surface in both cohesive and non-cohesive soil. Mohr-Coulomb plastic points indicate plasticizing of the soil in a zone in front of the blade with the failure surface as a boundary. This is in agreement with passive earth pressure theory were a wedge of soil is formed in front of a wall.

3.2.1 Cohesive soil

The figures below show the blade and the soil after 0,1 m displacement, as it is visualized in Plaxis.

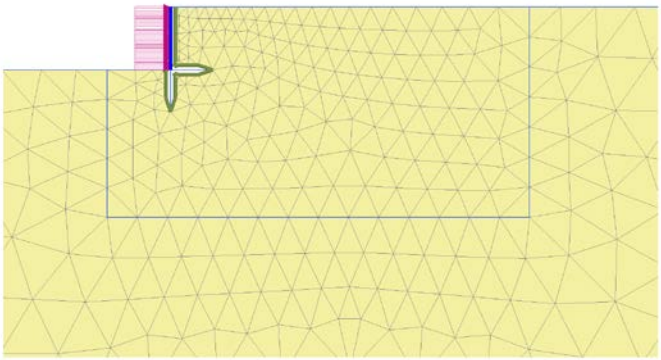

Figure 3.3. The finite element mesh before displacement of the blade.

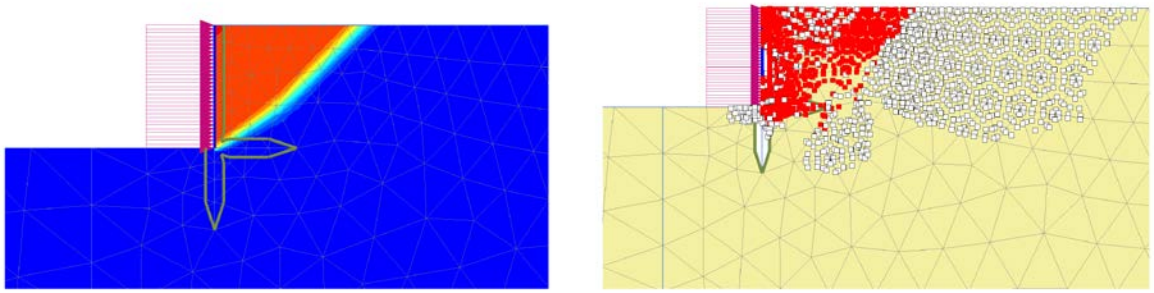

a) b)

Figure 3.4. (a) Total displacements of soil, light colours display large movements. (b) Mohr – Coulomb plastic points (dark dots) and tension cut-off points (white dots).

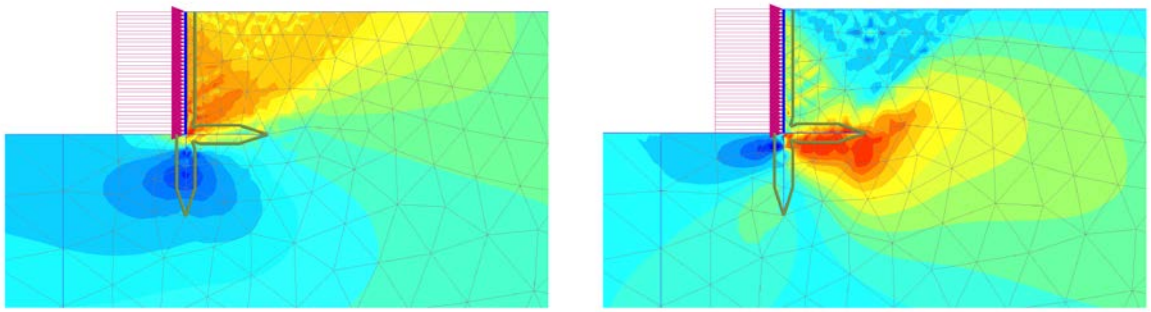

a) b)

Figure 3.5. (a) Cartesian total stresses, σ_{xx} in soil. (b) Cartesian shear stresses, σ_{xy} in soil. Light colours display high stresses.

3.2.2 Non-Cohesive soil

The figures below show the blade and the soil after 0,1 m displacement as it is visualized in Plaxis.

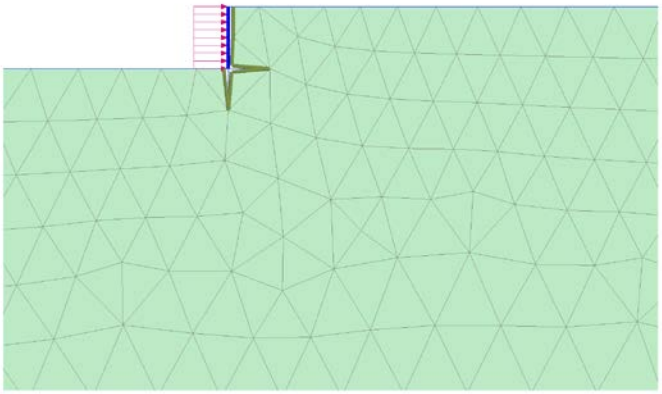

Figure 3.6. The finite element mesh before displacement of the blade.

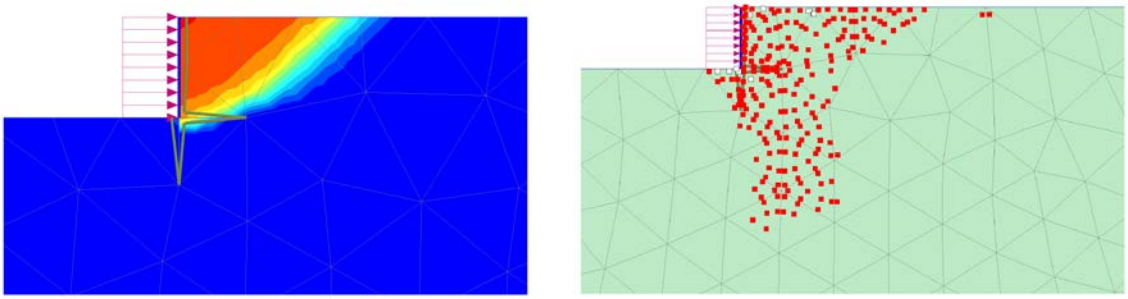

a) b)

Figure 3.7. (a) Total displacements of soil, light colours display large movements. (b) Mohr – Coulomb plastic points (dark dots) and tension cut-off points (white dots).

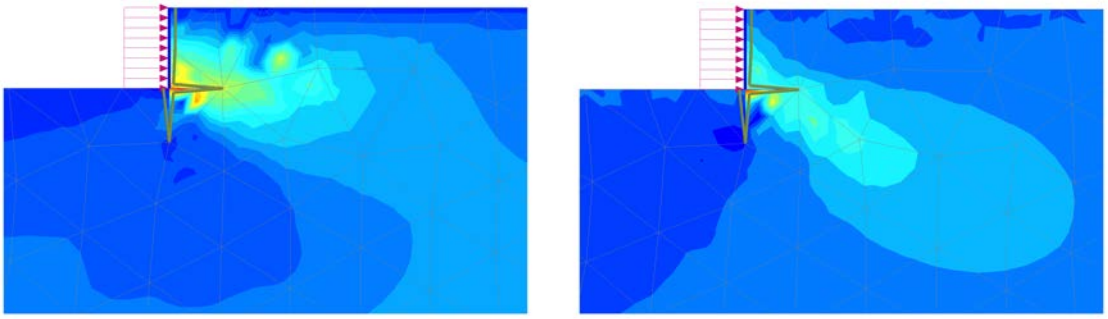

a) b)

Figure 3.8. (a) Cartesian total stresses, σ_{xx} in soil. (b) Cartesian shear stresses, σ_{xy} in soil. Light colours display high stresses.

3.2.3 Modelling blade and soil

The blade was modelled as a stiff plate of steel pushing the soil horizontally. The length of the blade was 0,3 m.

The soil mass was modelled in plane strain conditions assigned material properties according to the Mohr-Coulomb soil model. The non-linear behaviour of soil can be modelled at several levels of complexity, where the number of model parameters increases with the level of complexity, Brinkgreve et al. (2006). For example, the Hardening Soil model is more complex model were the stress-strain relationship is considered as hyperbolic, see Figure 3.9. In this study the ultimate strength of soil is of mayor interest and the behaviour of the soil before failure is of minor interest. It is thought that the Hardening Soil model suites to describe the later behaviour and that the Mohr-Coulomb soil model is sufficient in predicting the soil failure. The Mohr-Coulomb model was chosen for this study to analyse soil behaviour. It is the most common model used when modelling soil behaviour in practice, in civil and construction projects, and do not need, relatively other soil models, that many soil parameters as input. The results from the convergence study show that the difference in predicting the ultimate soil failure between the Mohr-Coulomb and Hardening Soil models is small. See chapter 3.3.

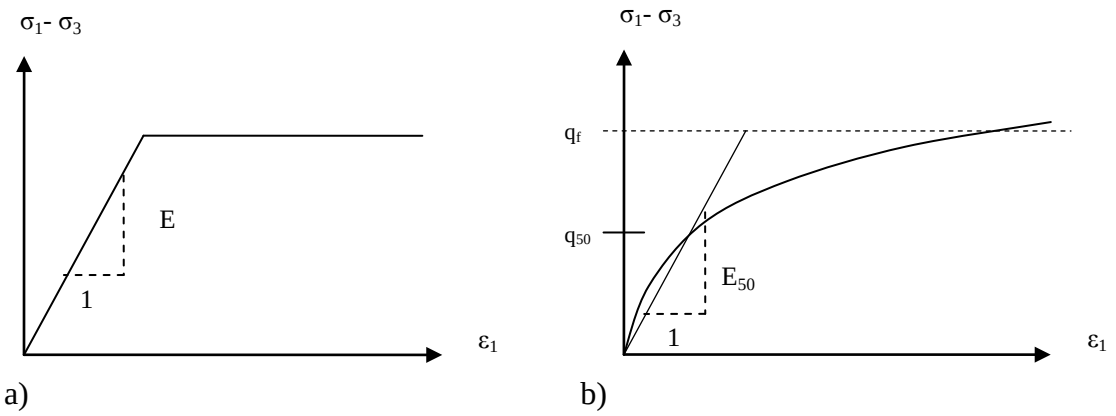

Figure 3.9. Stress – strain relationship according to; (a) Mohr-Coulomb soil model, and (b) Hardening soil model.

The Mohr-Coulomb soil model assumes linear elastic and perfectly plastic deformation of the soil and involves five input parameters: Young's modulus, E and Poisson's ratio, ν for soil elasticity: cohesion, c and friction angle, φ, for soil plasticity and the angle of dilatancy, ψ, for soil volume increase.

In Plaxis Young's modulus, E is used as the basic stiffness modulus in both the elastic model and the Mohr-Coulomb model. For soils like sands and normally consolidated clays the elastic stiffness modulus is best approximated with the secant slope of the stress-strain curve. The stiffness modulus depends on confining pressure, stress path during loading and unloading and amount of straining of the soil. Brinkgreve et al. (2006) recommend using a modulus value that is consistent with the stress level and expected stress path. In Plaxis there is an option to perform undrained effective stress analyses using undrained parameters ($\varphi = 0$ and $c = c_u$) in the material model.

With Poisson's ratio, v, the volume decrease at the very beginning of loading is modelled in Plaxis. In undrained behaviour Brinkgreve et al. (2006) recommend using the effective Poisson's ratio, v that is smaller than 0,35. Using higher values would mean that the water would not be sufficiently stiff.

In the Mohr-Coulomb model the cohesion, c is used together with the friction angle, φ to model the shear strength of the material. For an undrained condition Brinkgreve et al. (2006) prefers that the undrained shear strength parameter, c_u, is used since the user then has control over the shear strength independently of the actual stress state and stress path followed. The c_u parameter is used in combination with $\varphi = 0$ for cohesive soil. In non-cohesive soil the software can have problems with the performance when using almost zero cohesion. To avoid complications Brinkgreve et al. (2006) recommends a small value ($c > 0,2$ kPa) for the cohesion. In Plaxis the computing time increases more or less exponentially with the friction angle. High friction angles, especially higher than 35 degrees, considerably increase plastic computational effort.

Dilatancy is the volume increase of a soil mass due to soil particles moving and rolling over each other when the soil deforms. When sheared, heavily consolidated clays and non-cohesive soils show on dilatancy that depends on density and the friction angle. Normally consolidated clays tend to not show on dilatancy. In Plaxis the angle of dilatancy, ψ, is considered as a strength parameter increasing the shear strength of soil. For quartz sand the dilatancy angle approximately equals φ – 30 degrees and often is set to zero for φ-values less than 30 degrees. When the soil is modelled as undrained in Plaxis, with c_u and $\varphi = 0$, the angle of dilatancy has to be set to zero, otherwise the model will show unlimited soil strength due to suction.

3.2.4 The blade – soil interaction

The interaction between the blade and the soil is modelled with interfaces in Plaxis. Interfaces are no physical elements and have a "virtual thickness" which is an imaginary dimension used to define material properties of the interface. A higher virtual thickness generates more elastic deformations. In this study the virtual thickness factor is set to 0,1.

The interaction between the blade and the soil can vary from smooth to rigid (fully rough). The interface is defined with a strength reduction factor $R_{interaction}$ that models the roughness of the interaction, ($0 < R_{interaction} < 1,0$). This factor relates the interface strength (friction and adhesion) to the soil strength (friction angle and cohesion respectively). The behaviour of the interfaces is described with an elastic-plastic model and the Coulomb criterion is used to distinguish between elastic behaviour, small displacements within the interface, and plastic behaviour when permanent slip may occur. In Plaxis the interface properties are related to the soil properties with the strength reduction factor, $R_{interaction}$ as follows:

$$c_a = R\, c \qquad (3\text{-}1)$$

$$\tan(\delta) = R \tan(\varphi) < \tan(\varphi) \qquad (3\text{-}2)$$

where R is the strength reduction factor, c_a is the adhesion and δ is the soil-interface friction angle.

In reality the interface is weaker and more flexible than the associated soil layer which means that the strength reduction factor should be smaller than 1. The closer $R_{interaction}$ is 1,0 the

rougher the interaction becomes. The closer $R_{interaction}$ is 0 the smoother the interaction becomes which means that the blade and the soil moves more independently of each other, Carlstedt (2008).

3.2.5 Numerical calculations

Numerical calculations of the horizontal resistive force on the blade have been performed with Plaxis. A parametric study was carried out for the undrained cohesive and drained non-cohesive soils. One at a time the blade angle, α, the soil friction angle, φ and the undrained shear strength, c_u, of the soil were varied. The soil-blade friction, δ and adhesion, c_a were varied through the soil-tool interaction parameter, $R_{interaction}$. The blade depth was held constant at 0,3 m. The unit weight of soil, γ and the soil model parameters E, and ψ, were varied for the non-cohesive soil, see Table 3.5, but held constant for the cohesive soil.

In the calculations the blade was displaced 0,1 m, enough to see when the force achieves a constant value representing the plastic state of the soil occurring at some displacement. For different combinations of parameter settings the effects on the resultant horizontal force have been studied.

3.2.6 Soil properties used in the finite element analysis

Three types of soils were modelled: a cohesive soil with no internal friction, a non-cohesive soil with practically no cohesion and a moraine soil with both cohesion and internal friction. The cohesive soil was loaded under undrained conditions ($\varphi_u = 0$, $\psi = 0$). The non-cohesive soil was loaded under drained condition. Gravel, sand and silt moraine were loaded under drained condition while clay moraine was loaded under both drained and undrained conditions.

The cohesive soil was modelled as undrained and it was assumed that the soil particles had poor contact with each other and that the soil skeleton was instable. The angles of friction and dilatancy were assumed to be zero. The undrained cohesive soil was assigned values of undrained shear strength from 10 to 40 kPa. The value of the coefficient of lateral earth pressure, K_0 was set to equal 1,0. The stiffness modulus, E = 6000 MPa and Poisson ratio, ν = 0,35.

The non-cohesive soil was modelled to represent a granular soil where an increase of the friction and dilatancy angles causes an increase of the strength of the soil. With increasing friction properties and stiffness the soil was assumed to be more difficult to excavate. The non-cohesive soil was modelled as drained and it was assumed that there was no cohesion. A zero value of the cohesion leads to a dividing by zero during the Plaxis computations. Therefore a low value of c (= 0,3 kPa) was used when modelling non-cohesive soil. The weight of soil, γ, stiffness modulus, E, angle of dilatancy, ψ and coefficient of lateral earth pressure, K_0 varies with increasing soil friction angle, φ'. Poisson ratio, ν = 0,2. According to Das (2006), Jaky (1944) have proposed that the K_0 value can be calculated as follows:

$$K_0 = 1 - \sin \varphi \qquad (3\text{-}3)$$

Proposed values for different soil properties have been found in the literature, see tables below.

Table 3.1. Characteristic values of unit weight, γ, from Larsson (2008).

Soil type	Unit weight (kN/m^3)	
	Saturated	Unsaturated
Blasted rock	21	18
Gravel	22	19
Gravel moraine	23	20
Sand	20	18
Sand moraine	22	20
Silt	19	17
Silt moraine	21	20
Clay	17	17
Clay moraine	22	22

Table 3.2. Characteristic values of the soil friction angle, from Swedish Road Administration (2009).

Soil type	Soil friction angle, φ'	
	Loose	Dense
Blasted rock	-	45
Gravel	30	37
Gravel moraine	38	45
Sand	28	35
Sand moraine	35	42
Silt	26	33
Silt moraine	33	40
Clay	-	-
Clay moraine	-	-

Table 3.3. Approximate values of the soil friction angle, according to Hansbo (1975).

Soil type	Soil friction angle, φ'	
	Loose	Dense
Blasted rock	40	45
Gravel	30	37
Gravel moraine	38	45
Sand	28	35
Sand moraine	35	42
Silt	25	35
Silt moraine	-	-
Clay	20	30
Clay moraine	25	35

Table 3.4. Characteristic values of the Elastic Modulus, E, from Swedish Road Administration (2009).

Soil type	Elastic Modulus (Mpa)	
	Loose	Dense
Blasted rock	-	50
Gravel	10	40
Gravel moraine	10	40
Sand	5	20
Sand moraine	5	20
Silt	2	10
Silt moraine	2	10
Clay	-	-
Clay moraine	-	-

In Table 3.5 values for properties of the non-cohesive soil used in the analysis is presented. The unit weight, γ, the friction angle, φ, the angle of dilatancy, ψ, the stiffness modulus, E, and the coefficient of lateral earth pressure, K_0 varies with increased denseness and shear strength of soil and are related to each other. Values used in this study are presented in Table 3.5 and the arrangement of the properties is based on the friction angle and represents a reasonable range of values for non-cohesive soils. In this study the values where chosen in order to show on the difference in magnitude of the horizontal force due to different soil properties. The soil with the lowest values (when $\varphi = 30°$) represents a silty or sandy soil and the soil with the highest values (when $\varphi = 45°$) represents a dense gravely soil. The values of the different properties and the relations between them are reasonable in accordance to values presented in the literature, see: Hansbo (1975), Larsson (2008) and Swedish Road Administration (2009).

Table 3.5. Values of soil properties used in the FE-analysis for non-cohesive soil.

γ (kN/m^3)	φ' (°)	ψ (°)	E (Mpa)	K_0
18	30	0	10	0,5
18	35	5	20	0,426
19	40	10	30	0,357
19	45	15	40	0,293

In Table 3.6 values for properties of the moraine/c-φ soil used in the analysis is presented. Similarly as for non-cohesive soil the values of the different soil parameters varies depending on, particles size, denseness and shear strength. The values for the moraine/c-φ soil used in this study have been chosen from the literature. In Larsson (2008), Hansbo (1975) and Swedish Road Administration (2009) approximate values of soil properties have been proposed, see tables above. It is assumed that the values used in Table 3.6 represent a reasonable range of values for loose and dense moraine soils. Values for the stiffness modulus, E, for clay moraine could not be found in the literature and it was assumed that this value was 3 MPa. The values for the cohesion, c' in the moraine soil was assumed to range from 0 to 15 kPa, increasing for soil with increasing cohesion.

Table 3.6. Values of soil properties used in the FE-analysis for moraine/c-φ soil.

	γ (kN/m^3)		φ' (°)		E (Mpa)		c' (kPa)	Drained/
	Unsat	Sat	Loose	Dense	Loose	Dense		Undrained
Gravel moraine	20	23	38	45	10	40	0	Drained
Sand moraine	20	22	35	42	5	20	5	Drained
Silt moraine	20	21	33	40	2	10	10	Drained
Clay moraine	22	22	25	-	3	-	15	Drained
			-	-	3	-	15	Undrained

3.3 Convergence study

Before the parametric study was started a convergence study for the model of the problem was performed. The purpose of the convergence study was to see the effects of mesh size coarseness, extended interfaces (boundary conditions) and soil models on the horizontal force. From the convergence study initial values of these parameters were selected for the parametric study.

In Plaxis a special attention is needed when modelling the interaction between soil and a stiff structure with sharp corners. According to Brinkgreve et al. (2006) the abrupt change in boundary condition may lead to high unrealistic peaks in stresses and strains around the corner points. Therefore additional interface elements were used, from the corner point and 0,2 m into the soil mass. These elements were assigned a strength reduction factor, $R_{interaction}$ = 1 which allows for minimum disturbance and sufficient flexibility of the finite element mesh. As the blade was vertical the interface elements were chosen to have vertical and horizontal directions. This was also assumed by Rollins et al (2010) in their Plaxis calculations. For an inclined blade different angles of the interface elements normal and tangential to the blade were tried. The convergence study showed that the directions of the interface elements had a large impact on the resultant force. Also the effect with and without extended interfaces were compared.

In Plaxis the finite element mesh is distinguished into five levels of coarseness according to the size of the elements: very coarse, coarse, medium, fine and very fine. A finer coarseness gives more elements within a surface unit which enables a more accurate analysis. In areas were large stresses or displacements are expected Brinkgreve et al. (2006) recommends a finer mesh to be used. In this study a finer mesh was used in a small area close to the blade for the cohesive soil. The default mesh was set to be of medium coarseness. In the convergence study the effect from three types of meshes (global coarseness) were tested: medium, fine and very fine. The effect of mesh size was also investigated by Shamsabadi and Nordal (2006) when calculating soil resistance developed during movement of a bridge abutment. They also found that the mesh coarseness had a significant impact and that the medium mesh could be used mediating between accuracy and computing time.

The convergence study was carried out to evaluate the effects of the extended interfaces and mesh size around a vertical blade. Cohesive soil with c_u of 20, 30 and 40 kPa and non-cohesive soil with 30, 35 and 40 degree friction angle were tested at an $R_{interaction}$-value of 0,4.

The results show that the resultant force on the vertical blade in cohesive soil decreases up to 5% if extended interfaces are used and decreases up to 7% if a fine mesh instead of medium mesh is used. If both extended interfaces and fine mesh is used in the cohesive soil the resultant force decreases up to 12% compared to not using any of them. In non-cohesive soil the resultant force increases up to 15% if extended interfaces are used and decreases up to 17% if a fine mesh instead of a medium mesh is used around the blade. If both extended interfaces and fine mesh is used in the non-cohesive soil the resultant force decreases up to 4% compared to not using any of them.

Also the difference in results between Mohr-Coulomb and Hardening Soil models were studied. A non-cohesive soil with a soil friction angle of 45° was tested at an angle of dilatancy of 5° and 15° respectively, see Figure 3.10 and Figure 3.11. The results show that yielding progresses for a longer displacement with the Hardening Soil model. Though, the ultimate horizontal force will be about the same for both models. This might not be a surprise since the Hardening Soil model defines failure according to the Mohr-Coulomb soil model, with parameters c, φ and ψ.

Observe that the calculations are performed with a 0,7 m high blade which causes higher magnitude of the horizontal forces than other results in this study.

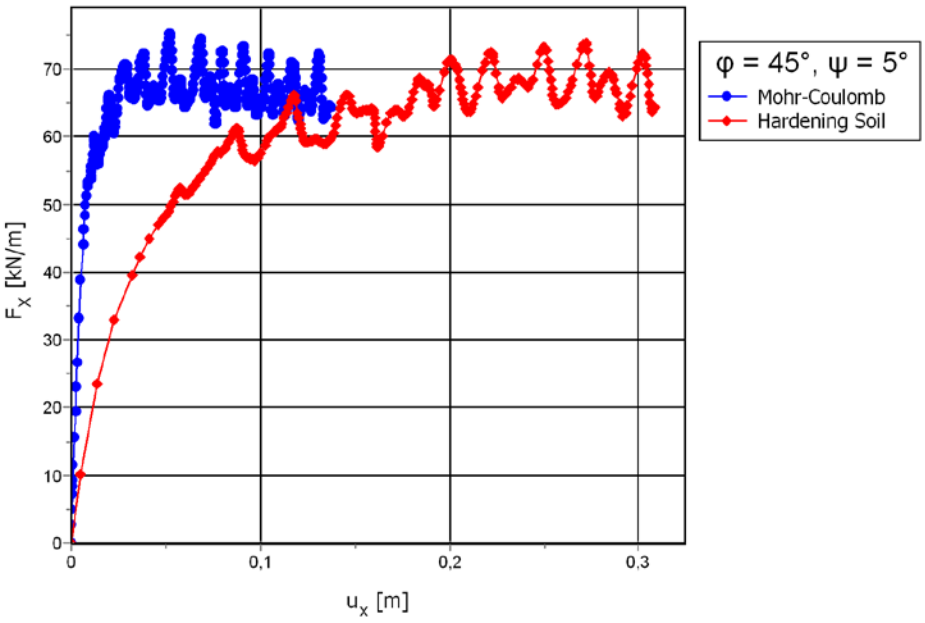

Figure 3.10. The variation of the horizontal force for non-cohesive soil modelled with Mohr-Coulomb and Hardening Soil material models. With φ = 45° and ψ = 5°.

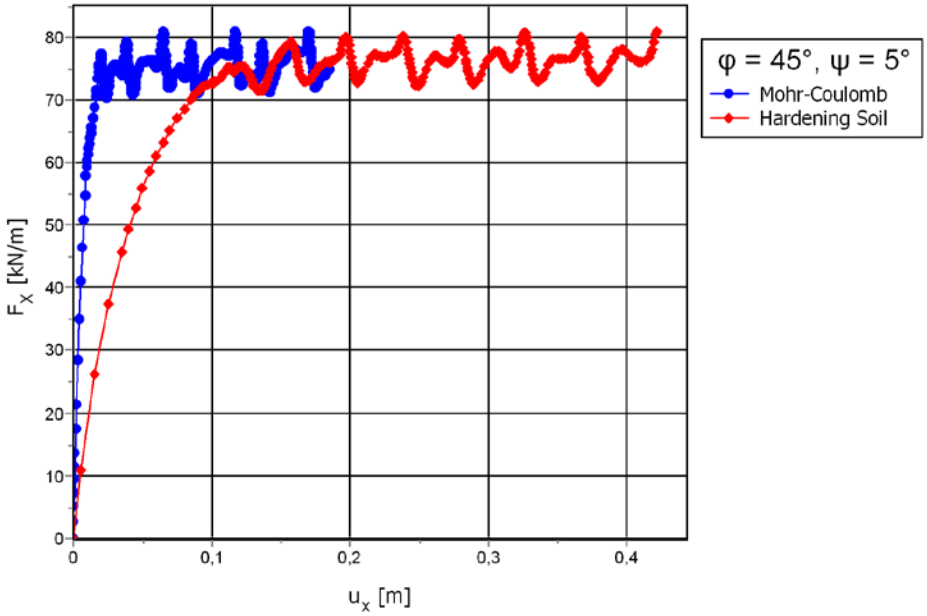

Figure 3.11. The variation of the horizontal force for non-cohesive soil modelled with Mohr-Coulomb and Hardening Soil material models. With $\varphi = 45°$ and $\psi = 15°$.

3.3.1 Cohesive soil

With the results from the convergence study it was decided that the soil-blade interaction in cohesive soil could be modelled with both extended interfaces and a fine mesh around the blade. There were problems with the calculations when extended interfaces were applied in a medium mesh but not in a fine mesh around the blade, as can be seen in Figure 3.12 to Figure 3.14 below.

Using extended interfaces with a mesh of medium coarseness gave difficulties with the convergence. In meshes with fine and very fine coarseness the use of the extended interfaces led to a reduced horizontal force with about 5% and 8% respectively compared to using medium coarseness. A fine mesh decreases the horizontal force with about 7% compared to use a mesh of medium coarseness. Using a very fine mesh decreases the force with additionally 7%.

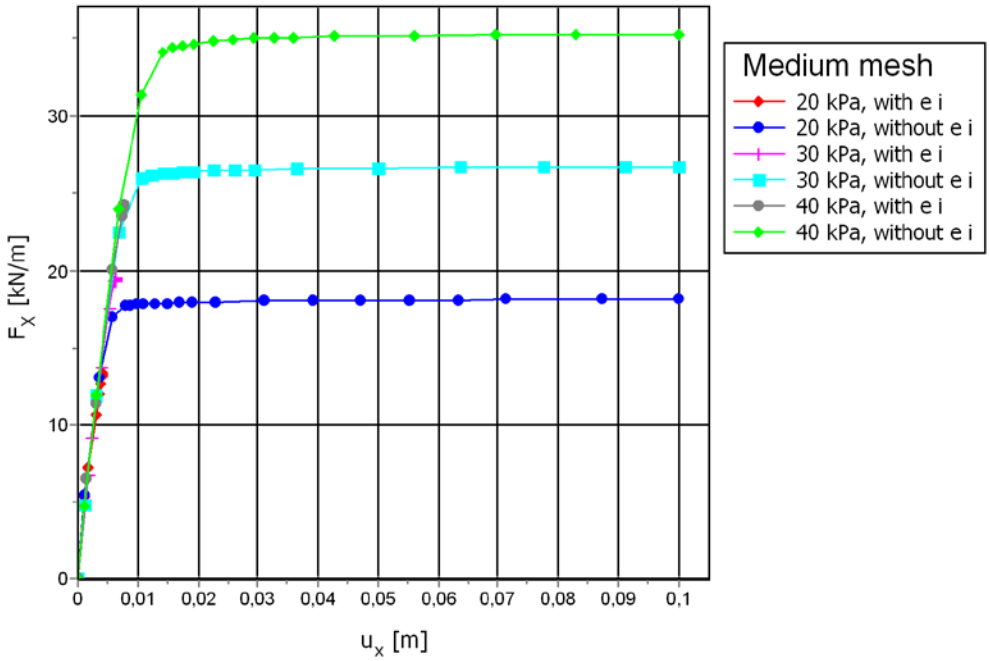

Figure 3.12. Force – displacement curves in medium mesh with and without extended interfaces (in cohesive soil). Due to convergence difficulties results from calculations with extended interfaces are only shown in the elastic part of the force – displacement curves.

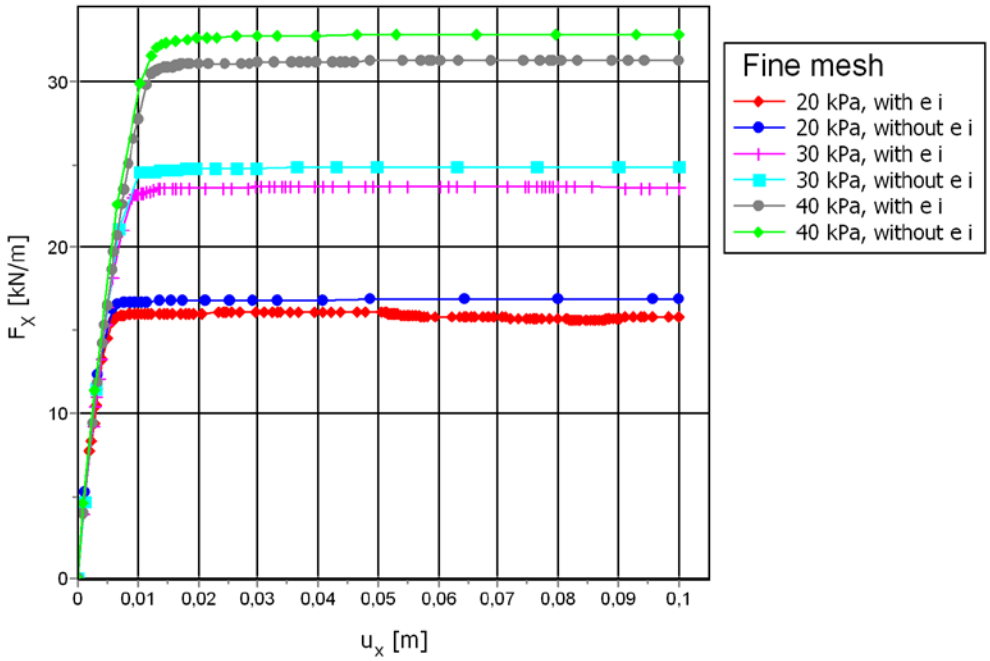

Figure 3.13 Force – displacement curves in fine mesh with and without extended interfaces (in cohesive soil).

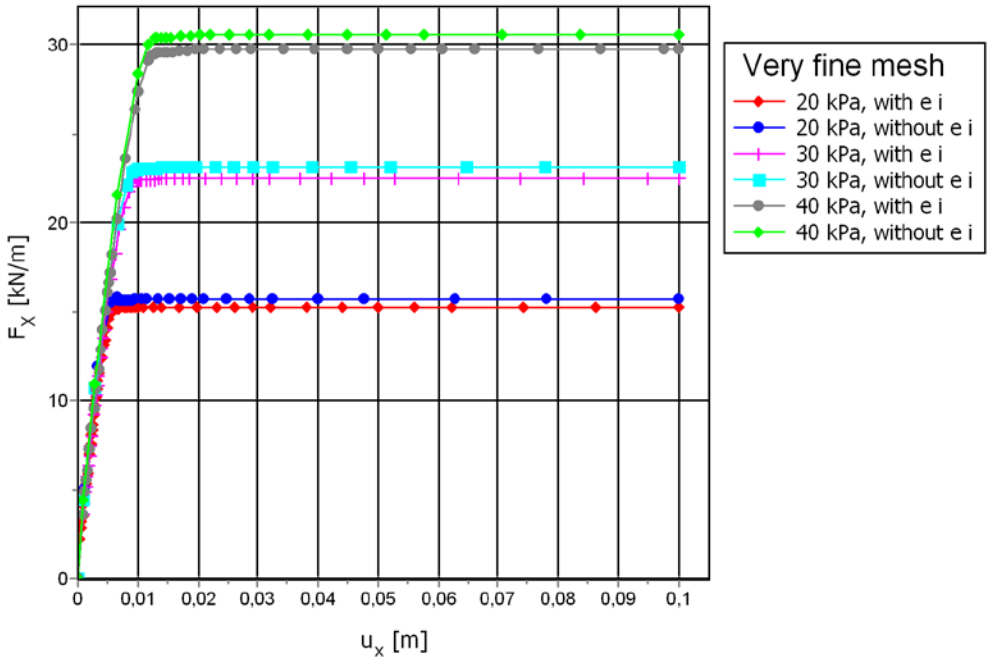

Figure 3.14. Force – displacement curves in very fine mesh with and without extended interfaces (in cohesive soil).

3.3.2 Non-Cohesive soil

The soil-blade interaction in non-cohesive soil was modelled with extended interfaces and a medium mesh around the blade, see Figure 3.15 to Figure 3.17. In calculations with fine and very fine meshes yielding problems arise due to lack of convergence. The finer mesh used; the larger pending of the force as the blade was displaced. The problems with convergence also increased with increasing soil friction angle. Therefore there is a greater discrepancy in the load – displacement curves with larger soil friction angle and in those curves generated in fine and very fine meshes.

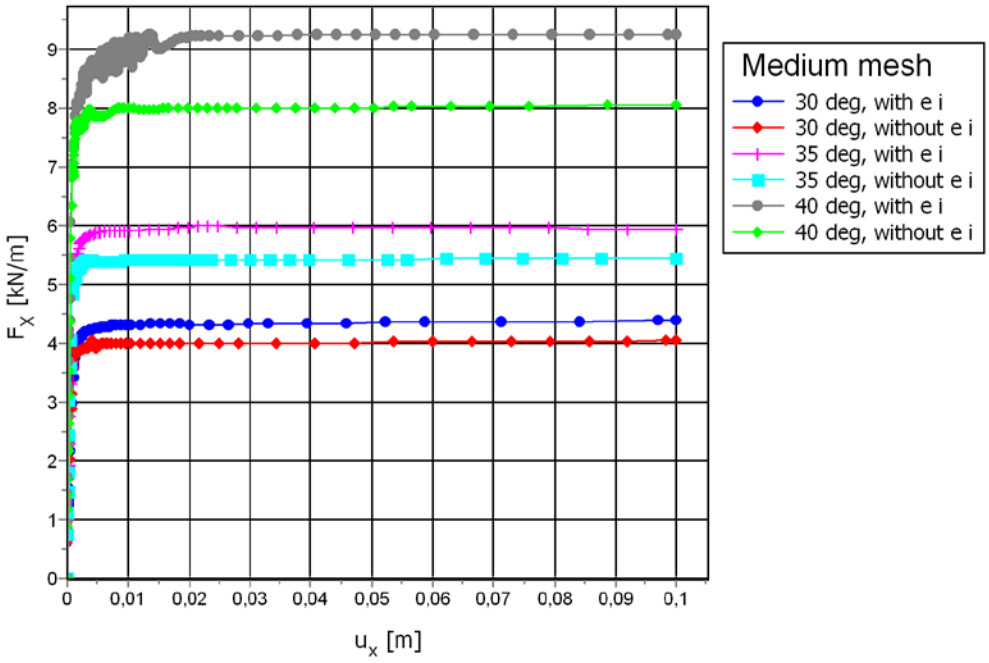

Figure 3.15. Force – displacement curves in medium mesh with and without extended interfaces (in non-cohesive soil).

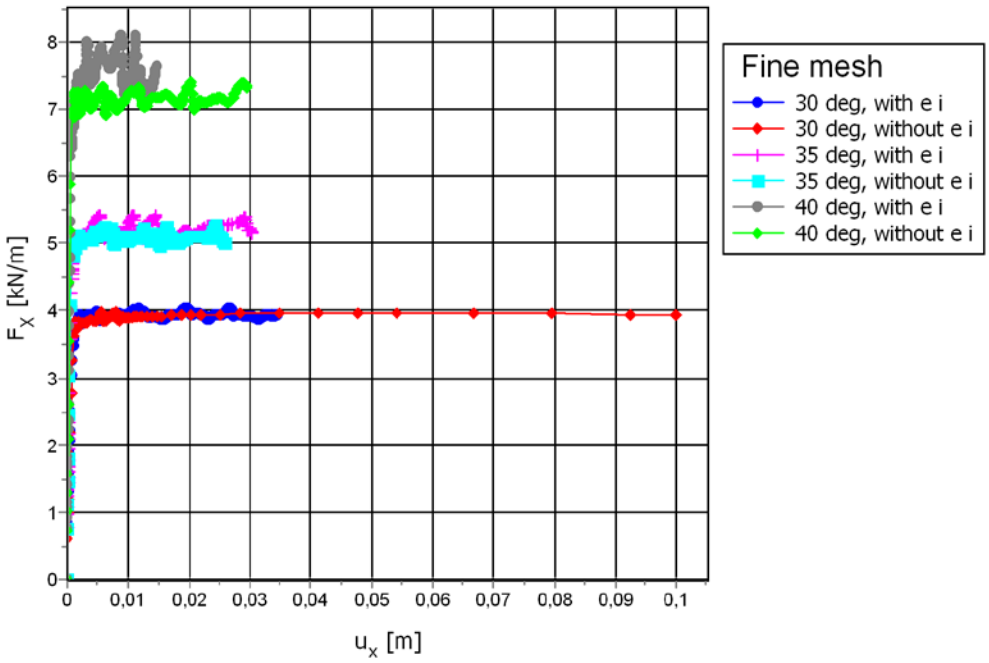

Figure 3.16. Force – displacement curves in fine mesh with and without extended interfaces (in non-cohesive soil).

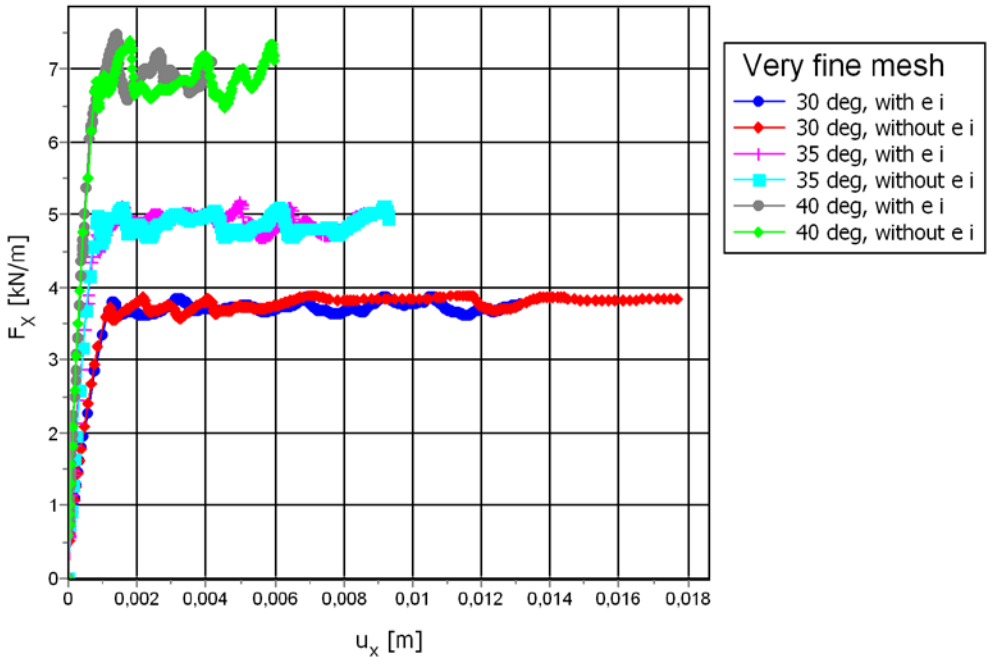

Figure 3.17. Force – displacement curves in very fine mesh with and without extended interfaces (in non-cohesive soil).

The use of extended interfaces in a medium mesh soil increases the horizontal force with about 6%, 11% and 15% for soils with 30, 35 and 40 degree friction angle respectively. When using them in soil with fine or very fine mesh the increase of the force is low, between 1 and 5%. Using a finer mesh decreases the horizontal force in non-cohesive soil. A fine mesh instead of medium coarseness decreases the force about 7 to 17%. Using a very fine mesh instead of a fine mesh decreases the force about 7 to 10%. The decrease is lower for soils with lower soil friction angle. The decrease is also lower when not using extended interfaces.

3.4 Parametric study - cohesive soil

3.4.1 Effect of undrained shear strength, c_u

Figure 3.18 to Figure 3.20 shows the resultant horizontal force on the blade during displacement at different values of undrained shear strength in the soil. For a vertical blade the force increases as the deformation is elastic and reaches a constant value after some displacement. For soil with undrained shear strength, c_u of 40 kPa the maximum force occurs after about 0,01 m displacement, when the soil yields continuously. The force will reach its maximum level at a shorter displacement in a soil of lower c_u than in a soil with higher c_u. For blades with blade angles of 60 degrees the force reaches a constant value at further displacement than for a vertical blade. Also the transition from elastic to plastic yielding is not as distinct as in the case with a blade angel of 90 degrees. It is assumed that soil failure have occurred as the force reaches a constant value.

The ultimate soil resistance, F_x increases with increasing undrained shear strength of soil. An increase of the undrained shear strength, c_u from 10 to 20 kPa yields an increase of about 90 % of the soil resistance, an increase from 20 to 30 kPa yields an increase of about 44% and an increase of 30 to 40 kPa yields an increase of about 35 % of F_x.

Figure 3.20 shows the ultimate horizontal force at 0,1 m displacement at a constant soil-tool interaction value ($R_{interaction}$ = 0,4). It shows that the force increases linearly with increasing undrained shear strength, c_u.

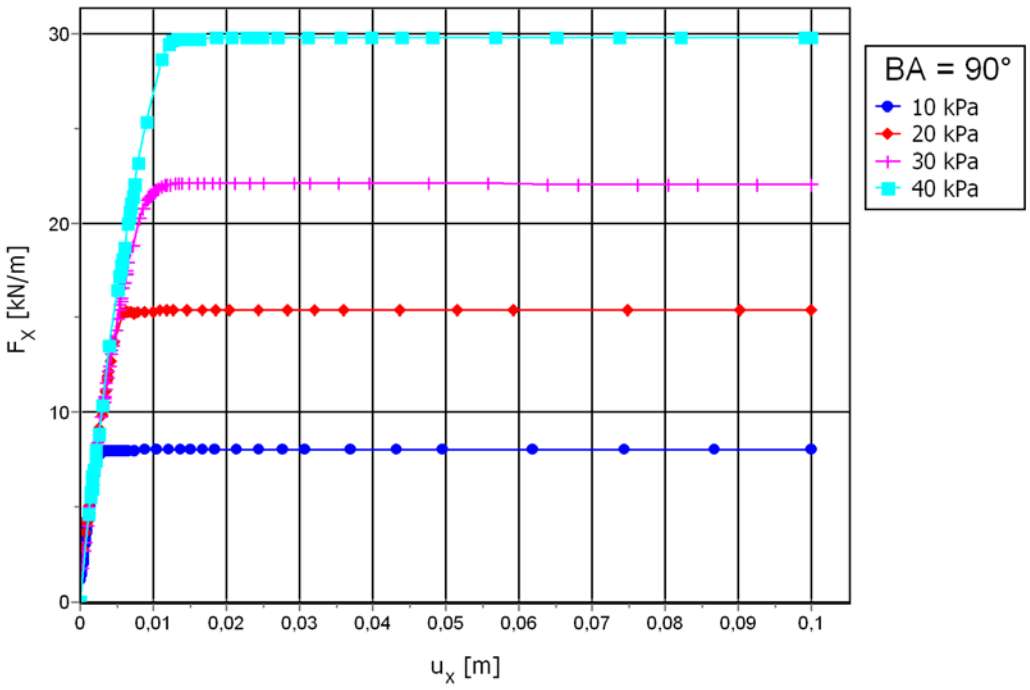

Figure 3.18. Force – displacement curve for a blade with a 90° blade angle (BA) at $R_{interaction}$ = 0,4 for different values of undrained shear strength, c_u for the soil.

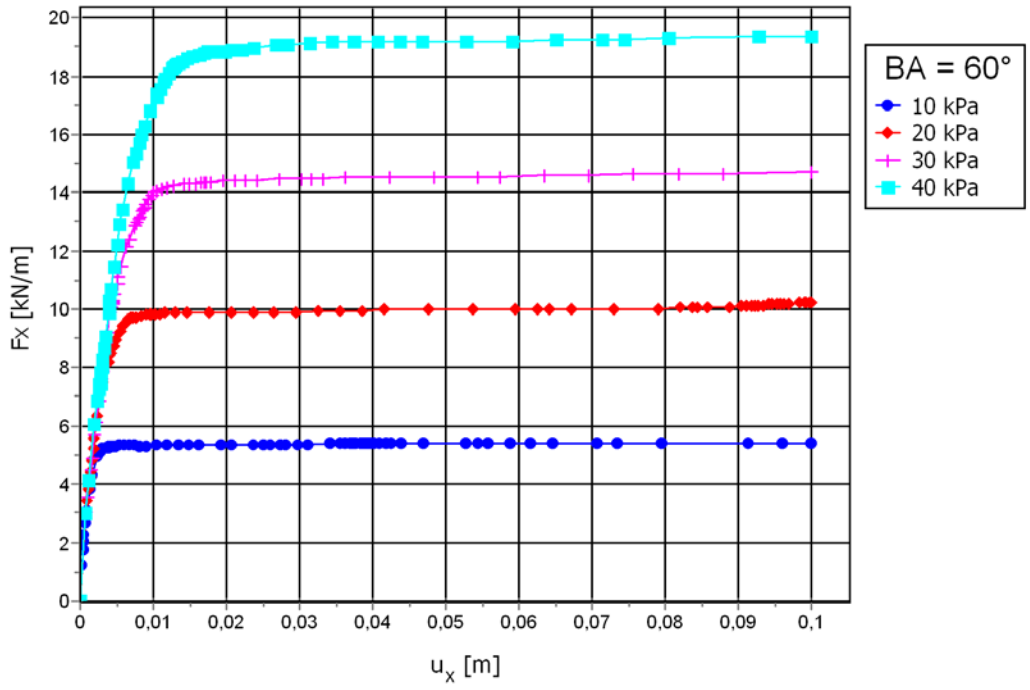

Figure 3.19. Force – displacement curve for a blade with a 60° blade angle (BA) at $R_{interaction}$ = 0,4 for different values of undrained shear strength, c_u for the soil.

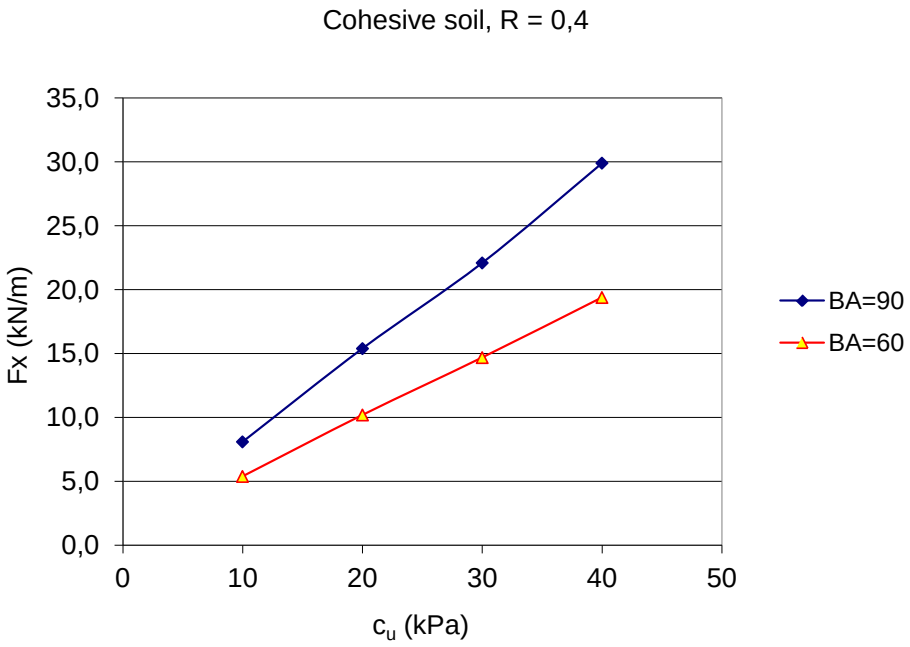

Figure 3.20. The variation of the ultimate horizontal force with c_u of the soil and for different blade angles (BA). Summary of values from Figure 3.18 and Figure 3.19.

3.4.2 Effect of soil-tool adhesion through $R_{interaction}$

Figure 3.21 and Figure 3.22 shows the variation of the horizontal force with the different values of adhesion between the soil and the blade. It is shown that the force – displacement curve is similar for every value of adhesion ($R_{interaction}$).

Figure 3.23 shows the variation of the ultimate horizontal force at different values of adhesion ($R_{interaction}$) with the vertical blade. The force seems to increase linearly with adhesion. For a soil with c_u = 20 kPa the force varies with the adhesion from about 15 kN/m at R = 0,2 to 18 kN/m at R = 1,0. For a soil with c_u = 30 kPa the force varies with the adhesion from about 21 kN/m at R = 0,2 to 25 kN/m at R = 1,0.

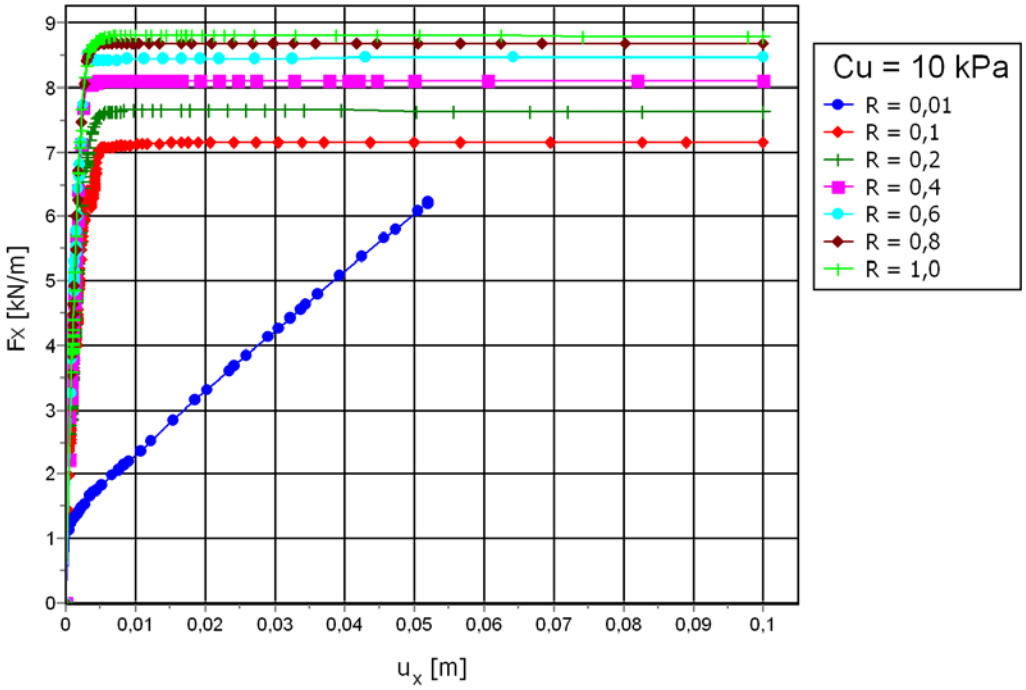

Figure 3.21. Force – displacement curve for a blade with a 90° blade angle in cohesive soil with c_u = 10 kPa at different values of soil-tool interaction, $R_{interaction}$.

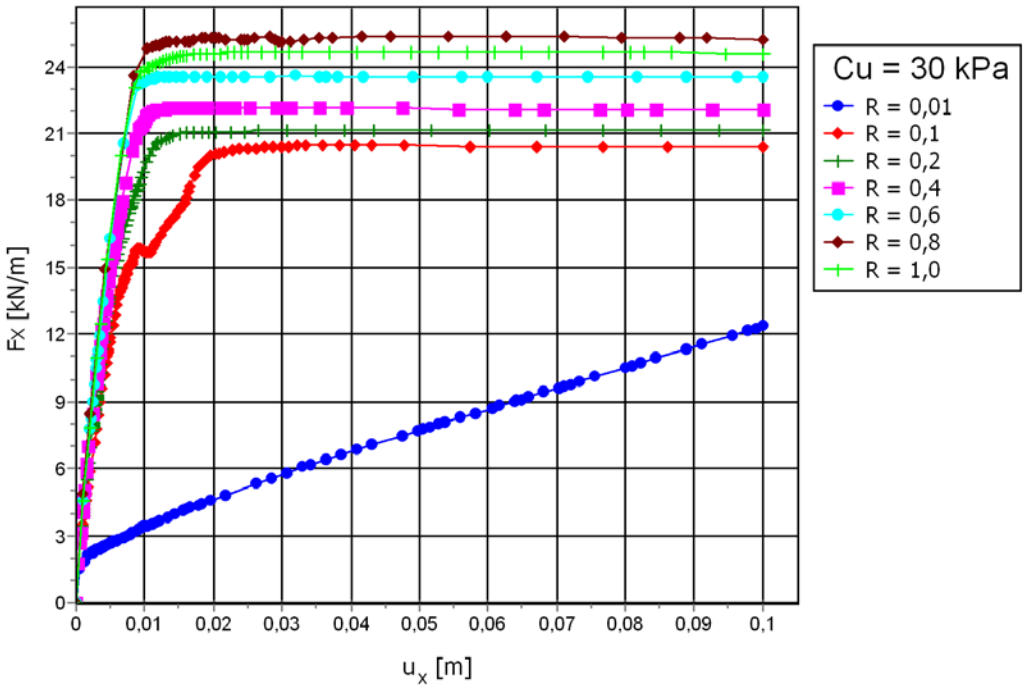

Figure 3.22. Force – displacement curve for a blade with a 90° blade angle in cohesive soil with c_u = 30 kPa at different values of soil-tool interaction, $R_{interaction}$.

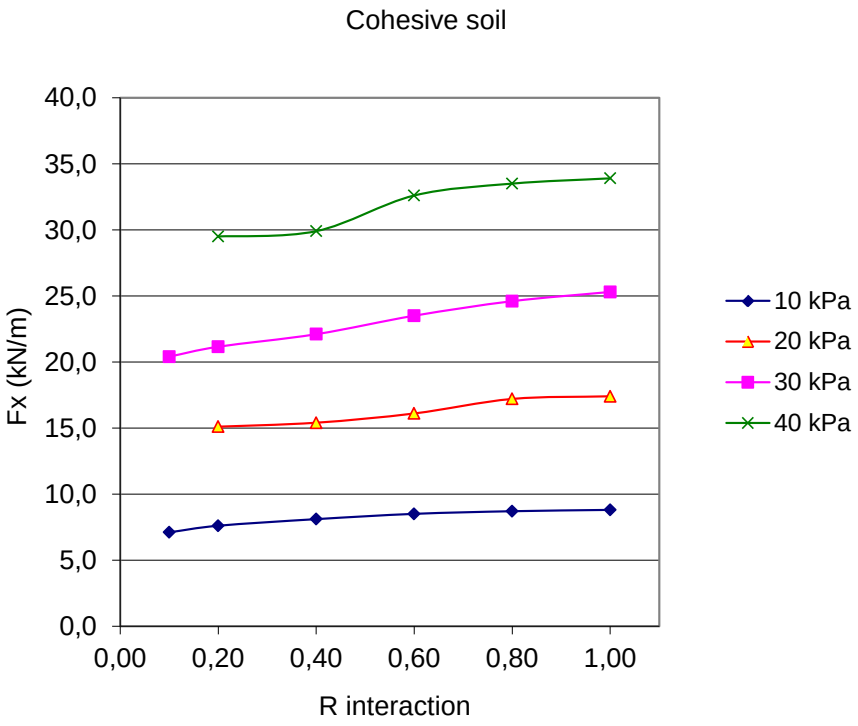

Figure 3.23. The variation of the ultimate horizontal force with different values of adhesion. Summary of values from Figure 3.21 and Figure 3.22.

3.4.3 Effect of blade angle, α

Figure 3.24 shows the increase of the ultimate horizontal force as the blade angle increases from 60 to 90 degrees. At a constant $R_{interaction}$ = 0,4 the increase of the force is larger at higher undrained shear strength, c_u. Figure 3.25 shows the rate of increase (in %) of the ultimate horizontal force as the blade angle increases from 60 to 90 degrees. The increase varies with different values of $R_{interaction}$ and undrained shear strength in a nonlinear way.

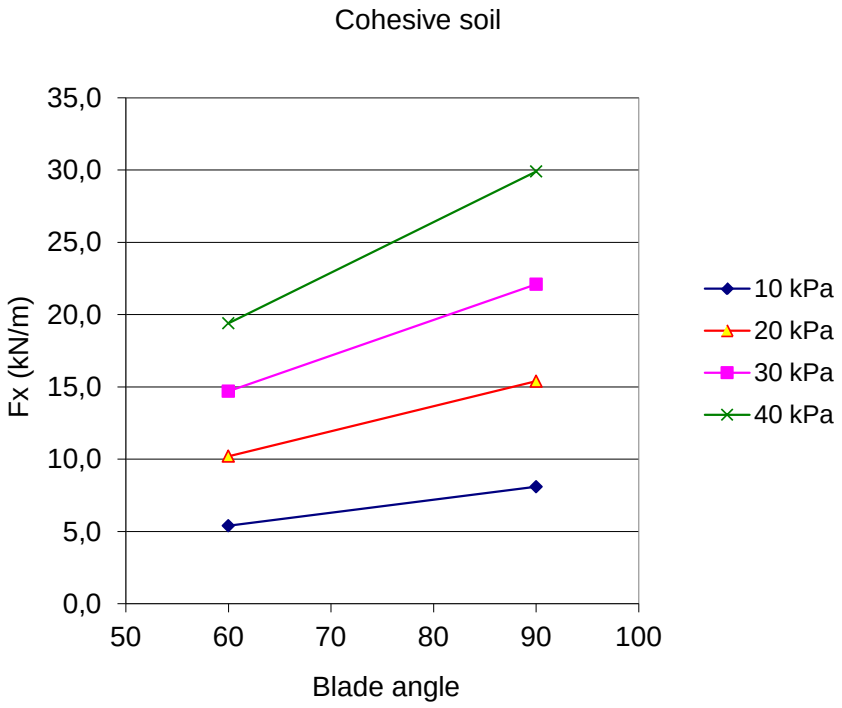

Figure 3.24. The variation of the ultimate horizontal force with blade angle and different values of c_u in the soil. R = 0,4. Summary of values from Figure 3.18 and Figure 3.19.

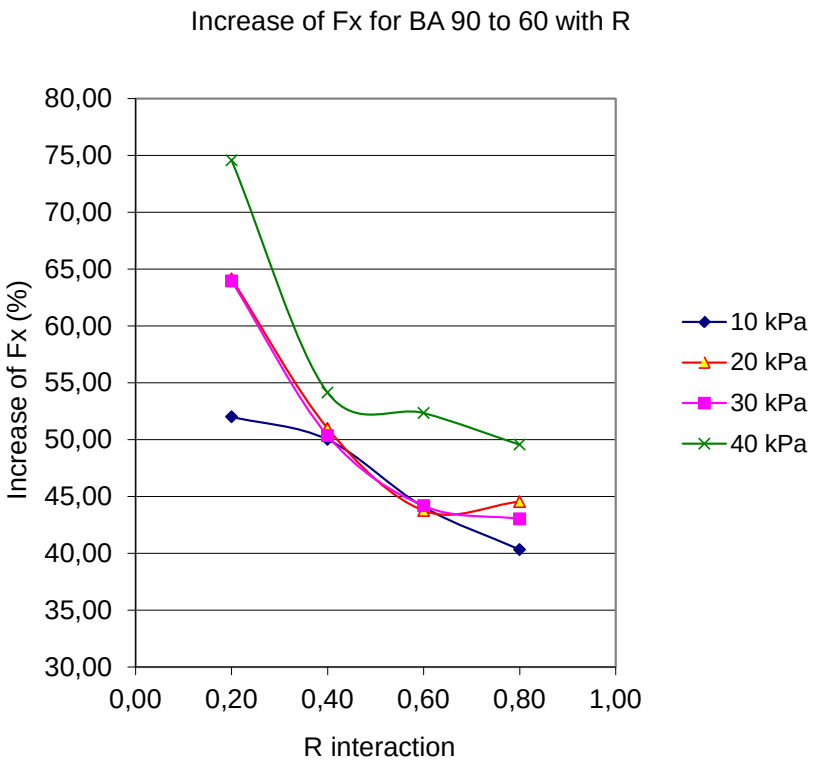

Figure 3.25. Calculated values of the increase of the ultimate horizontal force when the blade angle increases from 60 to 90 degrees at different values of $R_{interaction}$ in cohesive soil.

3.5 Parametric study - non-cohesive soil

3.5.1 Effect of soil friction parameters

Figure 3.26 to Figure 3.28 shows the resultant horizontal force on the blade during displacement at different values of the soil friction angle, φ, dilatancy angle, ψ, unit weight, γ, elastic modulus, E, and K_0 – value, see Table 3.5. The force – displacement curves are similar to the ones for cohesive soil. In the beginning the force increases rapidly and the soil is in an elastic state. At further displacement the force becomes constant as the soil becomes plastic and starts to yield. These curves differ with those reported by Schmulevich et al. (2007), were the force – displacement curve increases linearly during the 0,2 m displacement. Their experiments were performed in a soil box with sand and the soil accumulated in front of the blade during displacement. The non-cohesive soil was modelled with extended interfaces but without a finer mesh around the blade.

The ultimate soil resistance, F_x increases with increasing soil friction angle, φ. An increase of the soil friction angle from 30 to 35 degrees yields an increase of about 40 % of the soil resistance, an increase from 35 to 40 degrees yields an increase of about 55% and an increase of 40 to 45 degrees yields an increase of about 59 % of F_x.

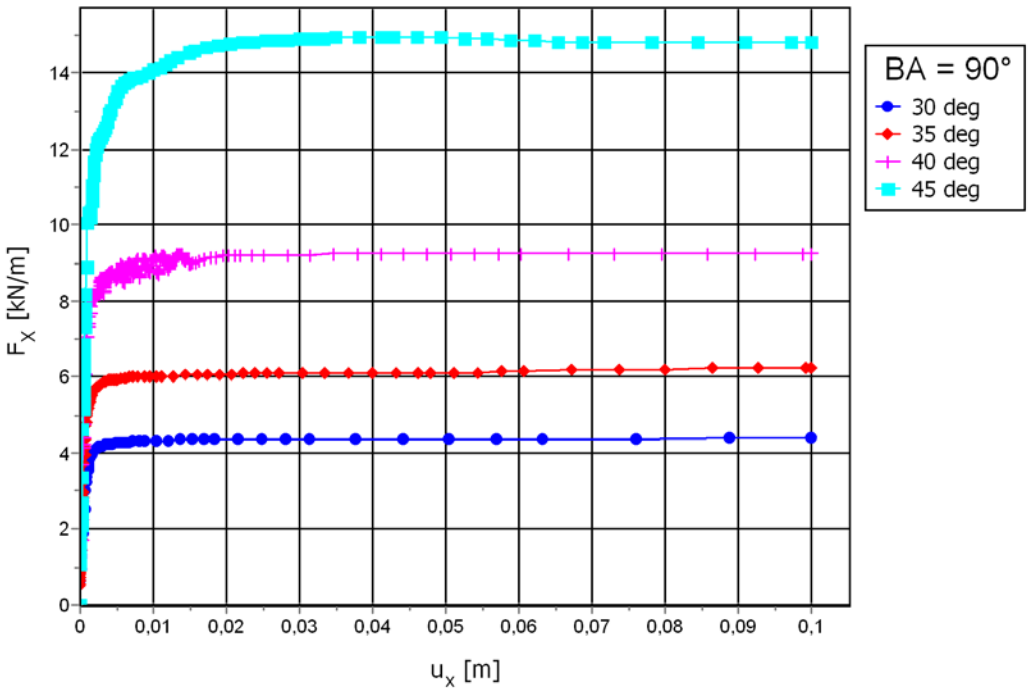

Figure 3.26. Force – displacement curve for a blade with a 90° blade angle (BA) $R_{interaction}$ = 0,4 for different values of internal friction angle of the soil.

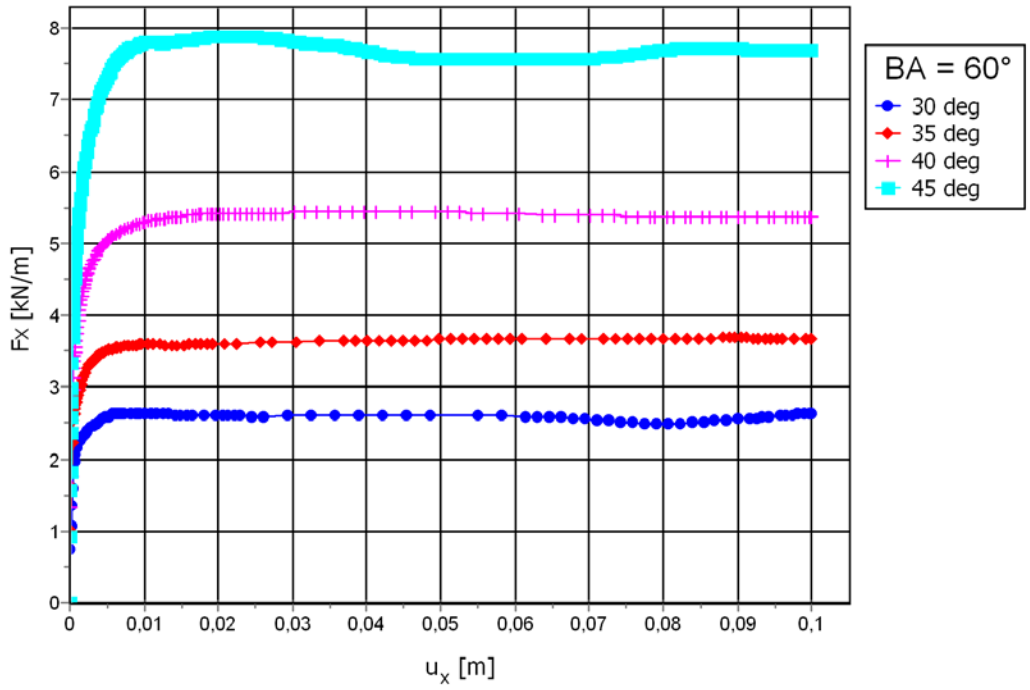

Figure 3.27. Force – displacement curve for a blade with a 60° blade angle (BA) at $R_{interaction}$ = 0,4 for different values of the internal friction angle of the soil.

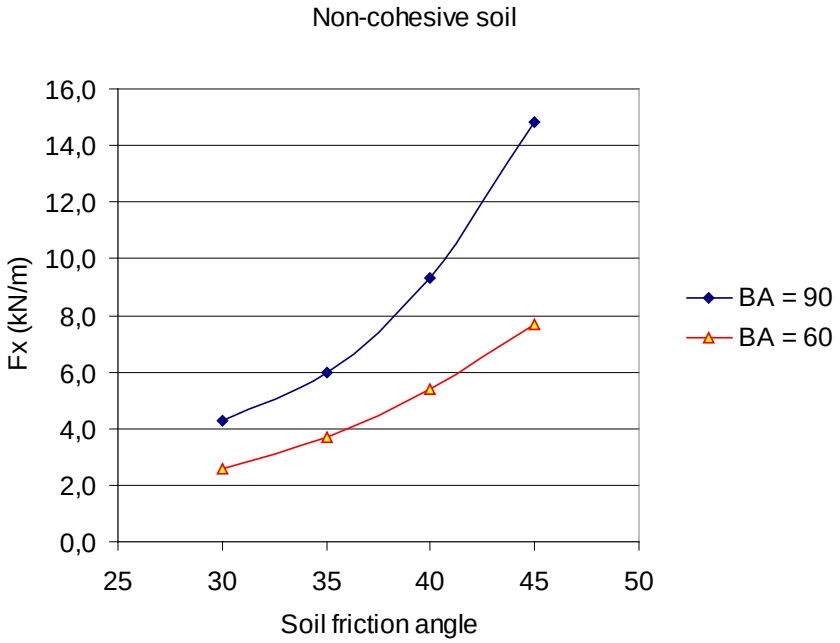

Figure 3.28. The variation of the ultimate horizontal force with the internal friction angle of the soil and different blade angles (BA). Summary of values from Figure 3.26 and Figure 3.27.

Figure 3.28 shows the ultimate horizontal force at 0,1 m displacement at a constant soil-tool interaction value ($R_{interaction}$ = 0,4). It shows that the force increases in a non-linear way with increasing internal friction angle of the soil.

3.5.2 Effect of soil-tool friction through $R_{interaction}$

Figure 3.29 to Figure 3.31 shows the variation of the horizontal force with different values of friction between the soil and the blade. It is shown that the force – displacement curve is similar for every value of soil-tool friction, δ, ($R_{interaction}$) but that the increment of the force is nonlinear.

Figure 3.31 shows the variation of the ultimate horizontal force at different values of soil-tool friction ($R_{interaction}$) with the vertical blade. The Plaxis results show a linear to non-linear increase of the force. For a soil with a 30 degree soil friction angle the force varies with the soil-tool friction from about 3,9 kN/m at R = 0,2 to 5,1 kN/m at R = 0,8. For a soil with a 40 degree soil friction angle the force varies with the soil-tool friction from about 8,1 kN/m at R = 0,2 to 12,0 kN/m at R = 0,8.

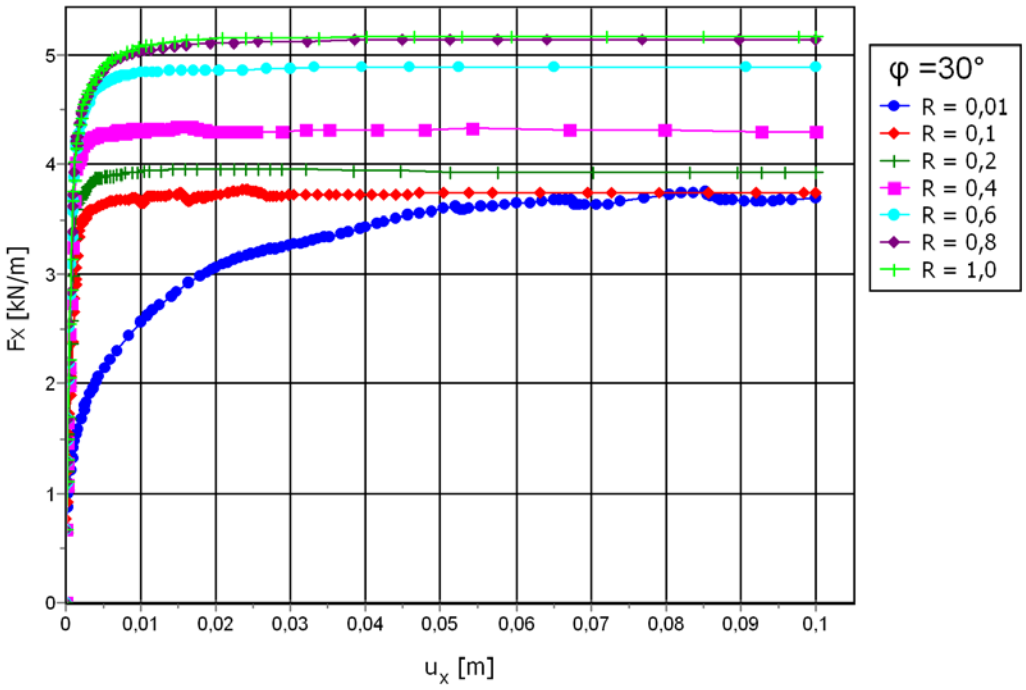

Figure 3.29. Force – displacement curves for a blade with a 90° blade angle in non-cohesive soil with 30 degree internal friction angle at different values of soil-tool friction, $R_{interaction}$.

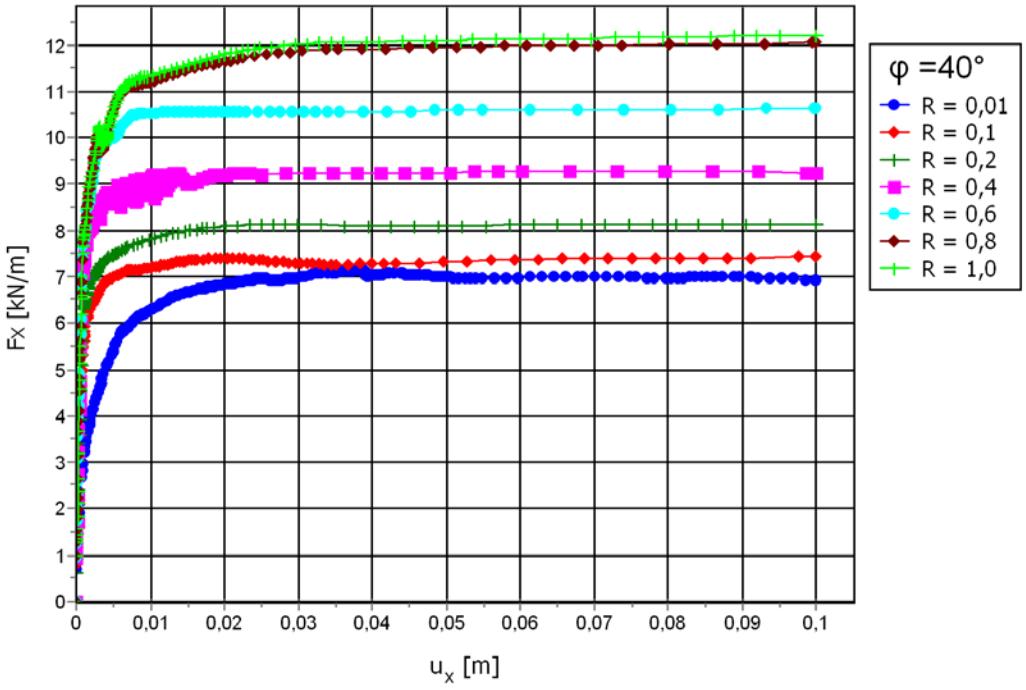

Figure 3.30. Force – displacement curves for a blade with a 90° blade angle in non-cohesive soil with 40 degree internal friction angle at different values of soil-tool friction, $R_{interaction}$.

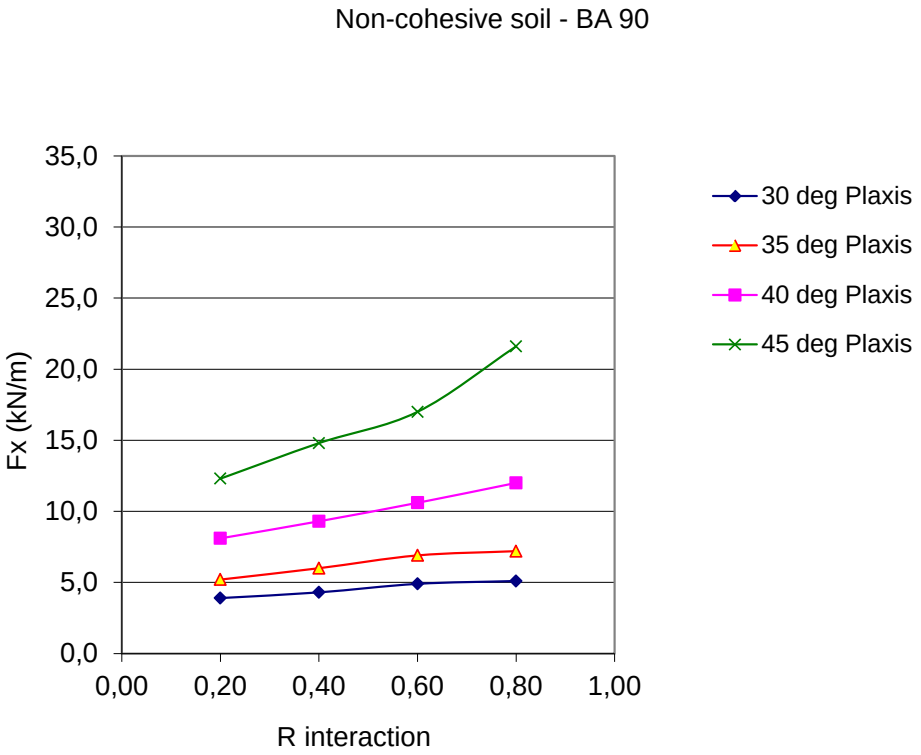

Figure 3.31. The variation of the ultimate horizontal force with different values of soil-tool friction. Summary of values from Figure 3.29 and Figure 3.30.

3.5.3 Effect of angle of dilatancy, ψ

Figure 3.32 to Figure 3.36 shows the variation of the horizontal force with different values of the angle of dilatancy, ψ. For different soil friction angles the dilatancy angle was varied between 0 and 20 degrees. The results show that the force tends to increase linearly with increasing angle of dilatancy.

In Figure 3.36 the variation of the ultimate horizontal force with dilatancy angle is presented. The force varies about 18% when the soil friction angle is 30° and about 48% when the soil friction angle is 45°.

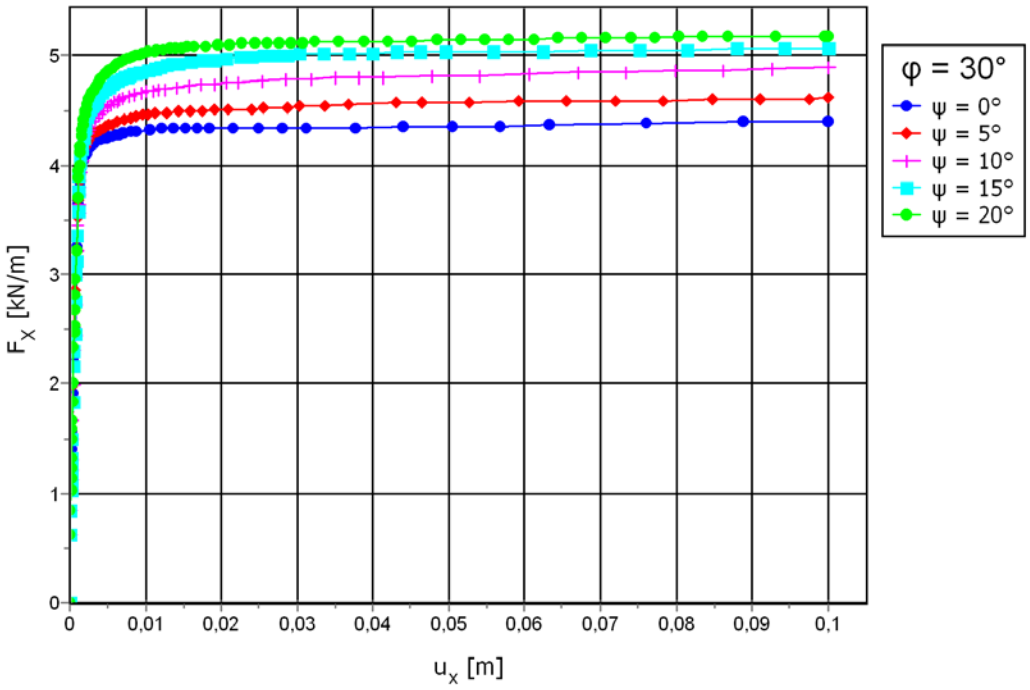

Figure 3.32. Force – displacement curves for a vertical blade in non-cohesive soil with 30 degree internal friction angle at different values of the angle of dilatancy, ψ.

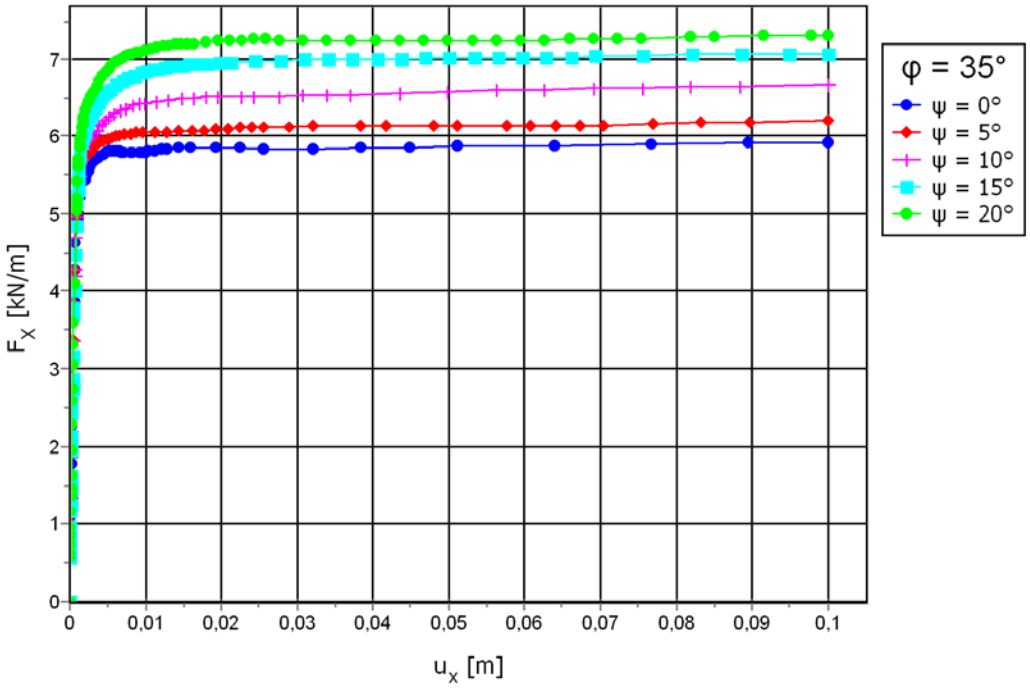

Figure 3.33. Force – displacement curves for a vertical blade in non-cohesive soil with 35 degree internal friction angle at different values of the angle of dilatancy, ψ.

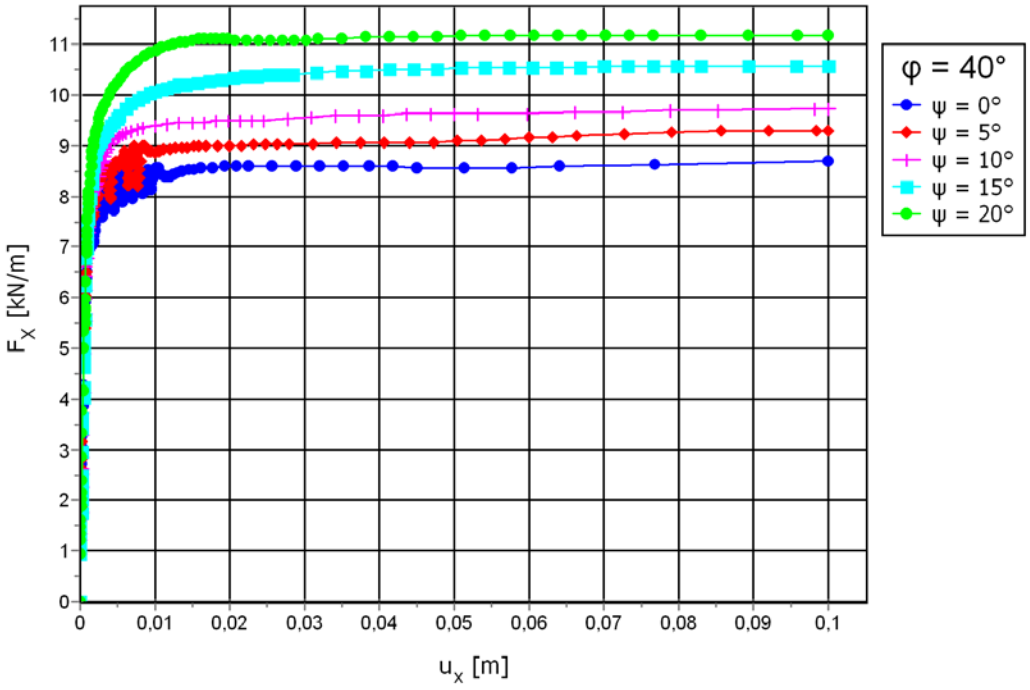

Figure 3.34. Force – displacement curves for a vertical blade in non-cohesive soil with 40 degree internal friction angle at different values of the angle of dilatancy, ψ.

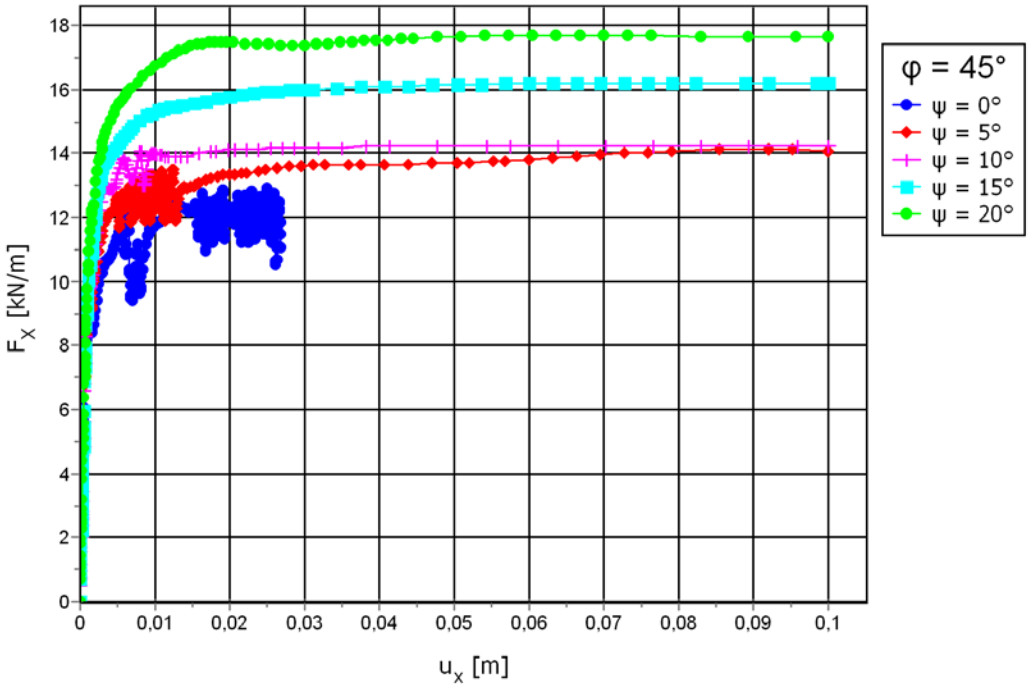

Figure 3.35. Force – displacement curves for a vertical blade in non-cohesive soil with 45 degree internal friction angle at different values of the angle of dilatancy, ψ.

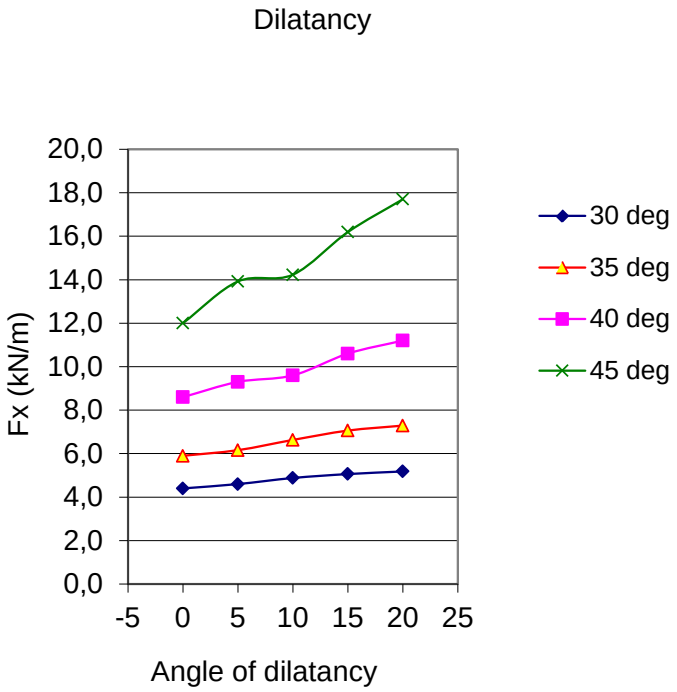

Figure 3.36. The increase of the ultimate horizontal force with angle of dilatancy for different internal friction angles of the soil. Summary of values from Figure 3.32 to Figure 3.35.

3.5.4 Effect of blade angle, α

Figure 3.37 shows the increase of the ultimate horizontal force as the blade angle increases from 60 to 90 degrees. At a constant $R_{interaction}$ = 0,4 the increase of the force is larger at higher friction angles. Figure 3.38 shows the increase (%) of the ultimate horizontal force as the blade angle increases from 60 to 90 degrees. The increase varies with different values of $R_{interaction}$ and soil friction angle in a nonlinear way.

The ultimate horizontal force, F_x increases with increasing blade angle, α. From two values it is not possible to tell if the increase is linear or non-linear. An increase of the blade angle from 60 to 90 degrees in a soil with a soil friction angle of 30 degrees causes an increase of the force with about 65 %. In soil with a soil friction angle of 40 degrees the force increases with about 72 %.

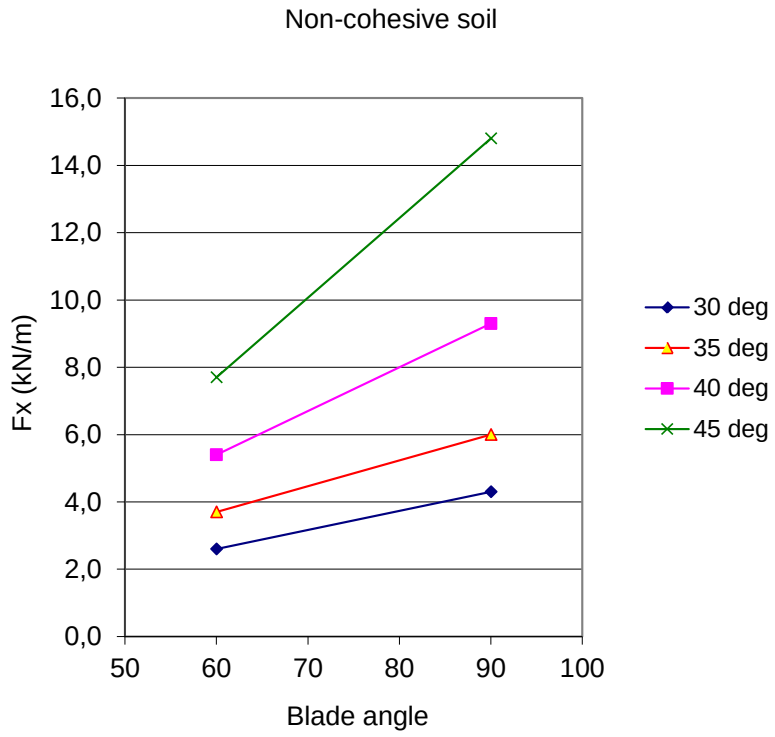

Figure 3.37. The variation of the ultimate horizontal force with blade angle and different values of the internal friction angle in soil. Summary of values from Figure 3.26 and Figure 3.27.

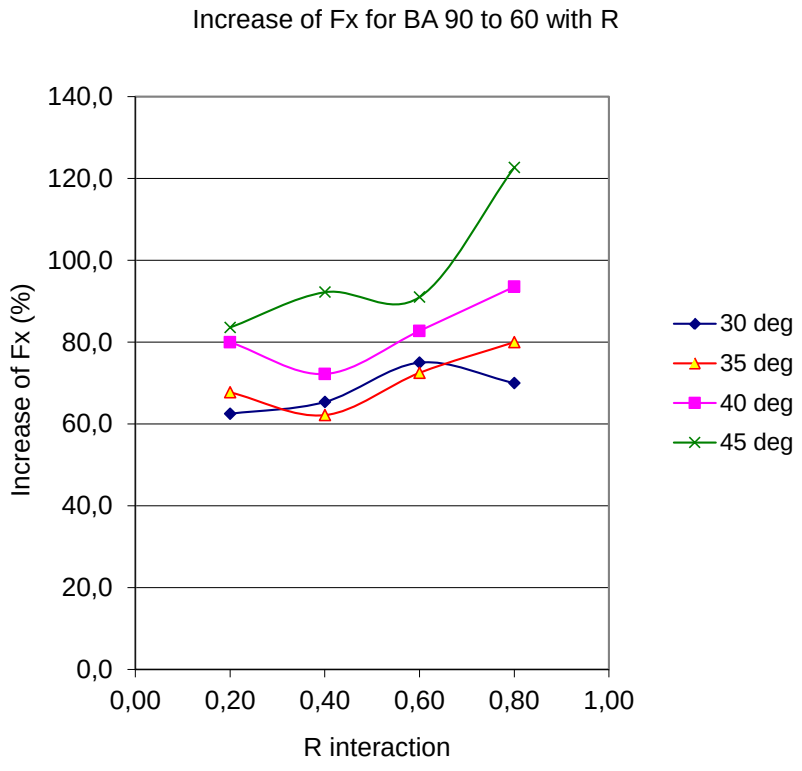

Figure 3.38. Calculated values of the increase of the ultimate horizontal force when the blade angle (BA) increases from 60 to 90 degrees at different values of $R_{interaction}$.

3.6 Modelling moraine/c-φ soil

An attempt of simulating moraine soil with different soil properties was performed. Values for loose and dense moraine soils were found in the literature, see Table 3.6 in Chapter 3.2.6. Gravel, sand, silt and clay moraine was simulated with appropriate values of unit weight, soil friction angle, elastic modulus and cohesion, see figures below. Clay moraine was modelled as drained and undrained. The ultimate horizontal force is higher for sand moraine than for gravel moraine and higher for silt moraine than for sand moraine. The effect of increasing cohesion relatively the decreasing particle size distribution (from gravel to clay moraine) had larger impact on the magnitude of the horizontal force than decreasing soil friction angle.

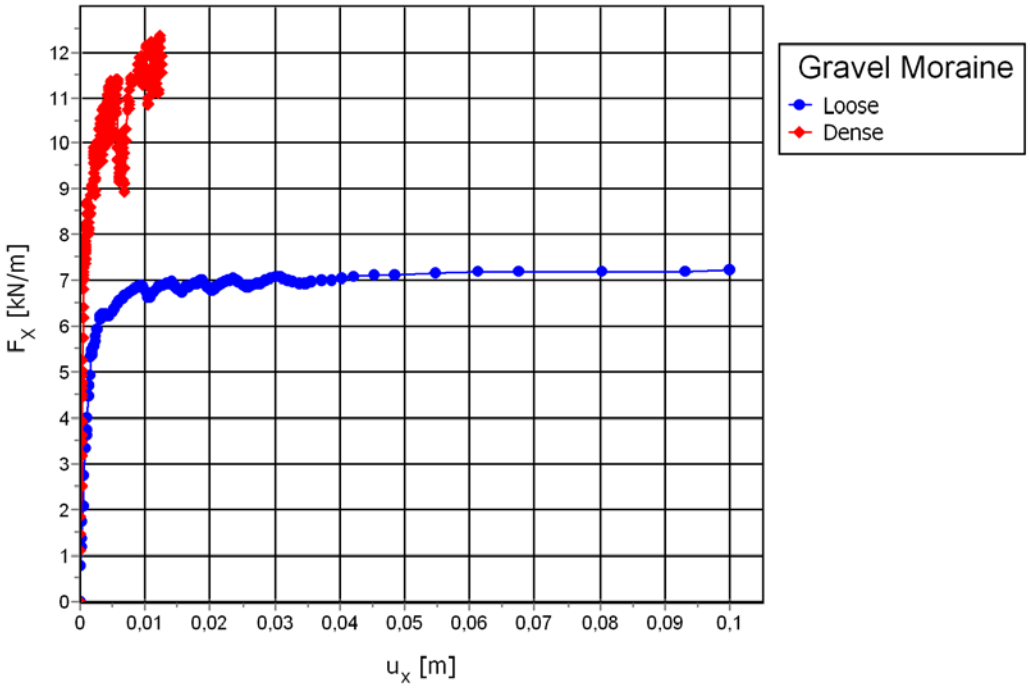

Figure 3.39. The variation of the horizontal force in loose and dense gravel moraine.

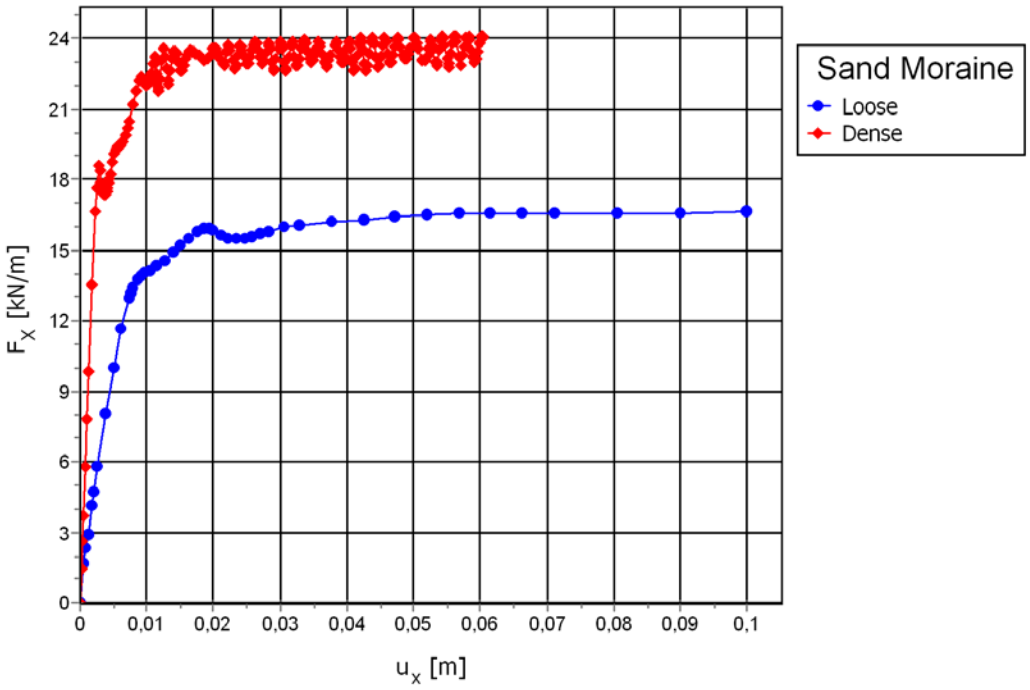

Figure 3.40. The variation of the horizontal force in loose and dense sand moraine.

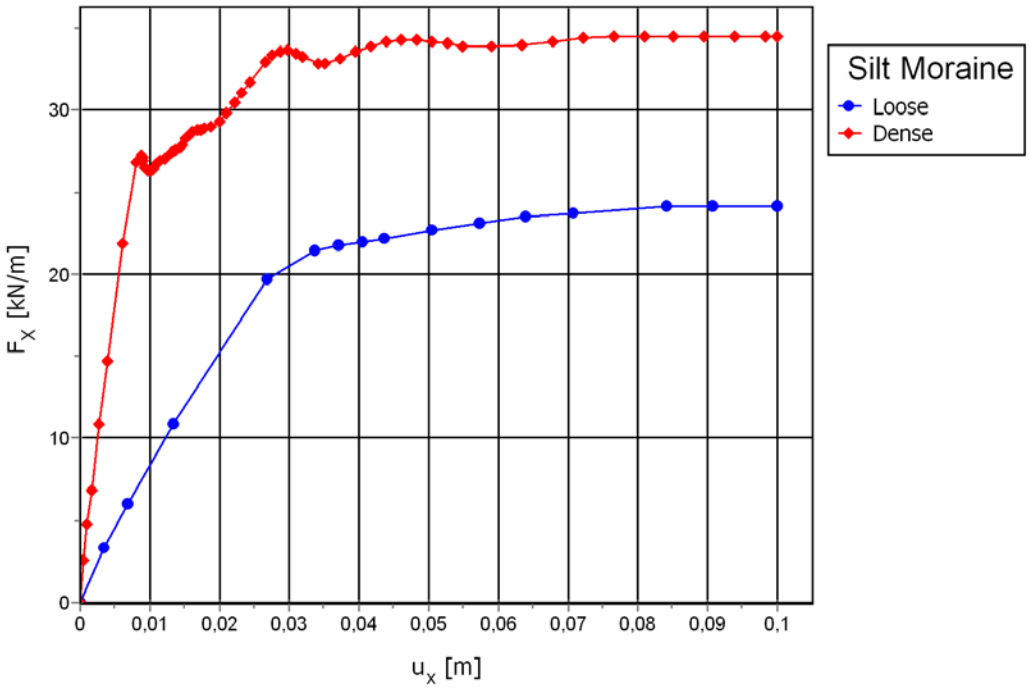

Figure 3.41. The variation of the horizontal force in loose and dense silt moraine.

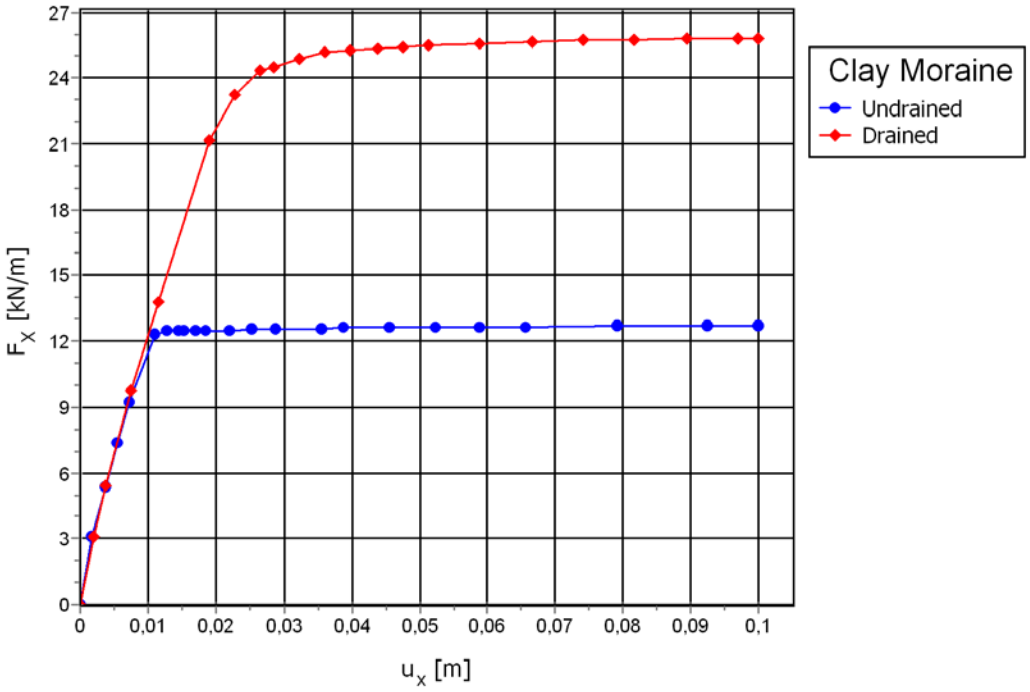

Figure 3.42. The variation of the horizontal force in drained and undrained clay moraine.

3.7 Conclusion

In this study, the displacement of a stiff vertical blade in a soil mass was simulated with the finite element method. The blade was displaced 0,1 m which was assumed to be enough in order to cause yielding of the soil mass. The blade was penetrated to a depth of 0,3 m.

The convergence study shows that the extended interface elements and the mesh coarseness had considerable impact on the magnitude of the horizontal resisting force. When modelling the cohesive soil it was concluded that extended interface elements and a fine mesh were required. For the non-cohesive soil extended interface elements and a medium mesh was needed.

Load – displacement curves were generated for the situation when the blade was displaced into the soil. Generally, it showed an increase of the force for a first short displacement (< 0,02 m). Thereafter, the resisting force tends to be constant with further displacement. The load – displacement curve shows an elastic-yielding-plastic behaviour.

The results show that the horizontal force increases with the increase of the parameter studied. In cohesive soil the ultimate horizontal force have a linear increase, at about 72 %, with undrained shear strength. In non-cohesive soil the ultimate horizontal force have a second order polynomial increase with soil friction angle. Though, at small values of the soil friction angle the increase of the horizontal force is so small the appearance will look linear. The adhesion causes a linear increase of the ultimate horizontal force. The soil-tool friction causes a non-linear increase of the ultimate horizontal force.

An increase of the blade angle from 60 to 90 degrees causes an increase of the horizontal force with about 65% in soil with $\varphi = 30°$ and about 72% in soil with $\varphi = 40°$.
The horizontal force increases linearly with angle of dilatancy.

The resulting horizontal force in a blade can be expected to be higher in a pure cohesive soil than in a pure non-cohesive soil.

Gravel, sand, silt and clay moraine were simulated with values of the soil parameters chosen from the literature. The results show that the impact from the cohesion parameter is larger than from the soil friction angle parameter on the ultimate horizontal force.

4 Discussion

4.1 Introduction

Excavation and moving of soil are common work tasks in construction projects. Large amounts of soil must be handled with different machines, tools and working methods. Different soils, with different soil properties present different degrees of difficulty to the excavation process. The difficulty of excavating the soil affects the choice of machines and tools to use and the time it takes to perform the work. The ability to excavate the soil, therefore, influences the total cost of the project. If the excavatability of the soil could be determined, the cost for excavating soil could be more accurately calculated and the choice of the best machines and tools to use would be simplified. An excavatability description system gives an objective point of view on the ability to excavate in soil, thus preventing disagreements.

In this study, the issue of excavating soil has been dealt with from a broad perspective. The area of study concerns several disciplines such as soil, soil mechanics, machine types, machine equipments and excavation work performance. Furthermore contractual agreements between contractors and clients could affect the interest in determining the excavatability of soil, since in the case of an excavation project the estimated additional cost due to the probability of encountering difficulties during excavation is included for in the total price. In this case the contractor has to consider the risk of higher costs when excavating compared to other expenses and the total cost.

The excavatability classification system used today in Sweden, Classification system -85, Magnusson & Orre (1985), is based on knowledge from the earlier studies in Sweden and Finland. There have been some disputes about the excavatability classification of soils between contractors and clients (or the client's consultant). The contractor has claimed that it is difficult to excavate in the soil and that it should have a higher excavatability class. The disputes have mainly regarded soil excavation in class 3 to 5 in the classification system, which concerns soils with a particle size of gravel or coarser, often dense and with cobbles or boulders. If disputes arise about the classification performed with the classification system it could be an indication that the system is not correctly calibrated, inaccurate or too coarse in its classification.

The excavatability of soil depends on soil properties or characteristics, such as unit weight, denseness or particle size distribution. The choice of machine type, equipment and appropriate methodology of excavating is based on soil properties and governed by the ability to excavate the soil. In order to determine the excavatability of the soil, that is, the ability to penetrate, cut and load the soil with a blade or bucket, the resistance of the soil can be determined. This can be done through modelling the tool in the soil during action and measuring or calculating the force or energy needed. Depending on, for example, the geometry of the tool that is used the force needed to excavate the soil will differ from one tool to another. In addition the friction or adhesion between the tool and soil will cause a difference of the resulting force on the tool. A mechanical analysis can be carried out to calculate the force. Depending on the tool used and the action performed (penetration, cutting or loading) the mechanical analysis will look different.

It is clear that different tools are used for different soils but can also be used for the same soil. For example loose sand can be cut and moved by a scraper blade, loaded by a wheel loader

bucket and excavated with an excavator bucket. The difference in energy requirement to excavate and move the sand with these different machines and tools will not rely on the soil properties. In order to decide the ability to excavate in one type of soil it is therefore necessary to be clear about which type of tool that is considered. Nevertheless, when excavating with different machines and tools the soil is the common factor. The properties of the soil govern the ability to excavate it. Therefore it is possible to create an excavatability classification of soil based on soil properties. But when this classification is constructed it is necessary to conduct correlations between results from different machines and tools as well as between tools and soil properties.

This study reviewed earlier systems for classification of the excavatability of soils with the purpose to find out which soil parameters and other parameters affect excavatability according to these systems. The excavation processes of three common types of machine-and-tool configurations have been studied. This was carried out to understand the excavation phases in each process and to find a concept or model to use in determining the resistance of the soil. For each blade- or bucket process different models for determining the resultant force on the tool have been studied. For blades (narrow and wide) and buckets the models of different authors have been reviewed. These models represent theories of soil behaviour during loading with certain boundary conditions and soil properties. The relationship between the soil properties and the force calculated by the model will provide a prediction of the resistance of the soil. Another way of studying soil behaviour is to conduct a finite element analysis. In this study, a two-dimensional blade displaced in a soil mass has been modelled to simulate a bulldozer blade working in the soil. The resultant force on the blade has been calculated for different soil properties, soil-tool properties and blade angles. Results from the finite element study have been compared to values calculated with the McKeys (1989) model. The results have also been compared to results from experiments in the literature.

4.2 Earlier studies on excavation and moving soil

The literature about excavatability of soil has not been extensive or consistent. Most of it is from Sweden and Finland and was carried out during the 1960s and 1970s. These studies have not been easy to find, and some studies are not even searchable in public directories. These studies concern empirically gained knowledge from excavation studies, dividing soil into different classes according to a soil classification system or geotechnical sounding resistance. There is no mechanical analysis used to assess the excavatability difficulties. During the literature search only a couple of systems from other countries were found. These systems differ from the Swedish and Finnish ones but give some examples of dividing soil into excavatability classes.

A lot more studies were found on other topics of excavation and earthmoving. They concerns soil-tool interaction and force prediction models on blades or buckets in the agricultural field, automatic excavation in the field of automation in the mining industry and passive earth pressure theory in the construction area. In the agricultural area several studies concerns prediction of forces on blades or buckets performing in soil. A drawback of these studies is that they almost always concern narrow blades with low width / depth ratios. Another drawback is that no study concerns soil that is fairly heterogeneous, such as moraine soil. This is due to the fact that since the majority of these studies have been performed in agricultural soils like clay, sand or equally uniform and loose soils. In the field of automated excavation some researchers have focused on defining force components acting on a bucket during excavation. An assumption is that the bucket will follow a specific trajectory of motion during

excavation. The resulting forces needed to keep the bucket in the path will then have to be determined.

4.2.1 Classification of excavatability

To find out possible parameters affecting the ability to excavate soil, a review of earlier classification systems of excavatability has been performed. In several studies, different soil properties and other parameters are claimed to affect the excavatability of a soil. In Table 2.24 in Chapter 2.8.1 these parameters are summarized. It is noted that the particle size distribution and the content of cobbles and boulders in the soil affect the excavatability. The particle size has an effect on the shear strength, density and denseness of a soil mass. Other parameters noted, for example cementation between particles, denseness and water content, are related to the strength of the soil. Parameters such as bulk density, porosity, relative density and dilatancy are related to each other in the sense that they are all measures of the denseness of the soil. Therefore, there is a possibility that different studies have different parameters even though they have similar aims. In the same way the cohesion and friction angle are parameters that are included in shear strength. The adhesion between soil and blade has also been mentioned.

According to Arhippainen and Korpela (1966), the excavatability of soil decreases with the decreasing grading of particles, since the shear strength increases. They also stated that the excavatability decreases with increasing content of cobbles since cobbles of larger size will not fit in the excavating bucket. According to the excavation tests by the Swedish Road Administration (1977), the water content in the moraine soil did not considerably change the resistance to soil loosening, not in comparison with other parameters. Though, according to the Swedish Road Administration (1972), increased water content can lead to a lower bearing capacity for machines, that is, lower shear strength of the soil. The ability to fill a bucket with soil depends on about the same soil parameters as for loosening the soil from the ground. It has been stated that the degree of filling the bucket is dependent on the ability of the soil to flow into the bucket. The filling degree is higher for fine grained and homogenous material and lesser for soil with high boulder content. In some studies it is mentioned that other parameters than those related to the soil affects the excavatability. The ability of excavating in a soil can be affected by parameters such as what season of the year it is, weather conditions, the skills of the operator, the bearing capacity of the machines, properties of the machine and tool as well as organization of the work.

4.2.2 The excavation process

When studying excavation and soil moving it is natural to study the excavation process, such as, how the blade or bucket interferes with the ground, how the machine and tool moves and the methodology used for excavating and moving the soil. In chapter 2.3 a literature study of these aspects was carried out. Three combinations of machine-and-tool sets have been distinguished: a bulldozer or scraper with a wide blade, a wheel loader with a wide bucket and an excavator with a narrow bucket. This division is based on the work task expected and the type of material to be handled. The purpose was to perform an orientation of the excavation process as defined or used by different authors. The aim was to understand a general excavation process for each machine-and-tool set. From this general process a model with specific boundaries can be created for a certain phase of excavation.

In this study a two-dimensional model of a bulldozer blade was considered. The model assumes the initial phase of cutting soil, when the soil breaks loose from the ground. The purpose was to be able to determine the force needed to break loose the soil. Therefore the excavation phase when the blade is fully loaded after some displacement was not of interest.

Another way to study the excavation process would be to follow some operators when working in a construction project. But in order to achieve representative basic data several operators have to be studied since the ability to excavate in soil is significantly affected by the skills of the operator. For an orientation of the excavation process a literature study was considered sufficient.

4.2.3 Studies related to excavating and moving soil

In chapter 2.4 studies regarding excavation and soil moving were presented. Some of these studies propose models for predicting the horizontal and vertical resultant forces on a blade or a bucket. Mechanical models for narrow blades, wide blades and buckets are presented. Many of the models found for buckets build on models used for blades. In these models soil properties, soil-tool properties and the geometry of the tool and soil failure are parameters that affects the resistive forces on the blade or a bucket.

Blades can be divided into narrow and wide blades. According to Hettiaratchi (1965) a narrow blade (tine) causes three-dimensional failure problems whereas the failure in front of a wide blade can be considered two-dimensional, see Figure 4.1. McKeys (1985) states that a two-dimensional approach is valid for blades with a width-depth ratio of at least 10. He refers to experiments conducted by Payne (1956) showing that the effect of the movement of soil to the edges of the blade have a larger impact on the total force for narrow than for wide blades. According to McKeys (1985), Payne (1956) classified narrow blades as those with a w/d ratio smaller than unity (< 1) and wide blades as those greater than 2. Blouin et al (2001) proposes a w/d ratio of 6 distinguishing narrow from wide blades.

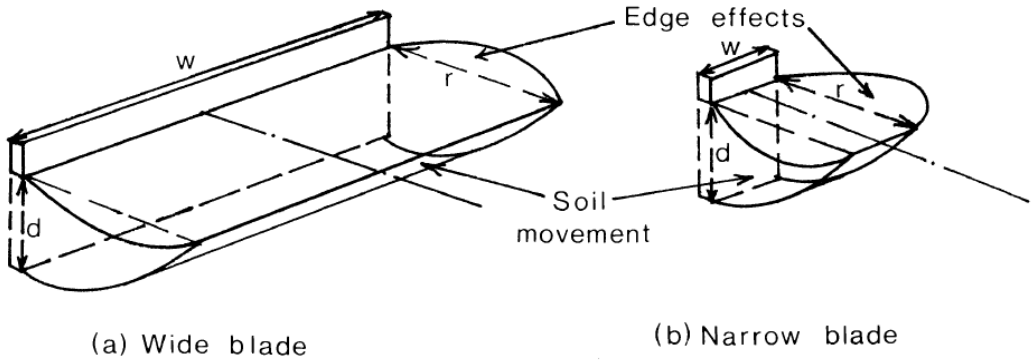

Figure 4.1. Soil movement patterns for wide and narrow cutting blades, according to Payne (1956), from McKeys (1985).

McKeys (1985) argues that the sides of a bucket causes the soil to move essentially in a two-dimensional manner inside the bucket, allowing for a two-dimensional analysis for both narrow and wide buckets. Referring to McKeys (1985), Singh (1995) and Luengo et al (1998) uses two-dimensional force prediction models in studies for narrow buckets.

In force prediction models for blades and buckets it is assumed that the resistance from the soil depends on different soil, tool and soil-tool parameters. Several of these models build on passive earth pressure theory on structures developed in the geotechnical field. In models presented in this study soil parameters such as weight, soil friction angle and cohesion; tool parameters including depth, width and inclination of the tool as well as soil-tool parameters such as soil-tool friction and adhesion have been considered. In addition the surcharge above the cut soil as well as the shape and extent of the soil failure zone in front of a blade can be considered in the models through different parameters. In other models, such as Zein Eldin & Al-Janobi (1995) and Ericsson & Slättengren (2000), the velocity and acceleration (inertia) of the tool and the soil is considered. In some force prediction models for buckets even the compaction of the soil in the bucket has been considered as well as uneven terrain.

4.2.4 Prediction of resistive forces

The theory of passive earth pressure on structures can be used in order to determine the resultant resistive force on a blade or bucket as it moves against the soil. In chapter 2.5 different aspects of passive earth pressure are dealt with. Results from classical methods as well as recent numerical approaches for calculating the passive pressure have been presented. It can be concluded that the main difference between the models concern the shape of the assumed failure surface and whether soil-interface friction and adhesion are considered. These factors and whether a two- or three-dimensional analysis is considered have a high impact on the results.

4.3 Modelling with the finite element method

With the finite element method accurate predictions of the deformation of soil are possible through numerical computations. The calculations are performed quickly and predictions of stresses, displacements and pore pressures can be achieved for any loading or prescribed displacement. In this study the finite element method was used to model a two-dimensional blade displaced in soil. The purpose was to predict the resultant horizontal force on the blade as different model parameters were varied.

In this study the choice of the values for the various parameters and boundary conditions significantly affected the results. Even if this is expected in the present study it is clear that a small increase of the undrained shear strength or soil friction angle has a significant impact on the magnitude of the soil resistance (resulting horizontal force). In the convergence study it was also noted how important it is with finite element specific issues as extended interfaces around corners of modelled objects. The difference in the result was considerable; the force decreased up to 5% in cohesive soil and increased up to 15% in non-cohesive soil, if extended interfaces were used. The mesh size also affected the results. Using a finer mesh than the medium mesh had a significant impact on the horizontal force. For the cohesive soil this was even required in order to obtain accurate results. The reason for this could be that the blade size was too small (0.3 m) relative to the size of the medium mesh and therefore a finer mesh was needed. The force decreased by up to 7% in cohesive soil and up to 17% in non-cohesive soil if a fine mesh was used instead of a medium mesh.

The force – displacement curves shown in the results indicates that the soil behaves in an elastic-plastic manner. This is consistent with the Mohr-Coulomb soil model, were the stress - strain curve is very distinct with a linearly increasing elastic part and a constant plastic part.

4.3.1 Cohesive soil

The results from the numerical analysis show that the ultimate horizontal force increases linearly with increasing undrained shear strength. This is shown in Figure 3.20 where the variation of the ultimate horizontal force with undrained shear strength is presented for a 90 and 60 degree blade angle, respectively.

The ultimate horizontal force increases about 20-25 percent as the $R_{interaction}$ − value, related to the adhesion, increases from 0 to 1. See Figure 3.21 to Figure 3.23. The increase of the horizontal force with adhesion is almost linear. This can be expected since the adhesion is linearly related to undrained shear strength or cohesion in Plaxis.

The horizontal force increases as the blade angle increases from 60 to 90 degrees, see Figure 3.24. This is logical since a larger volume of soil has to be displaced by the blade. The force is only modelled for 60 and 90 degrees blade angles so it is not possible to conclude anything about the magnitude in between these blade angles. In Figure 3.25 the increase of the horizontal force is shown for different values of adhesion as the blade angle increases from 60 to 90 degrees. The figure indicates that the force increases more if the $R_{interaction}$ − value (adhesion) is low. With high adhesion the increase of the force is about 45 kN, with low adhesion the increase is between 50 and 75 kN.

4.3.2 Non-Cohesive soil

For the non-cohesive soil the soil friction angle was varied together with the unit weight, γ the stiffness modulus, E and the angle of dilatancy, ψ. This makes it difficult to determine which parameter affects the ultimate horizontal force. However, it would not be realistic to increase the friction angle alone and let the other parameters be constant. In reality all these parameters increase as the denseness of the soil increases. In a dense soil the particles are close together and ordered in a way to minimise void space. This increases the density and the stiffness. It also increases the friction, and shearing resistance, since there are more contact points between the soil particles. The shearing resistance also increases as the soil particles have to roll over each other during deformation.

The results from the numerical analysis show that the ultimate horizontal force increases non-linearly with soil friction angle (and the increase of parameters γ, φ, ψ, E and K_0). This is shown in Figure 3.28 where the variation of the horizontal force with soil friction angle is presented for a 90 and 60 degree blade angle respectively.

In Figure 3.29 to Figure 3.31 in Chapter 3.5.2 the variation of the ultimate horizontal force with the $R_{interaction}$ − value is shown. The results show that the increase of the force could be linear or non-linear as the $R_{interaction}$ − value, related to the soil-blade friction angle, increases from 0 to 1. Since the soil-blade friction angle is non-linearly related to the soil friction angle in Plaxis, it would be reasonable if the increase of the force is non-linear with the soil-blade friction angle. For small values of the soil friction angle the increase of the soil-blade friction angle is small which might be the reason for the linear increase of the force at small values of the soil friction angle.

The results show that the ultimate horizontal force has a fairly linear increase with the angle of dilatancy, see Figure 3.36 in Chapter 3.5.3. The fluctuation of the force at higher soil friction angles is due to convergence problems. The increase of the force with angle of

dilatancy is larger for a higher soil friction angle. The increase depends on both the value of the soil friction angle as well as the unit weight.

In Figure 3.37 in chapter 3.5.4 the increase of the ultimate horizontal force with blade angle is shown for 90 and 60 degrees blade angles respectively. The increase of the force depends on the increased volume of the soil displaced. The increase of the force with blade angle is larger for a higher soil friction angle than for a lower one. In non-cohesive soil the increase of the horizontal force is about 70 to 80 percent for all $R_{interaction}$ – values as the blade angle increases from 60 to 90 degrees. The increase is slightly larger for higher $R_{interaction}$ – values. See Figure 3.38.

4.4 Comparison of earlier studies and modelling with the FEM

4.4.1 Cohesive soil

In the numerical analysis the ultimate horizontal force increases linearly with increasing undrained shear strength. Values calculated with McKeys (1989) model are in good agreement with the numerical results, see Figure 4.2, although, there is some difference between the values when using a blade angle of 60 degrees.

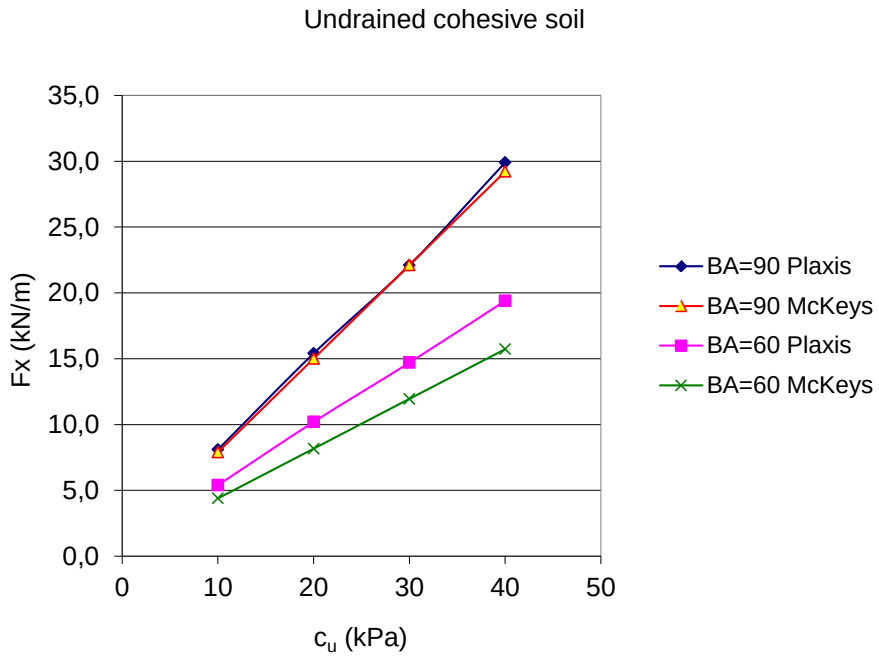

Figure 4.2. Variation of the ultimate horizontal force with undrained shear strength for a blade angle (BA) of 90° and 60° respectively. Results from the numerical analysis and McKeys (1989) model.

In the numerical analysis the ultimate horizontal force increases about 20-25 percent as the $R_{interaction}$ – value, related to the adhesion, increases from 0 to 1. The increase of the horizontal force with adhesion is almost linear, which the model by McKeys (1989) also indicates, see Figure 4.3.

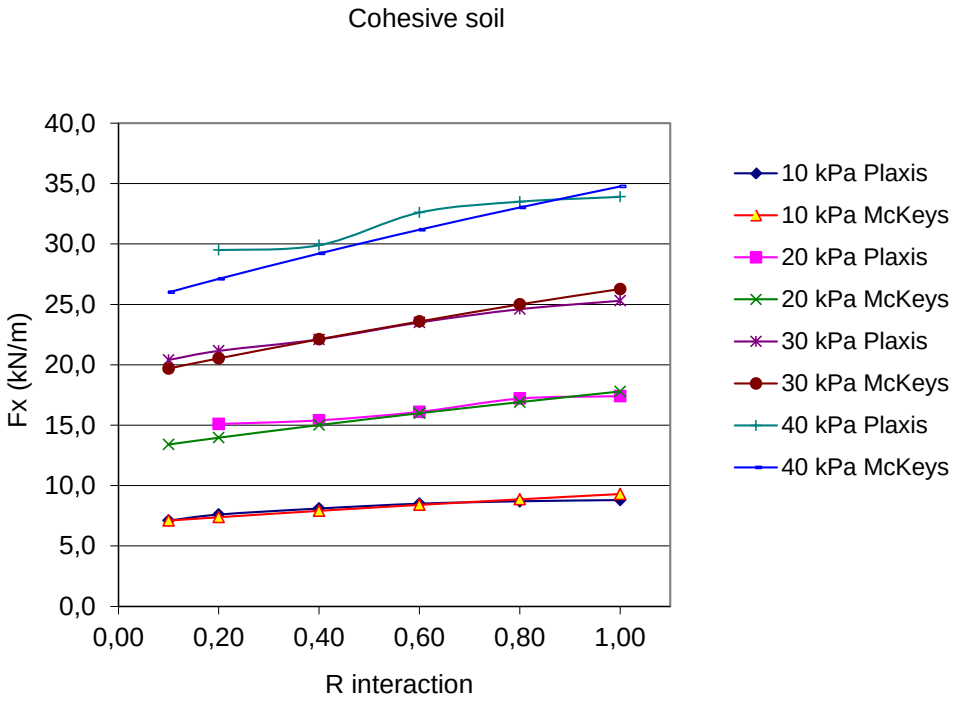

Figure 4.3. Variation of the ultimate horizontal force with the $R_{interaction}$ – value (adhesion). Results from the numerical analysis and McKeys (1989) model.

Results from the numerical analysis show that the ultimate horizontal force increases as the blade angle increases from 60 to 90 degrees. Results from McKeys' model indicate that the increase of the force with blade angle is linear, see Figure 4.4. Experimental results from Osman (1964), presented by Hettiaratchi (1965), in both clay and sand show a slightly nonlinear increase of the horizontal force with blade angle. The slight differences between the numerical analysis and McKeys' model can be due to difference in the failure surface and thereby the volume of loosened soil in front of the blade.

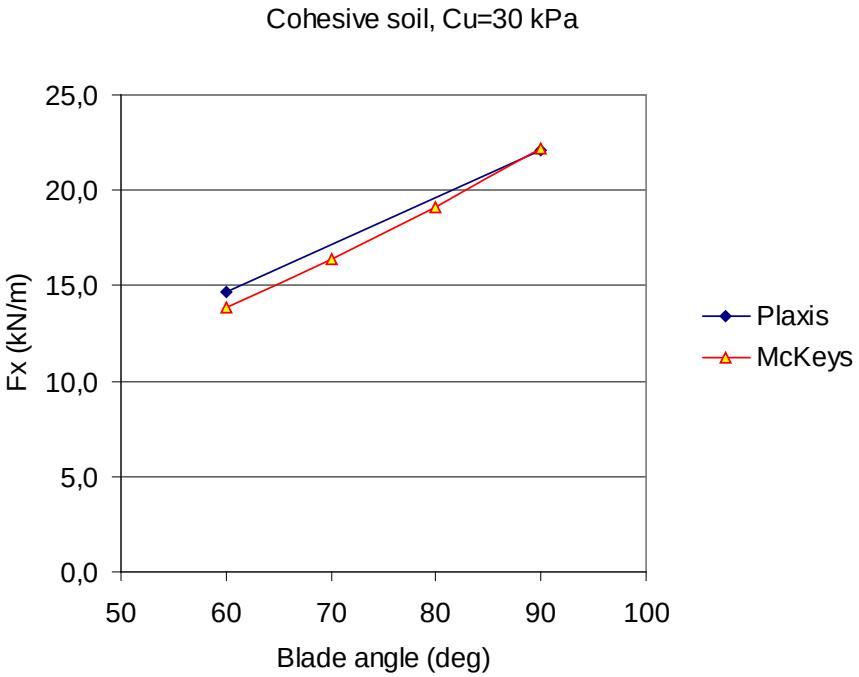

Figure 4.4. Variation of the ultimate horizontal force with blade angle. Results from the numerical analysis and McKeys (1989) model.

4.4.2 Non-Cohesive soil

In the numerical analysis the ultimate horizontal force increases non-linearly with the soil friction angle (soil friction parameters). There were good agreements between values from McKeys' (1989) model and the numerical model for a vertical blade, see Figure 4.5. The difference between the results can be explained by the fact that McKeys' model does not consider the angle of dilatancy which, in practise, causes an increase of the soil friction angle and thereby the horizontal force. McKeys' model is based on limit equilibrium of different forces on a soil mass. It does not consider the displacements or the Elastic modulus. The Elastic modulus does not affect the ultimate force, only the elastic part of the deformation. Predictions with a vertical blade, presented by Hettiaratchi (1965), with the model by Osman (1964) shows that the horizontal force increases with increasing soil friction angle as well as soil-tool friction angle. The increase is non-linear as in the numerical analysis. Jafari (2008) has presented results from a finite element study with a tilted blade. The results show that the horizontal force increases with increasing soil friction angle.

For a blade angle of 60° the increase of the force with soil friction angle is higher for the numerical model values than for McKeys' values.

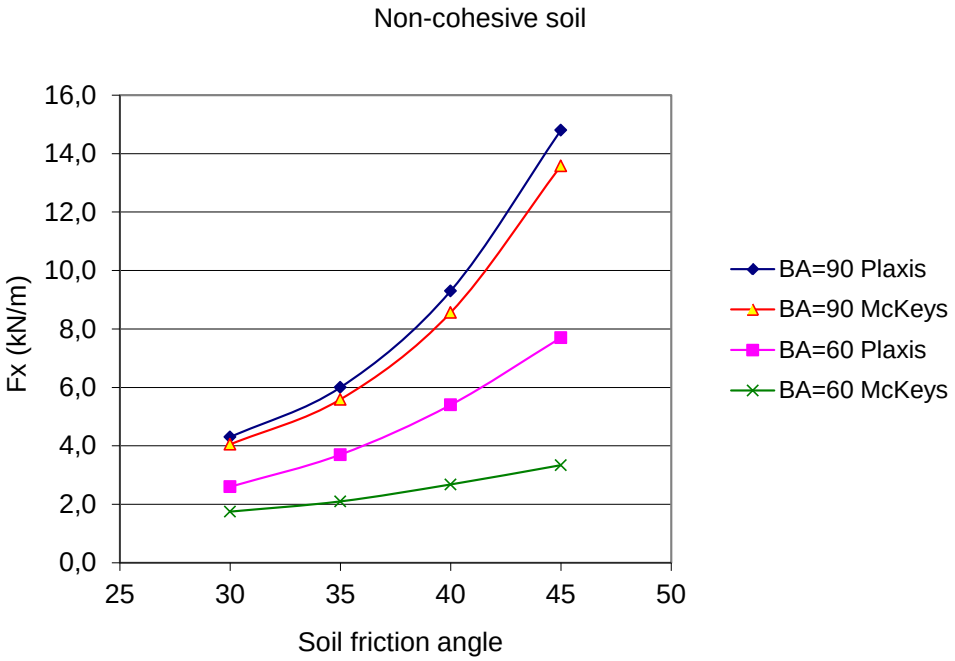

Figure 4.5. Variation of the ultimate horizontal force with soil friction angle for blade angles (BA) of 90° and 60° respectively. $R_{interaction}$ = 0,4. Results from the numerical analysis and McKeys (1989) model.

Results from the numerical analysis shows that the ultimate horizontal force increases non-linearly as the $R_{interaction}$ – value, related to the soil-tool friction, increases from 0 to 1. The results calculated with McKeys (1989) model show a highly non-linear behaviour for high values of the soil-tool friction angle in combination with high soil friction values, see Figure 4.6. This behaviour, with a high magnitude of the force at a high soil-tool friction angle is related to Coulomb's model for passive earth pressure, on which McKeys' model is built. In the literature this behaviour has been discussed, see for example Duncan & Mokwa (2001) or chapter 2.5. Coulombs model assumes a plane failure surface in the soil. In the numerical analysis the failure surface is more of a curve-linear shape, this can be seen in Figure 3.7. As the friction between the soil and the blade becomes larger the curved part of the failure shape will increase. This causes the difference between the sizes of the failure zones to increase. The difference will increase even more at higher soil friction angles.

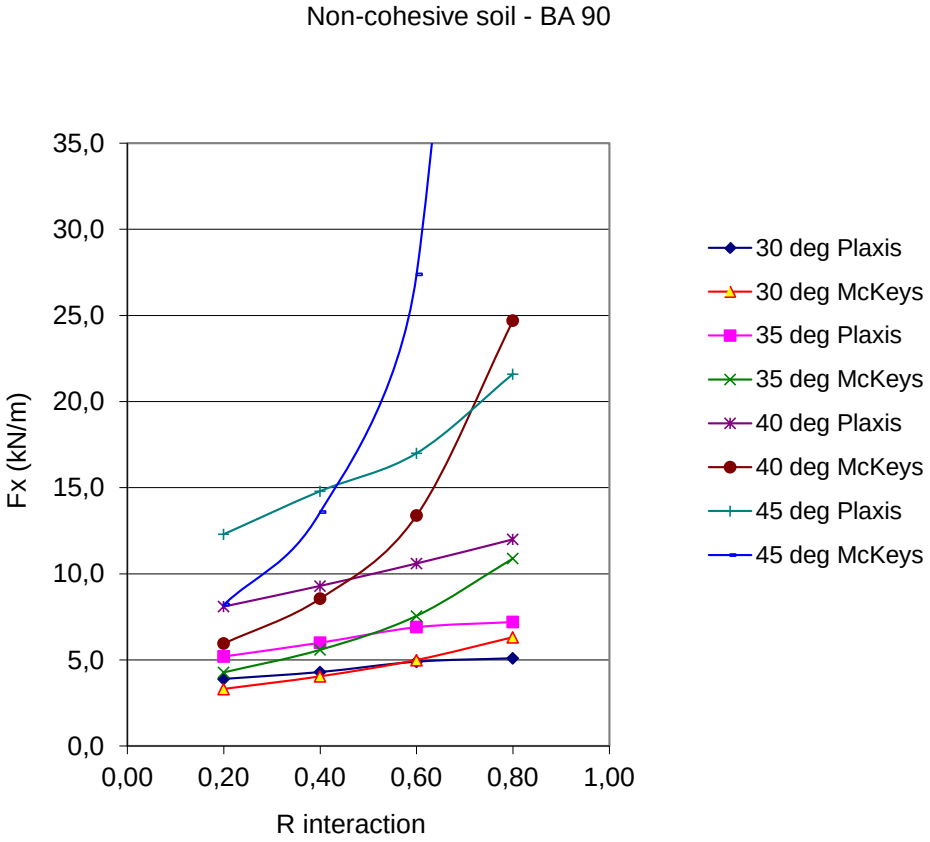

Figure 4.6. The variation of the ultimate horizontal force with the $R_{interaction}$ – value (soil-tool friction angle). Results from the numerical analysis and McKeys (1989) model.

The numerical analysis shows that the ultimate horizontal force increases with blade angle, see Figure 4.7. According to McKeys (1989) model the increase of the force with blade angle is non-linear. Experimental results from Osman (1964), presented by Hettiaratchi (1965), in both clay and sand show a slightly nonlinear increase of the horizontal force with blade angle.

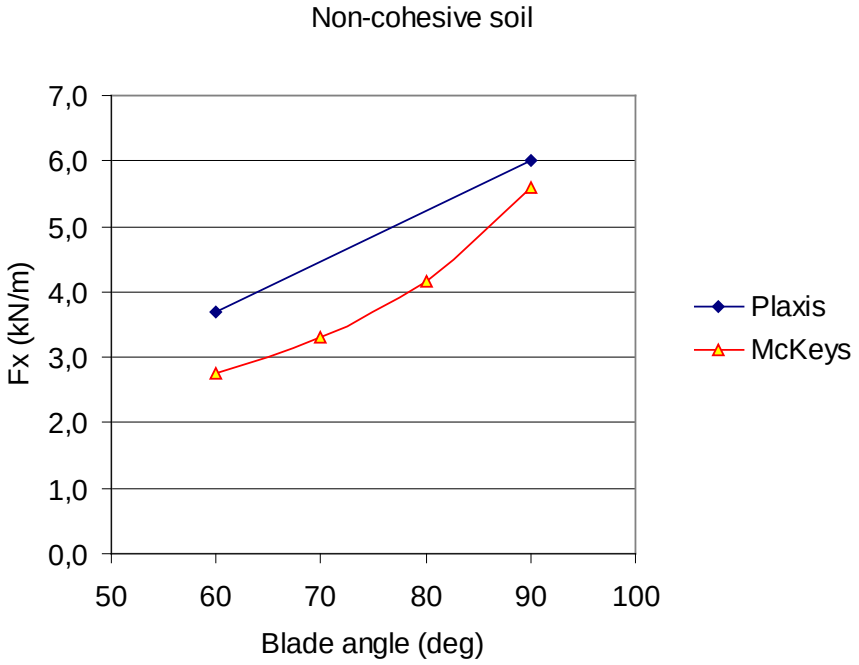

Figure 4.7. The variation of the ultimate horizontal force with blade angle. Results from the numerical analysis and McKeys (1989) model.

4.4.3 Moraine/c-φ soil

In the numerical analysis, in chapter 3.6, moraine was modelled as a "c-φ soil" with values of different parameters taken from the literature. Table 4.1 below shows values of the ultimate horizontal force calculated for different moraine soils with the numerical method and McKeys method. The values calculated with the two methods seem to agree very well, as shown in Figure 4.8. Loose soils have a lower resistance than dense soils. It is shown that the elastic modulus has no effect on the ultimate horizontal force, since the expression of the load in McKeys' model does not include such a parameter. For dense gravel moraine there were difficulties in achieving convergence in the numerical calculations, probably due to high soil friction angle and angle of dilatancy. Soil parameters can be found in Table 3.6 in Chapter 3.2.6.

Table 4.1. Values of the ultimate horizontal force calculated with the finite element method and McKeys' method in moraine soil. Values in (kN/m).

Soil type		(In Plaxis)	Plaxis	McKeys
Gravel Moraine	(Loose)	Drained	7,2	6,9
Gravel Moraine	(Dense)	Drained	-	13,0
Sand Moraine	(Loose)	Drained	16,6	16,5
Sand Moraine	(Dense)	Drained	23,5	26,2
Silt Moraine	(Loose)	Drained	24,1	24,8
Silt Moraine	(Dense)	Drained	34,4	37,1
Clay Moraine		Drained	25,8	24,9
Clay Moraine		Undrained	12,7	11,6

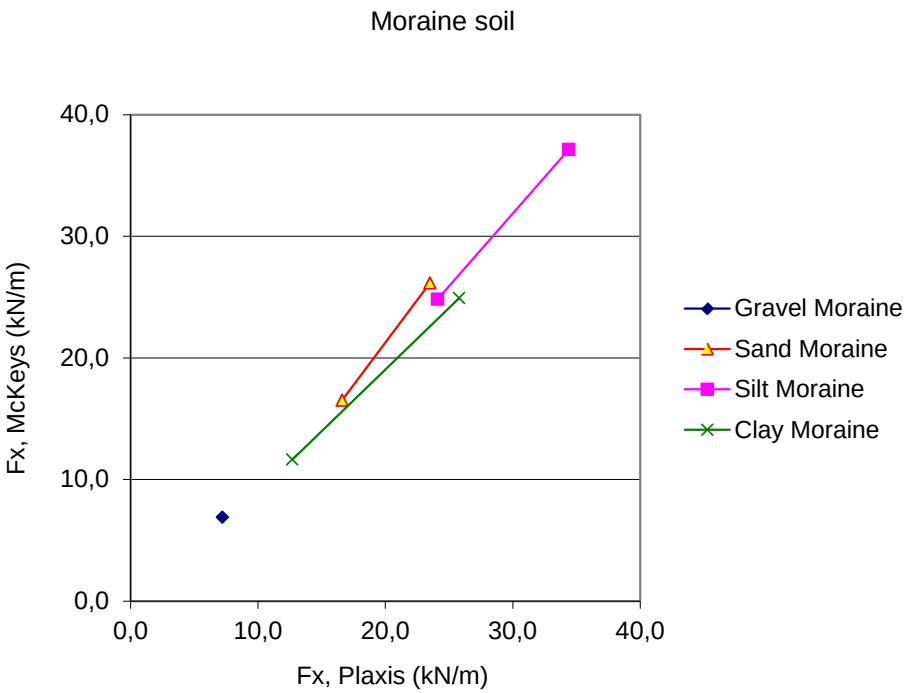

Figure 4.8. Agreement between values calculated with the numerical method and McKeys' method in moraine soil.

5 General conclusions and proposal for future research

5.1 General conclusions

Based on the study, it can be concluded that the ability to excavate soils is determined by soil properties. Parameters such as the unit weight (density), strength and denseness of the soil together with particle size, particle size distribution and content of cobbles and boulders affects the resistance developed in the soil as a blade or bucket is displaced into the soil.

To determine the excavatability of a soil type, the resistance can be calculated in terms of force per unit area (resistive force). Several authors have proposed relations for force prediction based on models where soil properties, soil-tool properties and the geometrical outline of the tool affect the failure of the soil in front of the tool.

The numerical analysis in this study showed that the magnitude of the resistance from cohesive soil was larger than that from non-cohesive soil, for the ranges of undrained shear strength and soil friction angle used. Moraine soil can be modelled with soil parameters used in the Mohr-Coulomb model. From the literature reasonable values of these soil parameters were found and used in the numerical study. The increase of the cohesion parameter had a larger impact on the magnitude of the ultimate horizontal resistive force than the decrease of the soil friction angle.

The results obtained in the numerical study were in good agreement with McKeys (1989) model for a vertical blade. However, the results for soil-tool interaction showed a poor correlation between the models. For a blade angle of 60 degrees the results were lower with McKeys' model.

Based on the literature review, the following general conclusions can be stated:

- The particle size, the particle size distribution, the content of cobbles and boulders, the shear strength and the denseness of the soil affects excavatability of the soil.
- The increase of the horizontal force due to different parameters is mostly non-linear. However, the increase of the horizontal force is linear with width and soil density.
- When defining a model for prediction of resistive forces on an excavating tool it is necessary to study the total excavation process, that is, how the tool interferes with the ground, how the machine and tool moves and the methodology used for excavating and moving the soil.

Based on the numerical analysis, the following general conclusions can be stated:

- In cohesive soil the horizontal force decreases when using extended interfaces. In non-cohesive soil the horizontal force increases when using extended interfaces.
- In both cohesive and non-cohesive soil the horizontal force decreases with finer mesh.
- For a cohesive soil the horizontal force increases linearly with undrained shear strength and adhesion.
- For a non-cohesive soil the horizontal force increases non-linearly with soil friction angle and soil-tool friction angle and linearly with dilatancy.

5.2 Proposal for future research

This study has highlighted some problem areas that would benefit from further investigation to obtain the necessary complementary knowledge about excavation in soil and to propose a new system for classification of excavatability. The following is proposed:

- It is necessary to study the penetration phase of a blade or bucket in order to understand the failure mechanism and to determine the resisting forces at this phase.

- The flow of soil into a narrow bucket has to be studied to clarify if there are any side effects on the resultant force. This can be performed through modelling of a bucket in three dimensions.

- In order to verify the magnitude of different parameter's effect on the resistive soil pressure, full scale excavation field tests need to be performed.

- According to the literature study, the content of boulders and cobbles in the soil to a large extent affects the ability to excavate the soil. This effect should be investigated further.

6 References

Alekseeva, T. V., Artem'ev, K. A., Bromberg, A. A., Voitsekhovskii, R. I., Ul'yanov, N. A. (1985) Machines for earthmoving work, theory and calculation. Balkema, Rotterdam, The Netherlands, p. 515.

Arhippainen, E., Korpela, K. (1966) Schaktbarhetsklassificering som hjälp vid bedömning av maskiners schaktförmåga, Utredningsrapport 20, Transportforskningskommissionen, Stockholm, Sweden, p. 47, In Swedish.

Axelsson, K. (1998) Introduktion till geotekniken, jämte jordmaterialläran. Luleå tekniska universitet, Luleå, Sweden. In Swedish.

Balovnev, V. I. (1983) New methods for calculating resistance to cutting of soil. Amerind Publishing Co., New Delhi, India, p. 103.

Bekker (1956) Theory of land locomotion – the mechanics of vehicle mobility. University of Michigan Press, Ann Arbor, Michigan, USA, p. 522.

Bergdahl, U., Ottosson, E., Stigson Malmborg, B. (1993) Plattgrundläggning. AB Svensk Byggtjänst och Statens Geotekniska Institut, Stockholm, Sweden, p. 282. In Swedish.

Bisse, E., Hemami, A., Boukas, E. K. (1995) A comparsion of the required energy in loading for four scooping strategies. Proc. of the Third Int. Symp. on Mine Mechanization and Automation, Golden, CO, USA, pp. 2-17 to 2-28.

Blouin, S., Hemami, A., Lipsette, M. (2001) Review of resistive force models for earthmoving processes. Journal of Aerospace Engineering, Vol. 14, No. 3, pp 102-111.

Brinch Hansen, J. (1966) Resistance of a rectangular anchor slab. Bulletin No. 21, Danish Geotechnical Institute, Copenhagen, p. 12-13.

Broms, B. (1966) Arbetsprogram för uppförande av nytt klassificeringssystem med hänsyn till jordarters schaktbarhet, Utredningsrapport 20, Transportforskningskommissionen, Stockholm, Sweden, p. 47, In Swedish.

Bradley, D. A., Seward, D. W. (1998) The development, control and operation of an autonomous robotic excavator. Journal of Intelligent and Robotic Systems, Vol. 21, No. 1, pp. 73-97.

Cannon, H. N. (1999) Extended earthmoving with an autonomous excavator. Carnegie Mellon University, PA, USA, p. 116.

Carlstedt, E. (2008) Soil-structure interaction for bridges with backwalls. Master Thesis, Div. of Structural Design and Bridges, Royal Institute of Technology, Stockholm, Sweden.

Cernica, J. N. (1995) Geotechnical Engineering: Soil Mechanics. John Wiley & Sons, USA, p. 451.

Chu, S. C. (1991) Rankine analysis of active and passive pressures on dry sand. Soils and Foundations, Vol. 31, No. 4, pp. 115-120.

Das, B. M. (2006) Principles of Geotechnical Engineering, sixth edition. Thomson Learning, Toronto, Canada, p. 686.

Davoudi, S., Alimardani, R., Keyhani, A., Atarnejad, R. (2008) A two-dimensional finite element analysis of a plane tillage tool in soil using a non-linear elasto-plastic model. American-Eurasian Journal of Agricultural and Environmental Science, Vol. 3, No. 2, pp 498-505.

Dechao, Z., Yusu, Y. (1992) A dynamic model for soil cutting by blade and tine. Journal of Terramechanics, Vol. 29, No. 3, pp. 317-327.

Duncan, M., Mokwa, R. L. (2001) Passive earth pressures: Theories and tests. Journal of Geotechnical and Geoenvironmental Engineering, Vol. 127, No. 3, pp. 248-257.

Ericsson, A., Slättengren, J. (2000) A model for predicting digging forces when working in gravel or other granulated material. 15th ADAMS European Users Conference, Rome, Italy.

Filla, R., Ericsson, A., Palmberg, J. O. (2005) Dynamic simulation of construction machinery: Towards an operator model. IFPE 2005 Technical Conference, Las Vegas, NV, USA, pp. 429-438.

Filla, R. (2005) Operator and machine models for dynamic simulation of construction machinery. Licentiate Thesis, Linköpings Universitet, Linköping, Sweden, p. 45.

Fine Ltd. (2011) GEO 5, Geotechnical software guide, User's guide version 13, Praha, Czech Republic.

Fransen, G. (1951) Handledning i schaktning med djupgrävmaskiner. State board of water power, Stockholm, Sweden, p. 136. In Swedish.

Gill, W. R., Vanden Berg, G. E. (1968) Agriculture handbook, number 316: Soil dynamics in tillage and traction. Agricultural Research Service, U. S. Department of Agriculture, Washington, D. C., USA, pp. 511.

Godwin, R. J., Spoor, G. (1977) Soil failure with narrow tines. Journal of Agricultural Engineering Research, No. 22, pp 213-228.

Godwin, R. J. (2006) A review of the effect of implement geometry on soil failure and implement forces. Soil and Tillage Research, Vol. 97, No. 2, pp. 331-340.

Haga, M., Watanabe, H., Fujishima, K. (2001) Digging control system for hydraulic excavator. Journal of Mechatronics, Vol. 11, No. 6, pp. 665-676.

Hansbo, S. (1975) Jordmateriallära, Almqvist & Wiksell Förlag AB, Stockholm, Sweden, p. 218. In Swedish.

Hemami, A., Daneshmend, L. (1992) Force analysis for automation of the loading operation in an LHD-loader. Proc. IEEE Conf. on Robotics and Automation, Nice, France, pp 645-650.

Hemami, A. (1994) Force analysis in the scooping/loading operation of an LHD loader. Proc. of the 2nd Int Symp. on Mine Mechanization and Automation, Luleå, Sweden, pp. 415-424.

Hemami, A. (1995) Fundamental analysis of automatic excavation. Journal of Aerospace Engineering, ASCE, Vol. 8, No. 4, pp. 175-179.

Hemami, A. (2008) Robotic excavation, Robotics and Automation in Construction, InTech, Croatia, www.intechopen.com, p. 404.

Hemami, A., Hassani, F. (2007) Simulation of the resistance forces of bulk media in a loading process. 24th Int. Symp. on Automation and Robotics in Construction, Kochi, India, pp. 163-168.

Hemami, A., Hassani, F. (2009) An overview of autonomous loading of bulk material. 26th Int. Symp. on Automation and Robotics in Construction, Austin, Texas, USA, pp. 405-411.

Hettiaratchi D. R. P. (1965) The present state of the theory of soil cutting, Journal of Terramechanics, Vol. 2, No. 1, pp 63-76.

Hettiaratchi, D. R. P., Witney, B. D., Reece, A. R. (1966) The calculation of passive pressure in two-dimensional soil failure. Jour. Agric. Eng. Res. Vol. 11, No. 2. pp. 89-107.

Hettiaratchi, D. R. P., Reece, A. R. (1967) Symmetrical Three Dimensional Soil Failure, Journal of Terramechanics, Vol. 4, No. 3, pp 45-67.

Hettiaratchi, D. R. P., Reece, A. R. (1974) The calculation of passive soil resistance. Geotechnique, Vol. 24, No. 3, pp. 289-310.

Hettiaratchi, D. R. P (1988) Theoretical soil mechanics and implement design. Soil and tillage research, Vol. 11, No. 3-4, pp. 352-347.

Hong, W. (2001) Modeling, Estimation, and Control of Robotic-Soil Interactions. Doctoral Thesis, Massachusetts institute of technology, MA, USA, p. 225.

Jafari, R. (2008) Sensitivity analysis of factors affecting on finite element analysis of soil-tool interaction, Proc. of the 1st WSEAS int. conf. on Finite differences – finite elements – finite volumes – boundary elements, Malta, p. 122-127.

Jaky, J. (1944) The coefficient of earth pressure at rest. J. Soc. Hung. Eng. Arch., pp. 355-358. In Hungarian.

Janbu, N. (1957) Earth pressures and bearing capacity calculations by generalized procedure of slices. Proc.4th Int. Conf. Soil Mech. and Found. Engrg., Vol. 2, pp. 207-212.

Karlsson, R., Hansbo, S. (1984) Jordarters indelning och benämning, Geotekniska laboratorieanvisningar 2, Swedish Geotechnical Society, Stockholm, Sweden, p. 48. In Swedish.

Korhonen, K-H., Gardemeister, R. (1972) Ett nytt system för klassificering av schaktbarhet, Utredningsrapport 35, Transportforskningskommissionen, Stockholm, Sweden, p. 19, In Swedish.

Larsson, R. (1989) Hållfasthet i friktionsjord, SGI Information 8. Swedish Geotechnical Institute, Linköping, Sweden, p. 49. In Swedish.

Larsson, R. (2008) Jords egenskaper, SGI Information 1, Swedish Geotechnical Institute, Linköping, Sweden, p. 60. In Swedish.

Larsson, R., Sällfors, G., Bengtsson, P. E., Alén, C., Bergdahl, U., Eriksson, L. (2007) Skjuvhållfasthet – utvärdering i kohesionsjord, SGI Information 3, Swedish Geotechnical Institute, Linköping, Sweden, p. 66. In Swedish.

Lipsett, M. G., Yousefi Moghaddam, R. (2011) Modeling Excavator-Soil Interaction. Bifurcations, Instabilities and Degradations in geomaterials, Springer-Verlag Berlin Heidelberg, Germany, pp. 347-366.

Luengo, O., Singh, S., Cannon, H. (1998) Modeling and Identification of Soil-Tool Interaction in Automated Excavation, in Proc. of the International Conference on Intelligent Robots and Systems, Canada.

Lundqvist, J. (1993) Geologi, processer – landskap – naturresurser, Studentlitteratur, Lund, Sweden, p. 232. In Swedish.

Luth, H. J., Wismer, R. D. (1965) Performance of plain soil cutting blades in sand. Transactions of the American Society of Agricultural Engineers, Vol. 14, No. 2, pp. 255-259, 262.

Magnusson, O. (1973) Jordars schaktbarhet, Rapport R51:1973, Byggforskningen, Stockholm, Sweden, p.243. In Swedish.

Magnusson, O., Orre, B. (1985) Schaktbarhet Klassificeringssystem -85, Rapport R130:1985, Byggforskningen, Stockholm, Sweden, p. 69. In Swedish.

Malaguti, F. (1994) Soil machine interaction in digging and earthmoving automation. Proc. of the 11th Int. Symp. on Automation and Robotics in Construction, Brighton, UK.

McKeys, E. (1985) Soil Cutting and Tillage, Elsevier, Amsterdam, The Netherlands, p. 217.

McKeys, E. (1989) Agricultural Engineering Soil Mechanics, Elsevier, Amsterdam, The Netherlands, p.292.

McKeys, E. & Ali, O. S. (1977) The cutting of soil with narrow blades, Journal of Terramechanics, Vol. 14, No. 2, pp 43-58.

Mokwa, R. L., Duncan, M. (1999) Addendum to final contract report on investigation of the resistance of pile caps and integral abutments to lateral loading, Documentation for spreadsheet PYCAP2, Virginia Transportation Research Council, Virginia, USA, p. 23.

Mouazen, A. M., Neményi, M. (1998) A review of the finite element modelling techniques of soil tillage, Journal of Mathematics and Computers in Simulation, Vol. 48, No. 1, pp 23-32.

NAVFAC (1986) (Naval Facilities Engineering Command), Design Manual 7.02 (DM-7.02), Foundations and earth structures, NAVFAC, Virginia, USA, p. 279.

Nezami, E. G., Hashash, Y, M. A., Zhao, D., Ghaboussi, J. (2007) Simulation of front end loader bucket-soil interaction using discrete element method. Int. J. for Numerical and Analytical Methods in Geomechanics, Vol. 31, No. 9, pp. 1147-1162.

O'Callaghan, J. R., Farrelly, K. M. (1964) Cleavage of soil by tined implements, Jour. Agric. Eng. Res., Vol. 9, No. 3. pp. 259-270.

Ohde, J. (1938) Zur theorie des erddruckes unter besinderer perucksiuchtigung der Erddruck verteilung, Bautechnik , No. 16, pp. In German.

Osman, M. S. (1964) The mechanics of soil cutting blades, Jour. Agric. Eng. Res. Vol. 9, No. 4. pp. 313-328.

Payne, P. C. J. (1956) The relationship between the mechanical properties of soil and the performance of simple cultivation implements, Jour. Agric. Eng. Res., Vol. 1, No. 1. pp. 23-50.

Brinkgreve, R. B. J., Broere, W., Waterman, D. (2006) PLAXIS 2D – Version 8 Manual. Plaxis bv, The Netherlands.

Qinsen, Y. Shuren, S. (1994) A soil-tool interaction model for bulldozer blades. Journal of Terramechanics, Vol. 31, No. 2, pp 55-65.

Rahardjo, H., Fredlund, D. (1983) General limit equilibrium method for lateral earth force. Can. Geotech. Journal, Vol. 21, pp. 166-175.

Reece, A. R. (1964) The fundamental equation of earth-moving mechanics. Proc. of the Institution of Mechanical Engineers, Vol. 179, Part 3F, London.

Reese, L. C. (1997) Analysis of laterally loaded piles in weak rock. Journal of Geotechnical and Geoenvironmental Engineering, Vol. 123, No. 11, pp. 1010-1017.

Resource Management Technical Report 298 (2005), Land evaluation standards for land resource mapping, Department of Agriculture, Government of Western Australia, Australia, pp 28.

Rollins, K. M., Nasr, M., Gerber, T. M. (2010) Numerical analysis of dense narrow backfills for increased passive resistance. Brigham Young University, Utah, USA, p. 192.

Selig, E. T., Nelson, R. D. (1964) Observations of soil cutting with blades, Journal of Terramechanics, Vol. 1, No.3. pp. 32-53.

Swedish Geotechnical Institute (2011) website, Information about soil types, Swedish Geotechnical Institute, Linköping, Sweden, In Swedish. Published on the internet at 2011-12-22: http://www.swedgeo.se/templates/SGIStandardPage____1098.aspx?epslanguage=SV.

Shamsabadi, A., Nordal, S. (2006) Modelling passive earth pressures on bridge abutments for nonlinear seismic soil-structure interaction using Plaxis. Plaxis publications, Delft, The Netherlands, p. 8.

Shiau, J., Smith, C. (2006) Numerical analysis of passive earth pressures with interfaces. 3rd European Conf. on Computational Mechanics Solids, Lisbon, Portugal, pp. 147-155.

Shiau, J. S., Augarde, C. E., Lyamin, A. V., Sloan, S. W. (2008) Finite element limit analysis of passive earth resistance in cohesionless soils. Soils and foundations, Vol. 48, No. 6, pp. 843-850.

Shmulevich, I., Asaf, Z., Rubinstein, D. (2007) Interaction between soil and a wide cutting blade using the discrete element method, Soil & Tillage Research, Vol. 97, pp 37-50.

Siemens, J. C., Weber, J. A., Thornburn, T. H. (1965) Mechanics of soil as influenced by model tillage tools, Vol. 8, No. 1, pp. 1-7.

Singh, S. (1995) Learning to predict resistive forces during robotic excavation. Proc. of 1995 IEEE Int. Conf. on Robotics and Automation, Vol. 2, pp. 2102-2107.

Singh, S. (1997) The state of the art in automation of earthmoving. ASCE Journal of Aerospace Engineering, Vol. 10, No. 4. pp. 179-188.

Sokolvski, V. V. (1960) Statics of Soil Media, Butterworths Scientific Publications, London, UK, p. 237.

Stafford, J. V., Tanner, D. W. (1983) Effect of rate of soil shear strength and soil-metal friction, I. shear strength. Soil and Tillage Research, Vol. 3, No. 3, pp. 245-260.

Swick, W. C., Perumpral, J. V. (1988) A model for predicting soil-tool interaction. Journal of Terramechanics, Vol. 25, No. 1, pp. 43-56.

Swedish Road Administration (1972) Internal document, Definition av bearbetbarhet för olika jordar, Utvecklings projekt 2.7, Delrapport, Swedish Road Administration, Borlänge, Sweden, p. 40. In Swedish.

Swedish Road Administration (1976) Internal document, Definition av bearbetbarhet för olika jordar, Utvecklings projekt 2.7, Slutrapport, Swedish Road Administration, Borlänge, Sweden, p. 33. In Swedish.

Swedish Road Administration (1977) Internal document, Testverksamhet angående jordarters bearbetbarhet vid väg 805 Allån – Alanäs, Internrapport 18, Swedish Road Administration, Borlänge, Sweden, p. 29. In Swedish.

Swedish Road Administration (2009) Tekniska Kravdokument Geo (TK Geo), Vägverket Publ. 2009:46, Swedish Road Administration, Borlänge, Sweden, p. 156. In Swedish.

Terzaghi, K. (1943) Theoretical soil mechanics. John Wiley and Sons, New York, USA, p. 510.

Volvo GPPE Performance Manual (2009), How to calculate cost and productivity – The TCO Handbook, Edition 1, Internal document, Volvo Construction Equipment, Eskilstuna, Sweden., p. 490.

Wilkinson, D. (1997) WebPages for Road Design, Part of Master of Engineering report, University of Durham, UK, Published on the internet at 2011-09-18: http://www.dur.ac.uk/~des0www4/cal/roads/index.html

Wu, L. (2003) A study on automatic control of wheel loaders in rock/soil loading. Dissertation, University of Arizona, Arizona, USA, p. 236.

Xia, K. (2008) A framework for earthmoving blade/soil model development, Journal of Terramechanics, Vol. 45, No. 5, pp 147-165.

Young, R. N., Hannah, A. W. (1977) Finite element analysis of plane soil cutting, Journal of Terramechanics, Vol. 14, No. 3, pp 103-125.

Yong, R. N., Chen, C. K. (1970) Analytical and experimental studies of soil cutting. Soil mechanics series No. 27, McGill University, Montreal, Canada, p. 32.

Zein Eldin and Al-Janobi (1995) Soil – tillage tool interaction analyses, Effect of tool parameters on soil – tillage tool interaction, State of the art review and bibliography. Misr. Journal of Agricultural Engineering, Vol. 12, No. 3, pp. 561-574.

Zelenin, A. N., Balovnev, V. I., Kerov, I. P. (1985) Machines for moving the earth, Amerind Publishing Co., New Delhi, India, p. 555.

Zhu, D. Y., Qian, Q. (2000) Determination of passive earth pressure coefficients by the method of triangular slices. Canadian Geotechnical Journal, Vol. 37, No. 2, pp 485-491.